University of Copenhagen

PhD Thesis

Numerical Methods for Nonlinear PDEs in Finance

Author:
Sima Mashayekhi

This thesis submitted in fulfilment of the requirements for the degree of Doctor of Philosophy

in the

Department of Mathematical Sciences
University of Copenhagen

September 2015

Sima Mashayekhi
Department of Mathematical Sciences
University of Copenhagen
Universitetsparken 5
DK-2100 København Ø
Denmark
sima.m@math.ku.dk
s-mashayekhi@araku.ac.ir

PhD thesis submitted to the PhD School of Science, Faculty of Science, University of Copenhagen, Denmark, in September 2015.

Academic advisors: **Jens Hugger**
University of Copenhagen, Denmark

Rolf Poulsen
University of Copenhagen, Denmark

Assessment Committee: **Trine Krogh Boomsma** (chair)
University of Copenhagen, Denmark

Lina von Sydow
Uppsala University, Sweden

David Skovmand
Copenhagen Business School, Denmark

ISBN 978-87-7078-935-6

Abstract

Nonlinear Black-Scholes equations arise from considering parameters such as feedback and illiquid markets effects or large investor preferences, volatile portfolio and nontrivial transaction costs into option pricing models to have more accurate option price. Here some finite difference schemes have been investigated to solve numerically such nonlinear equations.

However the analytical solution of the linear Black-Scholes equation is known, different numerical methods have been considered for solving the equation to make a general numerical scheme for solving other more complicated models with no analytical solutions such as nonlinear Black-Scholes models. Therefore at first some investigations for the standard linear Black-Scholes equation have been considered for instance choosing a suitable right boundary condition and applying some remedies for dealing with nonsmooth conditions of the equation. After that a number of nonlinear Black-Scholes models are reviewed and different numerical methods have been investigated for solving some of those models. At the end the numerical schemes have been compared with respect to order of convergence.

Acknowledgements

I would like to express my special appreciation and thanks to my supervisors Jens Hugger and Rolf Poulsen for their supports, ideas and encouraging my research. In particular, I thank Jens for his enthusiasm and invaluable advices, and Rolf for his insightful comments. I also sincerely thank Jeffrey S. Scroggs who provided me an opportunity to have a great experience of visiting North Carolina State University and doing some research during my five months stay abroad. Moreover, I would like to thank my committee members for their comments and suggestions.

A special thanks to my family. Words cannot express how grateful I am to my parents for their all kindness and support. I would also like to thank all of my friends, colleagues and the rest of the department of Mathematics for this great experience that I had during this recent years. At the end I would like express appreciation to my little daughter Saba for giving us a nicer life and especially my beloved husband who was always my support in the moments when there was no one to answer my queries.

Sima Mashayekhi
Copenhagen, Denmark
September 2015

List of Papers

This thesis is based on the following four papers:

- Sima Mashayekhi and Jens Hugger, K_α-Shifting, Rannacher Time Stepping and Mesh Grading in Crank-Nicolson FDM for Black-Scholes Option Pricing, To be appeared in *Journal of Communications in Mathematical Finance (CMF), (2015).*
- *Jens Hugger and Sima Mashayekhi, Standard Finite Difference Schemes for European Options, Working Paper, (2015).*
- *Jens Hugger and Sima Mashayekhi, Feedback Options in Nonlinear Numerical Finance, International Conference of Numerical Analysis and Applied Mathematics. AIP Conference Proceedings, Volume 1479 (2012) pp. 2266-2269.*
- *Sima Mashayekhi and Jens Hugger, Finite Difference Schemes for a Nonlinear Black-Scholes Model with Transaction Cost and Volatility Risk, Acta Mathematica Universitatis Comenianae (AMUC), Vol 84, No 2 (2015), pp. 255-266.*

Contents

List of Figures

List of Tables

Abbreviations

BE	**B**ackward **E**uler
B-S	**B**lack **S**choles
BVP	**B**oundary **V**alue **P**roblem
BS	**B**lack **S**choles
CN	**C**rank **N**icolson
CNK	**C**rank **N**icolson $\mathbf{K}_\alpha$-optimization
CNGS	**C**rank **N**icolson **G**rid **S**tretching
CNR	**C**rank **N**icolson **R**annacher
FDM	**F**inite **D**ifference **M**ethod
FE	**F**orward **E**uler
FtCS	**F**orward in **t**ime **C**entral in **S**
ImpUp	**I**mplicit **U**pwind
NFDM	**N**onstandard **F**inite **D**ifference **M**ethod
PDE	**P**artial **D**ifferencial **E**quation
PosPre	**P**ositive **P**reserving

Symbols

S	underlying risky asset
t	time
T	terminal time
γ	dividend yield
σ	volatility of the underlying risky asset
r	market interest rate
K	strike price (exercise price)
B	Bet
$\mathcal{H}$	Heaviside function

Chapter 1

Introduction

This thesis except this chapter as a general introduction consist of four chapters that are written as academic articles on different topics and therefore are self-contained. In this chapter an overview of linear and nonlinear Black-Scholes models, definitions and properties of the models are given. Some remedies to deal with non-smooth condition of the Black-Scholes equation has been investigated in Chapter 2 to restore the convergence order of the Crank Nicolson. In Chapter 3 some standard finite difference schemes have been considered for European option pricing and position of S_{max} as the right boundary condition of the Black-Scholes equation is considered. After investigation on linear Black-Scholes equation two different nonlinear Black-Scholes equations have been investigated in Chapters 4 and 5.

1.1 Linear Black-Scholes Model

The standard Black-Scholes model is a well known linear equation derived by Fischer Black and Myron Scholes in 1973 [5] and earlier by Robert Merton [33] for pricing options in financial derivatives. Standard finite difference schemes for solving the partial differential equation formulation of European vanilla options are standard textbook material today — see for example [11, 46, 26, 42]. Moreover numerous articles have investigated this area — for instance [7, 9, 10, 13, 35, 43, 45].

In section 1.1.1 we present the partial differential equation model for the European vanilla option on the unbounded domain and derive boundary conditions to be used for numerical solution on a bounded domain.

One of the main obstacles in numerical option pricing is the fact that the terminal condition at the expiration time for the option in general contains one or more discontinuities either in the option value (this is the case for example for the "cash or nothing call" or simply the bet option with one discontinuity or butterfly spread with three discontinuities) or in some derivatives of this (as for example for the put and call options having discontinuities in the first derivative of the option value with respect to the risky asset price S. This derivative is commonly denoted the option Δ). All finite difference methods involves solving the model PDE only in a finite number of mesh points. It turns out that the error committed with the various methods depends on the position of the discontinuity with respect to these mesh points.

Following research questions have been posed where have been answered in Chapters 2 and 3:

(1) How should the discontinuity be positioned with respect to the mesh points in order to obtain the minimal error for the various options and methods?

(2) How does these discontinuities influence the convergence properties of various numerical methods?

1.1.1 PDE model of European vanilla options on unbounded domain

The classical boundary value problem for a European option posed over the financially relevant domain $\Omega_\infty = \{(S,t) \in]0,\infty[\times]0,T[\}$ is found in most of the references in section 1.1 to be the following terminal value problem:

$$\begin{aligned}&\text{Find } V: \ (S,t) \in \bar{\Omega}_\infty \to \mathcal{R}, \ V \in \mathcal{C}^0(\bar{\Omega}_\infty) \cap \mathcal{C}^{2,1}(\Omega_\infty) \text{ so that} \\ &\frac{\partial V}{\partial t} + \frac{1}{2}\sigma^2 S^2 \frac{\partial^2 V}{\partial S^2} + (r-\gamma)S\frac{\partial V}{\partial S} - rV = 0 \text{ in } \Omega_\infty \\ &\text{and } V(S,T) \text{ is payoff function as the terminal condition in } \bar{\Omega}_\infty|_{t=T}. \end{aligned} \quad (1.1)$$

Here the dependent variable $V(S,t)$ is the value (price) of the option for a value S of the risky asset at time t. γ, $\sigma > 0$ and r — the *dividend yield*, *volatility* (on the underlying

risky asset) and *market interest rate* (on the riskfree asset) — are all assumed to be independent of the value S of the underlying risky asset and time t in the standard Black-Scholes model. The payoff is negotiated at time 0 between the buyer and seller of the option. We shall here consider 4 simple options:

1. The *put option* where at time $t = 0$ it is agreed that you (the buyer of the option) at time $t = T$ may sell the underlying risky asset at the *Strike Price* K to your opponent (the seller of the option) or you may choose to do nothing. This means that at expiry you get a profit of — and hence the value V^P of the option at expiry is — $V^P(S(T), T) = \max\{K - S(T), 0\}$.

2. The *call option* is another very common option where at time $t = 0$ it is agreed that you (the buyer of the option) at time $t = T$ may buy the underlying risky asset at the *Strike Price* K from your opponent (the seller of the option) or you may choose to do nothing. This means that at expiry you get a profit of — and hence the value V^C of the option at expiry is — $V^C(S(T), T) = \max\{S(T) - K, 0\}$.

3. The *cash-or-nothing call option* or the *(Simple) Bet Option* is an option where at time $t = 0$ it is agreed that you (the buyer of the option) at time $t = T$ get a lump sum of B (the *Bet*) from your opponent (the seller of the option) if at that time, the price of the risky asset is at least equal to the *Strike Price* K. This means that at expiry you get a profit of — and hence the value V^B of the option at expiry is — $V^B(S(T), T) = B\mathcal{H}(S(T) - K)$ where $\mathcal{H}(x) = \begin{cases} 1 & \text{for } x \geq 0 \\ 0 & \text{for } x < 0 \end{cases}$ is the Heaviside function.

4. The *smoothened put option* is introduced to serve as a reference in the investigation of the above options. A main feature of the put, call and bet options are the singularities in the terminal conditions at $S = K$.[1] For the smoothened put option we use the smooth terminal condition $V^{SP}(S(T), T) = K\frac{S_{\max} - S(T)}{S_{\max}}e^{-2S(T)}$. Here

[1] Note that for the put and call options, the value functions $V^P(\cdot, T)$ and $V^C(\cdot, T)$ are continuous whereas $\frac{\partial V^P}{\partial S}(\cdot, T)$ and $\frac{\partial V^C}{\partial S}(\cdot, T)$ are discontinuous as functions of S (at $S = K$), i.e. $V^P(\cdot, T) \in \mathcal{C}^0(]0, \infty[)$ and $V^C(\cdot, T) \in \mathcal{C}^0(]0, \infty[)$ while we have a singularity in the first derivative at expiry. Instead for the bet option $V^B(\cdot, T)$ is discontinuous at $S = K$, so that we have a singularity already in the function value at expiry. The bet option is included in order to investigate the influence of discontinuities in the payoff on the solution V. It is well known that even a finite number of discontinuities in the terminal or boundary conditions to a linear parabolic differential equation problem [DEP] does not destroy the infinite smoothness of the solution in the interior of the domain as long as the coefficients of the derivatives are smooth. (See for example [22] §3.1).

$S_{\max}$ is the upper bound on the computational domain in the S variable, to be introduced in more details later.

We shall use similar notation for any other relevant function such as V^P, V^C, V^B, V^{SP} and V for the value function, Δ^P, Δ^C, Δ^B, Δ^{SP} and Δ for the Delta-greek and so on. For some predetermined strike price K, bet B and $S_{\max}$ we shall consider different values of the 6 parameters T, K, B, r, γ and σ. However we shall define a *Standard Case* with the parameters $T = 1$, $K = 1$, $B = 0.3$, $r = 0.04$, $\gamma = 0$ and $\sigma = 0.2$.

1.1.2 Solutions and Greeks

For our first 3 option cases the option prices V are known from basic finance text books as for example [46] §5.4–5.5 (for $\gamma = 0$), [29] §2.2 (for put and call) or [20] §1.1.6 and §2.11.2 (for all cases) and are given by

$$V^P(S,t) = Ke^{-r(T-t)}N(-d_2) - e^{-\gamma(T-t)}SN(-d_1), \tag{1.2}$$

$$V^C(S,t) = -Ke^{-r(T-t)}N(d_2) + e^{-\gamma(T-t)}SN(d_1), \tag{1.3}$$

$$V^B(S,t) = Be^{-r(T-t)}N(d_2), \tag{1.4}$$

$$\text{where } N(d) = \frac{1}{\sqrt{2\pi}}\int_{-\infty}^{d} e^{-\frac{1}{2}y^2}dy \text{ and}$$

$$d_1 = \frac{\ln\frac{S}{K} + (r - \gamma + \frac{1}{2}\sigma^2)(T-t)}{\sigma\sqrt{T-t}},\ d_2 = \frac{\ln\frac{S}{K} + (r - \gamma - \frac{1}{2}\sigma^2)(T-t)}{\sigma\sqrt{T-t}}.$$

2D solution plots for the standard case at start ($t = 0$) and expiration ($t = T$) are shown in Figure 1.1. Corresponding 3D solution plots showing solutions for all time values $t \in (0, T)$ are shown in Figure 1.2.

From V the Deltas given by $\Delta = \frac{\partial V}{\partial S}$ can be computed. Only Δ^P and Δ^C are "challenging", but these are well known from for example [46] §5.4 (for $\gamma = 0$) or [20] §1.3.1 (for

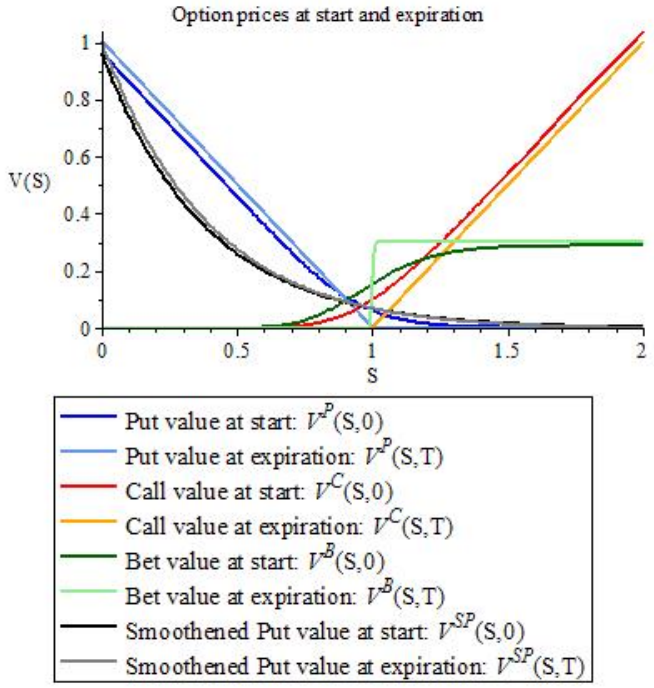

FIGURE 1.1: Solutions to put, call, bet and smoothened put options at start and expiration in the standard case ($T = 1$, $K = 1$, $B = 0.3$, $r = 0.04$, $\gamma = 0$ and $\sigma = 0.2$.

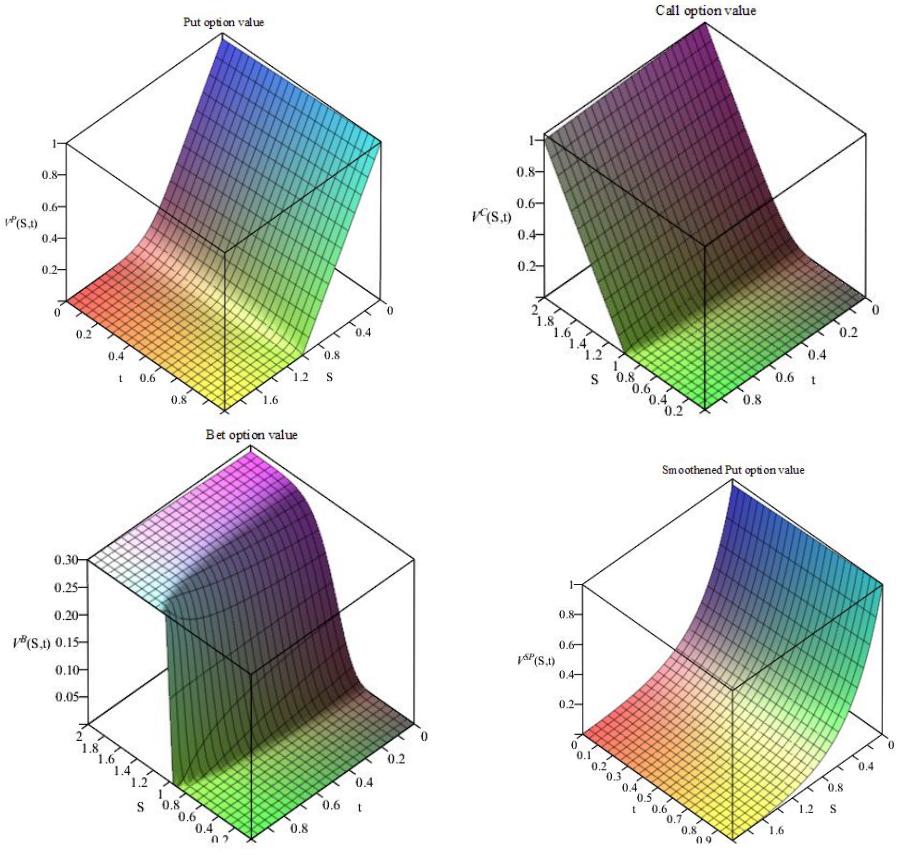

FIGURE 1.2: Solutions to put, call, bet and smoothened put options at times $t \in (0, T)$ in the standard case ($T = 1$, $K = 1$, $B = 0.3$, $r = 0.04$, $\gamma = 0$ and $\sigma = 0.2$)

all cases):

$$\Delta^P(S,t) = \frac{\partial V^P}{\partial S}(S,t) = e^{\gamma(T-t)}(N(d_1) - 1), \tag{1.5}$$

$$\Delta^C(S,t) = \frac{\partial V^C}{\partial S}(S,t) = e^{\gamma(T-t)}N(d_1), \tag{1.6}$$

$$\Delta^B(S,t) = \frac{\partial V^B}{\partial S}(S,t) = Be^{-r(T-t)}n(d_2), \tag{1.7}$$

where $n(d) = \dfrac{\partial N(d)}{\partial S}$ so that

$$n(d_1) = \frac{e^{-\frac{1}{2}d_1^2}}{\sqrt{2\pi}S\sigma\sqrt{T-t}} \text{ and } n(d_2) = \frac{e^{-\frac{1}{2}d_2^2}}{\sqrt{2\pi}S\sigma\sqrt{T-t}}.$$

2D Delta plots for the standard case at start ($t = 0$) and expiration ($t = T$) are shown in Figure 1.3. Corresponding 3D Delta plots showing Delta values for all time values

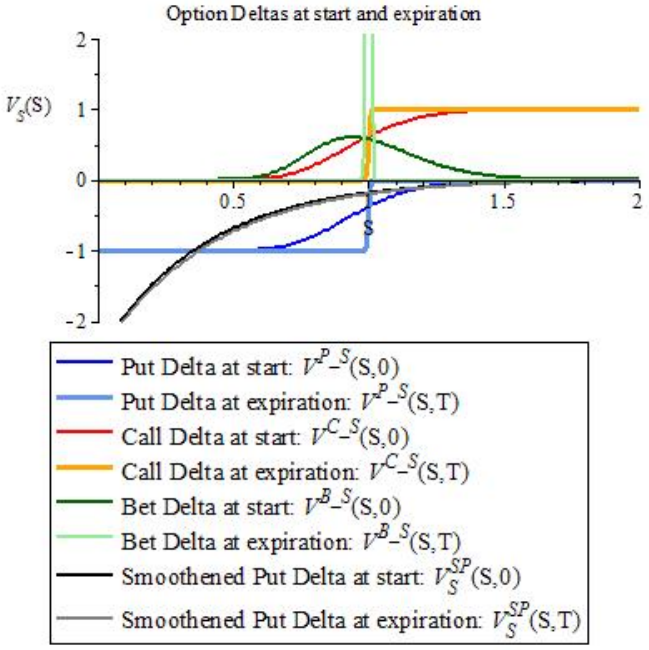

FIGURE 1.3: Deltas for put, call, bet and smoothened put options at start and expiration in the standard case ($T = 1$, $K = 1$, $B = 0.3$, $r = 0.04$, $\gamma = 0$ and $\sigma = 0.2$)

$t \in (0, T)$ are shown in Figure 1.4.

From V the Gammas given by $\Gamma = \frac{\partial^2 V}{\partial S^2}$ can be computed:

$$\Gamma^P(S,t) = \frac{\partial^2 V^P}{\partial S^2}(S,t) = e^{\gamma(T-t)}n(d_1), \tag{1.8}$$

$$\Gamma^C(S,t) = \frac{\partial^2 V^C}{\partial S^2}(S,t) = e^{\gamma(T-t)}n(d_1), \tag{1.9}$$

$$\Gamma^B(S,t) = \frac{\partial^2 V^B}{\partial S^2}(S,t) = -Be^{-r(T-t)}\frac{n(d_2)}{S}\left(\frac{d_2}{\sigma\sqrt{T-t}} + 1\right). \tag{1.10}$$

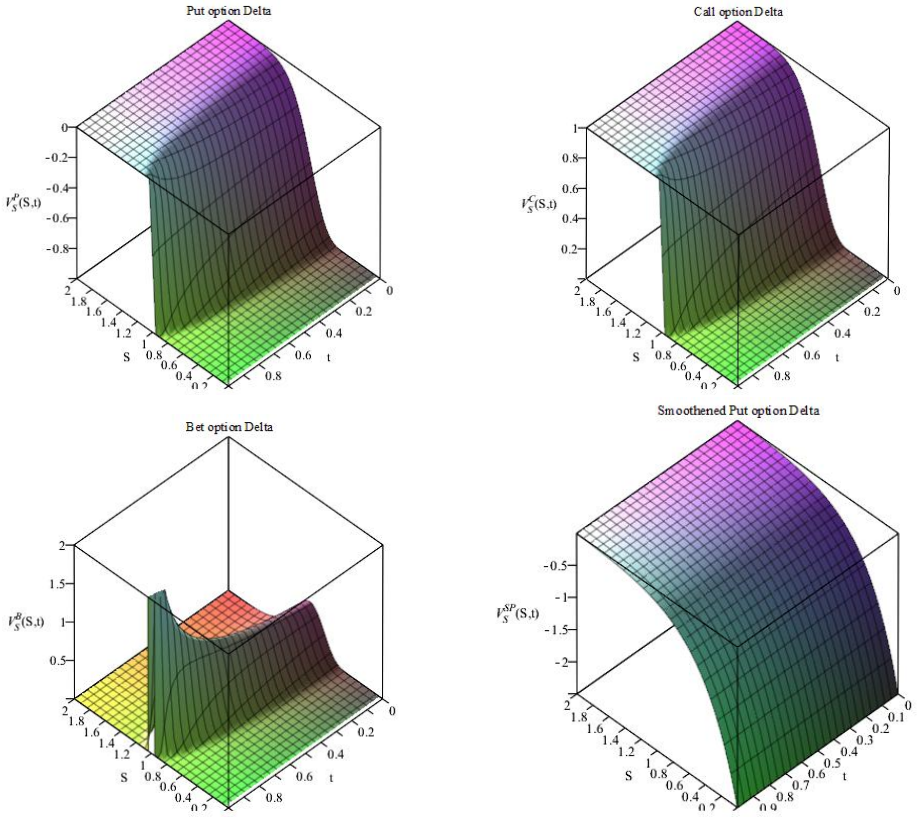

FIGURE 1.4: Deltas for put, call, bet and smoothened put options at times $t \in (0, T)$ in the standard case ($T = 1$, $K = 1$, $B = 0.3$, $r = 0.04$, $\gamma = 0$ and $\sigma = 0.2$)

2D Gamma plots for the standard case at start ($t = 0$) and expiration ($t = T$) are shown in Figure 1.5. Corresponding 3D Delta plots showing Gamma values for all time values

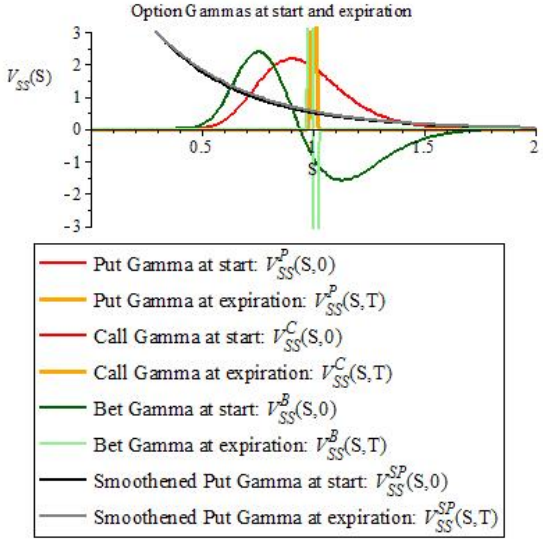

FIGURE 1.5: Gammas for put, call, bet and smoothened put options at start and expiration in the standard case ($T = 1$, $K = 1$, $B = 0.3$, $r = 0.04$, $\gamma = 0$ and $\sigma = 0.2$) - The put and call Gammas are identical

in $(0, T)$ are shown in Figure 1.6.

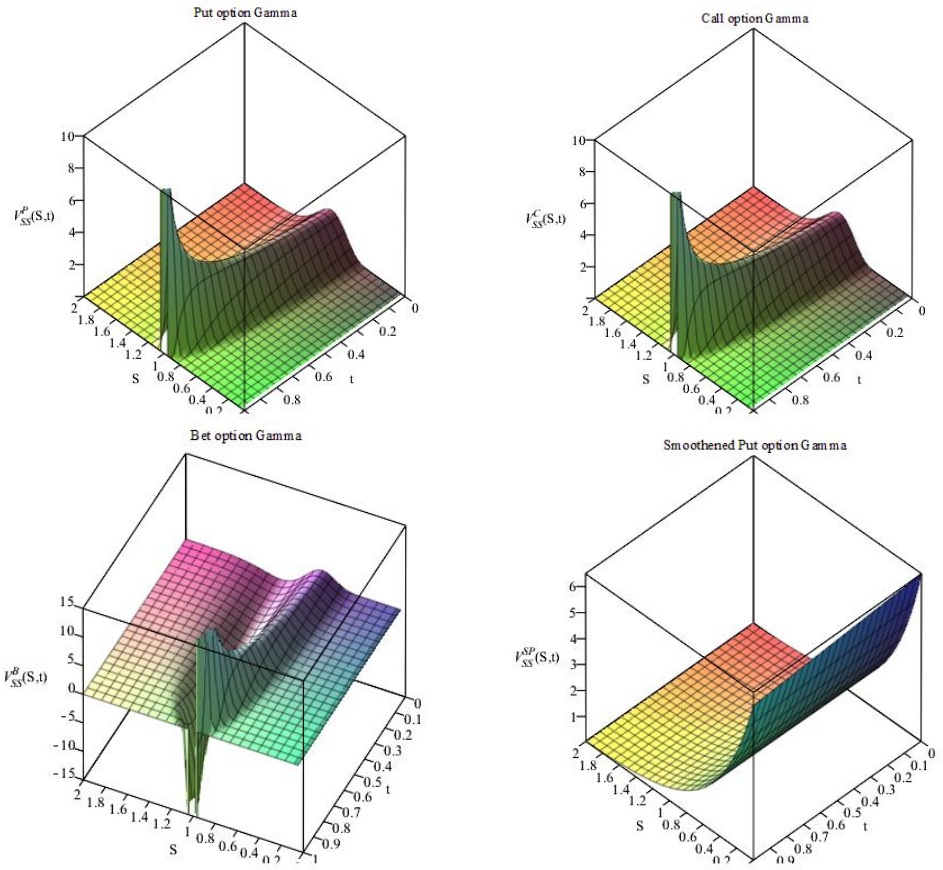

FIGURE 1.6: Gammas for put, call, bet and smoothened put options at times $t \in (0, T)$ in the standard case ($T = 1$, $K = 1$, $B = 0.3$, $r = 0.04$, $\gamma = 0$ and $\sigma = 0.2$)

For particular parameter selections, the solution, Δ and Γ of the smoothened put option can be computed for example using the Finance package of the Maple symbolic computation environment. The solutions, Δ's and Γ's are shown in Figures 1.1–1.6.

1.1.3 Limits

There are some interesting limits to the problem 1.1:

Volatility limit: For $\sigma = 0$ the option loses its stochastic aspect and behaves like a riskfree asset with the payoff function as the terminal value at time T and dividend γ in a world with interest rate r. The value at time t is then the amount of money that, if put in the bank at interest rate r would result in the same value of payoff at time T as if holding the option. But this amount is simply the terminal value back discounted by r so that $V(S,t)|_{\sigma=0} = V(S(T),T)e^{-r(T-t)}$. Here $S(T)$ is the value of the (now risk-free) risky asset at expiration $t = T$. To express it by S we simply back discount it by $r - \gamma$ since we could get the interest rate r by selling the stock and putting the money in the bank, but at the same time we would then lose the dividend rate γ. Hence $S = S(T)e^{-(r-\gamma)(T-t)}$. In conclusion

$$V(S,t)|_{\sigma=0} = V(Se^{(r-\gamma)(T-t)},T)e^{-r(T-t)} \tag{1.11}$$

As $\sigma \to 0$, the convection-diffusion equation loses its diffusion part and becomes a convection equation. Hence it is not known whether

$$\lim_{\sigma \downarrow 0} V(S,t) = V(S,t)|_{\sigma=0} \tag{1.12}$$

but it will be investigated whether the numerical solutions have this desirable property.

Expiration limit: For $t = T$ the option price is given by the payoff function $V(S,T)$. Even though $V^B(S,T)$ is discontinuous and $V^C(S,T)$ and $V^P(S,T)$ have discontinuous first derivatives the formulas for the exact solutions show that these singularities are instantaneously smoothened out for $t < T$ or $\tau > 0$ and also that

$$\lim_{t \uparrow T} V(S,t) = V(S,T). \tag{1.13}$$

Enforcing $V(S,T)$ as a terminal boundary condition and solving backwards in time, also a numerical solution will have this desirable property, but it will be investigated whether the discontinuities as expected give rise to problems in the numerical solution.

Left risky asset limit: For $S = 0$ the risky asset has lost all value corresponding to *Bankruptcy*. If bankruptcy happens at a time t^*, then (see note 2 in [23]) $S(t)$ remains zero for $t \geq t^*$. Hence the option has lost its stochastic aspect and behaves like a riskfree asset with interest rate r. Hence the value is simply the terminal value $V(S(T), T) = V(0, T)$ back discounted by r so that

$$\begin{aligned} V^P(0,t) &= Ke^{-r(T-t)} \\ V^C(0,t) &= 0 \\ V^B(0,t) &= 0 \\ V^{SP}(0,t) &= Ke^{-r(T-t)} \end{aligned} \quad . \tag{1.14}$$

This condition may (and will) be enforced as a boundary condition to the differential equation 1.1. Note that this is not entirely unquestionable since the PDE 1.1 in the limit $S \to 0$ loses all dependence on S. Hence a boundary condition in $S = 0$ may actually give rise to problems for a numerical solution.

Right risky asset limit: For $S \to \infty$ the limiting behavior is again determined by *certainty*, i.e. lack of stochastic uncertainty. If we are certain to get a payback M at time T then the value at $t \in (0, T)$ is as above the r-backdiscounted value of M, $Me^{-r(T-t)}$. For a put option with large $S >> K$ at some time $t \in (0, T)$ we are almost certain to end up at time T with the payback 0. As S is increasing, the certainty grows, and in the limit $S \to \infty$ the certainty becomes total resulting in $\lim_{S\to\infty} V^P(S, t) = 0$. The smoothened put will be given the same right boundary condition as the ordinary put. Similarly for a bet option with large $S >> K$ at some time $t \in (0, T)$ we are almost certain to end up at time T with the payback B. As S is increasing, the certainty grows, and in the limit $S \to \infty$ the certainty becomes total resulting in $\lim_{S\to\infty} V^B(S, t) = Be^{-r(T-t)}$. For a call option with large $S >> K$ at some time $t \in (0, T)$ we are almost certain to end up at time T with the payback $S(T) - K$. As S is increasing, the certainty grows, and in the limit $S \to \infty$ the certainty becomes total. The problem is, that $S(T)$ is stochastic so that the payoff is not certain. Considering instead a portfolio consisting of one call option and minus one risky asset then the payoff at time T on this portfolio is certain to be $-K$ in the limit as $S \to \infty$. Hence $\lim_{S\to\infty} (V(S(T), T) - S(T)) = -K$. To express the terminal risky asset price $S(T)$ by the asset price S at time t we follow the argument from the volatility limit and get $\lim_{S\to\infty} \left(V(S(T), T) - Se^{(r-\gamma)(T-t)}\right) = -K$. To express also the option price in terms of S and t we need — as explained for the volatility limit

— to back discount by the interest rate r. Clearly both the $-K$ and the $S(T)$ term must be back discounted so that $\lim_{S\to\infty}\left(V(S,t) - Se^{(r-\gamma)(T-t)}e^{-r(T-t)}\right) = -Ke^{-r(T-t)}$. In conclusion we have

$$\begin{aligned}
&\lim_{S\to\infty} V^P(S,t) = 0 \\
&\lim_{S\to\infty}(V^C(S,t) - Se^{-\gamma(T-t)}) = -Ke^{-r(T-t)} \\
&\lim_{S\to\infty} V^B(S,t) = Be^{-r(T-t)} \\
&\lim_{S\to\infty} V^{SP}(S,t) = 0
\end{aligned} \quad . \tag{1.15}$$

For numerical computations it is convenient to have a bounded computational domain. This is obtained by restricting S to some bounded interval $S \in (0, S_{\max})$. 1.15 indicate the following boundary condition in $S = S_{\max}$:

$$\begin{aligned}
&V^P(S_{\max},t) \simeq 0 \\
&V^C(S_{\max},t) \simeq S_{\max}e^{-\gamma(T-t)} - Ke^{-r(T-t)} \\
&V^B(S_{\max},t) \simeq Be^{-r(T-t)} \\
&V^{SP}(S_{\max},t) \simeq 0
\end{aligned} \quad \text{for } S_{\max} >> K. \tag{1.16}$$

In the limit $S_{\max} \to \infty$ this is a valid boundary condition but it will be investigated just how big $S_{\max}$ needs to be in order to get insignificant errors from the approximate boundary condition 1.16.

1.1.4 Differential equation on a bounded domain

We now have arrived at the following BVP to be discretized and solved:

$$\frac{\partial V}{\partial t} + \frac{1}{2}\sigma^2 S^2 \frac{\partial^2 V}{\partial S^2} + (r-\gamma)S\frac{\partial V}{\partial S} - rV = 0 \qquad \forall (S,t) \in (0, S_{\max}) \times (0,T) \tag{1.17}$$

with the following conditions

$$V(S,T) = \kappa(S,T), \quad V(0,t) = \kappa(0,t), \quad V(S_{\max},t) \simeq \kappa(S_{\max},t) \tag{1.18}$$

where function $\kappa(S,t)$ is defined as follow

$$\kappa(S,t) = \begin{cases} \max\{Se^{-\gamma(T-t)} - Ke^{-r(T-t)}, 0\} & \textit{call option} \\ \max\{Ke^{-r(T-t)} - Se^{-\gamma(T-t)}, 0\} & \textit{put option} \\ Be^{-r(T-t)}\mathcal{H}(S-K) & \textit{bet option} \\ K\frac{S_{\max}-S}{S_{\max}}e^{-2S-r(T-t)} & \textit{smoothened put} \end{cases} . \tag{1.19}$$

1.1.5 Transformations of differential equation

By the simple change of variables

$$\tau = T - t \ \forall t \in [0,T], \text{ i.e. } \forall \tau \in [0,T] \tag{1.20}$$

1.17–1.19 is transformed into the following initial value problem:

$$\begin{aligned} &\text{Find } U: \ (S,\tau) \in \bar{\Omega} \to \mathcal{R} \text{ where } \Omega = (0, S_{\max}) \times (0,T) \\ &\text{for some } S_{\max} >> K, \\ &\text{so that in a classical, weak or distributional sense} \\ &-\frac{\partial U}{\partial \tau} + \frac{1}{2}\sigma^2 S^2 \frac{\partial^2 U}{\partial S^2} + (r-\gamma)S\frac{\partial U}{\partial S} - rU = 0 \text{ in } \Omega \text{ and} \\ &U(S,0) = \kappa(S,T), \quad U(0,\tau) = \kappa(0,\tau), \quad U(S_{\max},\tau) \simeq \kappa(S_{\max},\tau) \end{aligned} \tag{1.21}$$

where the connection between 1.17 and 1.21 is that

$$U(S,\tau) = V(S,T-t), \ \forall (S,t) \in \bar{\Omega} \text{ i.e. } \forall (S,\tau) \in \bar{\Omega}. \tag{1.22}$$

The two formulations are equivalent, and we shall stick to the former, without losing generality. At any point it is easy to change to forward notation, simply changing from time t to reverse time τ as shown above.

Another common transformation of 1.17 is determined by

$$\begin{aligned} &\tau = \frac{1}{2}\sigma^2(T-t) \ \forall t \in [0,T], \text{ i.e. } \forall \tau \in [0,T]. \\ &x = \ln\left(\frac{S}{K}\right) \ \forall S \in [0, S_{\max}], \text{ i.e. } \forall x \in [-\infty, x_{\max}], \text{ where} \\ &x_{\max} = \ln\left(\frac{S_{\max}}{K}\right). \end{aligned} \tag{1.23}$$

1.17 is then transformed into the following initial value problem:

Find $W:\ (x,\tau)\in\bar{\Omega}_{\ln}\to\mathcal{R}$ where $\Omega_{\ln}=(-\infty,x_{\max})\times(0,T)$

for some $x_{\max}>>0$,

so that in a classical, weak or distributional sense

$$\frac{\partial W}{\partial\tau}=\frac{\partial^2 W}{\partial x^2}\text{ in }\Omega_{\ln}\text{ and} \tag{1.24}$$

$$W(-\infty,\tau)=\begin{cases} e^{-(\beta+\frac{r}{\frac{1}{2}\sigma^2})\tau} & \text{put or smoothened put option}\\ 0 & \text{call option}\\ 0 & \text{bet option}\end{cases},$$

$$W(x_{\max},\tau)\simeq\begin{cases} 0 & \text{put or smoothened put option}\\ e^{-\alpha x_{\max}-\beta\tau}\left(\frac{S_{\max}}{K}e^{-\frac{\gamma}{\frac{1}{2}\sigma^2}\tau}-e^{-\frac{r}{\frac{1}{2}\sigma^2}\tau}\right) & \text{call option}\\ \frac{B}{K}e^{-\alpha x_{\max}-(\beta+\frac{r}{\frac{1}{2}\sigma^2})\tau} & \text{bet option}\end{cases}$$

$$W(x,0)=\begin{cases} e^{-\alpha x}\max(1-e^x,0) & \text{put option}\\ e^{-\alpha x}\max(e^x-1,0) & \text{call option}\\ \begin{cases}\frac{B}{K}e^{-\alpha x} & \text{for } K(e^x-1)\geq 0\\ 0 & \text{for } K(e^x-1)<0\end{cases} & \text{bet option}\\ \frac{1}{K}e^{-\alpha x}(1-e^{x-x_{\max}})e^{-2Ke^x} & \text{smoothened put option}\end{cases},$$

where the connection between 1.17 and 1.24 is that

$$V(S,t)=Ke^{\alpha x+\beta\tau}W(x,\tau),\ \forall(S,t)\in\bar{\Omega}_\infty\text{ i.e. }\forall(x,\tau)\in\bar{\Omega}_{\ln}$$
$$\alpha=\frac{1}{2}\left(1-\frac{r-\gamma}{\frac{1}{2}\sigma^2}\right),\ \beta=-\frac{1}{4}\left(1-\frac{r-\gamma}{\frac{1}{2}\sigma^2}\right)^2-\frac{r}{\frac{1}{2}\sigma^2} \tag{1.25}$$

and where it is assumed that $\alpha<0$ in order to avoid problems at $x=-\infty$. The two formulations are equivalent, and while we shall stick to the former, we shall utilize known results from the second (the heat equation).

1.1.6 Numerical methods for solving European option on bounded domain

Some numerical methods for solving the option price model on the bounded domain are the following standard text book finite difference schemes:

a. *Forward* or *explicit Euler:* Forward[2] in time t, central in S [FtCS]. Error and stability condition for the heat equation: $\mathcal{O}(k+h^2)$ and $k \leq \frac{h^2}{2}$ respectively.

b. *Backward* or *implicit Euler:* Backward in time t, central in S [FtCS]. Error and stability condition for the heat equation: $\mathcal{O}(k+h^2)$ and A- and L-stable respectively.

c. *Crank Nicolson:* Central in time t, central in S [FtCS]. Error and stability condition for the heat equation: $\mathcal{O}(k^2+h^2)$ and A- but not L-stable respectively.

d. *Lax Friedrich:* Error and stability condition for the heat equation: $\mathcal{O}(h^2+k+\frac{h^2}{k})$ and $k \leq h$ respectively.

e. *Leapfrog:* Error and stability condition for the heat equation: $\mathcal{O}(k^2+h^2)$ and unconditionally unstable respectively.

f. *DuFort-Frankel:* Error and stability condition for the heat equation: $\mathcal{O}(h^2+k^2+\frac{k^2}{h^2})$ and A- but not L-stable respectively.

All these methods are consistent[3] except for the DuFort-Frankel method which is only conditionally consistent.

The numerical schemes are constructed on a net of nodal points (S_n, t_m), $n = 1, \ldots, N$, $m = 1, \ldots, M$ with step sizes h and k respectively, so that $S_n = (n-1)h$ and $t_m = (M-m)k$ and in particular $S_1 = 0$, $S_N = S_{\max}$, $t_1 = T$ and $t_M = 0$. Then the schemes consist of simple replacements [$\rightsquigarrow$] in 1.17-1.19: The Dirichlet terminal and boundary conditions are used as they are: $V(0,t_m) \rightsquigarrow \tilde{V}_{1,m} = V(0,t_m)$, $V(S_{\max},t_m) \rightsquigarrow \tilde{V}_{N,m} = V(S_{\max},t_m)$, $V(S_n,T) \rightsquigarrow \tilde{V}_{n,1} = V(S_n,T)$ for $n = 1,\ldots,N$ and $m = 1,\ldots,M$. The derivatives $DV(S_n,t_m)$ in the relevant (mainly interior) nodal points in 1.17-1.19 are replaced by

[2] Note that since we solve a backward DEP, The timesteps in Forward Euler is actually taking us backwards in time, and similarly for the other noncentral methods.

[3] The finite difference schemes converge to the DEP as the stepsizes go to 0.

finite differences $\delta\tilde{V}_{n,m}$ varying from method to method:

$$
\begin{aligned}
&\text{Find } \tilde{V}_{n,m} \text{ for } n = 1, \ldots, N \text{ and } m = 1, \ldots, M : \\
&\delta_t \tilde{V}_{n,m} + \frac{1}{2}\sigma^2 S_n^2 \delta_{SS} \tilde{V}_{n,m} + (r-\gamma) S_n \delta_S \tilde{V}_{n,m} - r\delta_0 \tilde{V}_{n,m} = 0 \\
&\text{for } n = 2, \ldots, N-1 \text{ and } m = 1, \ldots, M-1, \ (M-2 \text{ for Leapfrog and DuFort-Frankel}), \\
&\tilde{V}_{1,m} = \kappa(0, t_m), \ \text{for } m = 1, \ldots, M, \\
&\tilde{V}_{N,m} \simeq \kappa(S_{max}, t_m), \ \text{for } m = 1, \ldots, M, \\
&\tilde{V}_{n,1} = \kappa(S_n, T) \text{ for } n = 1, \ldots, N,
\end{aligned} \tag{1.26}
$$

For the various finite difference schemes we have the following replacements:

a. *Forward Euler:*

$$
\begin{aligned}
&V(S_n, t_m) \rightsquigarrow \delta_0 \tilde{V}_{n,m} = \tilde{V}_{n,m}, \\
&\tfrac{\partial V}{\partial t}(S_n, t_m) \rightsquigarrow \delta_t \tilde{V}_{n,m} = \tfrac{\tilde{V}_{n,m+1} - \tilde{V}_{n,m}}{k}, \\
&\tfrac{\partial V}{\partial S}(S_n, t_m) \rightsquigarrow \delta_S \tilde{V}_{n,m} = \tfrac{\tilde{V}_{n+1,m} - \tilde{V}_{n-1,m}}{2h}, \\
&\tfrac{\partial^2 V}{\partial S^2}(S_n, t_m) \rightsquigarrow \delta_{SS} \tilde{V}_{n,m} = \tfrac{\tilde{V}_{n+1,m} - 2\tilde{V}_{n,m} + \tilde{V}_{n-1,m}}{h^2}, \\
&\text{for } n = 2, \ldots, N-1, \ m = 1, \ldots, M-1.
\end{aligned}
$$

b. *Backward Euler:*

$$
\begin{aligned}
&V(S_n, t_{m+1}) \rightsquigarrow \delta_0 \tilde{V}_{n,m} = \tilde{V}_{n,m+1}, \\
&\tfrac{\partial V}{\partial t}(S_n, t_{m+1}) \rightsquigarrow \delta_t \tilde{V}_{n,m} = \tfrac{\tilde{V}_{n,m+1} - \tilde{V}_{n,m}}{k}, \\
&\tfrac{\partial V}{\partial S}(S_n, t_{m+1}) \rightsquigarrow \delta_S \tilde{V}_{n,m} = \tfrac{\tilde{V}_{n+1,m+1} - \tilde{V}_{n-1,m+1}}{2h}, \\
&\tfrac{\partial^2 V}{\partial S^2}(S_n, t_{m+1}) \rightsquigarrow \delta_{SS} \tilde{V}_{n,m} = \tfrac{\tilde{V}_{n+1,m+1} - 2\tilde{V}_{n,m+1} + \tilde{V}_{n-1,m+1}}{h^2}, \\
&\text{for } n = 2, \ldots, N-1, \ m = 1, \ldots, M-1.
\end{aligned}
$$

c. *Crank Nicolson:*

$$
\begin{aligned}
&V(S_n, t_{m+\frac{1}{2}}) \rightsquigarrow \delta_0 \tilde{V}_{n,m} = \tfrac{1}{2}\left(\tilde{V}_{n,m+1} + \tilde{V}_{n,m}\right), \\
&\tfrac{\partial V}{\partial t}(S_n, t_{m+\frac{1}{2}}) \rightsquigarrow \delta_t \tilde{V}_{n,m} = \tfrac{\tilde{V}_{n,m+1} - \tilde{V}_{n,m}}{k}, \\
&\tfrac{\partial V}{\partial S}(S_n, t_{m+\frac{1}{2}}) \rightsquigarrow \delta_S \tilde{V}_{n,m} = \tfrac{1}{2}\left(\tfrac{\tilde{V}_{n+1,m+1} - \tilde{V}_{n-1,m+1}}{2h} + \tfrac{\tilde{V}_{n+1,m} - \tilde{V}_{n-1,m}}{2h}\right), \\
&\tfrac{\partial^2 V}{\partial S^2}(S_n, t_{m+\frac{1}{2}}) \rightsquigarrow \delta_{SS} \tilde{V}_{n,m} = \tfrac{1}{2}\left(\tfrac{\tilde{V}_{n+1,m+1} - 2\tilde{V}_{n,m+1} + \tilde{V}_{n-1,m+1}}{h^2} + \tfrac{\tilde{V}_{n+1,m} - 2\tilde{V}_{n,m} + \tilde{V}_{n-1,m}}{h^2}\right), \\
&\text{for } n = 2, \ldots, N-1, \ m = 1, \ldots, M-1.
\end{aligned}
$$

d. *Lax Friedrich:*

$$
\begin{aligned}
&V(S_n, t_m) \rightsquigarrow \delta_0 \tilde{V}_{n,m} = \tilde{V}_{n,m}, \\
&\tfrac{\partial V}{\partial t}(S_n, t_m) \rightsquigarrow \delta_t \tilde{V}_{n,m} = \tfrac{\tilde{V}_{n,m+1} - \tilde{V}_{n,m}}{k} + \tfrac{h^2}{2k}\tfrac{\tilde{V}_{n+1,m} - 2\tilde{V}_{n,m} + \tilde{V}_{n-1,m}}{h^2},
\end{aligned}
$$

$\frac{\partial V}{\partial S}(S_n, t_m) \rightsquigarrow \delta_S \tilde{V}_{n,m} = \frac{\tilde{V}_{n+1,m} - \tilde{V}_{n-1,m}}{2h}$,
$\frac{\partial^2 V}{\partial S^2}(S_n, t_m) \rightsquigarrow \delta_{SS} \tilde{V}_{n,m} = \frac{\tilde{V}_{n+1,m} - 2\tilde{V}_{n,m} + \tilde{V}_{n-1,m}}{h^2}$,
for $n = 2, \ldots, N-1$, $m = 1, \ldots, M-1$.

e. *Leapfrog:*

$V(S_n, t_{m+1}) \rightsquigarrow \delta_0 \tilde{V}_{n,m} = \tilde{V}_{n,m+1}$,
$\frac{\partial V}{\partial t}(S_n, t_{m+1}) \rightsquigarrow \delta_t \tilde{V}_{n,m} = \frac{\tilde{V}_{n,m+2} - \tilde{V}_{n,m}}{2k}$,
$\frac{\partial V}{\partial S}(S_n, t_{m+1}) \rightsquigarrow \delta_S \tilde{V}_{n,m} = \frac{\tilde{V}_{n+1,m+1} - \tilde{V}_{n-1,m+1}}{2h}$,
$\frac{\partial^2 V}{\partial S^2}(S_n, t_{m+1}) \rightsquigarrow \delta_{SS} \tilde{V}_{n,m} = \frac{\tilde{V}_{n+1,m+1} - 2\tilde{V}_{n,m+1} + \tilde{V}_{n-1,m+1}}{h^2}$,
for $n = 2, \ldots, N-1$, $m = 1, \ldots, M-2$.

f. *DuFort-Frankel:*

$V(S_n, t_{m+1}) \rightsquigarrow \delta_0 \tilde{V}_{n,m} = \tilde{V}_{n,m+1}$,
$\frac{\partial V}{\partial t}(S_n, t_{m+1}) \rightsquigarrow \delta_t \tilde{V}_{n,m} = \frac{\tilde{V}_{n,m+2} - \tilde{V}_{n,m}}{2k} + \frac{k^2}{h^2} \frac{\tilde{V}_{n,m+2} - 2\tilde{V}_{n,m+1} + \tilde{V}_{n,m}}{k^2}$,
$\frac{\partial V}{\partial S}(S_n, t_{m+1}) \rightsquigarrow \delta_S \tilde{V}_{n,m} = \frac{\tilde{V}_{n+1,m+1} - \tilde{V}_{n-1,m+1}}{2h}$,
$\frac{\partial^2 V}{\partial S^2}(S_n, t_{m+1}) \rightsquigarrow \delta_{SS} \tilde{V}_{n,m} = \frac{\tilde{V}_{n+1,m+1} - 2\tilde{V}_{n,m+1} + \tilde{V}_{n-1,m+1}}{h^2}$,
for $n = 2, \ldots, N-1$, $m = 1, \ldots, M-2$.

1.2 Nonlinear Black-Scholes Models

The standard Black-Scholes equation is supposed in a complete market under some simplified assumptions such as liquid market with no transaction cost. Taking into account one or some of theses parameters to have more reliable option price causes a nonlinear Black-Scholes equation with a nonlinear volatility function. In Chapters 4-5 nonlinear Black-Scholes equations have been considered with nonlinear volatility that depends on time t, underlying asset price S and the second derivative of option price $V(S,t)$ with respect to S. Also several schemes have been applied and compared to solve the nonlinear Black-Scholes models in these two chapters. Here we review a number of nonlinear volatility models. Note that in these models σ_0 (the volatility of the underlying asset) is assumed constant and if we take $\sigma(t, S, V_{SS}) = \sigma_0$ we will have the classical linear Black-Scholes model.

1.2.1 Leland Model

The models that we have grouped together here are all addressing the issue of nonzero transaction cost assumed to be a fixed fraction of the volume of transactions. The original paper [30] takes

$$\sigma_L^2(t,S,V_{SS}) = \sigma_0^2\left[1 + Le \times \text{sign}\left(\frac{\partial^2 V}{\partial S^2}\right)\right] \tag{1.27}$$

for a call option, where Le is the Leland number given by

$$Le = \sqrt{\frac{2}{\pi}}\frac{\kappa}{\sigma_0\sqrt{\delta t}}.$$

κ denotes the round trip transaction cost per unit dollar of transaction and δt is the transaction frequency (interval between successive revisions of the portfolio). There was an error in the Leland argument, but it was apparently not published until 2003 in [47]. Some years before that Boyle and Vorst [6] modified the Leland number, replacing the factor $\sqrt{2/\pi} \simeq 0.8$ by 2, and showed using the binomial model that if the transaction frequency δt - taken equal to the time step in the binomial model - and the transaction cost κ tend to zero (while keeping the ratio $\frac{\kappa}{\sqrt{\delta t}}$ of the order one) then the discrete option price converges to the Black-Scholes price for a call option with a modified volatility of the form

$$\sigma^2(t,S,V_{SS}) = \sigma_0^2\left[1 + \frac{2\kappa}{\sigma_0\sqrt{\delta t}} \times \text{sign}\left(\frac{\partial^2 V}{\partial S^2}\right)\right].$$

For both of the above volatility models, the parameters κ and δt should be given so that $\sigma^2(t,S,V_{SS}) > 0$. Two years later Hoggard et al [21] derived the following nonlinear volatility model for a call option:

$$\sigma^2(t,S,V_{SS}) = \sigma_0^2\left[1 - \sqrt{\frac{2}{\pi}}\frac{2\kappa}{\sigma_0\sqrt{\delta t}} \times \text{sign}(\frac{\partial^2 V}{\partial S^2})\right]$$

including the negative of the product of the Leland factor $\sqrt{\frac{2}{\pi}}$ and the Boyle and Vorst factor 2. For a short position in a call option both Boyle and Vorst and Hoggard et al changes the sign on the modified Leland number, thus still having opposite signs. The Hoggard et al volatility model is known as the HWW transaction cost model.

1.2.2 Risk Adjusted Pricing Methodology(RAPM)

The RAPM model was introduced by Kratka in 1998 [27] as an attempt to include effects of transaction cost as well as risk from volatile portfolios into the Black-Scholes model. Jandačka and Ševčovič [25] later criticized the Kratka method for not being mathematically well-posed and scale invariant and presented the following alternative version:

$$\sigma_{JS}^2(t,S,V_{SS}) = \sigma_0^2\left[1+\mu(S\frac{\partial^2 V}{\partial S^2})^{\frac{1}{3}}\right] \tag{1.28}$$

where $\mu = 3\left(\frac{\kappa^2 R}{2\pi}\right)^{\frac{1}{3}}$. $\kappa \geq 0$ (denoted C in [25]) is the transaction cost from the Leland model and the *risk premium coefficient* $R \geq 0$ represents the marginal value of the investor's exposure to risk. More precisely, the change in the portfolio value arising from risk from the volatility of the portfolio per unit asset price and per unit time ($\frac{\Delta\Pi}{S\Delta t}$) is modelled by $R\frac{\mathrm{Var}(\Delta\Pi/S)}{\Delta t}$, Var being the variance. Jandačka and Ševčovič model [25] solves the nonlinear Black-Scholes problem by first deriving a quasilinear parabolic PDE for $H = S\frac{\partial^2 V}{\partial S^2}$ and solving this with a semi-implicit in time finite difference scheme and then plugging the numerical values of H into the exact solution for the standard Black-Scholes problem with constant volatility and integrating numerically using a trapezoidal quadrature. Kútik and Mikula [28] proposed a Crank-Nicolson-type scheme for the solution of the quasilinear H-equation from Jandačka and Ševčovič model [25] and compared it to the semi-implicit scheme in that paper. They found 2nd order convergence of the Crank-Nicolson scheme against linear convergence of the semi-implicit scheme.

1.2.3 Barles and Soner model

As for the RAPM, Barles and Soner [4] considers both transaction cost and risk from volatile portfolios. They start commenting on the Leland number that the size of the constant $\sqrt{\frac{2}{\pi}}$ is really irrelevant for the argument and may be replaced by any constant c without changing the argument thus basically validating all the different Leland constants in use. Then a different approach based on utility maximization is introduced

resulting in the following adjustment of the volatility:

$$\sigma_{BS}^2(t,S,V_{SS}) = \sigma_0^2\left[1+\Psi\left(e^{r(T-t)}\kappa^2 RS^2\frac{\partial^2 V}{\partial S^2}\right)\right] \tag{1.29}$$

where κ is the Leland transaction cost (denoted μ in [4]) and R is a *risk aversion factor* (denoted γ in [4]) and probably similar to the risk premium coefficient in Jandačka and Ševčovič model [25]. Finally $\Psi(x)$ is the solution of the nonlinear ODE

$$\Psi'(x) = \frac{\Psi(x)+1}{2\sqrt{x\Psi(x)}-x},\ x \neq 0 \tag{1.30}$$

with the initial condition $\Psi(0) = 0$. In appendix A of [4] the existence of a unique continuous viscosity solution to this problem has been shown. It is also shown that $\sigma_{BS}^2 \geq 0$ i.e. that the adjustment factor to σ_0^2 is nonnegative for any argument of Ψ. For the numerical experiments an unspecified explicit time stepping finite difference scheme is used with small time steps near maturity ($t = T$) and larger time steps away from maturity. Lesmana and Wang [31] present numerical results for the Barles and Soner model using instead an implicit first order time stepping and upwind asset price stepping finite difference method.

1.2.4 Feedback and illiquid market

Frey et al [16, 14, 15] do not consider transaction cost but look at the effects of assuming that the asset price depends on the hedging strategy (feedback) applied in an illiquid market with dynamic hedging. They argue for the nonlinear volatility model

$$\sigma_{FP}^2(t,S,V_{SS}) = \frac{\sigma_0^2}{\left(1-\rho\lambda(S)S\frac{\partial^2 V}{\partial S^2}\right)^2} \tag{1.31}$$

where $\rho > 0$ is a constant and $\lambda(S) > 1$ is a strictly convex function. For numerical computations they put in cut-off's to prevent $\sigma_{FP} \to 0$ and $\sigma_{FP} \to \infty$:

$$\tilde{\sigma}_{FP}^2(t,S,V_{SS}) = \sigma_0^2 \max\{\alpha_0, \frac{1}{\left(1-\min\{\alpha_1, \rho\lambda(S)S\frac{\partial^2 V}{\partial S^2}\}\right)^2}\} \tag{1.32}$$

where $\alpha_0 = 0.02$ and $\alpha_1 = 0.85$. Liu and Yong [32] continue the work on the Frey model but addresses also transaction cost. Frey's ρ factor is absorbed into the λ function and an expression for this function is given resulting in the model

$$\sigma_{LY}^2(t, S, V_{SS}) = \frac{\sigma_0^2}{\left(1 - \lambda(S,t) S \frac{\partial^2 V}{\partial S^2}\right)^2} \tag{1.33}$$

where $\lambda(S,t)$ is given by

$$\lambda(S,t) = \begin{cases} \frac{\gamma}{S}(1 - e^{-\beta(T-t)}) & \text{for } 0 \leq S \leq S_{max} \\ 0 & \text{otherwise} \end{cases}$$

where $\gamma > 0$ measures the price impact per traded share and is given the value 0.04 in the article. β is given the value 100 in the article. Liu and Yong [32] have also established sufficient conditions for existence and uniqueness of the solution of this generalized Black-Scholes equation.

1.2.5 Parameterized Illiquidity Model

Bakstein and Howison [3] develop a parameterized model for illiquidity effects arising from the discrete trading in an asset with transaction costs. Liquidity is defined via a combination of a trader's individual transaction cost and a price slippage impact, which is felt by all market participants:

$$\begin{aligned} \sigma_{BH}^2(t, S, V_{SS}) = \sigma_0^2 \Bigg[& 1 + 2\lambda S \frac{\partial^2 V}{\partial S^2} + \left(\lambda \mu S \frac{\partial^2 V}{\partial S^2}\right)^2 \\ & + \left(\frac{\kappa \mu}{\sigma_0 \sqrt{\delta t}}\right)^2 + 2\sqrt{\frac{2}{\pi}} \frac{\kappa}{\sigma_0 \sqrt{\delta t}} \operatorname{sign}\left(\frac{\partial^2 V}{\partial S^2}\right) + 2\sqrt{\frac{2}{\pi}} \lambda \mu^2 \frac{\kappa}{\sigma_0 \sqrt{\delta t}} S \left|\frac{\partial^2 V}{\partial S^2}\right| \Bigg] \end{aligned} \tag{1.34}$$

where $\lambda > 0$ models the market depth, which represents the elasticity of the asset price to the quantity traded and $\mu > 0$ models the slippage measure that transforms the average transaction price into the next published price. Finally κ and δt are the Leland transaction cost (denoted γ in the article) and transaction frequency. Bakstein and Howison [3] present a model according to which the parameters are observable from order-book data, rather than having to be estimated from market data.

In Chapter 4 we consider the feedback and illiquid market (1.2.4) and solve this model with Forward Euler, Backward Euler and Crank Nicolson schemes and also investigate how choosing the right boundary (S_{max}) can effect on option price and numerical error [24]. We investigate the Barles and Soner model (1.2.3) in Chapter 5. We consider some different finite difference schemes Forward Euler, Positive preserving, Crank Nicolson, Implicit Upwind and nonstandard finite difference mmethod for this nonlinear model and present some comparisons of the schemes and some numerical experiments.

Chapter 2

K_α-Shifting, Rannacher Time Stepping and Mesh Grading in Crank Nicolson FDM for Black-Scholes Option Pricing

Sima Mashayekhi and Jens Hugger

Abstract. Non-smooth conditions in partial differential equations cause discretization error in numerical schemes and lead to decay in the convergence rate. Here the K_α-shifting method is introduced for easy handling of uniform and nonuniform meshes and for one or more singularities in the terminal condition. Combining this method with Rannacher time stepping and mesh grading for the Crank-Nicolson Finite Difference Method on some examples including call options, bet options and a butterfly spread is shown to lead to higher accuracy and better convergence rate for the numerical solution.

Keywords: Black-Scholes model; Rannacher time stepping; finite difference schemes; Crank-Nicolson scheme; European options

Subjectclass: 65M06; 65M12; 65N06; 65N12

2.1 Introduction

We consider the well established Black-Scholes model for the pricing of a few standard European vanilla options on a bounded domain:

$$\frac{\partial V}{\partial t} + \frac{1}{2}\sigma^2 S^2 \frac{\partial^2 V}{\partial S^2} + (r-\gamma)S\frac{\partial V}{\partial S} - rV = 0 \qquad \forall (S,t) \in (0, S_{\max}) \times (0,T) \tag{2.1}$$

with the terminal and boundary conditions

$$V(S,T) = \kappa(S,T), \quad V(0,t) = \kappa(0,t), \quad V(S_{\max},t) \simeq \kappa(S_{\max},t) \tag{2.2}$$

where we are using the utility function

$$\kappa(S,t) = \begin{cases} \max\{Se^{-\gamma(T-t)} - Ke^{-r(T-t)}, 0\} & \textit{call option} \\ \max\{Ke^{-r(T-t)} - Se^{-\gamma(T-t)}, 0\} & \textit{put option} \\ Be^{-r(T-t)}\mathcal{H}(S-K) & \textit{bet option} \\ \max\{(K+a)e^{-r(T-t)} - Se^{-\gamma(T-t)}, 0\}\mathcal{H}(S-K) & \\ +\max\{Se^{-\gamma(T-t)} - (K-a)e^{-r(T-t)}, 0\}\mathcal{H}(K-S) & \textit{butterfly spread} \end{cases} \tag{2.3}$$

$V(S,t)$ is the (fair) option price for a value S of the risky asset at time t. r, σ and γ are the *market interest rate* (on a risk free asset), the *volatility* (of the underlying risky asset) and the *dividend yield* (on the risky asset) respectively. $S_{\max} >> K$ is the upper bound for the computational domain in the S variable and the terminal time T is the upper bound in the t variable. K is the *Strike Price* for the call and put, B the value of the *Bet* and a is the distance from the strike prices $K \pm a$ of the long options to the strike price K of the two short options in the butterfly spread. $\mathcal{H}$ is the Heaviside function.

In this article we provide numerical solutions using the standard Crank-Nicolson (CN) Finite Difference Method (FDM) with a few simple adaptations. Further we compute the Greeks Delta ($\Delta(S,t) = \frac{\partial V}{\partial S}(S,t)$) and Gamma ($\Gamma(S,t) = \frac{\partial^2 V}{\partial S^2}(S,t)$) using second order finite differences, centered in the interior points and one sided at the boundaries. These methods are easy to program and account for the majority of the PDE-methods in use today. The main underlying concept is that we would like to consider simple (if possible a priori) modifications to the in practice most commonly used methods in order to show how to improve results of these methods by simple adjustments without abandoning the methods.

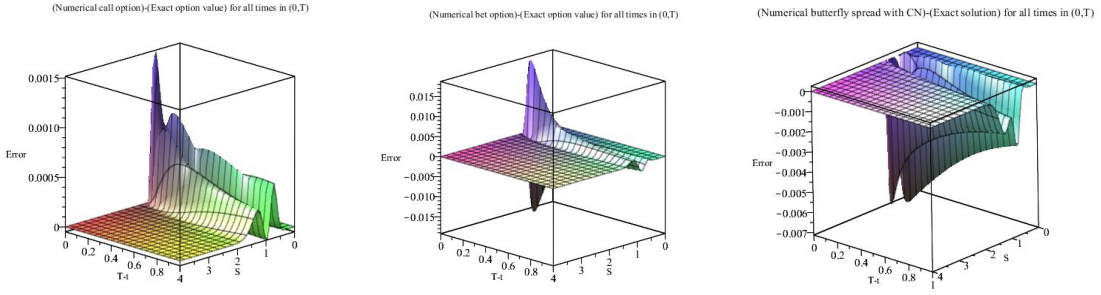

(a) $e(S,t)$ for call. (b) $e(S,t)$ for bet. (c) $e(S,t)$ for butterfly spread.

FIGURE 2.1: Plot of the error $e(S,t)$ as function of $S \in (0, S_{\max})$ and $t \in (0,T)$ for (a) call option, (b) bet option and (c) butterfly spread with $S_{\max} \simeq 4K$ in the *standard case* ($T = 1$, $K = 1$, $a = 0.2$, $B = 0.3$, $r = 0.04$, $\gamma = 0$, $\sigma = 0.2$ and $S_{\max} = 4K$) with the Crank-Nicolson (CN) method for a mesh with $h = 0.08$ and $k = 0.01$.

FDM's only provide results in grid points of the finite difference subdivisions. Results in other points are obtained by simple interpolation, typically linear but also higher order interpolations may be used if higher degree of precision is required. This is an issue if a value (or Greek) at a discontinuity is requested. If the discontinuity is a nodal point, derivatives must be defined with care and if not the interpolation in the point must be defined with care. We shall not require singularities to be nodal points since this as we shall show may result in increased error. Instead we refer to interpolation for such values. Using the Finite Element Method (including in the term all projection based methods finding solutions in a finite dimensional subspace of a sufficiently smooth function space) interpolation issues do not exist, but we shall not consider such methods here, as they are still not very common in practice, in particular not methods with enough smoothness to recover for example the Gamma ($\frac{\partial^2 V}{\partial S^2}$) since the Black-Scholes equation naturally leads to weak solutions in H^1 only offering a continuous solution V and one weak derivative ($\frac{\partial V}{\partial S}$).

The discontinuities in the terminal condition or its first derivative seen in (2.2) lead to decay in the convergence rate of most finite difference numerical schemes for "computable" stepsizes h in the S-variable and k in the t-variable, see for example [46, 44]. This happens also for the Crank-Nicolson (CN) method which is the one that we shall focus on in this article. Typical plots of the error e (CN solution minus exact solution in the nodal points) for call, bet and butterfly spread are shown in Figure 2.1, where the dominating error concentrated around the singularity $S = K$ or singularities

$S = K, K \pm a$ respectively is notable. The goal of this work is to investigate how the "size of the bump(s)" can be reduced without abandoning the CN method.

Rannacher [39] introduced a start-up procedure for Crank-Nicolson in which one or more initial time steps are replaced by small implicit Euler time steps in order to achieve the expected second order convergence in the follow up Crank-Nicolson method since the order of the standard Crank-Nicolson scheme may be reduced all the way down to zero in the case of rough terminal data. This approach, commonly known as Rannacher time stepping, is widely adopted in financial engineering practice and hence will be considered among the simple modifications allowed in this article.

Another approach, see [44, 38], addresses the decay in convergence order by considering the position of the strike price K with respect to the grid points used in the method. It is shown that having K in the middle between two nodal points in a finite difference scheme decreases the oscillations around the strike price when compared to having K located in a nodal point and consequently increases the accuracy of the finite difference method. Pooley et al [38] consider another alternative for reducing error from nonsmooth terminal conditions, namely smoothening of the terminal data either by a simple averaging over half of the cells to the left and right of the nodal point or by a projection (an L^2 projection is suggested) onto a set of continuous piecewise linear Finite Element basis functions. While the repositioning of a singular point can be performed a priori and hence can be implemented in any existing code at very low cost, the smoothening methods require reconstructing a code and thus falls outside the goal of this article to consider only simple adjustments easily applicable to existing code. Instead they are highly relevant when we in the future extend our work to finite element methods (see section 2.5).

It is also well known (see for example [40, 37]), that an alternative to Rannacher timestepping is nonuniform (exponentially increasing) time steps (or equivalently a square root of time variable change). Such methods show good promises even for singularities as strong as the Dirac delta function and hence can be used also for at least some Greeks. The method requires either a transformation of the problem or schemes accepting nonuniform time steps and hence falls outside the scope of this article and is relegated to future work (see section 2.5).

In this article we introduce a shifting grid points method (K_α-shifting) which puts the strike price at any preselected position between nodal points. In section 2.2 we explain

in more details the K_α-shifting method for uniform and nonuniform meshes with one or more singularities in the terminal value and show its effect for some numerical examples. Moreover we consider stability of the optimal choice of K_α with respect to different parameters in the Black-Scholes equation.

In section 2.3 we compare Crank-Nicolson with and without the K_α-shifting method and with and without Rannacher time stepping. We give results for uniform as well as nonuniform graded meshes.

In section 2.4 we compare the orders of convergence of these four methods for option prices and the Greeks Δ and Γ.

Finally some concluding remarks and possible future work is discussed in section 2.5.

2.2 K_α-shifting

The K_α-shifting method addresses the significance of the location of singular points in the terminal condition in relation to the end points of the S-elements. We consider "reasonable" parameter values $T = 1$, $K = 1$, $a = 0.2$, $B = 0.3$, $r = 0.04$, $\gamma = 0$, $\sigma = 0.2$ and $S_{\max} = 4K$ (denoted the *standard case*) and solve the call, bet and butterfly spread. (The put option is omitted since the put-call-parity makes it somewhat superfluous). For the put, call and bet options the single singularity occurs in $S = K$ whereas for the butterfly spread there are 3 singularities in $K - a$, K and $K + a$.

Consider first the case of uniform meshes with step sizes h in the S-variable and k in the t-variable and the case of one singularity in $S = K$. First the mesh interval containing K (controlled by $\tilde{\imath}_K$) and the relative position of K in this interval (controlled by α) are found from

$$\text{Find } \tilde{\imath}_K, \alpha: \ K - S_{\min} = (\tilde{\imath}_K + \alpha)\tilde{h} \text{ for some } \tilde{\imath}_K \in \mathcal{N} \text{ and } 0 \le \alpha < 1, \tag{2.4}$$

where $S_{\min}$ denotes the left endpoint of the computational S-domain which is 0 in our case, but may be $\neq 0$ in the generalizations of the K_α-shifting method below. Then $\tilde{h}$ is adjusted to h using

$$\text{Find } i_K, h: \ K - S_{\min} = (i_K + K_\alpha)h \text{ for some } i_K \in \mathcal{N}: \ \tilde{\imath}_K \le i_K \le \tilde{\imath}_K + 1. \tag{2.5}$$

i_K is given by

$$\begin{aligned} i_K &= \left\lceil \frac{K - S_{\min}}{\tilde{h}} - K_\alpha \right\rceil = \left\lceil \frac{K - S_{\min}}{\tilde{h}} - \alpha + (\alpha - K_\alpha) \right\rceil = \lceil \tilde{\imath}_K + (\alpha - K_\alpha) \rceil \\ &= \tilde{\imath}_K + \lceil \alpha - K_\alpha \rceil \in [\tilde{\imath}_K, \tilde{\imath}_K + 1], \end{aligned} \tag{2.6}$$

and hence

$$K - S_{\min} = \left(\left\lceil \frac{K - S_{\min}}{\tilde{h}} - K_\alpha \right\rceil + K_\alpha \right) h \Leftrightarrow h = \frac{K - S_{\min}}{\left\lceil \frac{K - S_{\min}}{\tilde{h}} - K_\alpha \right\rceil + K_\alpha}. \tag{2.7}$$

Note that the new S step size h is given by a simple updating formula from the known input parameters $\tilde{h}$ and K_α without actually ever computing $\tilde{\imath}_K$ and α. Also h is close to $\tilde{h}$ since

$$\begin{aligned} & \tilde{\imath}_K h \le i_K h \le K - S_{\min} \le (\tilde{\imath}_K + 1)\tilde{h} \\ & \text{and } (\tilde{\imath}_K + 2)h \ge (i_K + 1)h \ge K - S_{\min} \ge \tilde{\imath}_K \tilde{h} \\ \Downarrow & \\ & \frac{\tilde{\imath}_K}{\tilde{\imath}_K + 2}\tilde{h} \le h \le \frac{\tilde{\imath}_K + 1}{\tilde{\imath}_K}\tilde{h}. \end{aligned} \tag{2.8}$$

For very coarse meshes the adjustment of the S step size may be substantial, like $\frac{h}{\tilde{h}} \in [0.83, 1.1]$ for K situated in the 10'th interval ($\tilde{\imath}_K = 10$) but for more realistic meshes, the adjustment is minimal, like $\frac{h}{\tilde{h}} \in [0.98, 1.01]$ for K situated in the 100'th interval ($\tilde{\imath}_K = 100$).

Two further adjustment must be made, that are not part of the K_α-shifting method, but are necessary in order to adjust $S = \tilde{S}_{\max}$ (the user requested maximal S value in the computational domain) and $t = 0$ to be nodal points. First $\tilde{S}_{\max}$ is adjusted (increased) to $S_{\max}$ lying in the nodal point (in the S-variable) closest to but at least as big as $\tilde{S}_{\max}$ using

$$S_{\max} - S_{\min} = \left\lceil \frac{\tilde{S}_{\max} - S_{\min}}{h} \right\rceil h \ge \tilde{S}_{\max} - S_{\min}. \tag{2.9}$$

Finally $\tilde{k}$ is adjusted (reduced) to k so that $t = 0$ is a nodal point (in the t-variable) using

$$k = \frac{T}{\left\lceil \frac{T}{\tilde{k}} \right\rceil} \le \tilde{k} \text{ and } T - \left\lceil \frac{T}{\tilde{k}} \right\rceil k = 0 \text{ where } \left\lceil \frac{T}{\tilde{k}} \right\rceil \in \mathcal{N}. \tag{2.10}$$

These adjustments ($\tilde{h} \to h$, $\tilde{S}_{\max} \to S_{\max}$ and $\tilde{k} \to k$) are simple update formulas and hence cheap ($\mathcal{O}(1)$) that do not deteriorate the performance of the solution process and can be performed a priory and hence used with any existing code. They may result in slightly fluctuating errors when the requested step sizes are large and hence also the adjustments are potentially large. For "reasonable" step sizes however the results of the adjustments are negligible. Instead with the K_α-shifting method there are no fluctuation in the error caused by K "moving around" inside the i_K'th interval when adjusting the mesh interval size. This turns out to be a significant advantage in practical use, since the error from K moving around is significant (up to a factor of more than 10 for the maximal error).

The K_α-shifting method for uniform meshes easily generalizes to more than one singularity. Just divide the S domain into patches each containing one of the singularities. For each patch — starting from the left with the patch containing $S = 0$ — compute the adjusted step size and adjust the right endpoint of the patch to be a nodal point with the adjusted step size. In (2.4)–(2.9) just use the left patch endpoint as $S_{\min}$, the right endpoint of the patch as $\tilde{S}_{\max}$ and the adjusted right endpoint of the patch as $S_{\max}$. For small requested stepsize $\tilde{h}$ all the actual stepsizes will be very close in size, so that even uniform finite difference approximations will give good results in particular because patch boundaries are situated in areas where the computed solution is almost linear, but otherwise nonuniform finite differences across the patch boundaries may be used. The only issue is that for more than one singularity the method cannot be performed entirely a priory since it requires the ability to work with slightly different stepsizes in different parts of the domain and preferably also with nonuniform finite difference approximations across the patch boundaries, which a standard uniform mesh code will not be able to handle.

For nonuniform meshes constructed by a grading function the idea would be the following for a single singularity in $S = K$: If K is contained in the element number $[S_{i_K}, S_{i_K+1}[$ then simply relocate this element without resizing it to say $[S_0, S_1[$ so that K moves into K_α-position in the element. This relocation is then followed by a uniform scaling of the rest of the elements. The global scaling factors s_{K-} and s_{K+} for the elements before and after K respectively are given by

$$s_{K-} = \frac{S_0 - S_{\min}}{S_{i_K} - S_{\min}}, \quad s_{K+} = \frac{S_{\max} - S_1}{S_{\max} - S_{i_K+1}}, \tag{2.11}$$

so that the size of all elements before K are multiplied by s_{K-} and the size of all elements after K are multiplied by s_{K+}. A simpler alternative would be simply to use the K_α-shifting method for uniform meshes on the uniform mesh being graded. For small elements the grading function will be sufficiently close to linear to put the singularity close enough to the K_α-position.

For adaptively constructed nonuniform meshes with one singularity in $S = K$ the idea would be very similar to the first one for the grading function approach: If the element $[S_{i_K}, S_{i_K+1}[$ containing K in K_α-position is up for subdivision — let us for simplicity say uniform splitting into two equal elements — then the new elements are constructed, and the new element $[S_{i_K}, S_{i_K+1}[$ containing K (either $[S_{i_K}, \frac{S_{i_K}+S_{i_K+1}}{2}[$ or $[\frac{S_{i_K}+S_{i_K+1}}{2}, S_{i_K+1}[$) is relocated (but not resized), say to $[S_0, S_1[$ so that K is again in K_α-position in this element. This relocation is followed by global scalings of the elements to the left and right as for the grading function approach, using the scaling factors s_{K-} and s_{K+} defined in (2.11).

If finally $N > 1$ singularities are present with nonuniform meshes then N patches each containing exactly one singularity are constructed and each patch is scaled with individual scaling factors moving from the left to the right. If the nonuniform meshes are created with a grading function, the simple approach also generalizes. Just use the K_α-shifting method for uniform meshes with several singularities explained above on the uniform mesh being graded.

Turning to the computational examples, instead of using $\tilde{h}$, $\tilde{k}$ and $\tilde{S}_{max}$ we shall use the notation $h \simeq \ldots$, $k \simeq \ldots$ and $S_{\max} \simeq \ldots$ to account for the adjustments. For given values of all parameters we compute maximal absolute solution errors at time $t = 0$ over all S nodal points $S_1, \ldots, S_M$ as

$$E_V^0 = \max_{i=1\ldots,M} |V_{FDM}(S_i, 0) - V^{BS}(S_i, 0)| \tag{2.12}$$

where $V_{FDM}(S_i, 0)$ is the computed finite difference solution in the nodal point $S = S_i$ and $t = 0$ and $V^{BS}(S_i, 0)$ is the exact (Black-Scholes) solution in the same point. Similarly we define the maximal absolute errors E_Δ^0 and E_Γ^0 for the Greeks Δ and Γ.

In Figure 2.2 we show the maximal absolute solution errors $E_V^0(K_\alpha)$ at time $t = 0$ for two different sets of step sizes $(h, k) \simeq (0.08, 0.01)$ and $(h, k) \simeq (0.03, 0.001)$ and as a

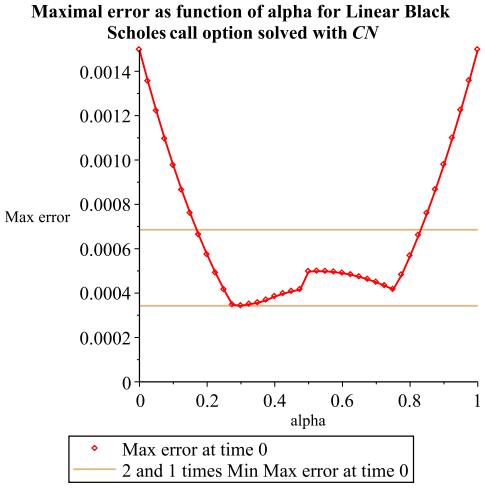

(a) $E_V^0(K_\alpha)$ for call with the coarse mesh.

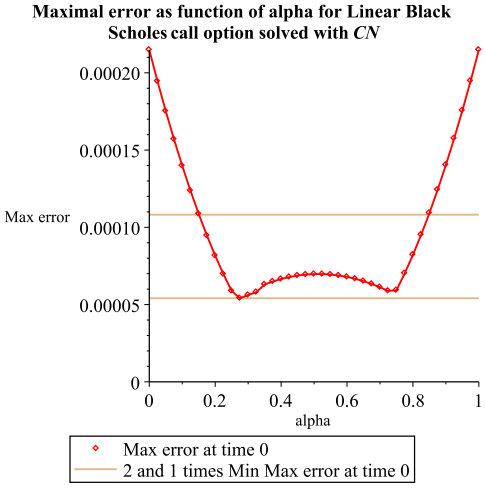

(b) $E_V^0(K_\alpha)$ for call with the fine mesh.

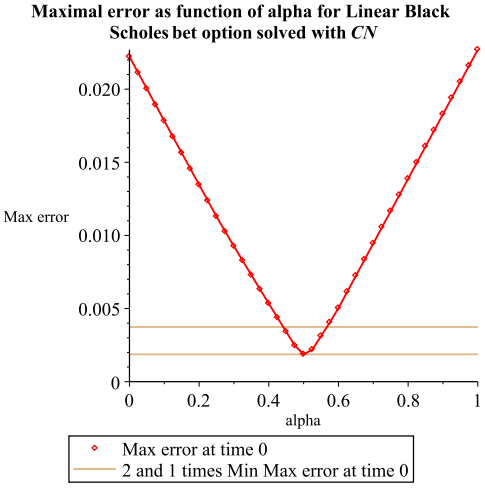

(c) $E_V^0(K_\alpha)$ for bet with the coarse mesh.

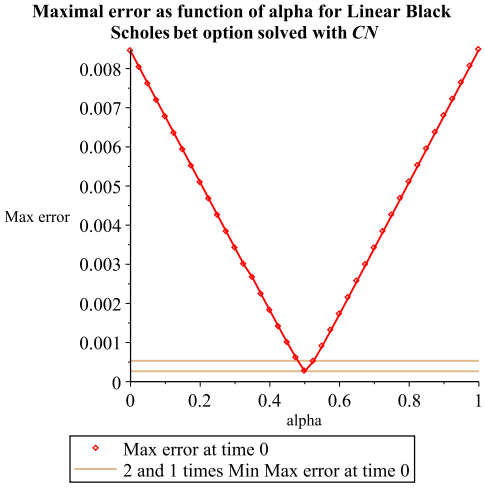

(d) $E_V^0(K_\alpha)$ for bet with the fine mesh.

FIGURE 2.2: Maximal error $E_V^0(K_\alpha)$ at time $t = 0$ as function of $K_\alpha \in [0, 1]$ for call and bet options in the standard case solved with CN using the coarse mesh $(h, k) \simeq (0.08, 0.01)$ and the fine mesh $(h, k) \simeq (0.03, 0.001)$.

function of 41 different K_α-values uniformly distributed from 0 to 1 for the call and the bet option solution values. When $K_\alpha = 0$ or 1 (or whenever $S = K$ is a nodal point) it becomes a numerical issue how to define $V(K, T)$ for the bet option. After some experimentation we have decided to use the convention $V(K, T) = 0$ for $K_\alpha < 0.5$ and $V(K, T) = B$ for $K_\alpha \geq 0.5$ giving the smoothest graphs. We are interested in $\hat{K}_\alpha$, the optimal K_α, minimizing E_V^0 over all values of $K_\alpha \in [0, 1[$. $\hat{K}_\alpha = 0.27$ turns out to be the optimal choice for the call option at time $t = 0$ (see Figures 2.2(a) and 2.2(b)) varying from 0.280 for the coarse mesh to 0.264 for the fine mesh when computed with 1001 uniformly distributed K_α-values from 0 to 1. Also we observe that the symmetric

position $K_\alpha = 1 - 0.27$ is quite good, and actually the entire interval $(0.2, 0.8)$ gives good results (at most the double maximal absolute solution error compared to the optimal location). The general conclusion is that for the call option (and similarly for the put) the strike price K should under no circumstances be located close to a nodal point.

Figures 2.2(c) and 2.2(d) show that $\hat{K}_\alpha = 0.50$ is the optimal choice for the bet option at time $t = 0$, varying from 0.508 for the coarse mesh to 0.504 for the fine mesh when computed with 1001 K_α-values. Unsurprisingly $\hat{K}_\alpha = 0.50$ is optimal also when solving with graded meshes. Hence the best location for the strike price is in the middle between two consecutive nodal points. The interval where the maximal error is at most the double of the optimal error is $(0.4, 0.6)$ and hence significantly smaller for the bet option than for the call. Also the price for locating the strike price closer to a nodal point is significantly bigger for the bet than for the call option. The general conclusion is that for the bet option the strike price K should under no circumstances be located close to a nodal point.

Figure 2.3 shows the maximal absolute errors at time $t = 0$ for the Greeks Δ and Γ for the call and bet options with the fine mesh $(h, k) \simeq (0.03, 0.001)$ and for 41 different K_α-values uniformly distributed from 0 to 1. Computing with 1001 uniformly distributed K_α-values from 0 to 1 we get the following optimal $\hat{K}_\alpha$-values: For the call option $\hat{K}_\alpha = 0.00$ and $\hat{K}_\alpha = 0.33$ for the Delta and Gamma respectively. Note however, that the value of K_α is of little importance for the Greeks of the call option, all minimal errors lying within a factor significantly below 2 from the smallest value. For the bet option $\hat{K}_\alpha = 0.51$ and $\hat{K}_\alpha = 0.53$ for the Delta and Gamma respectively. For the bet option the value of K_α is important also for the Greeks, the factor two interval being as small as $[0.48, 0.58]$. Concluding, for the bet option $K_\alpha = 0.5$ is the sensible choice for both the value, the Delta and the Gamma, whereas for the call K_α should be picked in the interval $[0.2, 0.8]$ and might be picked at $K_\alpha = 0.5$ without an increase of more than a factor 2 in the maximal error for the value, the Delta and the Gamma. The small irregularities visible in Figures 2.2–2.3 (for the coarse mesh solution of the call at $K_\alpha \simeq 0.5$ and for the fine mesh solutions of the call Greeks at $K_\alpha \simeq 0.35$) originate from various numerical "issues" related to the computation of either numerical or exact values. Since the irregularities do not influence the conclusions we have not investigated the exact causes in each case.

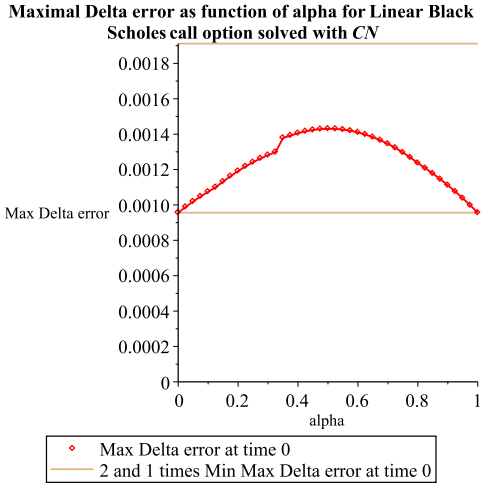

(a) $E^0_\Delta(K_\alpha)$ for call with the fine mesh.

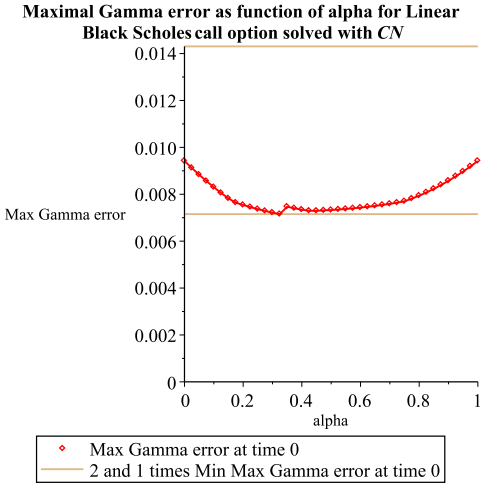

(b) $E^0_\Gamma(K_\alpha)$ for call with the fine mesh.

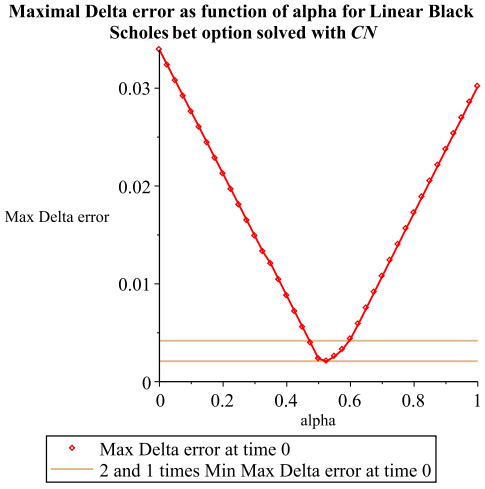

(c) $E^0_\Delta(K_\alpha)$ for bet with the fine mesh.

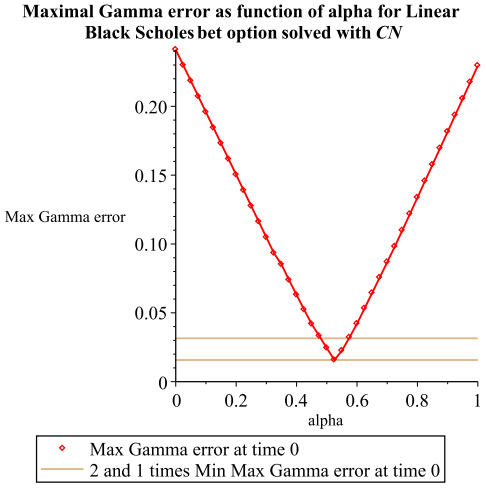

(d) $E^0_\Gamma(K_\alpha)$ for bet with the fine mesh.

FIGURE 2.3: Maximal error $E^0_\Delta(K_\alpha)$ and $E^0_\Gamma(K_\alpha)$ at time $t = 0$ for the Greeks Δ and Γ for the call and bet options as function of $K_\alpha \in [0, 1]$ in the standard case solved with CN using the fine mesh $(h, k) \simeq (0.03, 0.001)$.

The butterfly spread requires 3 optimal K_α-values denoted $\hat{K}^1_\alpha$, $\hat{K}^2_\alpha$ and $\hat{K}^3_\alpha$ for the singularities $K - a$, K and $K + a$ respectively. The corresponding 3 patches are chosen a priori as $[0, K - \frac{a}{2}]$, $[K - \frac{a}{2}, K + \frac{a}{2}]$ and $[K + \frac{a}{2}, \tilde{S}_{\max}]$ and then adjusted by the K_α-shifting method. For different values of N we have computed with N each of K^1_α-, K^2_α- and K^3_α-values uniformly distributed in $[0, 1]$ for a total of N^3 cases. Also we have computed for the coarse as well as for the fine mesh as defined above. Given the 3-dimensional parameter space $(K^1_\alpha, K^2_\alpha, K^3_\alpha) \in [0, 1]^3$ visualization of the results is somewhat challenging, so here we only show the results in tabular form in Table 2.1. For comparison we have also in Table 2.1 given the errors for the two most likely cases

TABLE 2.1: Optimal K_α-values for solution, Δ and Γ for the butterfly spread in the standard case solved with CN using the coarse mesh $(h,k) \simeq (0.08, 0.01)$ and the fine mesh $(h,k) \simeq (0.03, 0.001)$.

Mesh	No. K_α's	$\hat{K}_\alpha^1$	$\hat{K}_\alpha^2$	$\hat{K}_\alpha^3$	$\min_{K_\alpha} E_V^0(K_\alpha)$	$\frac{\max_{K_\alpha} E_V^0(K_\alpha)}{\min_{K_\alpha} E_V^0(K_\alpha)}$
	1	0.00	0.00	0.00	0.016762	1
	1	0.50	0.50	0.50	0.009338	1
Coarse V	11^3	0.50	0.33	0.33	0.000765	34.928762
	21^3	0.55	0.30	0.20	0.000622	46.712522
	41^3	0.53	0.28	0.18	0.000595	49.446807
	1	0.00	0.00	0.00	0.004325	1
	1	0.50	0.50	0.50	0.001495	1
Fine V	11^3	0.60	0.50	0.40	0.000105	93.523044
	21^3	0.60	0.50	0.40	0.000105	93.523044
	41^3	0.50	0.38	0.25	0.000091	–[a]
	1	0.00	0.00	0.00	0.114845	1
	1	0.50	0.50	0.50	0.039337	1
Coarse Δ	11^3	0.40	0.00	0.60	0.008357	29.840102
	21^3	0.45	0.05	0.65	0.008320	30.770937
	41^3	0.38	0.00	0.65	0.007997	34.449918
	1	0.00	0.00	0.00	0.020239	1
	1	0.50	0.50	0.50	0.006166	1
Fine Δ	11^3	0.20	0.00	0.80	0.001466	24.887289
	21^3	0.30	0.10	0.85	0.001354	26.942537
	41^3	0.28	0.08	0.85	0.001333	–[a]
	1	0.00	0.00	0.00	0.385213	1
	1	0.50	0.50	0.50	0.186919	1
Coarse Γ	11^3	0.40	0.10	0.90	0.116449	6.817861
	21^3	0.40	0.10	0.85	0.108821	7.503789
	41^3	0.40	0.10	0.85	0.108821	7.848675
	1	0.00	0.00	0.00	0.086126	1
	1	0.50	0.50	0.50	0.030656	1
Fine Γ	11^3	0.50	0.30	0.00	0.017846	6.569529
	21^3	0.55	0.35	0.05	0.017247	7.348245
	41^3	0.53	0.35	0.10	0.016665	–[a]

[a]Only selected subintervals of K_α are computed.

$K_\alpha = [0,0,0]$ which would likely occur if no thought is given to the location of the singularities (typically integer multiple of decimal steplengths) and $K_\alpha = [0.5, 0.5, 0.5]$ which would likely occur if it was decided to put the singularities in a fixed position different from nodal points without considering optimality of the position. First of all the results show that K_α-optimization gives a significant reduction with a factor from 5 to 30 in the error in the solution, Δ and Γ when compared to selecting $K_\alpha = [0,0,0]$. When compared to $K_\alpha = [0.5, 0.5, 0.5]$ we still record a significant reduction in the error

with an improvement of more than a factor 10 for the solution, less but still with a factor of about 5 for the Δ and least but still with a factor of around 2 for the Γ. This confirms our previous results that the K_α-optimization is less important for the Greeks than for the solution. For Γ basically any selection of K_α apart from putting the singularities in (or close to) nodal points is good.

All the results of this section indicate that positioning the strike price near the middle of a mesh interval might be a good although conservative approach giving reasonable results for many options. If looking for the very best the positioning of the strike price must be taking into consideration also the type of option.

For the K_α-optimization to be useful in practice it would need to be fairly stable against variations in the parameters. So next we investigate whether the conclusions depend on the particular selection of model parameters above. Here interest rate r and volatility σ are deemed the most important parameters, whereas T, B and K basically can be considered scaling parameters without much significance and the dividend yield γ is expected to behave like some sort of additional interest rate, a constant γ not creating new features by itself. Hence in the following two subsections we shall consider variations of the optimal K_α with interest rate r and volatility σ respectively.

2.2.1 Stability of K_α with respect to the interest rate

We redo the computations from Figure 2.2 only adding a third axis with the interest rate $r \in [-0.1, 0.1]$. Negative interest rates are considered since interest rates in Europe has fallen very close to zero after the financial crisis in 2010 and there has been discussions of whether negative interest rates were necessary in order to spawn investment in "growth" i.e. in risky assets.

Two typical results for the fine mesh are shown in Figure 2.4 where we have computed with equidistant r-values with the same difference 0.025 as is used for the K_α-values. For the call option the optimal K_α is situated in $(0.2, 0.3) \cup (0.7, 0.8)$. Further a K_α in the extended interval $(0.2, 0.8)$ only changes the minimal error for the call option by a factor of up to 2 whereas a K_α outside this interval may change the minimal error for the call option by a factor of up to 4.

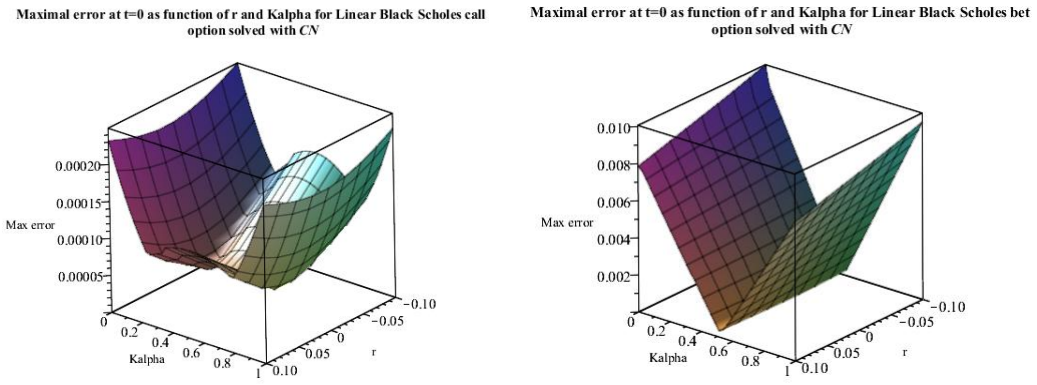

(a) $E_V^0(K_\alpha, r)$ for call with the fine mesh.

(b) $E_V^0(K_\alpha, r)$ for bet with the fine mesh.

FIGURE 2.4: Maximal error $E_V^0(K_\alpha, r)$ at time $t = 0$ as function of $K_\alpha \in [0, 1]$ and $r \in [-0.1, 0.1]$ for (a) the call and (b) the bet option in the standard case except for r solved with CN using the fine mesh $(h, k) \simeq (0.03, 0.001)$.

For the bet option the optimal K_α is situated in $(0.45, 0.55)$ and any K_α in this interval only changes the minimal error for the bet option by a factor of up to 2 whereas a K_α outside this interval may change the minimal error for the bet option by a factor of up to 10.

Summing up, the conclusions from section 2.2 hold for all values of r and t. A reasonable conservative choice is to pick $K_\alpha = 0.5$, but for the call option a more refined choice would be to select $K_\alpha = 0.725$ for negative interest rates and 0.275 for positive interest rates. Especially for the bet option a selection of $K_\alpha = 0$ is somewhat disastrous and should be avoided whether by choice or accident.

2.2.2 Stability of K_α with respect to the volatility

We redo the computations from Figure 2.2 this time adding a third axis with the volatility $\sigma \in (0.1, 0.4)$. Two results are shown in Figure 2.5. The conclusions are the same as before: For the call option the optimal K_α shift for some σ-values from a "lower" value close to the 0.275 observed typically for small values of σ to an "upper" value close to the symmetric value $0.725 = 1 - 0.275$ observed typically for large values of σ. The optimal K_α is situated in $(0.1, 0.3) \cup (0.7, 0.9)$. Further a K_α in the extended interval $(0.1, 0.9)$ only changes the minimal error for the call option by a factor of up to 2 whereas a K_α outside this interval may change the minimal error for the call option by a factor of up to 4.

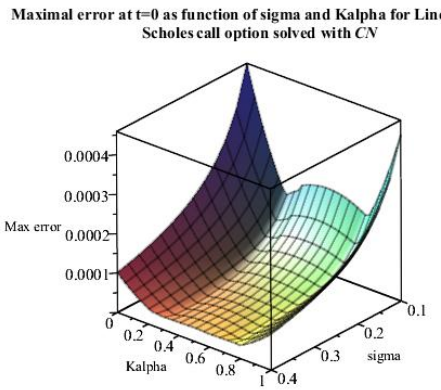

(a) $E_V^0(K_\alpha, \sigma)$ for call with the fine mesh.

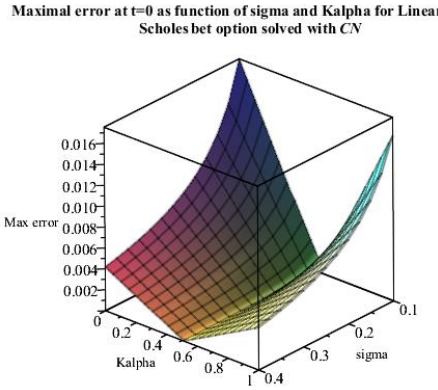

(b) $E_V^0(K_\alpha, \sigma)$ for bet with the fine mesh.

FIGURE 2.5: Maximal error $E_V^0(K_\alpha, \sigma)$ at time $t = 0$ as function of $K_\alpha \in [0, 1]$ and $\sigma \in [0.1, 0.4]$ for (a) the call and (b) the bet option in the standard case except for σ solved with CN using the fine mesh $(h, k) \simeq (0.03, 0.001)$.

The optimal K_α for the bet option is still located solidly in 0.5 except for a few cases with small σ, and for $K_\alpha \in (0.4, 0.6)$ the maximal error is at most the double of the minimal value of the maximal error, whereas a K_α outside this interval may change the minimal error for the bet option by a factor of up to 10.

Summing up, the conclusions from section 2.2 hold for all values of σ and r. A reasonable conservative choice is to pick $K_\alpha = 0.5$, but for the call option a more refined choice would be to select $K_\alpha = 0.725$ for large volatilities and 0.275 for small volatilities. Especially for the bet option a selection of $K_\alpha = 0$ is somewhat disastrous and should be avoided whether by choice or accident.

2.3 K_α-shifting, Rannacher time stepping and mesh grading

Recall Figure 2.1 showing the CN error as a function of $S \in (0, S_{\max})$ and $t \in (0, T)$. In this section we focus on reducing the size of the "bump" in the error close to $S = K$ for all values of $t \in (0, T)$. As in section 2.2 we consider the 2D-slice $t = 0$ but limit to the bet option with its larger error and hence bigger room for improvement than the call option. We shall investigate the error in the Greeks Δ and Γ as well as the error in the solution and compare the base results for the standard CN method to results obtained with CN with a Rannacher startup phase [CNR], CN with the optimal K_α [CNK_α] and

a new combination of CN with both a Rannacher startup phase as well as the optimal K_α [CNRK_α]. We compute with a uniform mesh but for the solution errors we also show results computed with a nonuniform mesh (method suffix GS for Grid Stretching, eg. CNGS) created with the mesh grading transformation

$$S(x) = K + \frac{1}{b}\sinh(c_1(1-x) + c_2 x) \text{ with } \begin{cases} c_1 = \operatorname{arc}\sinh(-bK) \\ c_2 = \operatorname{arc}\sinh(b(S_{\max} - K)) \end{cases} \tag{2.13}$$

changing a uniform mesh in $x \in [0,1]$ with stepsize dx into a nonuniform mesh in $S \in [0, S_{\max}]$ (See more details in Appendix 2.A). The grading of the S-mesh depends on the grading parameter b which we take to $b = 15$ (see [44, 36, 43]). The maximal absolute solution error (see (2.12)) with nonuniform meshes is denoted $E^0_{V,\mathrm{nu}}$.

We consider the Rannacher method in the form where the first iteration of the Crank-Nicolson method is replaced by four quarter-timesteps of the implicit Euler scheme. Giles et al [17] have shown that four quarter-timesteps of the implicit Euler method replacing the first CN step is more accurate than replacing the first two CN steps by four half-timesteps of implicit Euler due to a reduction of the low wavenumber error introduced by the Rannacher startup. Giles et al do so using an $x = \log S$ transformation of the S-variable and no transformation of the time variable giving a reasonable expectation that the conclusion will hold also without the transformation of the S-variable which we shall not apply here. Moreover Giles et al have shown that choosing $\lambda^\star = \frac{k\sigma}{h\sqrt{2T}} \in [0.5, 1]$ causes maximum accuracy for a given computational cost. This result is not expected to carry over to our case but keeping λ^* the same as in the Giles et al paper gives a good basis for comparison since $\log S$ is almost linear in the most interesting region around $S = K = 1$.

For comparison we consider the same parameter values as chosen by Giles et al [17]: $T = 2$, $K = 1$, $B = 0.3$, $r = 0.05$, $\gamma = 0$, $\sigma = 0.2$ and $S_{max} \simeq 5K$ (denoted the *Giles case*). Also we take $\lambda^\star = 0.5$ corresponding to $k = 5h$ and $h = 0.01$. (For the nonuniform meshes $dx = 0.01/S_{\max}$ to get the same number of elements in S). While h and k are not disclosed in [17], it is evident from [17, Fig. 1-2] that also they do consider the worst possible case ($K_\alpha = 0$). In Figures 2.6–2.9 we show the solution, Delta and Gamma errors at time $t = 0$ for the bet option with CN, CNR, CNK_α and CNRK_α.

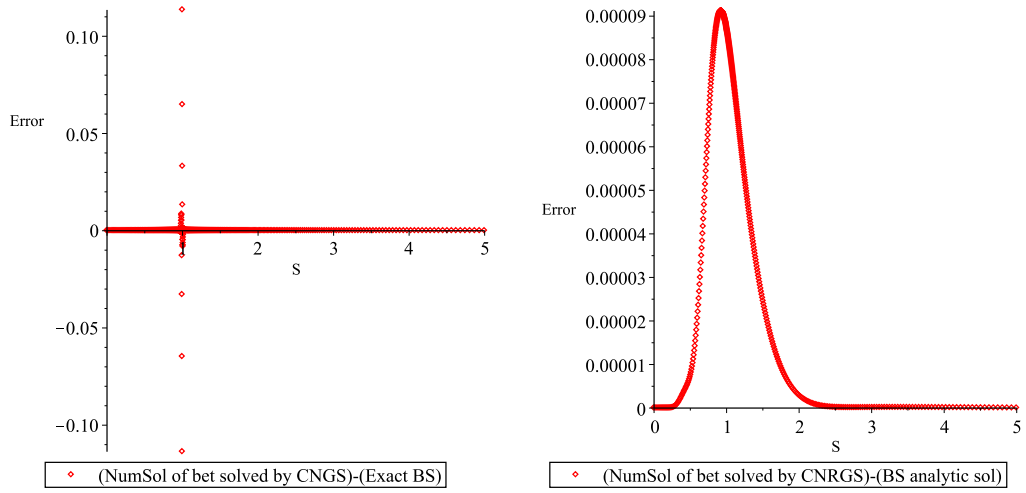

(a) $e_{\mathrm{nu}}(S,0)$ for bet with CNGS.

(b) $e_{\mathrm{nu}}(S,0)$ for bet with CNRGS.

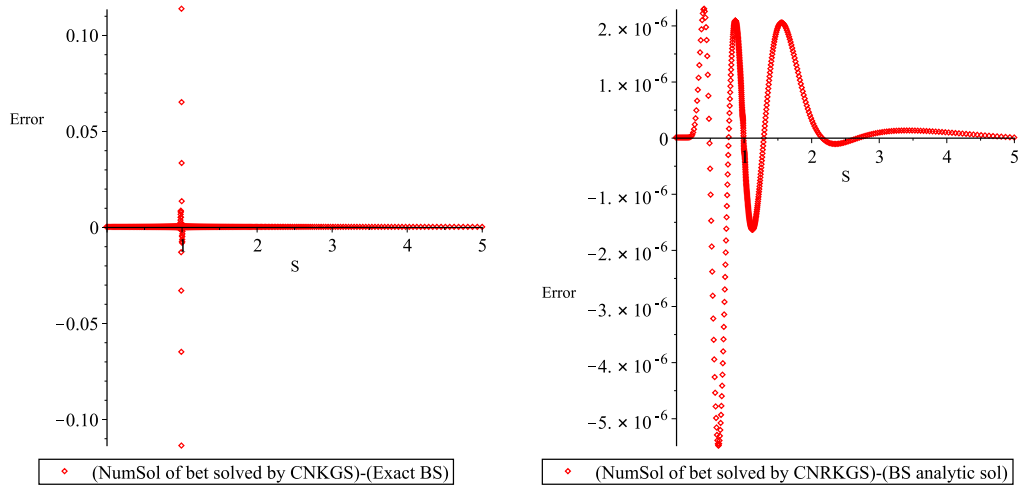

(c) $e_{\mathrm{nu}}(S,0)$ for bet with CNK_αGS.

(d) $e_{\mathrm{nu}}(S,0)$ for bet with CNRK_αGS.

FIGURE 2.6: Solution error $e_{\mathrm{nu}}(S,0)$ at time $t = 0$ as function of $S \in (0, S_{\max})$ with a mesh graded by (2.13) with $b = 15$ for the bet option in the Giles case with $dx = 0.01/S_{\max}$ and $k = 0.05$ solved with (a) CNGS with $K_\alpha = 0$, (b) CNRGS with $K_\alpha = 0$, (c) CNK_αGS with $K_\alpha = 0.5$ and (d) CNRK_αGS with $K_\alpha = 0.5$.

In Table 2.2 the maximal errors of the various cases considered in Figures 2.6–2.9 are listed.

The results show two features: A high frequency oscillation and a "bump" both occurring near $S = K$. For the standard CN method the oscillations are fairly small compared to the bump for the solution error, sizable for the Δ error and all dominating for the Γ error. Rannacher startup completely removes the oscillations for the solution and Δ error and very significantly reduces the oscillations for the Γ. Instead Rannacher startup does nothing to reduce the "bump". The K_α method reduces the size of the "bump"

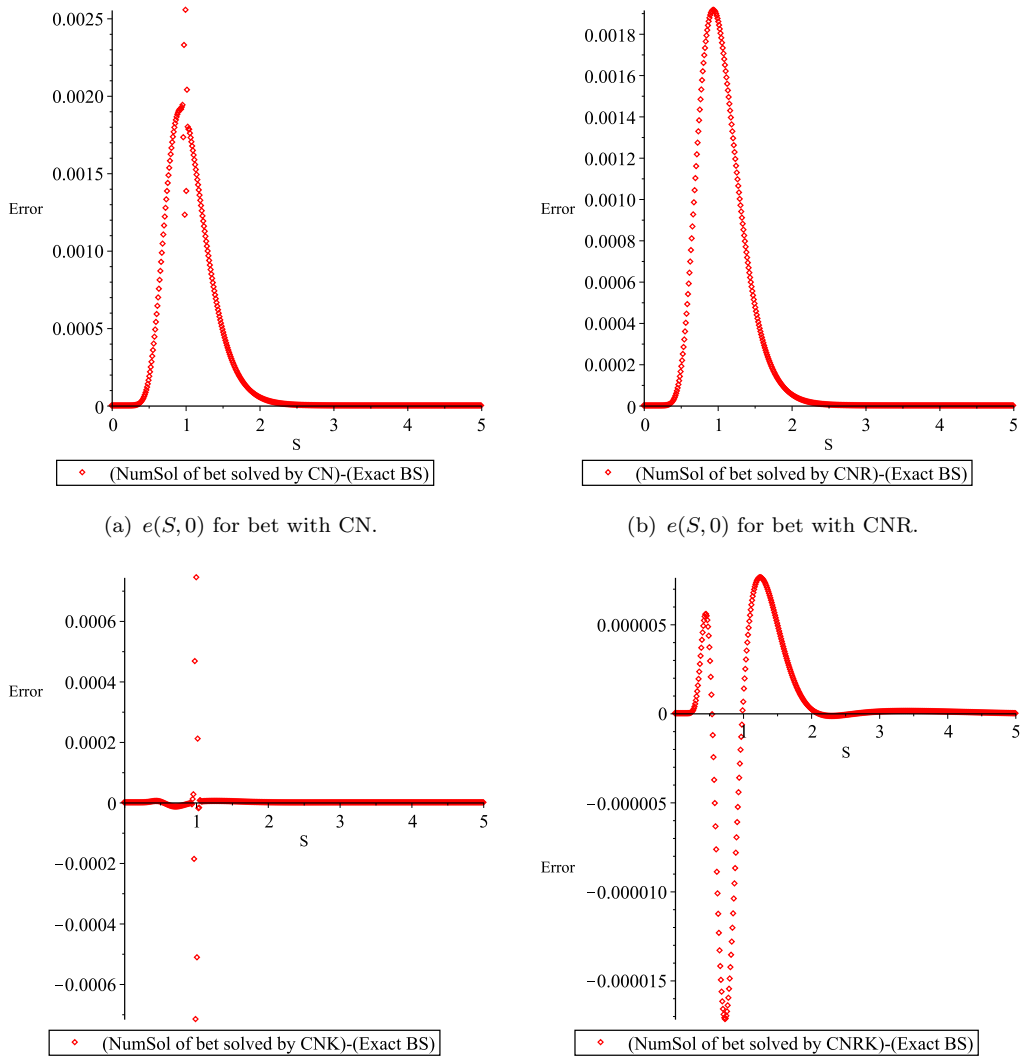

(a) $e(S,0)$ for bet with CN.

(b) $e(S,0)$ for bet with CNR.

(c) $e(S,0)$ for bet with CNK_α.

(d) $e(S,0)$ for bet with CNRK_α.

FIGURE 2.7: Solution error $e(S,0)$ at time $t = 0$ as function of $S \in (0, S_{\max})$ for the bet option in the Giles case with $h = 0.01$ and $k = 5h$ solved with (a) CN with $K_\alpha = 0$, (b) CNR with $K_\alpha = 0$, (c) CNK_α with $K_\alpha = 0.5$ and (d) CNRK_α with $K_\alpha = 0.5$.

but does not remove the oscillation like the Rannacher startup. Finally it is seen how adding the K_α-optimization together with the Rannacher startup completely removes the oscillatory part of the solution and Δ error and significantly reduces it for the Γ error. On top of this the size of the bump is significantly reduced for both solution, Δ and Γ error. For the total error for the CNRK_α-method, including oscillation and bump, the maximal solution error is reduced by a factor of 100 with respect to the CNR solution error. This factor reduces to 44 for the Delta error and 10 for the Gamma error, but in all cases the reduction is at least an order of magnitude. These factors are computed from Table 2.2. It should be noted that our results for CN and CNR are

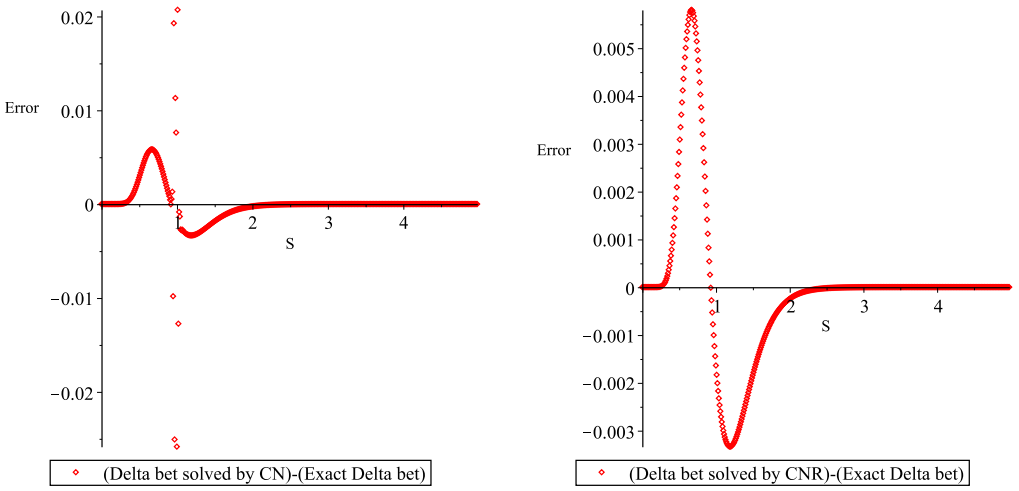

(a) $e_\Delta(S,0)$ for bet with CN.

(b) $e_\Delta(S,0)$ for bet with CNR.

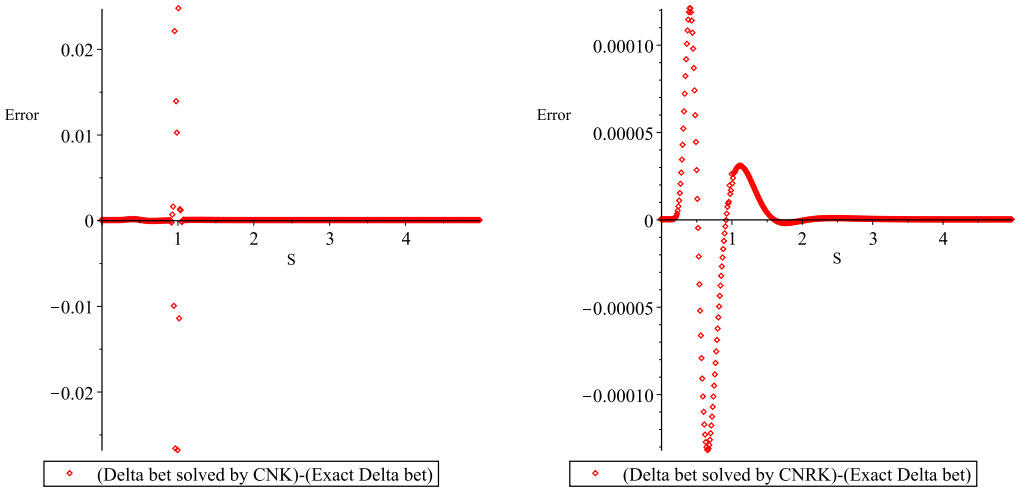

(c) $e_\Delta(S,0)$ for bet with CNK_α.

(d) $e_\Delta(S,0)$ for bet with CNRK_α.

FIGURE 2.8: Delta error $e_\Delta(S,0)$ at time $t=0$ as function of $S \in (0, S_{\max})$ for the bet option in the Giles case with $h = 0.01$ and $k = 5h$ solved with CN with $K_\alpha = 0$ (a), CNR with $K_\alpha = 0$ (b), CNK_α with $K_\alpha = 0.5$ (c) and CNRK_α with $K_\alpha = 0.5$ (d).

completely consistent with those of [17, Fig. 2].

After establishing the merit of the CNRK_α-method for the bet option for one mesh, we turn to the question of whether this is just a very particular case? So we solve for both the call and the bet option with a number of different values of $h \in [0.002, 0.1]$ in the Giles case. Also we again take $\lambda^\star = 0.5$ corresponding to $k = 5h$. For the K_α-shifting methods we use $K_\alpha = 0.275$ for the call option and $K_\alpha = 0.5$ for the bet option. For the non K_α-shifting methods actually we take $K_\alpha = 0$ to show some sort of "worst case scenario". For the "true" non K_α-shifting methods, the error will fluctuate erratically

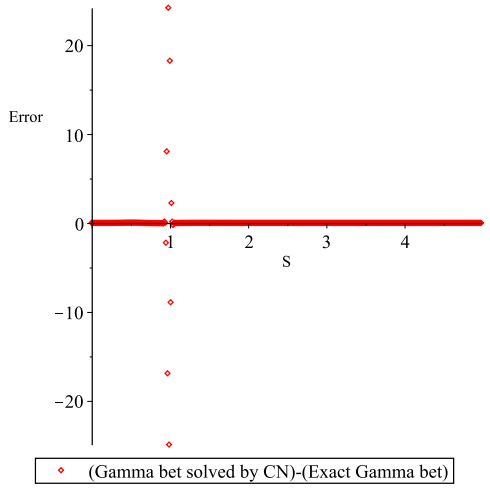

(a) $e_\Gamma(S,0)$ for bet with CN.

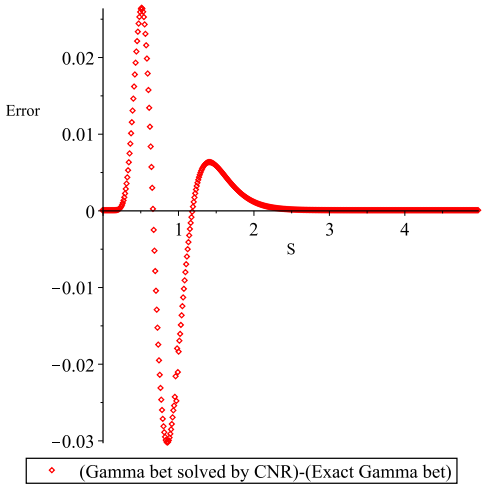

(b) $e_\Gamma(S,0)$ for bet with CNR.

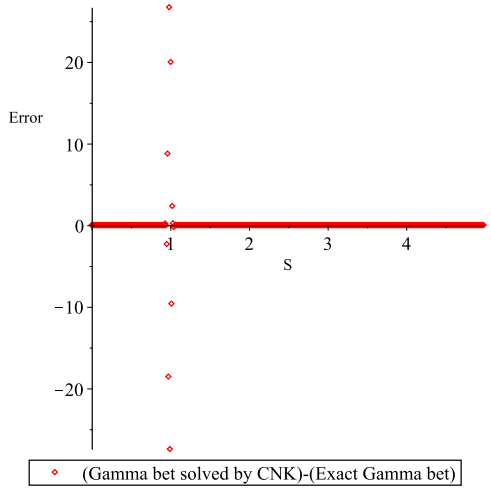

(c) $e_\Gamma(S,0)$ for bet with CNK_α.

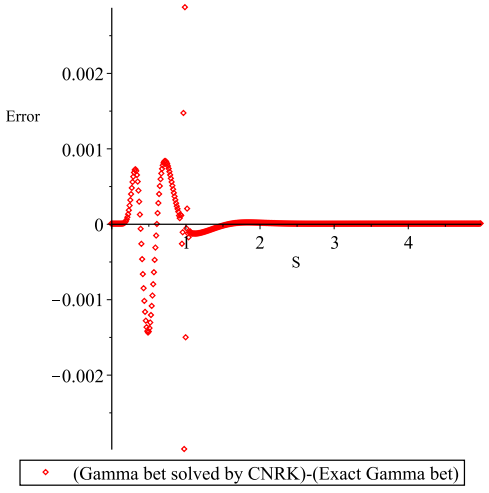

(d) $e_\Gamma(S,0)$ for bet with CNRK_α.

FIGURE 2.9: Gamma error $e_\Gamma(S,0)$ at time $t=0$ as function of $S \in (0, S_{\max})$ for the bet option in the Giles case with $h=0.01$ and $k=5h$ solved with (a) CN with $K_\alpha=0$, (b) CNR with $K_\alpha=0$, (c) CNK_α with $K_\alpha=0.5$ and (d) CNRK_α with $K_\alpha=0.5$.

TABLE 2.2: The maximal solution, Delta and Gamma errors over $S \in (0, S_{\max})$ at time $t=0$ for the bet option in the Giles case with $h=0.01$ and $k=5h$ ($dx = 0.01/S_{\max}$, for $E^0_{V,\text{nu}}$) solved with CN with $K_\alpha=0$, CNR with $K_\alpha=0$, CNK_α with $K_\alpha=0.5$ and CNRK_α with $K_\alpha=0.5$

Methods	$E^0_{V,\text{nu}}$	E^0_V	E^0_Δ	E^0_Γ
CN	0.113659	0.00255428	0.0258461	24.9258
CNR	9.11740e-05	0.00191539	0.00580019	0.0303068
CNK_α	0.113888	0.000743987	0.0268447	27.4361
CNRK_α	5.48878e-06	1.71763e-05	0.000132096	0.00298739

between this worst case scenario curve and the curve for the optimal K_α depending on whether the actual K_α is far from or close to optimal.

Apart from uniform meshes we also compute for nonuniform meshes created with the mesh grading function (2.13) indicated with a [GS] for grid stretching after the acronym for the method. As above, for the nonuniform meshes we take $dx = h/S_{\max}$ to get the same number of elements in S and $k = 5h$. In order to visualize the wide intervals of h-values and corresponding maximal errors we show the results on double logarithmic scales. Instead of showing plots of the errors for all values of $S \in (0, S_{\max})$ at $t = 0$ as we did in Figures 2.6–2.9 we now only show maximal errors over $S \in (0, S_{\max})$ at $t = 0$ in Figure 2.10.

It is seen, that Rannacher time stepping is essential in order to obtain convergence and for all cases Rannacher time stepping combined with mesh grading decreases the error although not the order of convergence. Rannacher time stepping combined with K_α-optimization is clearly the better choice when it comes to order of convergence and combining also with mesh grading decreases the error further without increasing the order of convergence. Hence only the CNRK_α- and CNRK_αGS-methods can be recommended for general use. The CN, CNR and CNK_α-methods (with or without mesh grading) must be considered unsuited for general use even though of course they can be used in particular cases especially if only limited precision is required. The conclusion is, that the CNRK_αGS-method is the overall winner as a general method for computing solution, Delta and Gamma values for put, call and bet options.

Our results for the call option in the left column of Figure 2.10 for CN and CNR are very similar in structure to those of Giles et al [see 17, Fig. 3]. In reality, the Giles et al results more resemble our results for CNK_α and CNRK_α. For the bet option shown in the right column of Figure 2.10 it is even more clear, that it is our results for CNK_α and CNRK_α that are comparable with the Giles et al results for CN and CNR [see 17, Fig. 4]. A personal communication with Mike Giles reveals that Giles et al [17] as a matter of fact consistently did use stepsizes putting the strike either in a nodal point [see 17, Fig. 1-2] or in the middle of a mesh interval [see 17, Fig. 3-4].

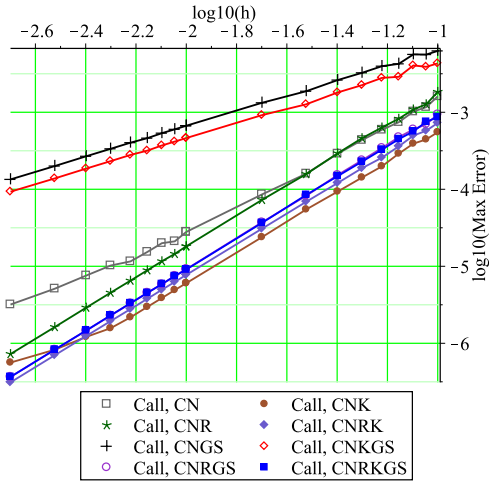

(a) Call maximal error.

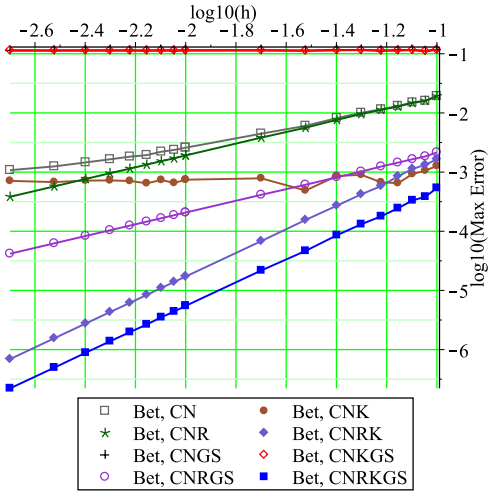

(b) Bet maximal error.

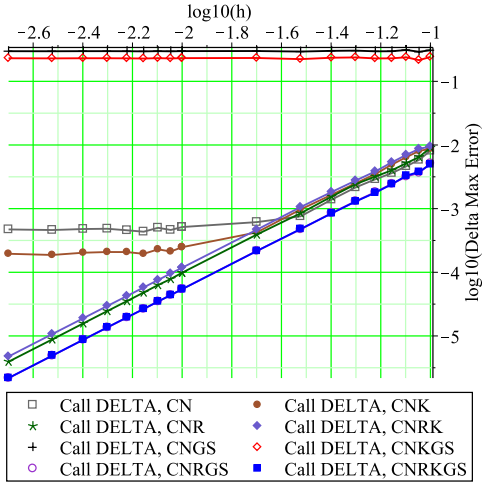

(c) Delta call maximal error.

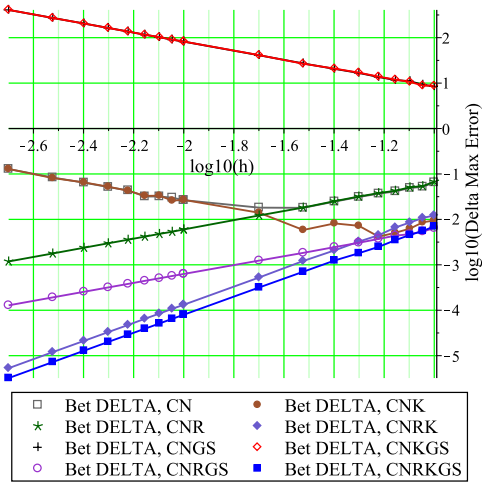

(d) Delta bet maximal error.

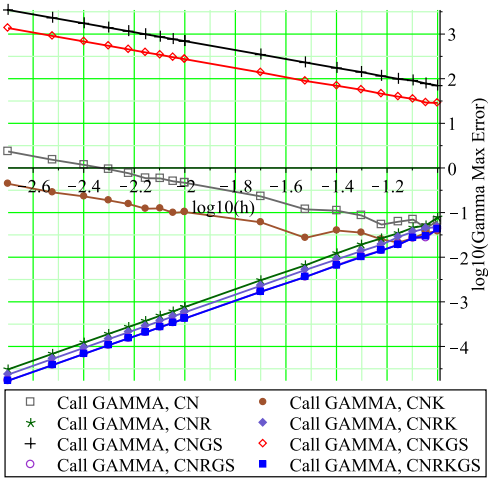

(e) Gamma call maximal error.

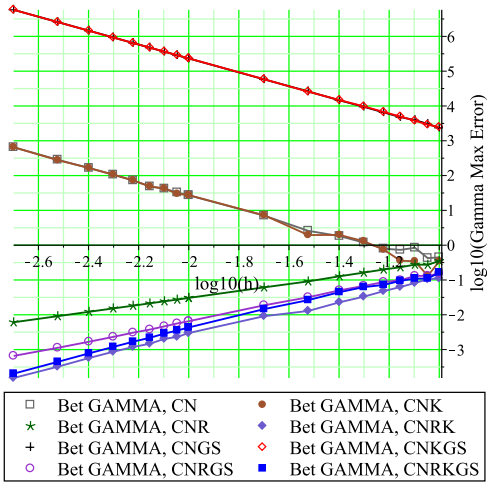

(f) Gamma bet maximal error.

FIGURE 2.10: Maximal solution (a)-(b), Δ (c)-(d) and Γ (e)-(f) errors at time $t = 0$ as function of $h \in (0.002, 0.1)$ for the call option with $K_\alpha = 0.275$ for the K_α methods and $K_\alpha = 0$ for the non K_α methods (left column) and bet option with $K_\alpha = 0.500$ for the K_α methods and $K_\alpha = 0$ for the non K_α methods (right column) in the Giles case with $k = 5h$ and $dx = h/S_{\max}$ for graded meshes. Each plot is showing error curves E_V^0, E_Δ^0 or E_Γ^0 respectively for uniform meshes for the 4 methods CN, CNR, CNK_α and CNRK_α and error curves $E_{V,\mathrm{nu}}^0$, $E_{\Delta,\mathrm{nu}}^0$ or $E_{\Gamma,\mathrm{nu}}^0$ respectively for graded meshes for the 4 methods CNGS, CNRGS, CNK_αGS and CNRK_αGS.

2.4 Order of Convergence

For problems without degenerations and singularities the maximal error with the Crank-Nicolson method should converge to zero as $\mathcal{O}(h^2) + \mathcal{O}(k^2)$ but the singular terminal conditions are known to decrease the orders of convergence for "computable" step sizes. The loss of convergence order is bigger the worse the singularity is and hence we focus on the bet option showing results for the error in the solution, the Δ and the Γ, the latter having the strongest singularity.

Figure 2.11 shows the maximal solution errors at time t = 0 for the bet option with logarithmic axes. The results are provided for the Giles case with $h \in (2^{-8}, 2^{-3})$ and $k \in (10^{-0.2}, 10^{-1.7})$. For the CN and CN$K_\alpha$ methods the (h,k)-plane is clearly divided into two regions with different behavior of the error: In one part a reduction in k reduces the error whereas a reduction in h increases the error. This part will be denoted the *bubble*. The rest of the (h,k)-plane is denoted the *asymptotic* part. The CNR and CNRK_α methods show no bubble part, only the asymptotic part. In order to estimate convergence orders in both h and k independently we use a weighted least squares fitting of the computational errors E_V^0 of the form

$$\min_{a,b,\alpha,\beta} \sum_{i,j} w_{i,j} \cdot ((E_V^0)_{i,j} - (a \cdot h_i^\alpha + b \cdot k_j^\beta))^2. \tag{2.14}$$

The stepsizes are recorded so that they decrease with increasing index, i.e. $h_{i+1} \leq h_i$ and $k_{j+1} \leq k_j$, and the simple weight function $w_{i,j} = i \cdot j$ putting higher weight on smaller step sizes is applied. Obviously selecting a different weight function may change the results somewhat. Separate fittings are made for the bubble and asymptotic parts. In the least squares minimizations the side conditions $0 \leq a$, $0 \leq b$, $0 \leq \alpha \leq 3$ and $0 \leq \beta \leq 3$ are imposed. In a few cases $\beta > 2$. In these cases β is restricted to $0 \leq \beta \leq 2$ and the least squares fitting is repeated. If the maximal fitting error is not increased on the leading digit, then the latter result is selected. The following convergence orders are

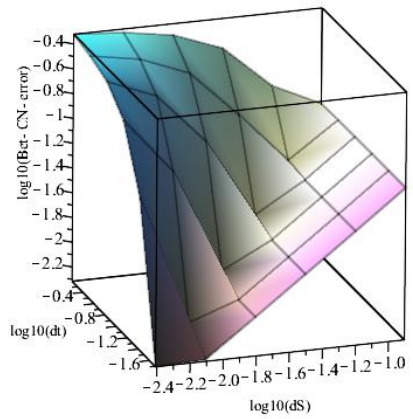

(a) E_V^0 for bet with CN.

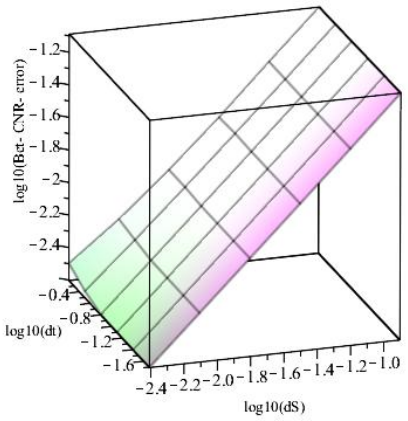

(b) E_V^0 for bet with CNR.

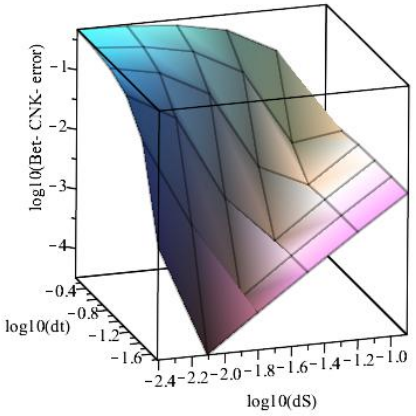

(c) E_V^0 for bet with CNK_α.

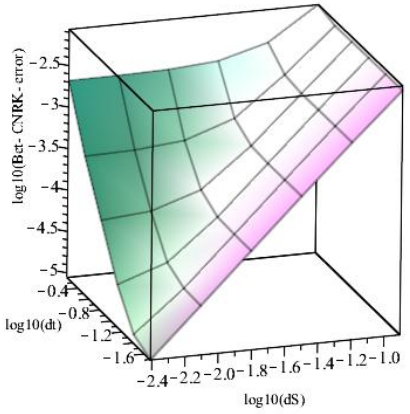

(d) E_V^0 for bet with CNRK_α.

FIGURE 2.11: Maximal error E_V^0 over $S \in (0, S_{\max})$ at time $t = 0$ as function of the step sizes $h = dS$ and $k = dt$ for the bet option in the Giles case for (a) CN ($K_\alpha = 0$), (b) CNR ($K_\alpha = 0$), (c) CNK_α ($K_\alpha = 0.5$) and (d) CNRK_α ($K_\alpha = 0.5$)

computed for the error in the bet option:

$$\begin{aligned}
E_V^0[CN] &\simeq \begin{cases} 0.5 \cdot k^{0.5} & \text{bubble} \\ 0.7 \cdot h^{1.1} + 0.002 & \text{asymptotic} \end{cases} \\
E_V^0[CNR] &\simeq 0.7 \cdot h^{1.0} + 0.001 \cdot k^{0.5} \quad \text{asymptotic} \\
E_V^0[CNK_\alpha] &\simeq \begin{cases} 0.6 \cdot k^{0.7} & \text{bubble} \\ 0.4 \cdot h^{1.9} & \text{asymptotic} \end{cases} \\
E_V^0[CNRK_\alpha] &\simeq 0.4 \cdot h^{1.9} + 0.005 \cdot k^{2.0} \quad \text{asymptotic}
\end{aligned} \tag{2.15}$$

Similar computations are performed for the Delta and Gamma errors of the bet option

but the convergence plots look very similar in structure to Figure 2.11 and are not shown here. Instead the approximate convergence results are given. The Delta errors for the bet option are computed as

$$\begin{aligned}
E^0_\Delta[CN] &\simeq \begin{cases} 77 \cdot k^{0.7} & \text{bubble} \\ 1.0 \cdot h^{0.8} & \text{asymptotic} \end{cases} \\
E^0_\Delta[CNR] &\simeq 1.1 \cdot h^{0.9} + 0.06 \cdot k^{2.0} \quad \text{asymptotic} \\
E^0_\Delta[CNK_\alpha] &\simeq \begin{cases} 77 \cdot k^{0.7} & \text{bubble} \\ 3.6 \cdot h^{1.9} & \text{asymptotic} \end{cases} \\
E^0_\Delta[CNRK_\alpha] &\simeq 3.7 \cdot h^{1.9} + 0.004 \cdot k^{2.0} \quad \text{asymptotic}
\end{aligned} \tag{2.16}$$

and the Gamma errors for the bet option are computed as

$$\begin{aligned}
E^0_\Gamma[CN] &\simeq \begin{cases} 36000 \cdot k^{0.3} & \text{bubble} \\ 8.0 \cdot h^{0.9} + 0.9 \cdot k^{2.0} & \text{asymptotic} \end{cases} \\
E^0_\Gamma[CNR] &\simeq 7.9 \cdot h^{1.0} + 1.0 \cdot k^{1.2} \quad \text{asymptotic} \\
E^0_\Gamma[CNK_\alpha] &\simeq \begin{cases} 35000 \cdot k^{0.3} & \text{bubble} \\ 18.3 \cdot h^{1.7} + 1.6 \cdot k^{2.0} & \text{asymptotic} \end{cases} \\
E^0_\Gamma[CNRK_\alpha] &\simeq 17.0 \cdot h^{1.7} + 0.03 \cdot k^{0.9} \quad \text{asymptotic}
\end{aligned} \tag{2.17}$$

We see evidence that the CN and CNR methods are missing one order of convergence in h i.e. in the S-direction. The convergence in k i.e. in the t-direction is quite imprecise. Because of the small coefficient the term is only visible for large values of k where the results are maybe not even in the asymptotic range. The CNK_α and CNRK_α methods reestablishes (almost) full quadratic convergence in h (1.9 for solution and Δ errors and 1.7 for Γ error). The convergence in k is also for these methods "problematic", but somewhat better than for the methods without K_α optimization.

Similar calculations for the call option results in the same conclusion only with a more perfect recovery of the optimal results since the singularity for the call option is weaker than for the bet option. Hence again, the CNRK_α method must be the one recommended for general use.

2.5 Conclusions and future work

We investigated the Crank-Nicolson finite difference method [CN] and simple improvements for European vanilla options (put, call, bet and butterfly spread).

We proposed the K_α method for uniform and nonuniform meshes with one or more singularities in the terminal condition and tested it with good results for uniform and graded meshes with 1 or 3 singularities.

We found that the Rannacher start up method removes high frequency oscillations in the CN-solution, Delta and Gamma error around the "bump" in the maximal error (see Figure 2.1) and partially reestablishes the optimal second order convergence in the t-direction of the CN method. Instead it does not decrease the size of the error bump or improve the order of convergence in the S-direction.

The K_α method instead reduces the size of the bump in the CN-error and partially reestablishes the optimal second order convergence in the S-direction of the CN method. Instead it does not remove the high frequency oscillations around the bump or improve the order of convergence in the t-direction.

The CN method with the addition of both the Rannacher and the K_α method removes the high frequency oscillations around the maximal error in the solution, Delta and Gamma and significantly reduces the size of the error bump. Further it partially reestablishes the optimal second order convergence in the S and t-direction of the CN method.

Finally we found that mesh grading further reduces the maximal error in all methods without changing orders of convergence thus establishing the merit of utilizing nonuniform meshes in the S-variable.

The Rannacher and K_α methods can be included into any finite difference scheme with very low cost, and is expected to give similar improvements as for the Crank-Nicolson method.

We have also shown that the optimal K_α-values depend on the option but that they are almost independent of the parameters (in particular of the interest r, the volatility σ and the step sizes h and k). For the call option the optimal K_α lies in $(0.2, 0.3)$ or $(0.7, 0.8)$ for the solution error but the error is not very sensitive to values of K_α in

$(0.2, 0.8)$. Values outside this interval may instead lead to significant increases in the error. For the Δ and Γ errors for the call the choice of K_α is almost insignificant but does have an optimal value at $K_\alpha = 0$ (and 1) and 0.3 respectively. For the bet option the optimal K_α is 0.5 for the solution, Δ as well as the Γ error and should be picked in $(0.45, 0.55)$. Values outside this interval may lead to significant increases in the error.

For possible future work we are planning to apply K_α-shifting to nonuniform S-grids considering both graded meshes and adaptive meshes. We intend to do this for finite difference grids, but also to extend to the finite element method, where theoretical results are more easily obtained.

Also we will apply K_α-shifting to problems without closed form solutions such as American options, Asian options, basket options, options with variable parameters (such as σ and γ) and options from a generalized Black-Scholes world taking into consideration for example nonvanishing trading cost, influence from trading volume on stock prices and other features leading to "nonlinear volatility" options.

Appendix

2.A Grid Stretching

The grid stretching transformation concentrates nodal points around non-smooth points of initial conditions for instance the strike price for European options and leads decreasing the error due to non-smoothness and then yields a better convergence rate. Hence, this method transforms underlying asset S with strike price K in the following form:

$$S = \phi(x) = \frac{1}{b}\sinh(c_2 x + c_1(1-x)) + K \tag{2.18}$$

where $c_1 = \sinh^{-1}(b(-K))$, $c_2 = \sinh^{-1}(b(S_{max} - K))$ are normalization constant that cause x is a number in $[0, 1]$ and b is a stretching parameter. Therefore Jacobian $J(x)$ and Hessian $H(x)$ of the transformation giving

$$J(x) = \frac{\partial\phi(x)}{\partial x} = \frac{(c_2 - c_1)}{b}\cosh(c_2 x + c_1(1-x)) + K)$$

and

$$H(x) = \frac{\partial^2\phi(x)}{\partial x^2} = \frac{(c_2 - c_1)^2}{b}\sinh(c_2 x + c_1(1-x)) + K)$$

By using the chain rule for the above functions,

$$\frac{\partial V}{\partial S} = \frac{1}{J(x)}\frac{\partial u}{\partial x}$$

and

$$\frac{\partial^2 V}{\partial S^2} = \frac{1}{J(x)^2}\frac{\partial^2 u}{\partial x^2} - \frac{H(x)}{J(x)^3}\frac{\partial u}{\partial x}$$

Therefore Black-Scholes equation (2.1) will be transformed to the following equation

$$\frac{\partial u}{\partial t} - \frac{1}{2}\sigma^2 \frac{\partial^2 \phi(x)}{\partial x^2}\frac{\partial^2 u}{\partial S^2} - \left[(r-\gamma)\frac{\partial \phi(x)}{\partial x} - \frac{1}{2}\sigma^2 \frac{\partial^2 \phi(x) H(x)}{J(x)^3}\right]\frac{\partial u}{\partial x} + ru = 0$$

where $u(x,t) = V(S,t)$. Figure 2.A.1 shows how the grid stretching transformation put more nodal points around the strike price. In this figure we assumed b(the stretching parameter) equal to 5, $K = 1$, $S_{max} = 4$ and the number of nodal points equal to 40. Oosterlee et al. [36] considered keeping constant the quantity of bK especially on coarse

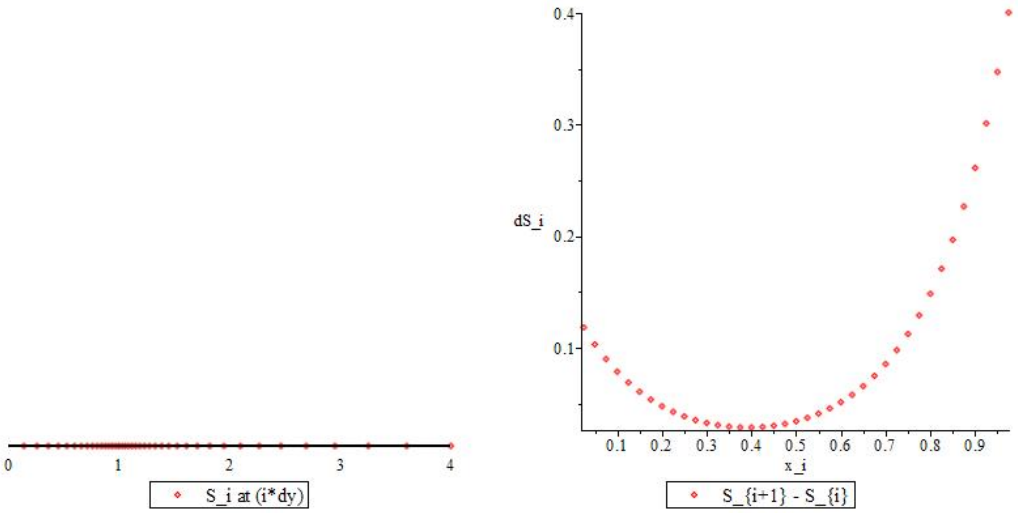

FIGURE 2.A.1: The position of nodal points S_i and the difference between consecutive nodal points with parameters $K = 1$, $Smax = 4$, $b = 5$ and $N = 40$ (the number of nodal points)

grids and they claimed $bK = 15$ ia an appropriate choice for a variety of option pricing parameters.

Chapter 3

Standard Finite Difference Schemes for European Options

Jens Hugger and Sima Mashayekhi

Abstract. Standard finite difference schemes like explicit, implicit and Crank Nicholson methods are used on a daily basis to solve standard European vanilla options or small variations of such like the put, call and bet options considered here.

The first question we have considered is, just how big values $S_{\max}$ of the risky asset do we need to compute with in order that errors from artificially cutting off the computations in $S = S_{\max}$ does not negatively influence the results in the computational domain, when applying the best available boundary conditions in $S_{\max}$? Extensive experimentation shows that $S_{\max} = 4K$, K being the strike price, is a fairly conservative selection, valid for most financially reasonable parameter values and all of the tested numerical methods.

The second question we have considered is that of convergence: How fast does various numerical finite difference methods converge? Here it turns out, that the singularities in the terminal conditions do "cost us some of the speed of convergence", but the methods are still converging. Within our computational domain it is possible to get errors below 0.001% for the put and call options and 0.1% for the bet option with the stronger singularity. Instead it has not been possible to determine understandable bounds for the stable region for the conditionally A-stable methods even though a (conservative) curve is given for the standard case in the computational domain.

The third and fourth questions we have considered are about limiting cases: Do the numerical results when the volatility vanishes go towards the known "no volatility solution"? Here the answer turns out to be affirmative. Do the numerical results when the time approaches the expiration time for the option go towards the known "terminal solution"? Here the answer turns out to be more questionable.

Keywords: European vanilla option, finite difference methods, Heat equation, boundary value problem, discontinuous boundary condition, numerical solution

Subjectclass: 35K61, 65M06

3.1 Introduction

The classic Black-Scholes equation for pricing the European vanilla options on a bounded domain is the following BVD:

$$\frac{\partial V}{\partial t} + \frac{1}{2}\sigma^2 S^2 \frac{\partial^2 V}{\partial S^2} + (r-\gamma)S\frac{\partial V}{\partial S} - rV = 0 \qquad \forall (S,t) \in (0, S_{\max}) \times (0,T) \tag{3.1}$$

with the terminal and boundary conditions

$$V(S,T) = \kappa(S,T), \quad V(0,t) = \kappa(0,t), \quad V(S_{\max},t) \simeq \kappa(S_{\max},t) \tag{3.2}$$

where we are using the utility function

$$\kappa(S,t) = \begin{cases} \max\{Se^{-\gamma(T-t)} - Ke^{-r(T-t)}, 0\} & \textit{call option} \\ \max\{Ke^{-r(T-t)} - Se^{-\gamma(T-t)}, 0\} & \textit{put option} \\ Be^{-r(T-t)}\mathcal{H}(S-K) & \textit{bet option} \\ K\frac{S_{\max}-S}{S_{\max}}e^{-2S-r(T-t)} & \textit{smoothened put} \end{cases} . \tag{3.3}$$

$V(S,t)$ is the option price of the underlying asset S at time t. r, σ and γ are the *market interest rate* (on a risk free asset), the *volatility* (of the underlying risky asset) and the *dividend yield* (on the risky asset) respectively. $S_{\max} >> K$ is the upper bound for the computational domain in the S variable and the terminal time T is the upper bound in the t variable. K is the *Strike Price* for the call and put, B the value of the *Bet* and $\mathcal{H}$ is the Heaviside function.

Chapter 2 shows that the computational error depends on the location of the singular point $S = K$ with respect to the nodal points of the mesh. So we chose $K_\alpha = 0.3$ for put and call options and $K_\alpha = 0.5$ for bet option as the optimal selection of K_α.

We consider three standard finite difference schemes explicit Euler, implicit Euler and Crank Nicolson methods for the numerical solution of (3.1–3.3) with investigation on the following issues in sections 3.2–3.4 and then in section 3.5 we conclude the work.

1. Sensitivity to $S_{\max}$: Limiting the risky asset price S to values $S < S_{\max}$ for some positive asset price $S_{\max}$ turns out to allow only an approximated boundary condition in $S = S_{\max}$. The error generated by this inexact boundary condition turns out to be damped away from $S_{\max}$ when $S_{\max}$ is sufficiently large.

Therefor the question is how big should $S_{\max}$ be selected for the error generated by the incorrect boundary condition to not influence significantly the computational results for the asset prices of interest?

For the standard case $T = 1$, $K = 1$, $B = 0.3$, $r = 0.04$, $\gamma = 0$ and $\sigma = 0.2$ and a number of stepsizes h and k in the S and t directions respectively we study the sensitivity to the selection of $S_{\max}$ by computing with $S_{\max} = 1.25K$, $1.5K$, $2K$ and $4K$ and comparing the errors at time $t = 0$. We also compute for several nonstandard cases, varying the various parameter values, and considering only a few step sizes. The goal is to select an $S_{\max}$ that "works in most cases" to be used for the remainder of the computations.

2. Convergence: For the standard case $T = 1$, $K = 1$, $B = 0.3$, $r = 0.04$, $\gamma = 0$ and $\sigma = 0.2$, the $S_{\max}$ selected in (1) and the K_α selected based on chapter 2 we study the observed convergence properties of the method by varying the stepsizes h and k in the S and t directions respectively. The goal is to obtain observed orders of convergence.

3. Volatility limit: we check if the numerical results approximate the exact solution also when the market volatility σ goes to zero.
$\lim_{\sigma \downarrow 0} V(S,t) = V(S,t)|_{\sigma=0} = \kappa(S,t)$.
The experiments will be performed for the standard case except for $\sigma \to 0$ and with the $S_{\max}$ selected in (1).

4. Expiration limit: $\lim_{t \uparrow T} V(S,t) = V(S,T) = \kappa(S,T)$.
We investigate whether the singularities in κ show up in V in Ω. The experiments will be performed for the standard case and with the $S_{\max}$ selected in (1).

3.2 Numerical results for the explicit Euler method

3.2.1 Computational results for the standard case

We consider our standard case with parameter values $T = 1$, $K = 1$, $B = 0.3$, $r = 0.04$, $\gamma = 0$ and $\sigma = 0.2$. We compute the maximal error at time $t = 0$ i.e.

$$e_0 = \max_{1 \le n \le N} |\tilde{V}_{n,M} - V(S_n, 0)| \tag{3.4}$$

with the exact solution $V(S_n, 0)$ given by (1.2–1.4) (and by Maple for the smoothened put option) and where $\tilde{V}_{n,M}$ have been computed with approximate stepsizes h in the S-direction and k in the t-direction. k is adjusted to get an integer number of steps between 0 and T and for reasons of K_α-shifting explained in Chapter 2, h is adjusted so that K is located in a position $0.3h$ from the start of an S-interval ($K_\alpha = 0.3$). Finally $S_{\max}$ is adjusted to lie in a nodal point. Values for h, k and $S_{\max}$ are reported before these adjustments. We compute with $S_{\max} \simeq 4K$, $2K$, $1.5K$ and $1.25K$ for the put option. Based on the results for these cases we compute only with $S_{\max} \simeq 4K$ for the call and bet options and $S_{\max} \simeq 30K$ for the smoothened put option. The resulting maximal errors are shown in tables below. Additionally we show the initial error at $t = 0$ for all values of S

$$e_{0,n} = \tilde{V}_{n,M} - V(S_n, 0), \text{ for } n = 1, \ldots, N \tag{3.5}$$

for the put option for $h \simeq 0.1$ and $k \simeq 0.001$ and for $h \simeq 0.01$ and $k \simeq 0.00001$ for each selection of $S_{\max}$ in figures below.

To compute the errors, a 32 bit Maple code is used on a standard 64 bit notebook computer running Windows 7. The computing times for each of the values in the following tables are insignificant (up to a few seconds) apart from the last two columns taking up to 5 minutes per entry again apart from the last error ($h \simeq 0.001$ and $k \simeq 0.00001$) taking about an hour for $S_{\max} \simeq 1.25$ and increasing gradually to "several hours" (overnight run) for $S_{\max} \simeq 4$, setting the limit for how long time we allow an individual computation to take.

First we show computational results for the put option. We compute with $S_{\max} \simeq 4K$, $2K$, $1.5K$ and $1.25K$ and the resulting maximal errors are shown in Tables 3.2.1–3.2.4 below.

TABLE 3.2.1: Maximal error e_0 for the put option at $t = 0$ with $S_{\max} \simeq 4K$ and $K_\alpha = 0.3$ in the standard case with the forward Euler method

h \ k	.3	.2	.1	.01	.001	.0001	.00001
.5	0.00743837	0.00713173	0.00691619	0.00673155	0.00671354	0.00671174	0.00671156
.4	0.00510416	0.00465733	0.00434556	0.00407992	0.00405408	0.0040515	0.00405124
.3	0.00330838	0.00273907	0.00280946	0.0032261	0.00326644	0.00327047	0.00327087
.2	0.00248046	0.00173754	0.00174807	0.00238843	0.00245008	0.00245622	0.00245683
.1	0.0108413	0.00193851	0.000666593	0.000495351	0.000551367	0.000556939	0.000557495
.08	0.0915953	0.0295096	0.00105769	0.000278598	0.000336479	0.000342234	0.000342809
.06	0.595397	0.663165	0.292642	0.00014363	0.000207122	0.000213432	0.000214069
.05	1.63976	4.81078	8.41182	47.2881	0.000149196	0.00015549	0.000156127
.04	6.02711	56.3561	701.131	2.24429e+12	9.42570e-05	0.000100889	0.000101557
.03	32.6835	1277.01	611264	2.79243e+26	4.89039e-05	5.54650e-05	5.61361e-05
.02	248.668	51318.3	2.01551e+09	2.34431e+47	3.95663e+184	2.55921e-05	2.62812e-05
.01	8557.03	3.06243e+07	1.73748e+15	3.81028e+93	4.85708e+779	5.9550e-06	6.7561e-06
.001	8.86874e+08	3.28432e+16	2.12565e+34	1.19895e+285	2.50670e+1998	5.58607e+18226	3.42919e+104005

TABLE 3.2.2: Maximal error e_0 for the put option at $t = 0$ with $S_{\max} \simeq 2K$ and $K_\alpha = 0.3$ in the standard case with the forward Euler method

h \ k	.3	.2	.1	.01	.001	.0001	.00001
.5	0.00740498	0.00706996	0.00683287	0.00662891	0.00660898	0.00660699	0.00660679
.4	0.00510416	0.00465693	0.00434345	0.00407532	0.00404918	0.00404658	0.00404632
.3	0.00330838	0.00273907	0.00280946	0.00322612	0.00326647	0.00327049	0.00327089
.2	0.00248046	0.00173754	0.00174807	0.00238843	0.00245008	0.00245622	0.00245684
.1	0.0108413	0.00193851	0.000666593	0.000495351	0.000551367	0.000556939	0.000557495
.08	0.0915953	0.0295096	0.00105769	0.000278598	0.000336479	0.000342234	0.000342809
.06	0.595397	0.663165	0.292642	0.00014363	0.000207122	0.000213432	0.000214069
.05	1.63976	4.81078	8.41182	8.58571e-05	0.000149196	0.00015549	0.000156127
.04	6.02711	56.3561	701.131	5.95539e-05	9.42570e-05	0.000100889	0.000101557
.03	32.6835	1277.01	611264	1.84602e+12	4.89039e-05	5.54650e-05	5.61361e-05
.02	248.668	51318.3	2.01551e+09	2.89985e+46	1.90594e-05	2.55921e-05	2.62812e-05
.01	8557.03	3.06243e+07	1.73748e+15	3.81028e+93	3.55043e+232	8.7574e-06	8.7574e-06
.001	8.86874e+08	3.28432e+16	2.12565e+34	1.19895e+285	2.50670e+1998	9.84577e+14179	1.88245e+32710

TABLE 3.2.3: Maximal error e_0 for the put option at $t = 0$ with $S_{\max} \simeq 1.5K$ and $K_\alpha = 0.3$ in the standard case with the forward Euler method

h \ k	.3	.2	.1	.01	.001	.0001	.00001
.5	0.00719295	0.00706996	0.00683287	0.00662891	0.00660898	0.00660699	0.00660679
.4	0.00463336	0.00443712	0.0040623	0.00374328	0.00371226	0.00370916	0.00370886
.3	0.00294854	0.0027368	0.00280985	0.00322743	0.0032679	0.00327194	0.00327234
.2	0.00200846	0.00172792	0.00175017	0.0023947	0.00245687	0.00246306	0.00246368
.1	0.00415232	0.00193851	0.000666593	0.000657543	0.000657543	0.000657543	0.000657543
.08	0.0429848	0.0295096	0.00104401	0.00104401	0.00104401	0.00104401	0.00104401
.06	0.734071	0.663165	0.292642	0.00105242	0.00105242	0.00105242	0.00105242
.05	3.21598	4.81078	8.41182	0.000840836	0.000840836	0.000840836	0.000840836
.04	20.7412	56.3561	701.131	0.00106134	0.00106134	0.00106134	0.00106134
.03	227.045	1277.01	611264	0.000931848	0.000931848	0.000931848	0.000931848
.02	3941.24	51318.3	2.01551e+09	3.08433e+34	0.000976963	0.000976963	0.000976963
.01	562262	3.06243e+07	1.73748e+15	3.81022e+93	0.0010275	0.0010275	0.0010275
.001	5.91920e+12	3.28432e+16	2.12565e+34	1.19895e+285	2.50670e+1998	7.76348e+11971	3.24985e+25823

TABLE 3.2.4: Maximal error e_0 for the put option at $t = 0$ with $S_{\max} \simeq 1.25K$ and $K_\alpha = 0.3$ in the standard case with the forward Euler method

h \ k	.3	.2	.1	.01	.001	.0001	.00001
.5	0.00612437	0.00612437	0.00612437	0.00612437	0.00612437	0.00612437	0.00612437
.4	0.00463336	0.00443712	0.0040623	0.00374328	0.00371226	0.00370916	0.00370886
.3	0.00278618	0.00278618	0.00286254	0.00330471	0.00334768	0.00335196	0.00335239
.2	0.00532862	0.00532862	0.00532862	0.00532862	0.00532862	0.00532862	0.00532862
.1	0.0087067	0.0087067	0.0087067	0.0087067	0.0087067	0.0087067	0.0087067
.08	0.0429848	0.0138345	0.00762432	0.00762432	0.00762432	0.00762432	0.00762432
.06	0.734071	0.663165	0.0482418	0.0080478	0.0080478	0.0080478	0.0080478
.05	3.21598	4.81078	5.36216	0.0074617	0.0074617	0.0074617	0.0074617
.04	20.7412	56.3561	677.905	0.00851633	0.00851633	0.00851633	0.00851633
.03	227.045	1277.01	611264	0.00933452	0.00933452	0.00933452	0.00933452
.02	3941.24	51318.3	2.01551e+09	1.24698e+17	0.00942338	0.00942338	0.00942338
.01	562262	3.06243e+07	1.73748e+15	8.36689e+90	0.00913899	0.00913899	0.00913899
.001	5.91920e+12	3.28432e+16	2.12565e+34	1.19895e+285	1.99598e+1989	1.26388e+10423	6.75542e+23568

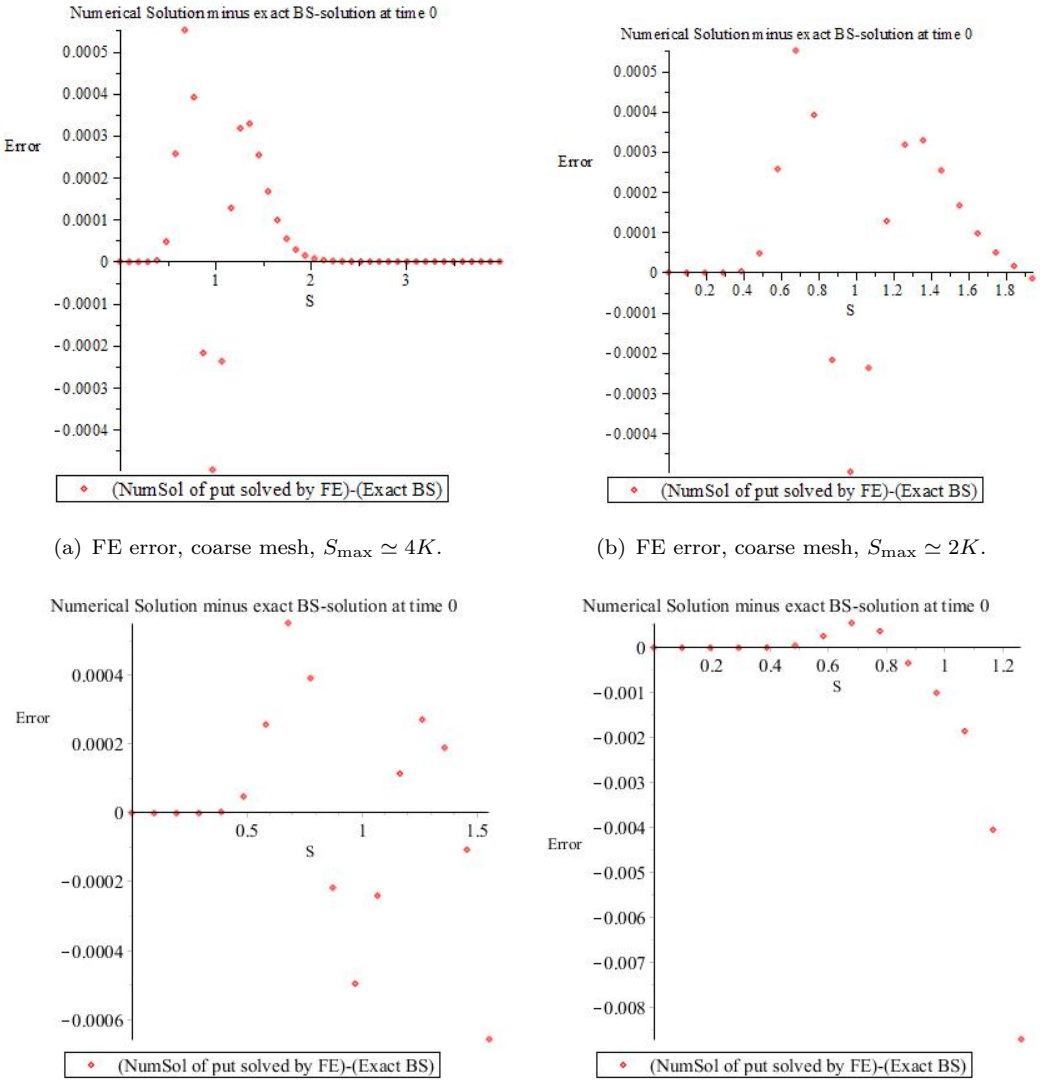

(a) FE error, coarse mesh, $S_{\max} \simeq 4K$.

(b) FE error, coarse mesh, $S_{\max} \simeq 2K$.

(c) FE error, coarse mesh, $S_{\max} \simeq 1.5K$.

(d) FE error, coarse mesh, $S_{\max} \simeq 1.25K$.

FIGURE 3.2.1: Error $\{e_{0,n}\}_{n=1}^{N}$ at $t = 0$ for the put option with $S_{\max} \simeq$ (a) $4K$, (b) $2K$, (c) $1.5K$ and (d) $1.25K$ for stepsizes $h \simeq 0.1$ and $k \simeq 0.001$ and $K_\alpha = 0.3$ in the standard case with the forward Euler method.

Next we show — still for the put option — $\{e_{0,n}\}_{n=1}^{N}$ for $h \simeq 0.1$ and $k \simeq 0.001$ and for $h \simeq 0.01$ and $k \simeq 0.00001$ for each selection of $S_{\max}$ in Figures 3.2.1–3.2.2.

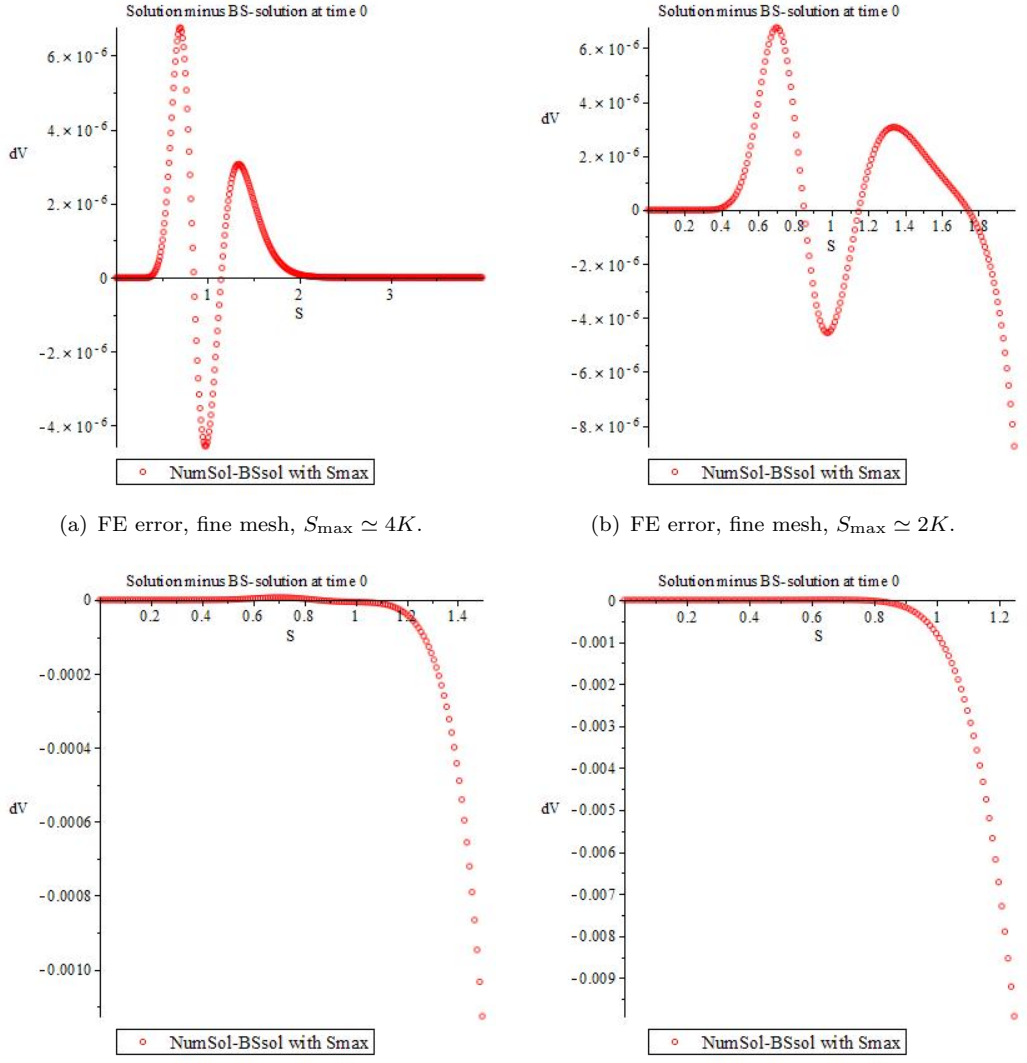

(a) FE error, fine mesh, $S_{\max} \simeq 4K$.

(b) FE error, fine mesh, $S_{\max} \simeq 2K$.

(c) FE error, fine mesh, $S_{\max} \simeq 1.5K$.

(d) FE error, fine mesh, $S_{\max} \simeq 1.25K$.

FIGURE 3.2.2: Error $\{e_{0,n}\}_{n=1}^{N}$ at $t = 0$ for the put option with $S_{\max} \simeq$ (a) $4K$, (b) $2K$, (c) $1.5K$ and (d) $1.25K$ for stepsizes $h \simeq 0.01$ and $k \simeq 0.00001$ and $K_\alpha = 0.3$ in the standard case with the forward Euler method.

Turning to the call option, the maximal error e_0 at time $t = 0$ with $S_{\max} \simeq 4K$ for the call option corresponding to Table 3.2.1 is shown in Table 3.2.5.

TABLE 3.2.5: Maximal error e_0 for the call option at $t = 0$ with $S_{\max} \simeq 4K$ and $K_\alpha = 0.3$ in the standard case with the forward Euler method

h \ k	.3	.2	.1	.01	.001	.0001	.00001
.5	0.00769685	0.00728627	0.00699325	0.00673924	0.00671431	0.00671182	0.00671157
.4	0.00536264	0.00481187	0.00442263	0.00408761	0.00405485	0.00405158	0.00405125
.3	0.00356686	0.00289361	0.0027324	0.00321841	0.00326567	0.00327039	0.00327086
.2	0.00273894	0.00189207	0.001671	0.00238074	0.00244931	0.00245614	0.00245682
.1	0.018031	0.560793	554.292	0.00050304	0.000552135	0.000557015	0.000557503
.08	0.0918538	5.15677	101216.	0.000286287	0.000337248	0.00034231	0.000342816
.06	0.595656	47.3567	1.70551e+07	2.32531e+27	0.000207891	0.00021351	0.000214072
.05	1.64001	177.894	3.50119e+08	4.67393e+46	0.000149964	0.000155568	0.000156128
.04	6.02736	1085.51	2.17304e+10	3.87789e+70	9.50257e-05	0.000100965	0.000101558
.03	32.6837	13054.2	6.16465e+12	3.61905e+100	4.96718e-05	5.55403e-05	5.61268e-05
.02	248.669	281922	6.06568e+15	2.40486e+136	6.90317e+294	2.56686e-05	2.62522e-05
.01	8557.03	8.75659e+07	2.85592e+21	2.82917e+198	2.61827e+1043	6.03150e-06	6.62002e-06
.001	8.86874e+08	1.33514e+17	1.01450e+41	6.46243e+399	1.20367e+3092	3.81939e+20988	7.83496e+106762

Then looking at the bet option, the maximal error e_0 at time $t = 0$ with $S_{\max} \simeq 4K$ for the bet option corresponding to Table 3.2.1 and 3.2.5 is shown in Table 3.2.6. Finally

TABLE 3.2.6: Maximal error e_0 for the bet option at $t = 0$ with $S_{\max} \simeq 4K$ and $K_\alpha = 0.5$ in the standard case with the forward Euler method

h \ k	.3	.2	.1	.01	.001	.0001	.00001
.5	0.0151327	0.0160641	0.0167154	0.0172708	0.0173249	0.0173303	0.0173308
.4	0.0151327	0.0160641	0.0167154	0.0172708	0.0173249	0.0173303	0.0173308
.3	0.0153395	0.0172512	0.0185667	0.0196757	0.0197830	0.0197937	0.0197948
.2	0.0018399	0.0056229	0.0085849	0.0110874	0.0113291	0.0113532	0.0113556
.1	0.3445796	0.2079453	274.481	0.0026521	0.0028800	0.0029027	0.0029050
.08	1.49439	0.9410296	9537.11	0.0016191	0.0018450	0.0018676	0.0018699
.06	17.5034	36.3931	6.70313e+06	4.29681e+28	0.0009594	0.0009812	0.0009833
.05	50.7228	243.656	1.34536e+08	4.18966e+47	0.0006937	0.0007136	0.0007156
.04	208.533	2878.77	7.97850e+09	1.30621e+71	0.0004343	0.0004537	0.0004556
.03	1156.695	54263.16	1.23731e+12	1.22676e+98	0.0002439	0.0002643	0.0002664
.02	14333.2	3.81941e+06	2.26010e+15	1.59028e+136	3.20829e+299	0.0001144	0.0001164
.01	914805	4.02255e+09	5.99658e+20	2.35827e+197	4.2964e+1043	0.0000272	0.0000292
.001	8.92510e+11	3.89745e+19	5.97178e+38	1.98691e+396	1.0626e+3088	3.3316e+15551	5.6970e+101379

we show computational results for the smoothened put option. Likely because of the lack of singularity at $S = K$ the maximal error shows a more significant dependence on $S_{\max}$. For example for the mesh $h = 0.5$, $k = 0.3$ we observe the slow decrease in the maximal error with increasing $S_{\max}$ shown in Table 3.2.7. Computing with $S_{\max} \simeq 30K$ the resulting maximal errors are shown in Table 3.2.8 below.

TABLE 3.2.7: Maximal error e_0 for the smoothened put option at $t = 0$ with different values of $S_{\max}$ and in the standard case with the forward Euler method

$S_{\max}$	4	8	12	20	30	40	80
e_0	0.00211441	0.00194163	0.00188404	0.00183646	0.00181393	0.00180266	0.00178576

TABLE 3.2.8: Maximal error e_0 for the smoothened put option at $t = 0$ with $S_{\max} \simeq 30K$ in the standard case with the forward Euler method

h \ k	.3	.2	.1	.01	.001	.0001	.00001	0.000001
.5	0.00174456	0.00170318	0.00162096	0.00154756	0.00154025	0.00153952	0.00153945	0.00153981
.4	0.000958889	0.000915192	0.000828236	0.000750474	0.000742723	0.000741949	0.000741873	0.00074163
.3	0.000623236	0.000579629	0.000492918	0.000422407	0.000415393	0.000414691	0.000414618	0.000414586
.2	0.000497333	0.000454331	0.000368881	0.000292605	0.000285009	0.00028425	0.00028418	0.000283717
.1	0.000294504	0.000250077	0.00370947	7.72736e+022	7.26825e+764	7.45196e-005	7.44454e-005	7.40195e-05
.08	0.000264834	0.000220447	0.982961	4.44241e+176	2.44328e+1017	4.48330e-05	4.47481e-05	4.41198e-05
.06	0.000246947	0.000202473	286.39	4.36105e+199	1.81505e+1264	3.24554e+293	2.65257e-05	2.59330e-05
.05	0.000239666	0.00146648	5.36896e+07	3.67745e+213	4.04348e+1410	7.49605e+2689	1.92572e-05	1.83604e-05
.04	0.000251355	0.010996	3.32478e+09	4.88994e+232	1.38130e+1609	7.41537e+5383	1.23878e-05	1.12536e-05
.03	0.00169661	0.16102	1.23513e+12	1.14286e+259	8.24320e+1879	2.15613e+8587	6.7196e-06	1.14450e-05
.02	0.0424713	8.84656	6.00126e+15	1.40665e+292	1.32217e+2217	2.30563e+12244	3.0852e-06	1.32023e-05
.01	13.2113	9.33967e+08	8.80241e+22	2.03646e+201	2.70492e+1047	1.07367e+14390	0.0433444	1.92865e-05
.001	9.97943e+06	9.33068e+16	2.83332e+41	2.83332e+41	8.41379e+4819	1.41552e+38528	∞	∞

3.2.2 Computational results for nonstandard cases

Now let us consider some other parameter values than the ones given by the standard case in order to be able to investigate the robustness in the selection of $S_{\max}$. Recall the standard case having parameter values $T = 1$, $K = 1$, $B = 0.3$, $r = 0.04$, $\gamma = 0$ and $\sigma = 0.2$. We consider the following variations in the parameters: $T = 0.1$, 1, 10. $K = 0.1$, 1, 10. $r = 0.01$, 0.04, 0.1. $\sigma = 0.01$, 0.2, 0.9. Instead we shall keep the dividend yield $\gamma = 0$ based on the assumption that this parameter is insignificant for *realistic* dividends. We shall however test this hypothesis by considering $\gamma = 0$, 0.5 and 1.0 but with the other parameters fixed as in the standard case, i.e. $T = 1$, $K = 1$, $B = 0.3$, $r = 0.04$ and $\sigma = 0.2$. Here 0.5 is considered a very conservative upper bound for *realistic* dividends, and 1.0 (100% dividend) is included in order to see how things work in the extreme. The bet value B is similarly tested by considering $B = 0.01$, 0.3, 1.0 and 10.0 but with the other parameters fixed as in the standard case, i.e. $T = 1$, $K = 1$, $\gamma = 0$, $r = 0.04$ and $\sigma = 0.2$. Since B is a parameter in the model only for the bet option, variation in B is considered only in this case.

We restrict to the same two meshes that we used above for Figures 3.2.1 and 3.2.2: A coarse mesh with $h \simeq 0.1$ and $k \simeq 0.001$ and a fine mesh with $h \simeq 0.01$ and $k \simeq 0.00001$,

in both cases with $K_\alpha = 0.3$. For each mesh, we shall find the smallest value of $S_{\max}$ where the error in $S = S_{\max}$ is negligible compared to the maximal error e_0 and report the results in tables below.

For comparison we show in figures below $\{e_{0,n}\}_{n=0}^{N}$ (see 3.5) for the standard case except for $T = 0.1$ and $T = 10$ for the coarse and fine meshes.

As for the standard case we first show results for the put option. The smallest values of $S_{\max}$ where the error in $S = S_{\max}$ is negligible compared to the maximal error e_0 are shown in Table 3.2.9 and 3.2.10 and the results for the fine mesh are shown in Table 3.2.11 and 3.2.12.

TABLE 3.2.9: Smallest $S_{\max}$ not giving significant error at $S = S_{\max}$ with the coarse mesh $h \simeq 0.1$, $k \simeq 0.001$ and $K_\alpha = 0.3$ in various nonstandard cases with the forward Euler method for the put option. "-" indicates an unstable case. "(NN)" indicates a nearly unstable case.

	$K = 10$				$K = 1$				$K = 0.1$			
	r \ σ	.01	.2	.9	r \ σ	.01	.2	.9	r \ σ	.01	.2	.9
$T = 10$	.001	1.25K	-	-	.001	$1.5K$	$(15K)$	-	.001	$2K$	$(10K)$	-
	.04	1.25K	-	-	.04	$2K$	$(11K)$	-	.04	$1.25K$	$(8K)$	-
	.1	1.25K	-	-	.1	$3K$	$(4K)$	-	.1	$1.25K$	$(3K)$	-
	r \ σ	.01	.2	.9	r \ σ	.01	.2	.9	r \ σ	.01	.2	.9
$T = 1$	.001	1.25	-	-	.001	$1.5K$	$3K$	-	.001	$2K$	$3K$	$(30K)$
	.04	1.25	-	-	.04	$1.5K$	$3K$	-	.04	$2K$	$3K$	$(30K)$
	.1	1.25	-	-	.1	$1.5K$	$2K$	-	.1	$2K$	$3K$	$(30K)$
	r \ σ	.01	.2	.9	r \ σ	.01	.2	.9	r \ σ	.01	.2	.9
$T = .1$	.001	$1.25K$	$1.5K$	-	.001	$1.5K$	$1.5K$	$4K$	.001	$2K$	$2K$	$4K$
	.04	$1.25K$	$1.5K$	-	.04	$1.5K$	$1.5K$	$4K$	.04	$2K$	$2K$	$4K$
	.1	$1.25K$	$1.5K$	-	.1	$1.5K$	$1.5K$	$4K$	.1	$2K$	$2K$	$4K$

TABLE 3.2.10: Smallest $S_{\max}$ not giving significant error at $S = S_{\max}$ with the coarse mesh $h \simeq 0.1$, $k \simeq 0.001$ and $K_\alpha = 0.3$ in the standard case except for γ with the forward Euler method for the put option. "-" indicates an unstable case. "(NN)" indicates a nearly unstable case.

γ	0	0.5	1.0
$\min S_{\max}$	3K	4K	6K

TABLE 3.2.11: Smallest $S_{\max}$ not giving significant error at $S = S_{\max}$ with the fine mesh $h \simeq 0.01$, $k \simeq 0.00001$ and $K_\alpha = 0.3$ in various nonstandard cases with the forward Euler method for the put option. "-" indicates an unstable case. "(NN)" indicates a nearly unstable case.

	$K = 10$				$K = 1$				$K = 0.1$			
	r \ σ	.01	.2	.9	r \ σ	.01	.2	.9	r \ σ	.01	.2	.9
$T = 10$	.001	2K	-	-	.001	1.25K	-	-	.001	1.25K	-	-
	.04	3K	-	-	.04	1.25K	-	-	.04	1.25K	(10K)	-
	.1	4K	-	-	.1	1.25K	(8K)	-	.1	1.25K	4K	-
$T = 1$	r \ σ	.01	.2	.9	r \ σ	.01	.2	.9	r \ σ	.01	.2	.9
	.001	1.25K	-	-	.001	1.25K	3K	-	.001	1.5K	3K	-
	.04	1.25K	-	-	.04	1.25K	3K	-	.04	1.5K	3K	-
	.1	1.25K	-	-	.1	1.25K	3K	-	.1	1.5K	3K	-
$T = .1$	r \ σ	.01	.2	.9	r \ σ	.01	.2	.9	r \ σ	.01	.2	.9
	.001	1.25K	-	-	.001	1.25K	1.5K	-	.001	1.5K	1.5K	4K
	.04	1.25K	-	-	.04	1.25K	1.5K	-	.04	1.5K	1.5K	4K
	.1	1.25K	-	-	.1	1.25K	1.5K	-	.1	1.5K	1.5K	4K

TABLE 3.2.12: Smallest $S_{\max}$ not giving significant error at $S = S_{\max}$ with the fine mesh $h \simeq 0.01$, $k \simeq 0.00001$ and $K_\alpha = 0.3$ in the standard case except for γ with the forward Euler method for the put option. "-" indicates an unstable case. "(NN)" indicates a nearly unstable case.

γ	0	0.5	1.0
$\min S_{\max}$	3K	4K	8K

Still considering the put option we show for comparison in Figure 3.2.3 $\{e_{0,n}\}_{n=0}^{N}$ (see 3.5) for the standard case except for $T = 0.1$ and $T = 10$ for the coarse and fine meshes. Figure 3.2.1a should be compared to Figure 3.2.3a and 3.2.3b and Figure 3.2.2a should be compared to Figure 3.2.3c and 3.2.3d.

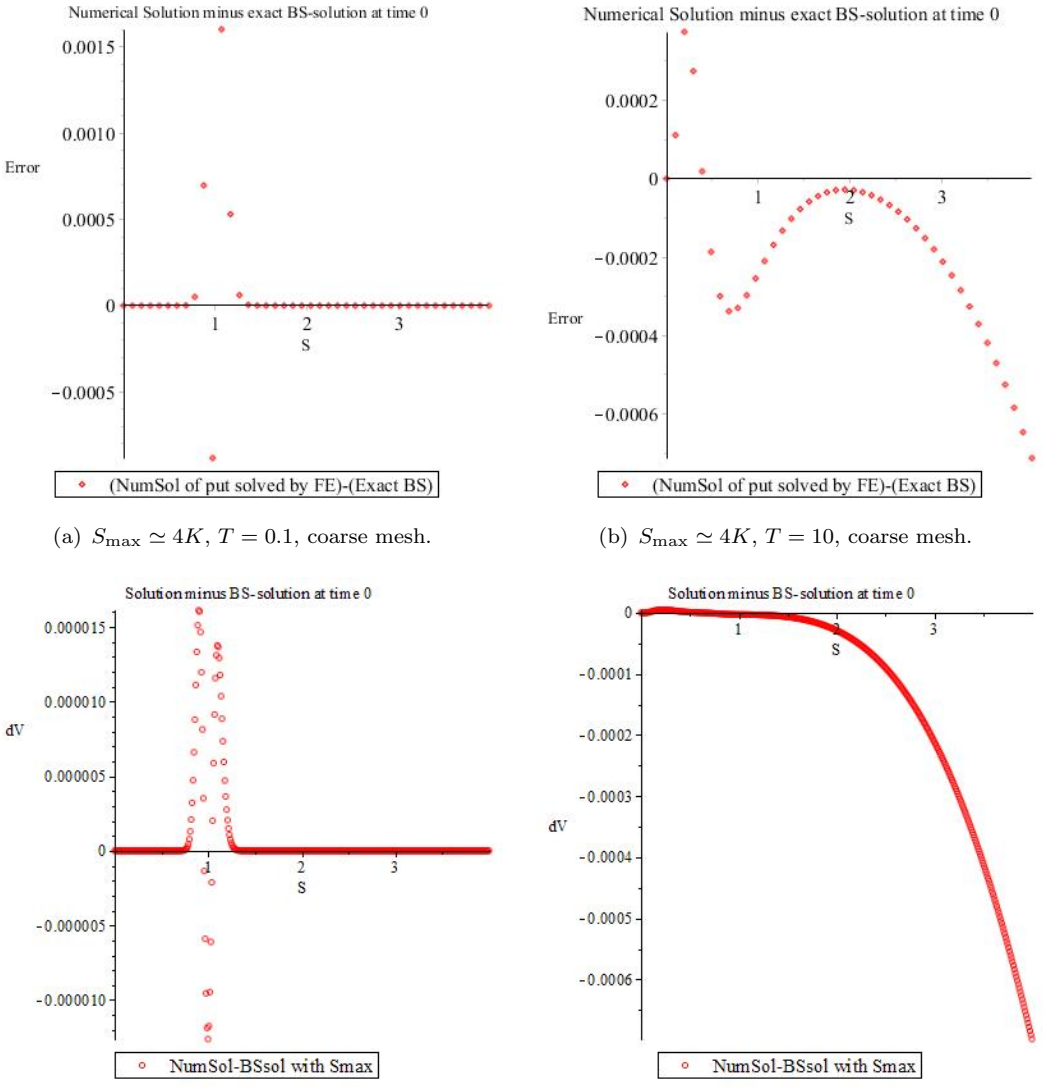

(a) $S_{\max} \simeq 4K$, $T = 0.1$, coarse mesh.

(b) $S_{\max} \simeq 4K$, $T = 10$, coarse mesh.

(c) $S_{\max} \simeq 4K$, $T = 0.1$, fine mesh.

(d) $S_{\max} \simeq 4K$, $T = 10$, fine mesh.

FIGURE 3.2.3: Error $\{e_{0,n}\}_{n=1}^{N}$ at $t = 0$ for the put option with $S_{\max} \simeq 4K$ (a) $h \simeq 0.1$, $k \simeq 0.001$, $T = 0.1$, (b) $h \simeq 0.1$, $k \simeq 0.001$, $T = 10$, (c) $h \simeq 0.01$, $k \simeq 0.00001$, $T = 0.1$ and (d) $h \simeq 0.01$, $k \simeq 0.00001$, $T = 10$ and $K_\alpha = 0.3$, in the standard case apart from the value of T with the forward Euler method.

Doing identical calculations for the call option (only for the coarse mesh, i.e. corresponding to tables 3.2.9 and 3.2.10) results in almost identical results regarding the optimal choice of $S_{\max}$. Only is the call option slightly more prone to instability than the put option resulting in a few additional unstable cases. The results are shown in tables 3.2.13 and 3.2.14.

Finally, doing identical calculations for the bet option (only for the coarse mesh, i.e. corresponding to tables 3.2.9 and 3.2.10) again result in almost identical results regarding

TABLE 3.2.13: Smallest $S_{\max}$ not giving significant error at $S = S_{\max}$ with the coarse mesh $h \simeq 0.1$, $k \simeq 0.001$ and $K_\alpha = 0.3$ in various nonstandard cases with the forward Euler method for the call option. "-" indicates an unstable case. "(NN)" indicates a nearly unstable case.

	$K = 10$				$K = 1$				$K = 0.1$			
	r \ σ	.01	.2	.9	r \ σ	.01	.2	.9	r \ σ	.01	.2	.9
$T = 10$	.001	1.25K	-	-	.001	1.5K	(15K)	-	.001	2K	(10K)	-
	.04	1.25K	-	-	.04	2K	(11K)	-	.04	2K	(8K)	-
	.1	1.25K	-	-	.1	3K	(4K)	-	.1	1.25K	(3K)	-
$T = 1$	r \ σ	.01	.2	.9	r \ σ	.01	.2	.9	r \ σ	.01	.2	.9
	.001	1.25K	-	-	.001	1.5K	3K	-	.001	2K	3K	(30K)
	.04	1.25K	-	-	.04	1.5K	3K	-	.04	2K	3K	(30K)
	.1	1.25K	-	-	.1	1.5K	3K	-	.1	2K	3K	(30K)
$T = .1$	r \ σ	.01	.2	.9	r \ σ	.01	.2	.9	r \ σ	.01	.2	.9
	.001	1.25K	-	-	.001	1.5K	1.5K	-	.001	2K	2K	4K
	.04	1.25K	-	-	.04	1.5K	1.5K	-	.04	2K	2K	4K
	.1	1.25K	-	-	.1	1.5K	1.5K	-	.1	2K	2K	4K

TABLE 3.2.14: Smallest $S_{\max}$ not giving significant error at $S = S_{\max}$ with the coarse mesh $h \simeq 0.1$, $k \simeq 0.001$ and $K_\alpha = 0.3$ in the standard case except for γ with the forward Euler method for the call option. "-" indicates an unstable case. "(NN)" indicates a nearly unstable case.

γ	0	0.5	1.0
min $S_{\max}$	3K	4K	6K

the optimal choice of $S_{\max}$. Only is the bet option slightly more prone to instability than the put option resulting in a few additional unstable cases. The results corresponding to Table 3.2.9 are shown in Table 3.2.15. Instead the bet option is slightly more sensitive

TABLE 3.2.15: Smallest $S_{\max}$ not giving significant error at $S = S_{\max}$ with the coarse mesh $h \simeq 0.1$, $k \simeq 0.001$ and $K_\alpha = 0.5$ in various nonstandard cases with the forward Euler method for the bet option. "-" indicates an unstable case. "(NN)" indicates a nearly unstable case.

	$K = 10$				$K = 1$				$K = 0.1$			
	r \ σ	.01	.2	.9	r \ σ	.01	.2	.9	r \ σ	.01	.2	.9
$T = 10$	.001	1.25K	-	-	.001	1.5K	(15K)	-	.001	2K	(10K)	-
	.04	1.25K	-	-	.04	2K	(11K)	-	.04	2K	(8K)	-
	.1	1.25K	-	-	.1	3K	(6K)	-	.1	1.25K	(4K)	-
$T = 1$	r \ σ	.01	.2	.9	r \ σ	.01	.2	.9	r \ σ	.01	.2	.9
	.001	1.25K	-	-	.001	1.5K	3K	-	.001	2K	3K	(30K)
	.04	1.25K	-	-	.04	1.5K	3K	-	.04	2K	3K	(30K)
	.1	1.25K	-	-	.1	1.5K	3K	-	.1	2K	3K	(30K)
$T = .1$	r \ σ	.01	.2	.9	r \ σ	.01	.2	.9	r \ σ	.01	.2	.9
	.001	1.25K	-	-	.001	1.5K	1.5K	-	.001	2K	2K	4K
	.04	1.25K	-	-	.04	1.5K	1.5K	-	.04	2K	2K	4K
	.1	1.25K	-	-	.1	1.5K	1.5K	-	.1	2K	2K	4K

than the put and call options to changes in the dividend than the put and call options. The results showing this fact are shown to the left in Table 3.2.16. Also, the bet option is completely insensitive to changes in B which is demonstrated to the right in Table 3.2.16.

We show no results for the smoothened put option for nonstandard cases.

TABLE 3.2.16: Smallest $S_{\max}$ not giving significant error at $S = S_{\max}$ with the coarse mesh $h \simeq 0.1$, $k \simeq 0.001$ and $K_\alpha = 0.5$ in the standard case except for γ (to the left) and B (to the right) with the forward Euler method for the bet option. "-" indicates an unstable case. "(NN)" indicates a nearly unstable case.

γ	0	0.5	1.0
min $S_{\max}$	3K	5K	7K

B	0.01	0.3	1.0	10
min $S_{\max}$	3K	3K	3K	3K

3.2.3 Sensitivity to $S_{\max}$

We start with the put option in the standard case. For $S_{\max} \simeq 1.25K$ Table 3.2.4 shows significantly bigger error values than Table 3.2.1–3.2.3 for all step sizes. Also Figures 3.2.1–3.2.2 show that the error is dominated by the contribution at $S_{\max}$ both for the coarse and fine step sizes.

For $S_{\max} \simeq 1.5K$ Table 3.2.3 shows error values of the same order of magnitude as Table 3.2.1–3.2.2 for coarse step sizes. For fine step sizes instead the error values are significantly bigger. Also Figures 3.2.1–3.2.2 show that the error is dominated by the contribution at $S_{\max}$ both for the coarse and fine step sizes.

For $S_{\max} \simeq 2K$ Table 3.2.2 shows error values of the same order of magnitude as Table 3.2.1 for all step sizes. But Figures 3.2.1–3.2.2 show that the error is dominated by the contribution at $S_{\max}$ for the fine step sizes.

For $S_{\max} \simeq 4K$ we have errors of the same order of magnitude as for $S_{\max} = 2K$ but Figures 3.2.1–3.2.2 show that the error is insignificant close to $S_{\max}$ for all step sizes.

The conclusion is that $S_{\max} \simeq 4K$ is required if a high degree of robustness against variation in step sizes is required while $S_{\max} \simeq 2K$ may be used for coarse meshes.

Moving to the nonstandard cases, still considering the put option, tables 3.2.9 and 3.2.11 indicate that $S_{\max}$ is fairly independent of T, K, r and σ as long as we stay away from instabilities. $S_{\max} = 4K$ seems to work for all "not nearly unstable" selections of

parameters. Note that for the nonstandard cases with $T = 10$ and $\sigma \geq 0.2$ all cases are unstable (or nearly so). This explains the results shown in Figure 3.2.3 (b) and (d) where the error in $S_{\max}$ dominates for $S_{\max} = 4K$.

Tables 3.2.10 and 3.2.12 indicate that $S_{\max}$ is likewise fairly independent of γ. $S_{\max} = 4K$ seems to work for all *realistic* dividends. For extreme dividends (like $\gamma = 1.0$) bigger values of $S_{\max}$ are needed.

For the call and bet options the conclusion remains that $S_{\max} = 4K$ is a good choice for all but extreme cases (Unstable, nearly unstable, or extreme parameter cases).

Hence the computational results indicate that $S_{\max}$ is fairly independent of the parameters T, K, r, σ, γ and B as long as we stay away from instabilities and extreme dividends. $S_{\max} = 4K$ seems to work for all selections of parameters with these two exceptions. For extreme dividends (like $\gamma = 1.0$) bigger values of $S_{\max}$ are needed.

3.2.4 Convergence

Convergence is expressed by

$$e_0 \simeq C_S h^\alpha + C_t k^\beta \tag{3.6}$$

where e_0 is the maximal error (see 3.4), h is the S-stepsize, k is the t-stepsize, α is the order of convergence in S, β is the order of convergence in t and C_S and C_t are proportionality constants. we use the weighted least squares (2.14) in order to estimate convergence order of convergence in both h and k directions independently and we get the following result:

$$e_0 \simeq 0.068 h^2 \tag{3.7}$$

Plotting the maximal errors e_0 for the put option at time $t = 0$ from Table 3.2.1 with logarithmic axes, we get the result shown in Figure 3.2.4. This plot indicates the expected (from the forward Euler method implemented) quadratic convergence in S until we reach instability. Instead we do not see the expected linear convergence in t but this is merely because of a small proportionality constant:

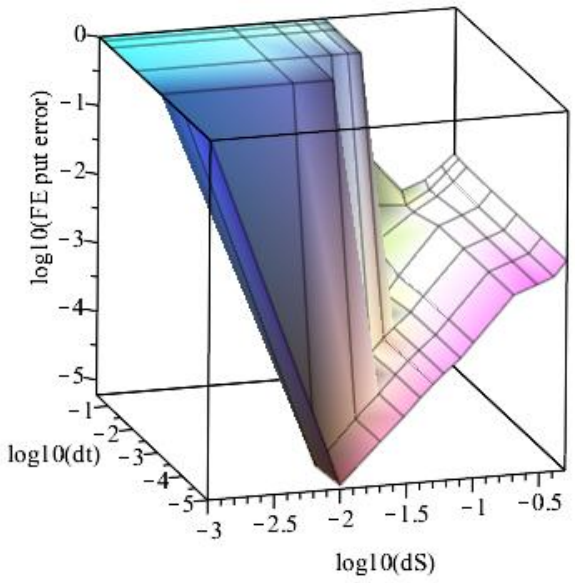

FIGURE 3.2.4: Plot of maximal error e_0 at time $t = 0$ (see 3.4) as a function of stepsizes $dS = h$ and $dt = k$ (logarithmic axes) for the put option in the standard case ($T = 1$, $K = 1$, $B = 0.3$, $r = 0.04$, $\gamma = 0$ and $\sigma = 0.2$) with $S_{\max} = 4K$ and $K_\alpha = 0.3$ with the forward Euler method. In this case the maximal error is attained in the interior of the S-interval, close to $S = K$.

A further investigation shows that the slow linear divergence in t appears to be connected with the discontinuity in the first derivative with respect to S of the terminal condition. This discontinuity generates an error that decays slowly as t decreases from T towards 0 and is — very slowly — increasing as k is reduced. In Figure 3.2.5 we show the error

$$e_{0,nm} = \tilde{V}_{n,m} - V(S_n, t_m) \text{ for } n = 1, \ldots, N,\ m = 1, \ldots, M, \tag{3.8}$$

i.e. the error as a function of both S and t for 5 different meshes:

$$\begin{aligned}
&\text{Mesh 1:} && h \simeq 0.1,\ k \simeq 0.1,\\
&\text{Mesh 2:} && h \simeq 0.1,\ k \simeq 0.01,\\
&\text{Mesh 3:} && h \simeq 0.1,\ k \simeq 0.001,\\
&\text{Mesh 4:} && h \simeq 0.05,\ k \simeq 0.001,\\
&\text{Mesh 5:} && h \simeq 0.03,\ k \simeq 0.001.
\end{aligned}$$

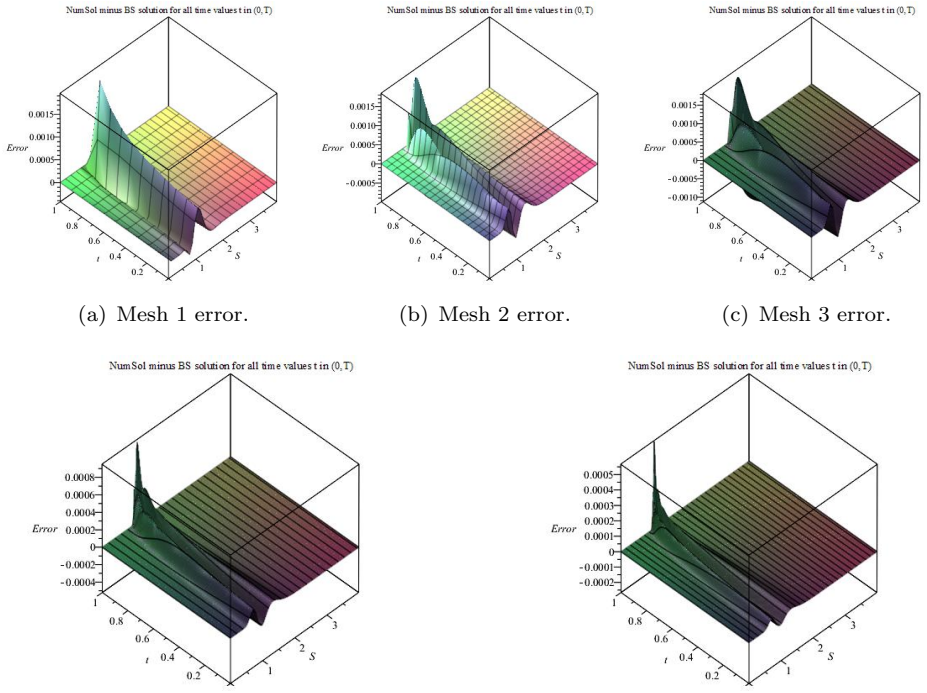

(a) Mesh 1 error. (b) Mesh 2 error. (c) Mesh 3 error.

(d) Mesh 4 error. (e) Mesh 5 error.

FIGURE 3.2.5: Plot of the error as a function of S and t for the put option with $S_{\max} = 4K$ and $K_\alpha = 0.3$ in the standard case ($T = 1$, $K = 1$, $B = 0.3$, $r = 0.04$, $\gamma = 0$ and $\sigma = 0.2$) with the forward Euler method for mesh 1 (a), mesh 2 (b), mesh 3 (c), mesh 4 (d) and mesh 5 (e).

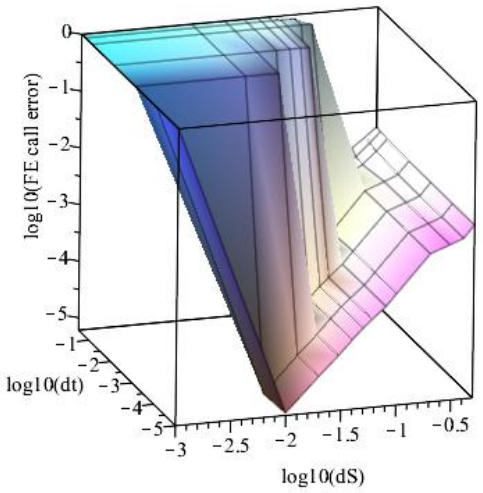

FIGURE 3.2.6: Plot of maximal error e_0 at time $t = 0$ (see 3.4) as a function of stepsizes $dS = h$ and $dt = k$ (logarithmic axes) for the call option in the standard case ($T = 1$, $K = 1$, $B = 0.3$, $r = 0.04$, $\gamma = 0$ and $\sigma = 0.2$) with $S_{\max} = 4K$ and $K_\alpha = 0.3$ with the forward Euler method. In this case the maximal error is attained in the interior of the S-interval, close to $S = K$.

Therefore for the put option solved with the forward Euler method we observe the expected quadratic convergence in S, whereas we because of the discontinuity in the first derivative $\frac{\partial V}{\partial S}$ at $(S, t) = (K, T)$ see no convergence in t in the computational domain. It would be expected that a linear convergence in t would show up once h becomes small enough to "resolve the singularity". But because of the conditional lack of stability, this requires such small values of k that they are out of our computational domain.

Now the convergence plot for the call option based on the data in Table 3.2.5 is shown in Figure 3.2.6. Using the same the weighted least squares formula as we did for the put option we get the following convergence result:

$$e_0 \simeq 0.068h^2 \tag{3.9}$$

As for the put option we get divergence in t in the computational part of the stability region. Also 3D error plots for the call option are identical to those of the put option in Figure 3.2.5 to the naked eye, so they are not shown here. Furthermore the conclusion is the same as for the put option

Then the convergence plot for the bet option based on the data in Table 3.2.6 is shown

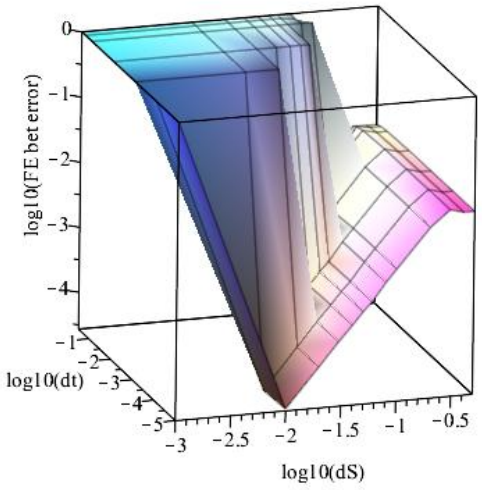

FIGURE 3.2.7: Plot of maximal error e_0 at time $t = 0$ (see 3.4) as a function of stepsizes $dS = h$ and $dt = k$ (logarithmic axes) for the bet option in the standard case ($T = 1$, $K = 1$, $B = 0.3$, $r = 0.04$, $\gamma = 0$ and $\sigma = 0.2$) with $S_{\max} = 4K$ and $K_\alpha = 0.5$ with the forward Euler method. In this case the maximal error is attained in the interior of the S-interval, close to $S = K$.

in Figure 3.2.7. Using the same the weighted least squares formula as we did for the put and call options we get the following convergence result:

$$e_0 \simeq 0.017h^{1.4} \tag{3.10}$$

As for the put and call options we get divergence in t in the computational part of the stability region, but unlike these two options, for the bet option we also loose some of the quadratic convergence in S (the order dropping from 2 to 1.4), likely because of the stronger singularity in the terminal data, the bet having a discontinuity in the value whereas the put and call have discontinuities only in the first derivative with respect to S of the value.

As for the put option a further investigation of the divergence in t is performed, plotting $e_{0,nm}$ from 3.8 for the 5 meshes "Mesh $1 \ldots, 5$". For the bet option, the "Mesh 1" case is unstable, whereas the other cases show the same general behaviour as those of the put and call options. Instead the shape of the error curve is different, starting out with a significantly greater error 0.05. Also this value does not decrease for Mesh 3 and 4 as for the put and call options. The results are shown in Figure 3.2.8. The conclusion is different from the one for the put and call options. This is likely caused by the stronger

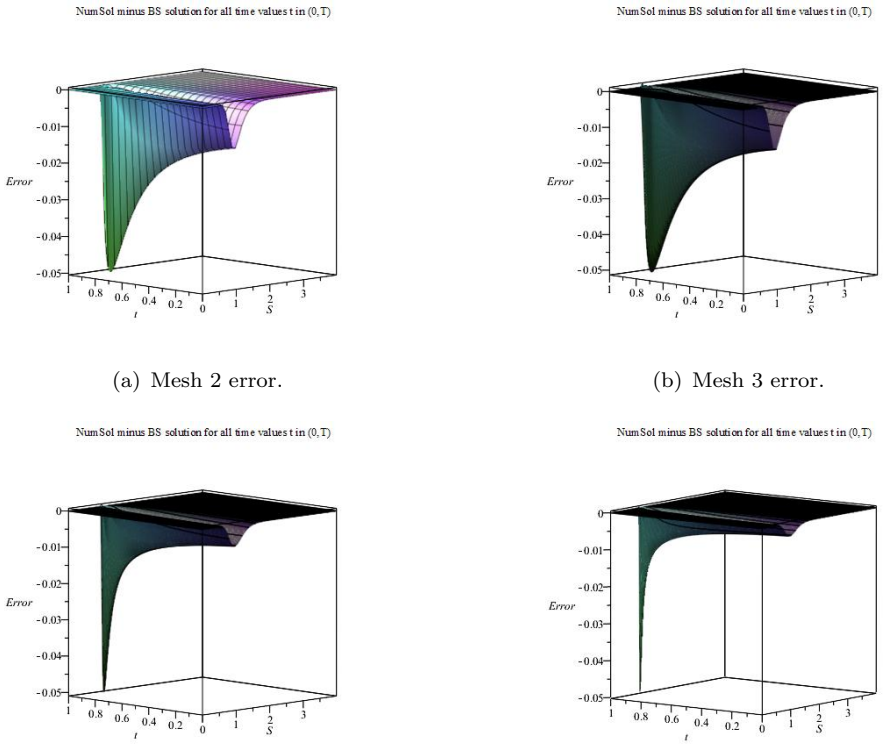

(a) Mesh 2 error.

(b) Mesh 3 error.

(c) Mesh 4 error.

(d) Mesh 5 error.

FIGURE 3.2.8: Plot of the error as a function of S and t for the bet option with $S_{\max} = 4K$ and $K_\alpha = 0.5$ in the standard case ($T = 1$, $K = 1$, $B = 0.3$, $r = 0.04$, $\gamma = 0$ and $\sigma = 0.2$) with the forward Euler method for mesh 2 (a), mesh 3 (b), mesh 4 (c) and mesh 5 (d).

singularity in the terminal condition. For the bet option there is a singularity in the price V itself at $(S, t) = (K, T)$ and not just in the derivative $\frac{\partial V}{\partial S}$ as for the put and call. For the bet option solved with the forward Euler method we observe a reduction in the order of convergence in S compared to the expected quadratic convergence. As for the put and call options, also for the bet option we see no convergence in t in the computational domain. It would be expected that a quadratic convergence in S and a linear convergence in t would show up once h becomes small enough to "resolve the singularity". But because of the conditional lack of stability, this requires such small values of k that they are out of our computational domain. Because of the stronger singularity, the domain where we get the expected convergence orders is probably further out of range for the bet option than for the put and call options.

Finally the convergence plot for the smoothened put option based on the data in Table 3.2.8 is shown in Figure 3.2.9 with the following convergence result:

$$e_0 \simeq 0.005h^2 + 0.001k \tag{3.11}$$

Unlike the results for the put, call and bet options we finally see the expected quadratic

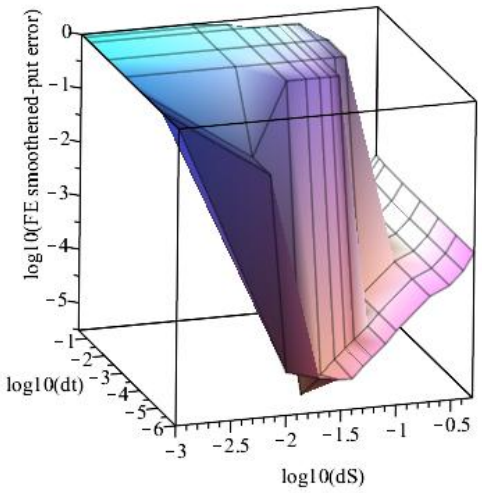

FIGURE 3.2.9: Plot of maximal error e_0 at time $t = 0$ (see 3.4) as a function of stepsizes $dS = h$ and $dt = k$ (logarithmic axes) for the smoothened put option the standard case ($T = 1$, $K = 1$, $B = 0.3$, $r = 0.04$, $\gamma = 0$ and $\sigma = 0.2$) with $S_{\max} = 30K$ with the forward Euler method. In this case the maximal error is attained in the interior of the S-interval, between $S = 0$ and $S = K$

convergence in S and linear (albeit slow) convergence in t in the computational part of the stability region.

As for the other options a further investigation of the convergence properties is performed by visualizing the global shape of the error function, plotting $e_{0,nm}$ from 3.8. The 5 meshes "Mesh $1 \ldots, 5$" used for the put, call and bet options are all unstable for the smoothened put option, (see Table 3.2.8) so we need to turn to finer meshes. Hence we

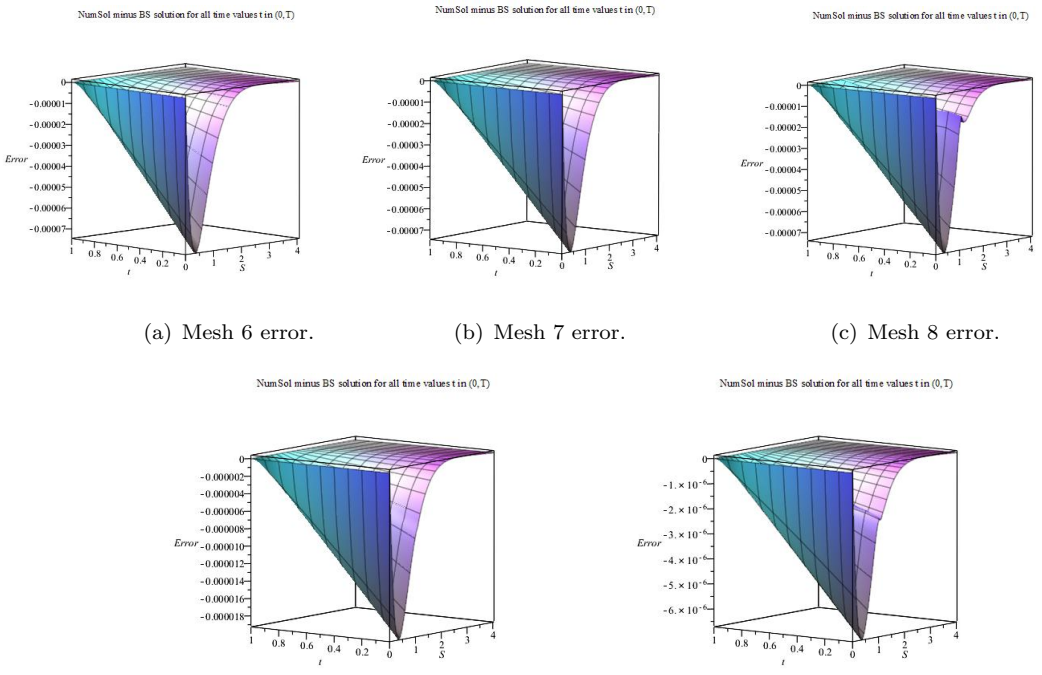

(a) Mesh 6 error. (b) Mesh 7 error. (c) Mesh 8 error.

(d) Mesh 9 error. (e) Mesh 10 error.

FIGURE 3.2.10: Plot of error as a function of S and t for the smoothened put option with $S_{\max} = 30K$ in the standard case ($T = 1$, $K = 1$, $B = 0.3$, $r = 0.04$, $\gamma = 0$ and $\sigma = 0.2$) for mesh 6 (a), mesh 7 (b), mesh 8 (c), mesh 9 (d), mesh 10 (e)

compute for

$$\begin{aligned} \text{Mesh 6:} \quad & h \simeq 0.1, \ k \simeq 0.0001, \\ \text{Mesh 7:} \quad & h \simeq 0.1, \ k \simeq 0.00001, \\ \text{Mesh 8:} \quad & h \simeq 0.1, \ k \simeq 0.000001, \\ \text{Mesh 9:} \quad & h \simeq 0.05, \ k \simeq 0.00001, \\ \text{Mesh 10:} \quad & h \simeq 0.03, \ k \simeq 0.00001. \end{aligned}$$

The results are shown in Figure 3.2.10. To be able to compare directly to the similar plots for the put, call and bet options, all results are shown only for $S \in [0, 4]$ even though the computations are made with $S_{\max} = 30K$.

For the smoothened put option the error increases linearly with time as $t \to 0$ and the maximal errors lies in the region $S \in (0, K)$ at $t = 0$. The linear decrease in the maximal error with k is not visible to the naked eye whereas the quadratic decrease in the maximal error with h is highly visible. The error obviously can not be blaimed on a singularity

in the boundary condition at $(S,t) = (K,T)$, since such a singularity is not present in the smoothened put option. Instead the error may be blaimed on the degeneracy in the PDE as $S \to 0$ where the S-dependency in the PDE vanishes conflicting with the boundary condition in $S = 0$ (recall the discussion in section 1.1.3 under "Left risky asset limit"). The results show, that this degeneracy although dominating the error is not so significant that we loose the expected convergence orders. So the degeneracy shows up only in the size of the constants C_S and C_t in 3.6.

For comparison, the convergence results with the forward Euler method are repeated here:

$$\begin{aligned} \text{Put:} \qquad & e_0 \simeq 0.068h^2 \\ \text{Call:} \qquad & e_0 \simeq 0.068h^2 \\ \text{Bet:} \qquad & e_0 \simeq 0.017h^{1.4} \\ \text{Smoothened put:} \qquad & e_0 \simeq 0.005h^2 + 0.001k \end{aligned}$$

The conclusion is that the discontinuity in the derivative $\frac{\partial V}{\partial S}$ at $(S,t) = (K,T)$ for the put and call options means the loss of one order of convergence in t (with respect to the expected linear convergence for the forward Euler method) in the computational domain. Instead the expected quadratic order of convergence in S is observed in the computational domain. The discontinuity in V at $(S,t) = (K,T)$ for the bet option means the loss of both one order of convergence in t (with respect to the expected linear convergence for the forward Euler method) as well as part of the expected quadratic order of convergence in S in the computational domain. It would be expected that a quadratic convergence in S and a linear convergence in t would show up once h becomes small enough to "resolve the singularity". But because of the conditional lack of stability, this requires such small values of k that they are out of our computational domain. Because of the stronger singularity, the domain where we get the expected convergence orders is probably further out of range for the bet option than for the put and call options. These speculations could merit further research but are not treated here. Also it has not been possible to establish understandable bounds for the stability regions, possibly for the same reason – we need smaller step sizes.

The smoothened put option has no discontinuity in V or its derivatives and we do get the expected orders of convergence even though the "constants" in 3.6 (in particular

the t-constant C_t) are small. The error is dominated by a contribution estimated to originate from the degeneracy in the PDE at $S = 0$ described in section 1.1.3 under "Left risky asset limit".

The recovery of the full order of convergence for the smoothened put further confirms the conclusion from above, that the decrease in orders of convergence for the put, call and bet options are explained by the discontinuity in V or some derivative with respect to S of V at expiration time $t = T$.

3.2.5 Volatility limit

As mentioned in section 1.1.3 for $\sigma = 0$ the pricing problem loses its stochastic aspect and the exact solution is easily accessible (see 1.11). At the same time, the convection-diffusion equation loses its diffusion part and becomes a convection equation and it is unknown whether the limit of the solution to the convection-diffusion problem equals the solution to the limiting convection problem (see 1.12). This is what we investigate here for the numerical solution and for simplicity we show results only for the put option. We consider the option price when volatility tends to 0 and Table 3.2.17 shows the maximal error e_0 for a number of volatilities tending to zero for the put option for the coarse and fine mesh $h \simeq 0.1$, $k \simeq 0.001$ and $h \simeq 0.01$, $k \simeq 0.00001$ respectively.

TABLE 3.2.17: Maximal error e_0 for the put option at $t = 0$ with $S_{\max} \simeq 4K$ and $K_\alpha = 0.3$ in the standard case except for σ with the coarse and fine meshes $h \simeq 0.1$, $k \simeq 0.001$ and $h \simeq 0.01$, $k \simeq 0.00001$ respectively with the forward Euler method.

σ	0.4	0.2	0.01	0.001	0.0001	0.00001	0.
Coarse mesh	0.147944	0.0715007	0.00694667	0.00659941	0.00659593	0.00659589	0.00659589
Fine mesh	0.150188	0.0745655	0.00318934	0.00272693	0.00274538	0.00274558	0.00274557

We can see that when σ goes to zero the maximal errors tend to the maximal error for the option price with zero volatility and by a closer inspection (see also Figure 3.2.11(e),(f) and 3.2.12)(e),(f) it turns out that also the numerical solution for a given value of σ converges to the numerical no volatility solution as $\sigma \to 0$. Hence 1.12 holds for the numerical solutions.

The error that occurred in the option price with no volatility is concentrated around $S = K$ originating in the non-continuous derivative of the initial condition here. This is shown in Figures 3.2.11(e),(f) and 3.2.12(e),(f) for the coarse and fine mesh respectively.

The leftmost plots of Figures 3.2.11 and 3.2.12 show the changes of option price when the volatility tends to zero and the rightmost plots show the difference between the numerical solution with different values of σ and the exact solution with $\sigma = 0$ for the coarse and fine mesh respectively.

Similar results are obtained for the call and bet options leading to the conclusion, that 1.12 holds for the numerical solutions in all cases considered here and probably for a much wider range of options.

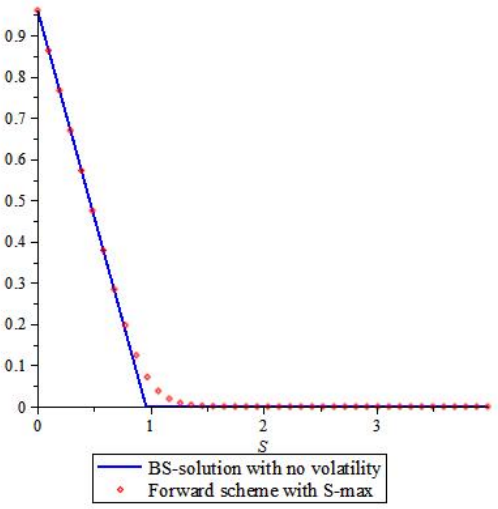

(a) Option Price, $\sigma = 0.2$.

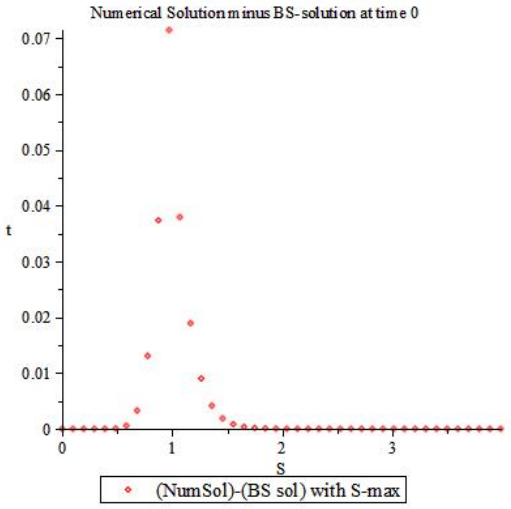

(b) Error curve, $\sigma = 0.2$.

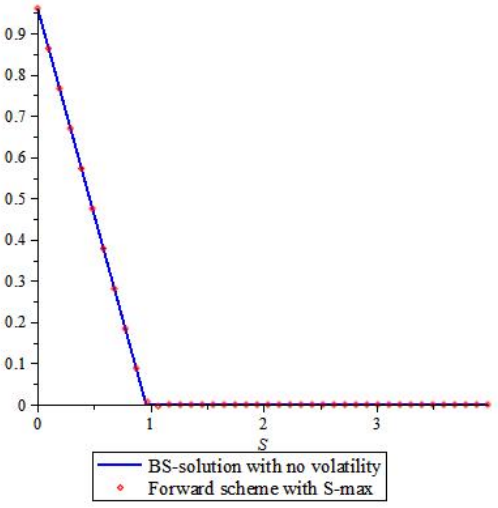

(c) Option Price, $\sigma = 0.001$.

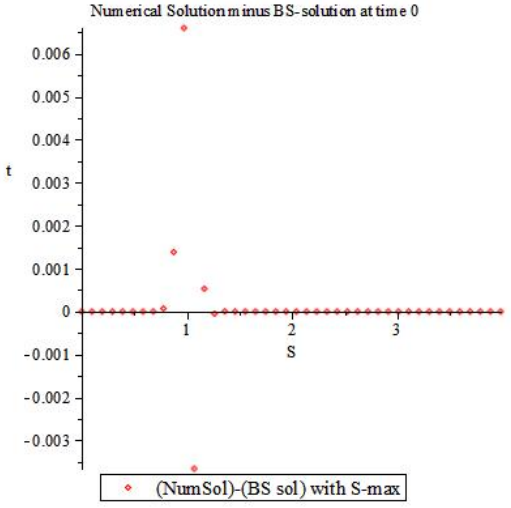

(d) Error curve, $\sigma = 0.001$.

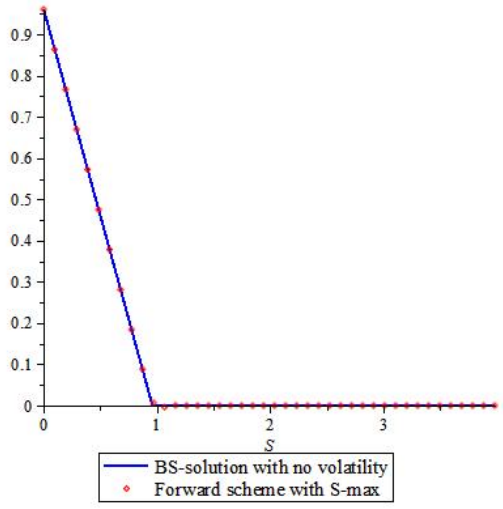

(e) Option Price, $\sigma = 0$.

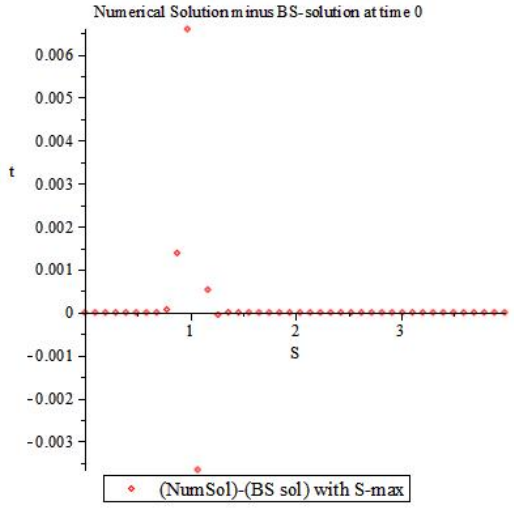

(f) Error curve, $\sigma = 0$.

FIGURE 3.2.11: The left curves show option price and the right curves error $\{e_{0,n}\}_{n=1}^{N}$ for the put option at $t = 0$ with $S_{\max} \simeq 4K$ and $K_\alpha = 0.3$ in the standard case except for σ with(a)-(b) $\sigma = 0.2$, (c)-(d) $\sigma = 0.001$, and (e)-(f) $\sigma = 0$ with the coarse mesh $h \simeq 0.1$, $k \simeq= 0.001$ and with the forward Euler method

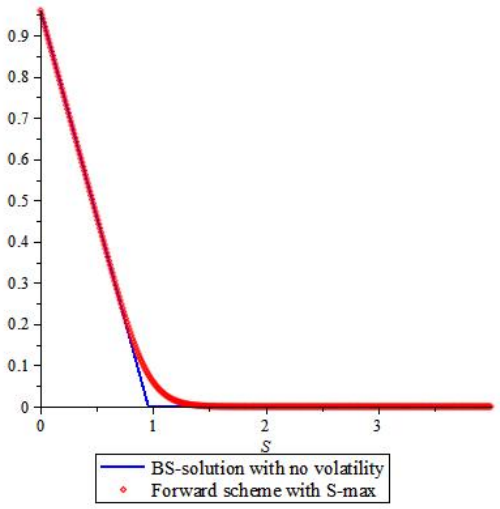

(a) Option Price, $\sigma = 0.2$.

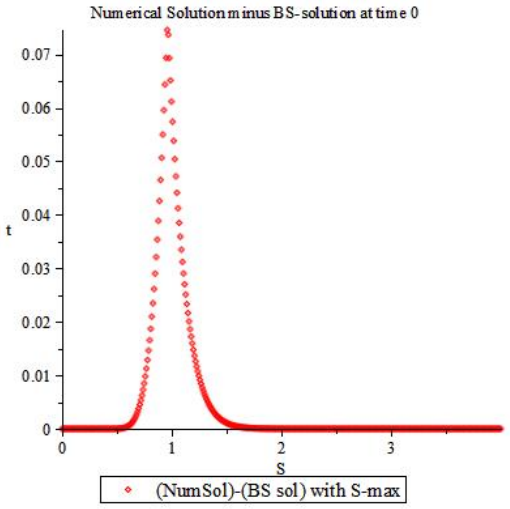

(b) Error curve, $\sigma = 0.2$.

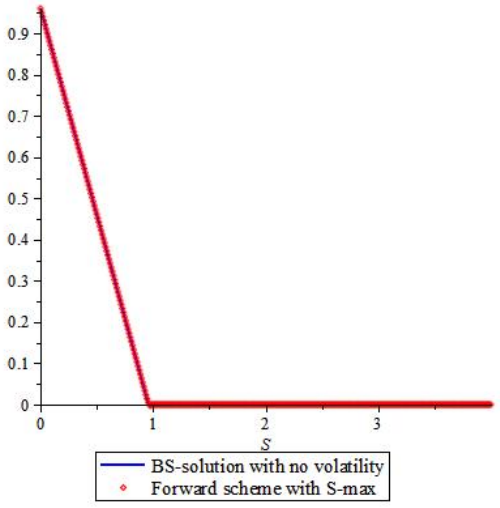

(c) Option Price, $\sigma = 0.001$.

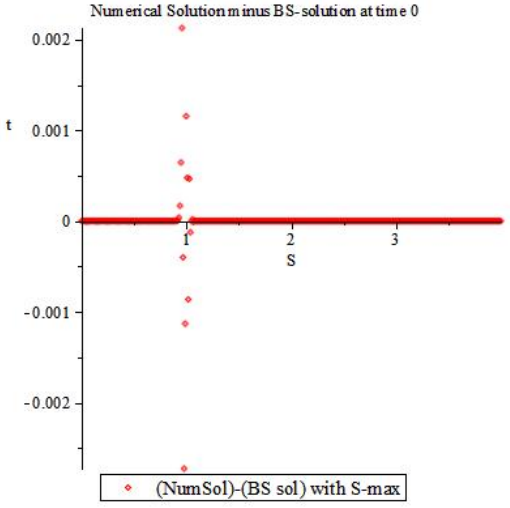

(d) Error curve, $\sigma = 0.001$.

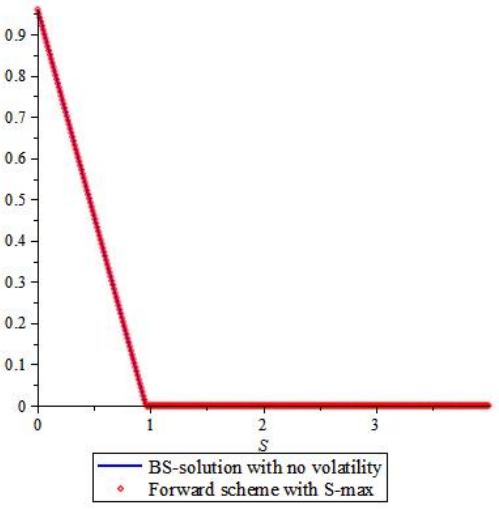

(e) Option Price, $\sigma = 0$.

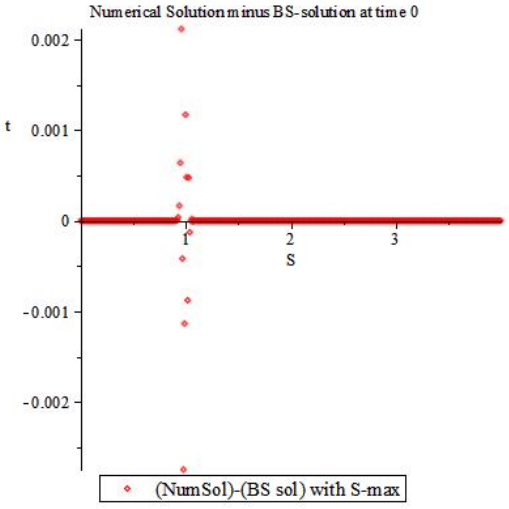

(f) Error curve, $\sigma = 0$.

FIGURE 3.2.12: The left curves show option price and the right curves error $\{e_{0,n}\}_{n=1}^{N}$ for the put option at $t = 0$ with $S_{\max} \simeq 4K$ and $K_\alpha = 0.3$ in the standard case except for σ with(a)-(b) $\sigma = 0.2$, (c)-(d) $\sigma = 0.001$, and (e)-(f) $\sigma = 0$ with the fine mesh $h \simeq 0.01$, $k \simeq= 0.00001$ and with the forward Euler method

3.2.6 Expiration limit

We have concluded in subsection 3.2.4 that the singularity at $S = K$ for $t = T$ for the put, call and bet options give rise to large errors for all values of t down to 0 and for S-values close to K. Here we investigate the expiration limit i.e. $\lim_{t\uparrow T} \tilde{V}(S,t) - V(S,T)$ where $\tilde{V}$ is the numerical solution.

TABLE 3.2.18: Maximal error e_0 for the put option at $t = T - k$ with $S_{\max} \simeq 4K$ and $K_\alpha = 0.3$ in the standard case with the forward Euler method

h \ k	.1	.01	.001	.0001	.00001	.000001
.5	0.00330986	0.000365137	3.65209e-05	3.65220e-06	3.65200e-07	3.65200e-08
.1	0.00195856	0.000859999	0.000149512	1.49515e-05	1.49515e-06	1.49515e-07
.01	0.115326	0.00736102	0.000173821	8.18825e-05	1.40976e-05	1.40977e-06

TABLE 3.2.19: Maximal error e_0 for the put option at $t = T - 5k$ with $S_{\max} \simeq 4K$ and $K_\alpha = 0.3$ in the standard case with the forward Euler method

h \ k	.1	.01	.001	.0001	.00001	.000001
.5	0.00591054	0.00181311	0.000182598	1.82608e-05	1.82600e-06	1.82500e-07
.1	0.000971536	0.00182457	0.000647555	7.47198e-05	7.47536e-06	7.47550e-07
.01	921821	4.51905	8.46229e-05	0.00018975	6.13366e-05	7.04452e-06

TABLE 3.2.20: Maximal error e_0 for the call option at $t = T - k$ with $S_{\max} \simeq 4K$ and $K_\alpha = 0.3$ in the standard case with the forward Euler method

h \ k	.1	.01	.001	.0001	.00001	.000001
.5	0.00331785	0.000365217	3.65217e-05	3.65217e-06	3.65217e-07	3.65217e-08
.1	0.00196655	0.000860079	0.000149513	1.49515e-05	1.49515e-06	1.49515e-07
.01	0.115334	0.0073611	0.000173821	8.18826e-05	1.40976e-05	1.40977e-06

TABLE 3.2.21: Maximal error e_0 for the call option at $t = T - 5k$ with $S_{\max} \simeq 4K$ and $K_\alpha = 0.3$ in the standard case with the forward Euler method

h \ k	.1	.01	.001	.0001	.00001	.000001
.5	0.00594985	0.00181351	0.000182602	1.82608e-05	1.82609e-06	1.82609e-07
.1	0.00676164	0.00182497	0.000647559	7.47198e-05	7.47535e-06	7.47569e-07
.01	1.16591e+06	4.51905	0.000173821	0.000189751	6.13366e-05	7.04452e-06

TABLE 3.2.22: Maximal error e_0 for the bet option at $t = T - k$ with $S_{\max} \simeq 4K$ and $K_\alpha = 0.5$ in the standard case with the forward Euler method

h \ k	.1	.01	.001	.0001	.00001	.000001
.5	0.00352959	0.000360024	3.60002e-05	3.60000e-06	3.60000e-07	3.60000e-08
.1	0.00479606	0.00433301	0.00066	6.60000e-05	6.60000e-06	6.60000e-07
.01	5.9237	0.486603	0.00422699	0.00415875	0.000606	6.06000e-05

TABLE 3.2.23: Maximal error e_0 for the bet option at $t = T - 5k$ with $S_{\max} \simeq 4K$ and $K_\alpha = 0.5$ in the standard case with the forward Euler method

h \ k	.1	.01	.001	.0001	.00001	.000001
.5	0.00945254	0.00178699	0.00017987	1.79987e-05	1.79999e-06	1.80000e-07
.1	0.00479606	0.014457	0.00317254	0.000329586	3.29959e-05	3.29996e-06
.01	1.21441e+08	627.543	0.00422699	0.013079	0.00293048	0.000302635

TABLE 3.2.24: Maximal error e_0 for the smoothened put option at $t = T - k$ with $S_{\max} \simeq 30K$ in the standard case with the forward Euler method

h \ k	.1	.01	.001	.0001	.00001	.000001
.5	0.00016328	1.55526e-05	1.55440e-06	2.71270e-07	1.18485e-05	4.90119e-05
.1	1.64707e-05	8.41900e-07	1.34900e-07	1.21080e-06	1.57217e-05	8.20377e-05
.01	9.28420e-06	1.04300e-07	2.99900e-07	2.52440e-06	2.14538e-05	0.000283342

TABLE 3.2.25: Maximal error e_0 for the smoothened put option at $t = T - 5k$ with $S_{\max} \simeq 30K$ in the standard case with the forward Euler method

h \ k	.1	.01	.001	.0001	.00001	.000001
.5	0.000814118	7.77619e-05	7.74500e-06	7.80100e-07	1.58410e-06	1.18576e-05
.1	8.17004e-05	4.19010e-06	3.73600e-07	4.12400e-07	3.49770e-06	4.63119e-05
.01	1551.52	0.0151725	1.21505e-07	5.16000e-07	3.85330e-06	3.60322e-05

3.3 Numerical results for the backward Euler method

In this section we consider the Backward Euler method for the standard case $T = 1$, $K = 1$, $B = 0.3$, $r = 0.04$, $\gamma = 0$ and $\sigma = 0.2$ with the same computational setup as described in section 3.2.1. Since the backward Euler method is implicit, the computing times are significantly higher than for the forward Euler method.

3.3.1 Computational results for the standard case

First we compute the maximal error e_0 (see 3.4) at time $t = 0$ with $S_{\max} \simeq 4K$, $2K$, $1.5K$ and $1.25K$ for the put option in the standard case with the backward Euler method. The results are shown in tables 3.3.1–3.3.4. Also the errors $\{e_0, n\}_{n=1}^{N}$ (see 3.5) are plotted in Figures 3.3.1–3.3.2 for a coarse and a fine mesh and $S_{\max} \simeq 4K$, $2K$, $1.5K$ and $1.25K$.

TABLE 3.3.1: Maximal error e_0 for the put option at $t = 0$ for $S_{\max} \simeq 4K$ and $K_\alpha = 0.3$ in the standard case with the backward Euler method.

h \ k	.3	.2	.1	.01	.001	.0001
.5	0.00609529	0.00633076	0.00651671	0.00669163	0.00670955	0.00671134
.4	0.00384639	0.00362807	0.00377233	0.00402266	0.00404835	0.00405093
.3	0.00462138	0.00411196	0.003704	0.00331544	0.00327538	0.00327136
.2	0.00448745	0.00372868	0.00311489	0.00252487	0.00246372	0.00245758
.1	0.00345368	0.00230403	0.00141278	0.000619103	0.000563741	0.000558176
.08	0.00328116	0.00210526	0.00120253	0.000406398	0.000349258	0.000343511
.06	0.00322514	0.00202104	0.00109011	0.000283795	0.000221138	0.000214835
.05	0.00323412	0.00201015	0.0010629	0.000225674	0.000163177	0.000156889
.04	0.00323177	0.00199248	0.00103742	0.000174862	0.000108983	0.00010236
.03	0.00321785	0.00197012	0.0010115	0.000134884	6.34725e-5	5.69204e-5
.02	0.00319782	0.00194879	0.000990868	0.00011523	3.35668e-5	2.70425e-5
.01	0.00318483	0.00193659	0.000978546	0.000102356	1.41839e-5	7.41565e-6
.001	0.00317989	0.00193236	0.000974538	9.81804e-5	9.86248e-6	1.02276e-6

TABLE 3.3.2: Maximal error e_0 for the put option at $t = 0$ for $S_{\max} \simeq 2K$ and $K_\alpha = 0.3$ in the standard case with the backward Euler method

h \ k	.3	.2	.1	.01	.001	.0001
.5	0.00592172	0.00618406	0.00639076	0.00658473	0.00660456	0.00660655
.4	0.00384835	0.00362908	0.00376364	0.0040174	0.00404339	0.004046
.3	0.00462213	0.00411226	0.00370411	0.00331547	0.0032754	0.00327138
.2	0.00448786	0.00372881	0.00311492	0.00252487	0.00246373	0.00245759
.1	0.00345381	0.00230406	0.00141279	0.000619103	0.000563741	0.000558176
.08	0.00328127	0.00210527	0.00120253	0.000406398	0.000349258	0.000343511
.06	0.0032253	0.00202108	0.00109011	0.000283796	0.000221138	0.000214835
.05	0.00323426	0.00201018	0.0010629	0.000225674	0.000163177	0.000156889
.04	0.00323189	0.0019925	0.00103742	0.000174862	0.000108983	0.00010236
.03	0.00321795	0.00197013	0.0010115	0.000134884	6.34725e-5	5.69205e-5
.02	0.00319791	0.00194881	0.000990869	0.00011523	3.35668e-5	2.70425e-5
.01	0.00318492	0.0019366	0.000978547	0.000102356	1.41839e-5	8.75748e-6
.001	0.00317997	0.00193237	0.000974539	9.81804e-5	9.8625e-6	8.21241e-06

TABLE 3.3.3: Maximal error e_0 for the put option at $t = 0$ for $S_{\max} \simeq 1.5K$ and $K_\alpha = 0.3$ in the standard case with the backward Euler method

h \ k	.3	.2	.1	.01	.001	.0001
.5	0.00608397	0.00618406	0.00639076	0.00658473	0.00660456	0.00660655
.4	0.00375692	0.00366857	0.00348810	0.00367456	0.00370539	0.00370848
.3	0.00431481	0.00411786	0.00370732	0.00331706	0.00327687	0.00327283
.2	0.00404811	0.00375119	0.00312869	0.00253232	0.00247063	0.00246444
.1	0.00275091	0.00231131	0.00141581	0.00065754	0.00065754	0.00065754
.08	0.00257032	0.00212018	0.00120921	0.00104401	0.00104401	0.00104401
.06	0.00251582	0.00204956	0.00109854	0.00105242	0.00105242	0.00105242
.05	0.00249824	0.00202773	0.00107062	0.00084084	0.00084084	0.00084084
.04	0.00249322	0.00201610	0.00106134	0.00106134	0.00106134	0.00106134
.03	0.00246513	0.00198700	0.00101864	0.00093185	0.00093185	0.00093185
.02	0.00244382	0.00196552	0.00099786	0.00097696	0.00097696	0.00097696
.01	0.00243401	0.00195532	0.00102750	0.00102750	0.00102750	0.00102750
.001	0.00243205	0.00195318	0.00107541	0.00107541	0.00107541	0.00107541

TABLE 3.3.4: Maximal error e_0 for the put option at $t = 0$ for $S_{\max} \simeq 1.25K$ and $K_\alpha = 0.3$ in the standard case with the backward Euler method

h \ k	.3	.2	.1	.01	.001	.0001
.5	0.00612437	0.00612437	0.00612437	0.00612437	00612437	0.00612437
.4	0.00375692	0.00366857	0.0034881	0.00367456	00370539	0.00370848
.3	0.00446444	0.00425374	0.00381534	0.0033999	0.0033572	0.00335292
.2	0.00532862	0.00532862	0.00532862	0.00532862	0.00532862	0.00532862
.1	0.0087067	0.0087067	0.0087067	0.0087067	0.0087067	0.0087067
.08	0.00762432	0.00762432	0.00762432	0.00762432	0.00762432	0.00762432
.06	0.0080478	0.0080478	0.0080478	0.0080478	0.0080478	0.0080478
.05	0.0074617	0.0074617	0.0074617	0.0074617	0.0074617	0.0074617
.04	0.00851633	0.00851633	0.00851633	0.00851633	0.00851633	0.00851633
.03	0.00933452	0.00933452	0.00933452	0.00933452	0.00933452	0.00933452
.02	0.00942338	0.00942338	0.00942338	0.00942338	0.00942338	0.00942338
.01	0.00913899	0.00913899	0.00913899	0.00913899	0.00913899	0.00913899
.001	0.0095676	0095676	0.0095676	0.0095676	0.0095676	0.0095676

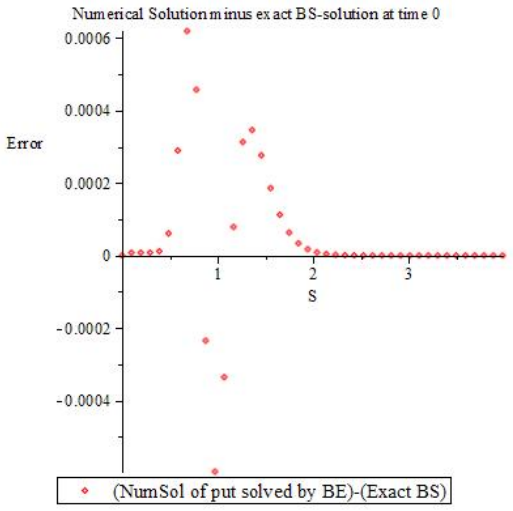

(a) BE error, coarse mesh, $S_{\max} \simeq 4K$.

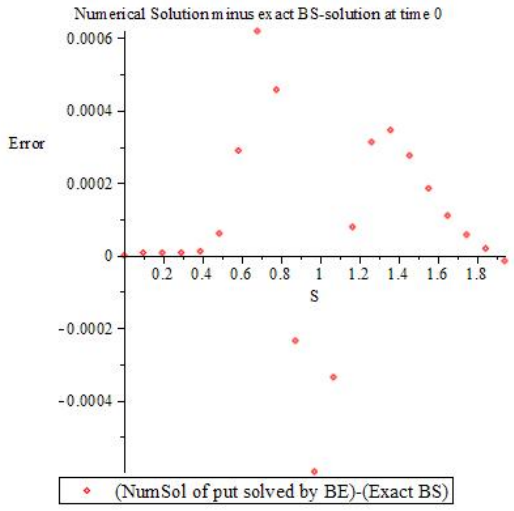

(b) BE error, coarse mesh, $S_{\max} \simeq 2K$.

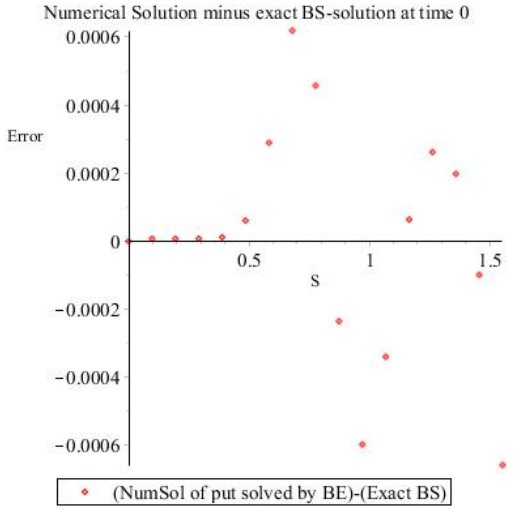

(c) BE error, coarse mesh, $S_{\max} \simeq 1,5K$.

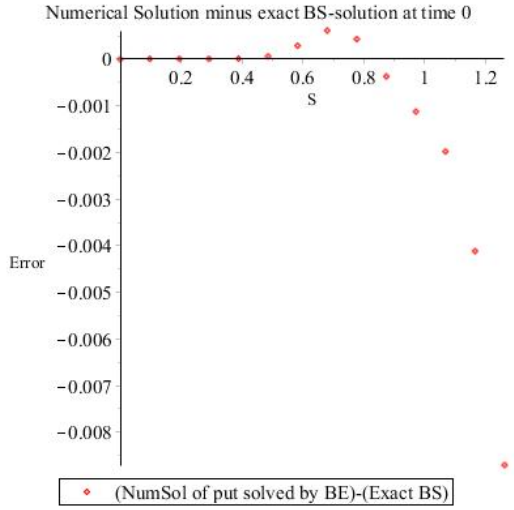

(d) BE error, coarse mesh, $S_{\max} \simeq 1.25K$.

FIGURE 3.3.1: Error $\{e_{0,n}\}_{n=1}^{N}$ at $t = 0$ for the put option and $S_{\max} \simeq$ (a) $4K$, (b) $2K$, (c) $1.5K$ and (d) $1.25K$ for stepsizes $h \simeq 0.1$ and $k \simeq 0.01$ and $K_\alpha = 0.3$ in the standard case with the backward Euler method.

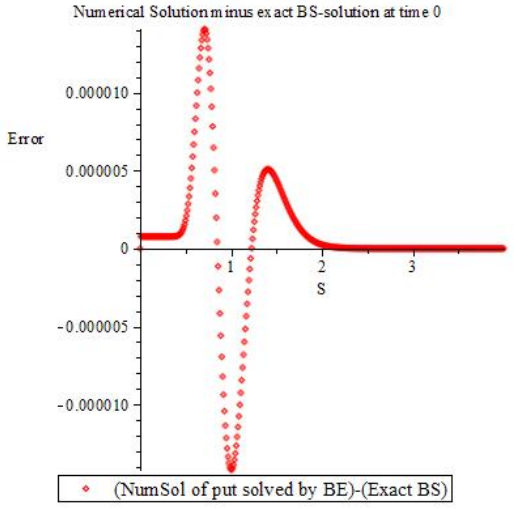

(a) BE error, fine mesh, $S_{\max} \simeq 4K$.

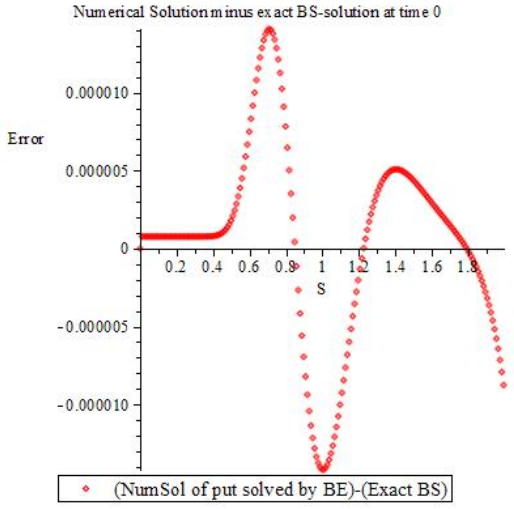

(b) BE error, fine mesh, $S_{\max} \simeq 2K$.

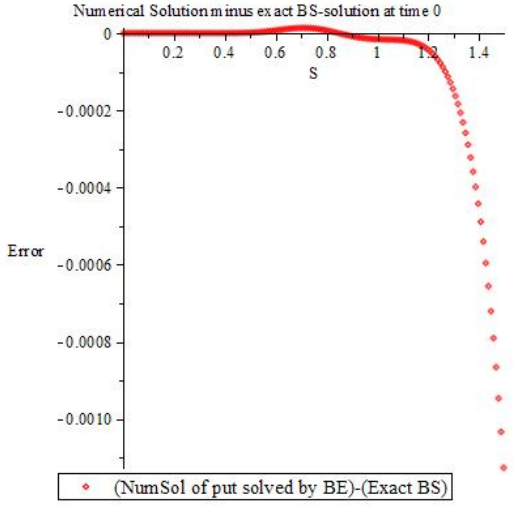

(c) BE error, fine mesh, $S_{\max} \simeq 1,5K$.

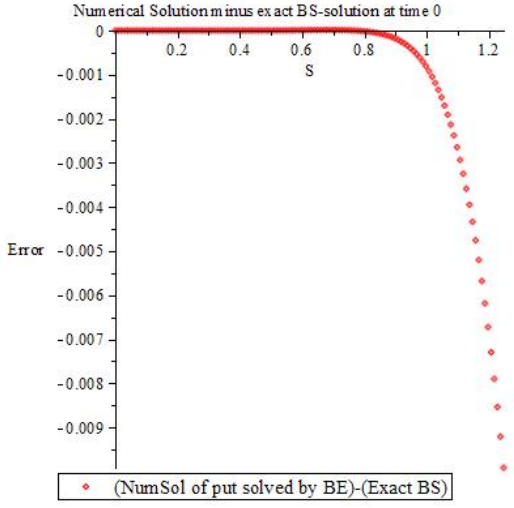

(d) BE error, fine mesh, $S_{\max} \simeq 1.25K$.

FIGURE 3.3.2: Error $\{e_{0,n}\}_{n=1}^{N}$ at $t = 0$ for the put option and $S_{\max} \simeq$ (a) $4K$, (b) $2K$, (c) $1.5K$ and (d) $1.25K$ for stepsizes $h \simeq 0.01$ and $k \simeq 0.001$ and $K_\alpha = 0.3$ in the standard case with the backward Euler method.

Next we consider the maximal error e_0 at time $t = 0$ with $S_{\max} \simeq 4K$ for the call option in the standard case with the backward Euler method. The results are shown in Table 3.3.5.

TABLE 3.3.5: Maximal error e_0 for the call option at $t = 0$ with $S_{\max} \simeq 4K$ and $K_\alpha = 0.3$ in the standard case with the backward Euler method.

h \ k	.3	.2	.1	.01	.001	.0001
.5	0.00584133	0.00617784	0.00644005	0.00668395	0.00670878	.00671127
.4	0.00410038	0.00378099	0.00369567	0.00401498	0.00404758	0.00405085
.3	0.00487537	0.00426488	0.00378066	0.00332312	0.00327615	0.00327144
.2	0.00474144	0.0038816	0.00319155	0.00253255	0.00246449	0.00245766
.1	0.00370767	0.00245695	0.00148944	0.000611419	0.000562973	0.000558099
.08	0.00353515	0.00225818	0.00127919	0.000398713	0.00034849	0.000343434
.06	0.00347913	0.00217397	0.00116677	0.000276111	0.00022037	0.000214758
.05	0.00348811	0.00216308	0.00113956	0.000218683	0.000162408	0.000156813
.04	0.00348576	0.00214541	0.00111408	0.000176433	0.000108215	0.000102283
.03	0.00347183	0.00212304	0.00108816	0.000142568	6.27039e-5	5.68435e-5
.02	0.00345181	0.00210172	0.00106753	0.000122914	3.27982e-5	2.69657e-5
.01	0.00343882	0.00208951	0.00105521	0.00011004	1.49526e-5	7.33879e-6
.001	0.00343326	0.00208528	0.0010512	0.000105865	1.06311e-5	1.11788e-6

Now we consider the maximal error e_0 at time $t = 0$ with $S_{\max} \simeq 4K$ for the bet option in the standard case with the backward Euler method. The results are shown in Table 3.3.6. Finally we consider the maximal error e_0 at time $t = 0$ with $S_{\max} \simeq 30K$

TABLE 3.3.6: Maximal error e_0 for the bet option at $t = 0$ with $S_{\max} \simeq 4K$ and $K_\alpha = 0.5$ in the standard case with the backward Euler method.

h \ k	.3	.2	.1	.01	.001	.0001
.5	0.0191664	0.0184684	0.0179142	0.0173906	0.0173369	0.0173315
.4	0.0191664	0.0184684	0.0179142	0.0173906	0.0173369	0.0173315
.3	0.0233774	0.0220285	0.0209460	0.0199133	0.0198068	0.0197961
.2	0.0193172	0.0163493	0.0139397	0.0116225	0.0113826	0.0113586
.1	0.0102039	0.0075571	0.0053355	0.0031568	0.0029305	0.0029078
.08	0.0098829	0.0068268	0.0043824	0.0021216	0.0018953	0.0018726
.06	0.0084057	0.0056381	0.0033703	0.0012254	0.0010078	0.0009860
.05	0.0084496	0.0054217	0.0030508	0.0009371	0.0007381	0.0007181
.04	0.0079794	0.0051162	0.0028181	0.0006869	0.0004774	0.0004580
.03	0.0078160	0.0049174	0.0026128	0.0004926	0.0002892	0.0002689
.02	0.0077169	0.0047655	0.0024506	0.0003494	0.0001392	0.0001188
.01	0.0076450	0.0046647	0.0023648	0.0002628	0.0000525	0.0000317
.001	0.0076188	0.0046369	0.0023344	0.0002343	0.0000237	2.63038e-6

for the smoothened put option in the standard case with the backward Euler method. The results are shown in Table 3.3.7.

TABLE 3.3.7: Maximal error e_0 for the smoothened put option at $t = 0$ with $S_{\max} \simeq 30K$ in the standard case with the backward Euler method.

h \ k	.3	.2	.1	.01	.001	.0001
.5	0.00133865	0.00137846	0.00145861	0.00153132	0.00153862	0.00153935
.4	0.000528457	0.000570851	0.000656069	0.000733258	0.000741002	0.000741777
.3	0.000222407	0.000260449	0.000337129	0.000406829	0.000413835	0.000414536
.2	9.80089e-005	0.000116921	0.000200182	0.000275735	0.000283323	0.000284082
.1	0.000157431	0.000117528	3.74274e-005	6.60896e-005	7.36013e-005	7.43528e-005
.08	0.000176201	0.000136901	5.8008e-005	3.63254e-005	4.39059e-005	4.46643e-005
.06	0.000192115	0.000149016	6.82257e-005	1.79547e-005	2.56681e-005	2.64405e-005
.05	0.000199072	0.000155875	7.15357e-005	1.07863e-005	1.84008e-005	1.9174e-005
.04	0.000205495	0.000162334	7.56172e-005	4.36875e-006	1.15366e-005	1.23051e-005
.03	0.000211081	0.000167848	8.09551e-005	6.3233e-006	5.88777e-006	6.65884e-006
.02	0.000214585	0.000171347	8.44484e-005	7.25001e-006	2.2793e-006	3.04957e-006
.01	0.000216855	0.000173615	8.67112e-005	8.01286e-006	7.10504e-007	7.05265e-007
.001	0.000217601	0.000174376	8.74691e-005	8.76639e-006	8.70483e-007	4.77757e-007

3.3.2 Computational results for nonstandard cases

Here we consider robustness in the selection of $S_{\max}$ against variations in the other parameters in the problem when solving with the backward Euler method like we have done for the forward Euler method in section 3.2.2. As we have mentioned before, since backward Euler is an implicit method it is also computationally more demanding than the forward Euler method. Therefore we choose somewhat coarser meshes both for the coarse mesh and for the fine mesh calculations. We choose a coarse mesh with $h \simeq 0.1$ and $k \simeq 0.01$ and a fine mesh with $h \simeq 0.01$ and $k \simeq 0.001$. For each mesh, we shall find the smallest value of $S_{\max}$ where the error in $S = S_{\max}$ is negligible compared to the maximal error e_0.

As observed when solving with the forward Euler method, we expect no significant differences between the results for the put, call and bet options. Hence we compute only for the put option. The results for the coarse mesh are shown in Tables 3.3.8 and 3.3.9 and the results for the fine mesh are shown in Tables 3.3.10 and 3.3.11. In Figure 3.3.3 we show $\{e_{0,n}\}_{n=0}^{N}$ (see 3.5) for the standard case except for $T = 0.1$ and $T = 10$ for the coarse and fine meshes. Figure 3.3.3(a) and (b) should be compared to Figure 3.3.1(a) and Figure 3.3.3(c) and (d) should be compared to Figure3.3.2(a).

TABLE 3.3.8: Smallest $S_{\max}$ not giving significant error at $S = S_{\max}$ with the coarse mesh $h \simeq 0.1$, $k \simeq 0.01$ and $K_\alpha = 0.3$ in various nonstandard cases for the put option with the backward Euler method. "-" indicates a case where it has not been possible to establish a functional $S_{\max}$.

	$K = 10$				$K = 1$				$K = 0.1$			
	σ / r	.01	.2	.9	σ / r	.01	.2	.9	σ / r	.01	.2	.9
$T = 10$	.001	$1.25K$	-	-	.001	$1.5K$	$15K$	-	.001	$4K$	$14K$	-
	.04	$1.25K$	-	-	.04	$3K$	$10K$	-	.04	$8K$	$8K$	-
	.1	$1.25K$	$6K$	-	.1	$4K$	$4K$	-	.1	$10K$	$4K$	-
$T = 1$	σ / r	.01	.2	.9	σ / r	.01	.2	.9	σ / r	.01	.2	.9
	.001	$1.25K$	$3K$	-	.001	$1.5K$	$3K$	$70K$	.001	$4K$	$5K$	$50K$
	.04	$1.25K$	$3K$	-	.04	$2K$	$3K$	$60K$	.04	$4K$	$5K$	$40K$
	.1	$1.25K$	$3K$	-	.1	$2K$	$3K$	$60K$	.1	$4K$	$4K$	$30K$
$T = .1$	σ / r	.01	.2	.9	σ / r	.01	.2	.9	σ / r	.01	.2	.9
	.001	$1.25K$	$1.5K$	$4K$	.001	$1.5K$	$2K$	$4K$	.001	$4K$	$4K$	$7K$
	.04	$1.25K$	$1.5K$	$4K$	.04	$1.5K$	$2K$	$4K$	.04	$4K$	$4K$	$7K$
	.1	$1.25K$	$1.5K$	$4K$	.1	$1.5K$	$2K$	$4K$	.1	$4K$	$4K$	$7K$

TABLE 3.3.9: Smallest $S_{\max}$ not giving significant error at $S = S_{\max}$ with the coarse mesh $h \simeq 0.1$, $k \simeq 0.01$ and $K_\alpha = 0.3$ in the standard case except for γ in the put option with the backward Euler method.

γ	0	0.5	1.0
$\min S_{\max}$	$3K$	$3K$	$5K$

TABLE 3.3.10: Smallest $S_{\max}$ not giving significant error at $S = S_{\max}$ with the fine mesh $h \simeq 0.01$, $k \simeq 0.001$ and $K_\alpha = 0.3$ in various nonstandard fine for the put option with the backward Euler method. "-" indicates a case where it has not been possible to establish a functional $S_{\max}$.

	$K = 10$				$K = 1$				$K = 0.1$			
	σ / r	.01	.2	.9	σ / r	.01	.2	.9	σ / r	.01	.2	.9
$T = 10$	.001	-	-	-	.001	$1.25K$	-	-	.001	$1.5K$	$20K$	-
	.04	-	-	-	.04	$1.25K$	-	-	.04	$3K$	$15K$	-
	.1	-	-	-	.1	$1.25K$	-	-	.1	$4K$	$4K$	-
$T = 1$	σ / r	.01	.2	.9	σ / r	.01	.2	.9	σ / r	.01	.2	.9
	.001	$1.25K$	-	-	.001	$1.25K$	$3K$	-	.001	$1.5K$	$3K$	$50K$
	.04	$1.25K$	-	-	.04	$1.25K$	$3K$	-	.04	$1.5K$	$3K$	$50K$
	.1	$1.25K$	-	-	.1	$1.25K$	$3K$	-	.1	$2K$	$3K$	$50K$
$T = .1$	σ / r	.01	.2	.9	σ / r	.01	.2	.9	σ / r	.01	.2	.9
	.001	$1.25K$	$1.5K$	$4K$	.001	$1.25K$	$1.5K$	$4K$	.001	$1.5K$	$2K$	$4K$
	.04	$1.25K$	$1.5K$	$4K$	.04	$1.25K$	$1.5K$	$4K$	.04	$1.5K$	$2K$	$4K$
	.1	$1.25K$	$1.5K$	$4K$	.1	$1.25K$	$1.5K$	$4K$	.1	$1.5K$	$2K$	$4K$

TABLE 3.3.11: Smallest $S_{\max}$ not giving significant error at $S = S_{\max}$ with the fine mesh $h \simeq 0.01$, $k \simeq 0.001$ and $K_\alpha = 0.3$ in the standard case except for γ in the put option with the backward Euler method.

γ	0	0.5	1.0
$\min S_{\max}$	$3K$	$3K$	$5K$

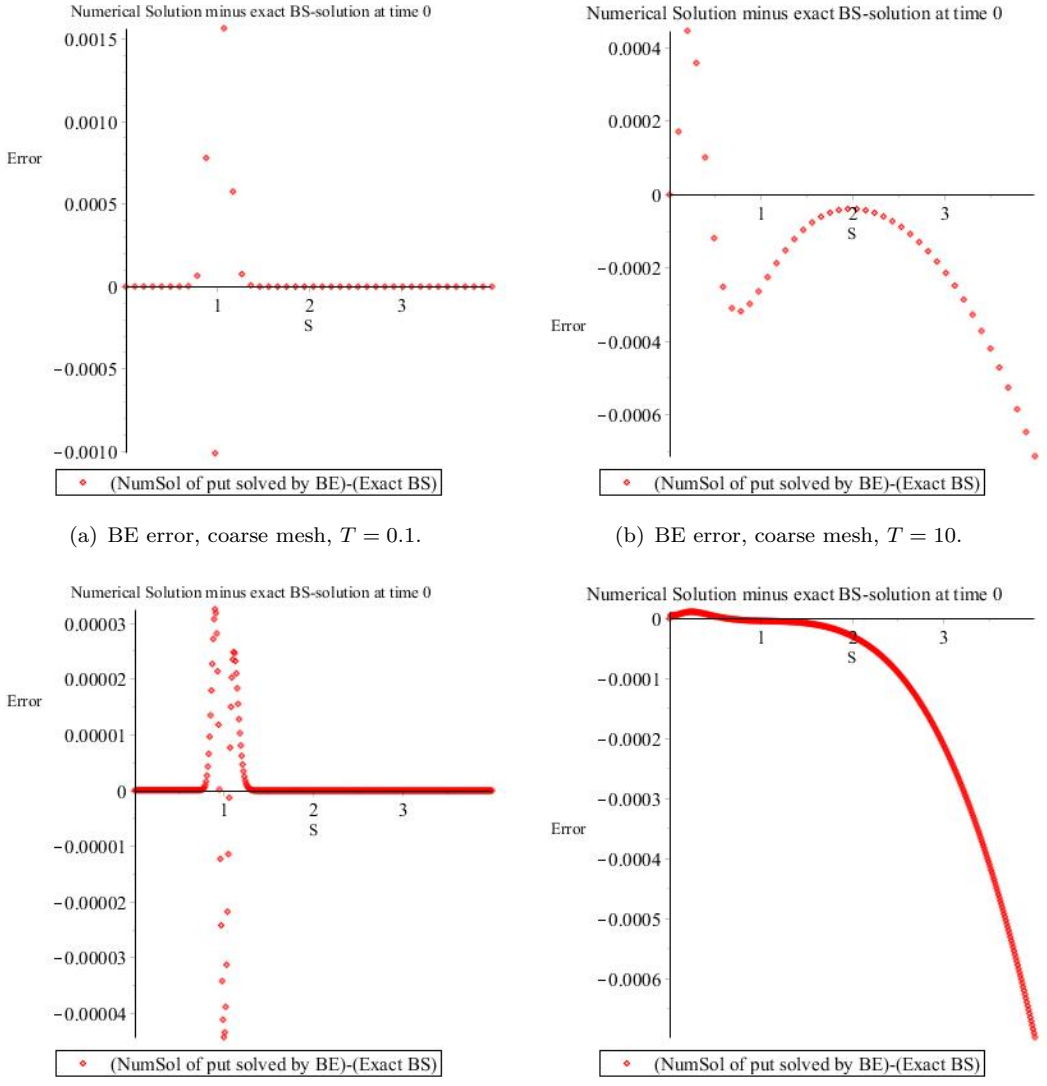

(a) BE error, coarse mesh, $T = 0.1$.

(b) BE error, coarse mesh, $T = 10$.

(c) BE error, fine mesh, $T = 0.1$.

(d) BE error, fine mesh, $T = 10$.

FIGURE 3.3.3: Error $\{e_{0,n}\}_{n=1}^{N}$ at $t = 0$ for the put option with $S_{\max} \simeq 4K$ (a) $h \simeq 0.1$, $k \simeq 0.01$, $T = 0.1$, (b) $h \simeq 0.1$, $k \simeq 0.01$, $T = 10$, (c) $h \simeq 0.01$, $k \simeq 0.001$, $T = 0.1$ and (d) $h \simeq 0.01$, $k \simeq 0.001$, $T = 10$ and $K_\alpha = 0.3$, in the standard case apart from the value of T with the backward Euler method.

3.3.3 Sensitivity to $S_{\max}$

Tables 3.3.8 and 3.3.10 show the smallest $S_{\max}$ with the backward Euler method are very similar to tables 3.2.9 and 3.2.11 show the smallest $S_{\max}$ with the forward Euler method. There is a big difference however. Whereas the forward Euler method is only conditionally stable, the backward Euler method is unconditionally stable. Hence the large values of $S_{\max}$ for the backward Euler case — in particular for $\sigma = 0.9$ but also in some cases for $\sigma = 0.2$ — can not be explained by instability as we did for the forward Eular case. We may "discard" the results with $\sigma = 0.9$ as being extreme cases since $\sigma > 0.5$ is generally considered such, but this is not sufficient to explain the results. Instead looking at the error plots corresponding to the ones in Figure 3.3.3 — which are the ones used for deciding on the minimal $S_{\max}$ — it seems that the error originating near $S = K$ from the discontinuity in the first derivative in the terminal condition decay more and more slowly as σ is increasing. Hence the reason for the non-vanishing error in $S = S_{\max}$ is not that the boundary condition is introducing an error, but that the error from $S = K$ has simply not yet vanished. For example for the coarse mesh $h = 0.1$ and $k = 0.01$ in the case $T = 10$, $K = 0.1$, $B = 0.3$, $r = 0.001$, $\gamma = 0$ and $\sigma = 0.2$ the maximal error with the "preferred" $S_{\max} = 14K$ is $e_0 = 0.0020457$ whereas the maximal error with $S_{\max} = 4K$ is almost the same, namely $e_0 = 0.0020464$.

Hence the results with the backward Euler method confirm the results with the forward Euler method: $S_{\max} \simeq 4K$ seems to be adequate independently of the numerical scheme used for the solution.

3.3.4 Convergence

First we consider the put option in the standard case with $S_{\max} = 4K$ solved with the backward Euler method. Plotting the maximal errors e_0 (see 3.4) at time $t = 0$ from Table 3.3.1 with logarithmic axes, we get the result shown in Figure 3.3.4. From the data in Table 3.3.1 we get the following convergence result:

$$e_0 \simeq 0.069h^2 + 0.006k \tag{3.12}$$

Unlike what is observed for the forward Euler method, here we get the expected quadratic convergence in S and linear convergence in t.

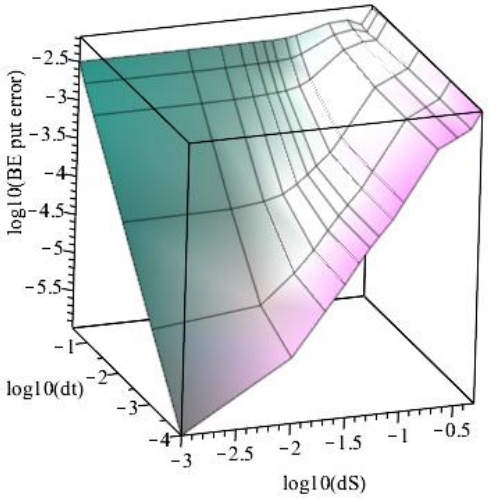

FIGURE 3.3.4: Plot of maximal error e_0 at time $t = 0$ (see 3.4) as a function of stepsizes $dS = h$ and $dt = k$ (logarithmic axes) for the put option in the standard case with $S_{\max} = 4K$ and $K_\alpha = 0.3$ with the backward Euler method. In this case the maximal error is attained in the interior of the S-interval, close to $S = K$.

In Figure 3.3.5 we show the error $e_{0,nm}$ (see 3.8) as a function of both S and t for 5 different meshes: Mesh 1: $h \simeq 0.1$, $k \simeq 0.1$, Mesh 2: $h \simeq 0.1$, $k \simeq 0.01$, Mesh 3: $h \simeq 0.1$, $k \simeq 0.001$, Mesh 4: $h \simeq 0.05$, $k \simeq 0.001$, Mesh 5: $h \simeq 0.03$, $k \simeq 0.001$.

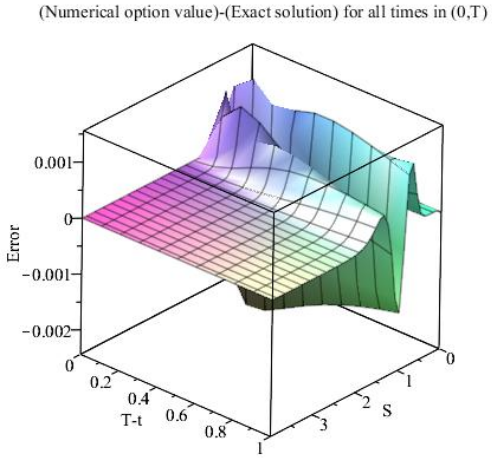

(a) Mesh 1 error.

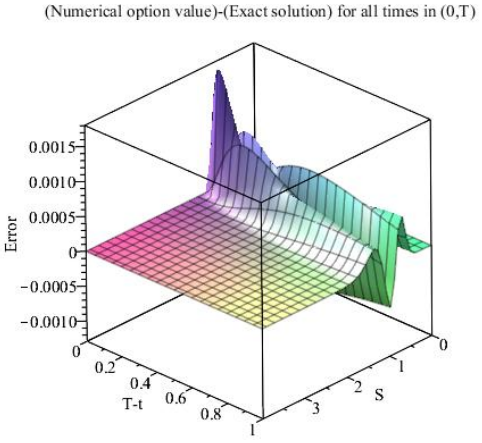

(b) Mesh 2 error.

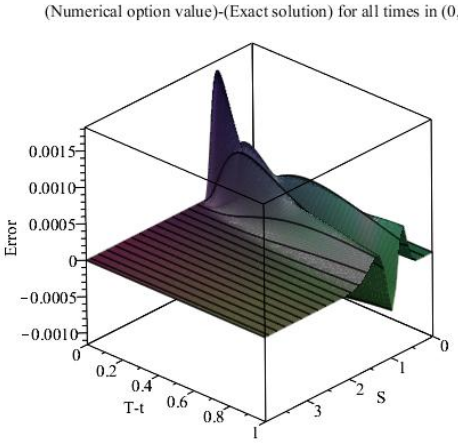

(c) Mesh 3 error.

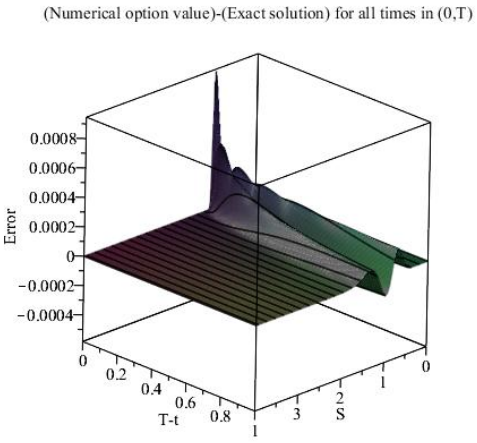

(d) Mesh 4 error.

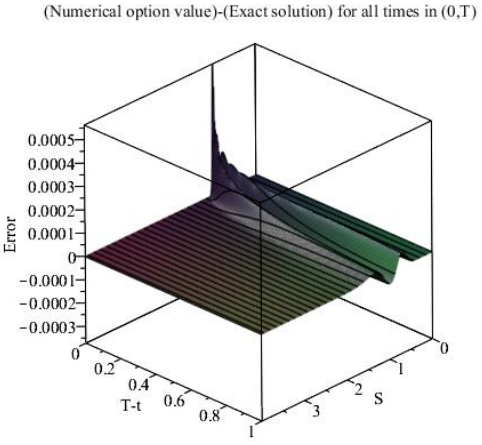

(e) Mesh 5 error.

FIGURE 3.3.5: Plot of the error as a function of S and t for the put option with $S_{\max} = 4K$ and $K_\alpha = 0.3$ with the backward Euler method for mesh 1 (a), mesh 2 (b), mesh 3 (c), mesh 4 (d) and mesh 5 (e).

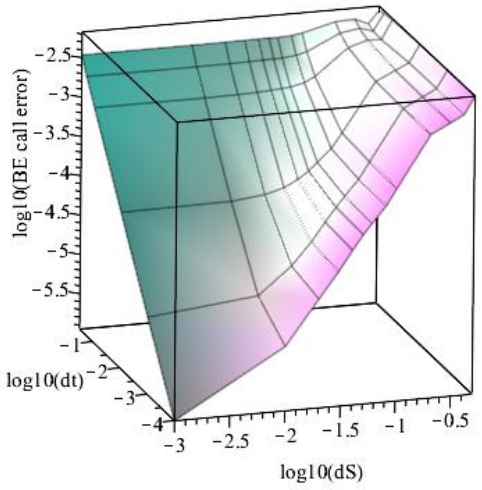

FIGURE 3.3.6: Plot of maximal error e_0 at time $t = 0$ (see 3.4) as a function of stepsizes $dS = h$ and $dt = k$ (logarithmic axes) for the call option in the standard case with $S_{\max} = 4K$ and $K_\alpha = 0.3$ with the backward Euler method. In this case the maximal error is attained in the interior of the S-interval, close to $S = K$.

Next we turn to the call option in the standard case with $S_{\max} = 4K$ solved with the backward Euler method. Plotting the maximal errors e_0 (see 3.4) at time $t = 0$ from Table 3.3.5 with logarithmic axes, we get the result shown in Figure 3.3.6. From the data in Table 3.3.5 we get the following convergence result:

$$e_0 \simeq 0.07h^2 + 0.006k \tag{3.13}$$

Unlike what is observed for the forward Euler method, here we get the expected quadratic convergence in S and linear convergence in t.

Then we consider the bet option in the standard case with $S_{\max} = 4K$ solved with the backward Euler method. Plotting the maximal errors e_0 (see 3.4) at time $t = 0$ from Table 3.3.6 with logarithmic axes, we get the result shown in Figure 3.3.7. From the data in Table 3.3.6 we get the following convergence result:

$$e_0 \simeq 0.016h^{1.4} + 0.001k \tag{3.14}$$

As observed for the forward Euler method, for the bet option we get a reduction in the expected quadratic convergence in S. We still observe the expected linear convergence in t.

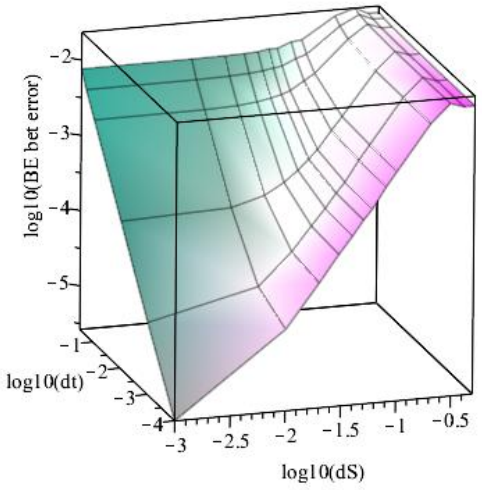

FIGURE 3.3.7: Plot of maximal error e_0 at time $t = 0$ (see 3.4) as a function of stepsizes $dS = h$ and $dt = k$ (logarithmic axes) for the bet option in the standard case with $S_{\max} = 4K$ and $K_\alpha = 0.5$ with the backward Euler method. In this case the maximal error is attained in the interior of the S-interval, close to $S = K$.

Finally we consider the smoothened put option in the standard case with $S_{\max} = 30K$ solved with the backward Euler method. Plotting the maximal errors e_0 (see (3.4)) at time $t = 0$ from Table 3.3.7 with logarithmic axes, we get the result shown in Figure 3.3.8 with the following convergence result:

$$e_0 \simeq 0.005h^2 + 0.01k \tag{3.15}$$

For comparison, the convergence results with the backward Euler method are repeated here:

$$\begin{aligned} \text{Put:} \qquad & e_0 \simeq 0.069h^2 + 0.006k \\ \text{Call:} \qquad & e_0 \simeq 0.07h^2 + 0.006k \\ \text{Bet:} \qquad & e_0 \simeq 0.016h^{1.4} + 0.001k \\ \text{Smoothened put:} \qquad & e_0 \simeq 0.005h^2 + 0.01k \end{aligned}$$

The conclusion is that the discontinuity in the derivative $\frac{\partial V}{\partial S}$ at $(S,t) = (K,T)$ for the put and call options shows up in the computational results, but that we observe no loss of convergence neither in t nor in S (with respect to the expected linear convergence in

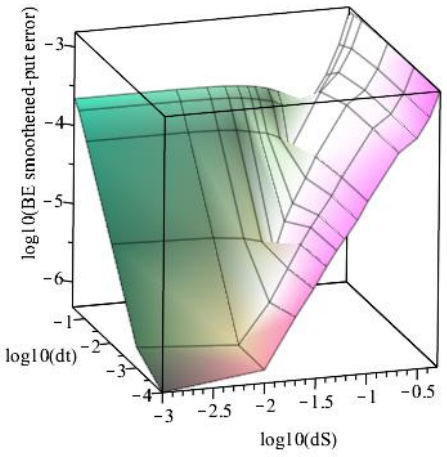

FIGURE 3.3.8: Plot of maximal error e_0 at time $t = 0$ (see (3.4)) as a function of step sizes $dS = h$ and $dt = k$ (logarithmic axes) for the smoothened put option in the standard case ($T = 1$, $K = 1$, $B = 0.3$, $r = 0.04$, $\gamma = 0$ and $\sigma = 0.2$) with $S_{\max} = 30K$ with the backward Euler method.

t and quadratic convergence in S for the backward Euler method) in the computational domain. Instead the stronger discontinuity in V at $(S, t) = (K, T)$ for the bet option means the loss of one order of convergence in S (with respect to the expected quadratic convergence for the backward Euler method) whereas there is no loss in the order of convergence in t in the computational domain. It would be expected that a quadratic convergence in S and a linear convergence in t would show up once h becomes small enough to "resolve the singularity". Only for the bet option the singularity can not be resolved inside the computational domain. These speculations could merit further research but are not treated here. And as we expected for the smoothened put option with no discontinuity in V or its derivatives we get the expected second order and linear convergence in S and t respectively.

3.3.5 Volatility limit

Now we consider the put option price when volatility tends to 0 with the backward Euler method and Table 3.3.12 shows the maximal error e_0 when σ tends to zero.

In Figure 3.3.9(e)-(f) we show for the fine mesh $h \simeq 0.01$, $k \simeq 0.001$ the changes in option price when the volatility tends to zero to the left and the difference between numerical solution with different values of σ and exact solution with $\sigma = 0$ to the right.

TABLE 3.3.12: Maximal error e_0 for the put option at $t = 0$ with $S_{\max} \simeq 4K$and $K_\alpha = 0.3$ in the standard case except σ with the coarse and fine meshes $h \simeq 0.1$, $k \simeq 0.01$ and $h \simeq 0.01$, $k \simeq 0.001$ respectively with the backward Euler method.

σ	0.4	0.2	0.01	0.001	0.0001	0.00001	0.
Coarse mesh	0.147722	0.0714003	0.00698829	0.00664124	0.00663775	0.00663772	0.00663772
Fine mesh	0.150168	0.0745572	0.00320859	0.00270294	0.00272136	0.00272155	0.00272155

We conclude, as for the forward Euler method, that the numerical solutions computed with the backward Euler method satisfy 1.12.

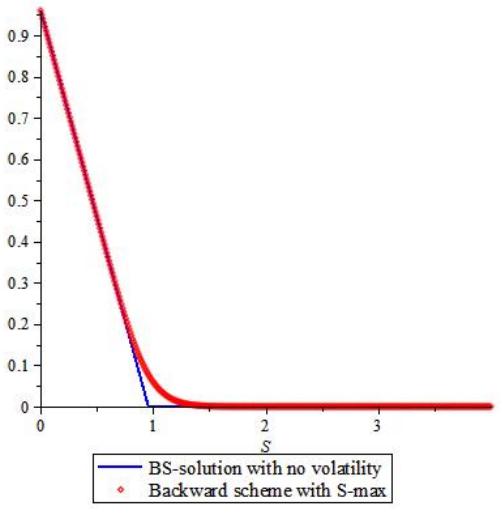

(a) Option Price, $\sigma = 0.2$.

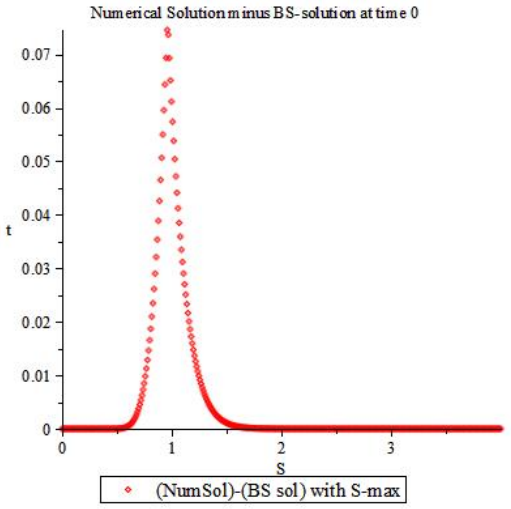

(b) Error curve, $\sigma = 0.2$.

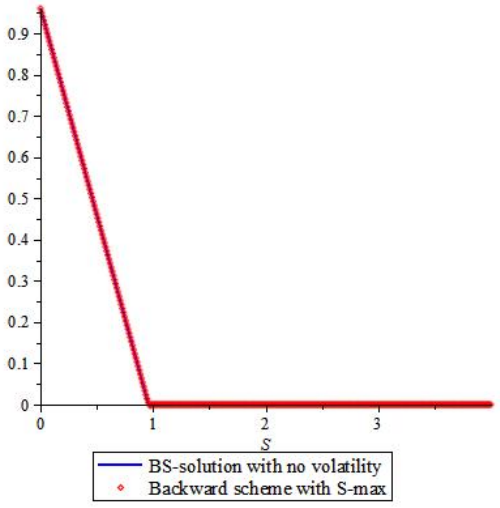

(c) Option Price, $\sigma = 0.001$.

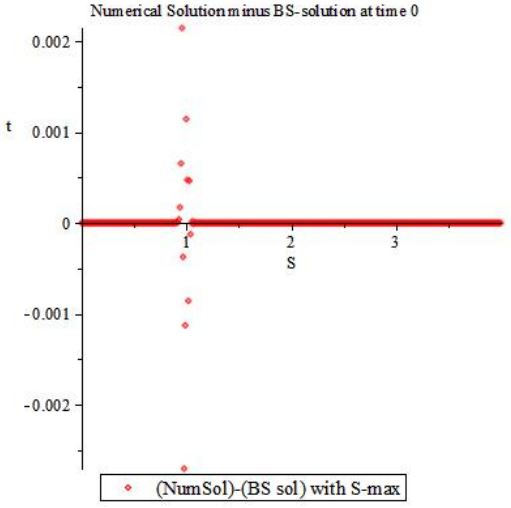

(d) Error curve, $\sigma = 0.001$.

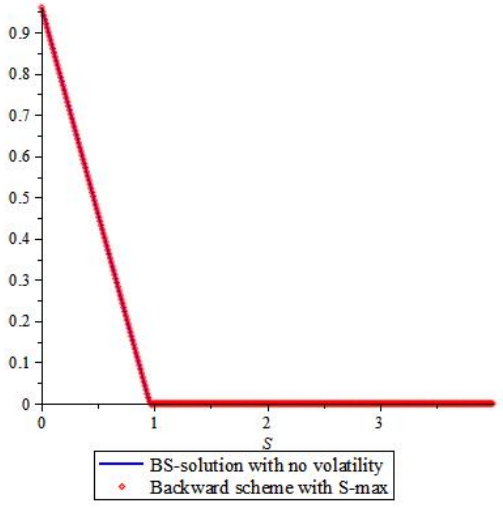

(e) Option Price, $\sigma = 0$.

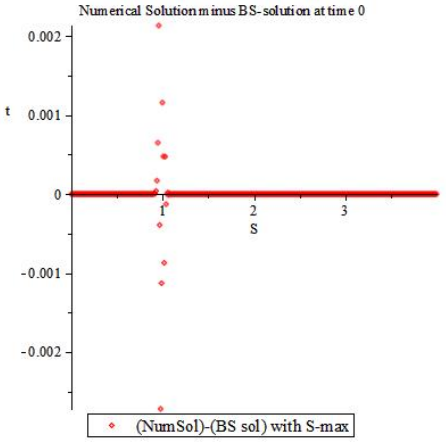

(f) Error curve, $\sigma = 0$.

FIGURE 3.3.9: The left curves show option price and the right curves error $\{e_{0,n}\}_{n=1}^{N}$ for the put option at $t = 0$ with $S_{\max} \simeq 4K$ and $K_\alpha = 0.3$ in the standard case except for σ with(a)-(b) $\sigma = 0.2$, (c)-(d) $\sigma = 0.001$, and (e)-(f) $\sigma = 0$ with the fine mesh $h \simeq 0.01$, $k \simeq= 0.001$ and with the backward Euler method

3.3.6 Expiration limit

Here we compute the expiration limit for the options as we did in subsection 3.2.6 with the for ward Euler method.

TABLE 3.3.13: Maximal error e_0 for the put option at $t = T - k$ with $S_{\max} \simeq 4K$ and $K_\alpha = 0.3$ in the standard case with the backward Euler method

h \ k	.1	.01	.001	.0001	.00001	.000001
.5	0.00331879	0.000365234	3.65219e-05	3.65218e-06	3.65217e-07	3.65217e-08
.1	0.00184363	0.000824394	0.00014914	1.49477e-05	1.49511e-06	1.49514e-07
.01	0.0028557	0.000898223	0.00019204	7.77653e-05	1.40544e-05	1.40934e-06

TABLE 3.3.14: Maximal error e_0 for the put option at $t = T - 5k$ with $S_{\max} \simeq 4K$ and $K_\alpha = 0.3$ in the standard case with the backward Euler method

h \ k	.1	.01	.001	.0001	.00001	.000001
.5	0.00565441	0.00181357	0.000182603	1.82608e-05	1.82609e-06	1.82609e-07
.1	0.0020224	0.00178869	0.000645733	7.47011e-05	7.47517e-06	7.47567e-07
.01	0.00139073	000454277	0.000201432	0.000189783	6.11255e-05	7.04235e-06

TABLE 3.3.15: Maximal error e_0 for the call option at $t = T - k$ with $S_{\max} \simeq 4K$ and $K_\alpha = 0.3$ in the standard case with the backward Euler method

h \ k	.1	.01	.001	.0001	.00001	.000001
.5	0.00331084	0.000365154	3.65211e-05	3.65217e-06	3.65217e-07	3.65217e-08
.1	0.00185158	0.000824314	0.000149139	1.49477e-05	1.49511e-06	1.49514e-07
.01	0.00286365	0.000898302	0.00019204	7.77653e-05	1.40544e-05	1.40934e-06

TABLE 3.3.16: Maximal error e_0 for the call option at $t = T - 5k$ with $S_{\max} \simeq 4K$ and $K_\alpha = 0.3$ in the standard case with the backward Euler method

h \ k	.1	.01	.001	.0001	.00001	.000001
.5	0.00561531	0.00181317	0.000182599	1.82608e-05	1.82609e-06	1.82609e-07
.1	0.00206151	0.00178829	0.000645729	7.47011e-05	7.47517e-06	7.47567e-07
.01	0.00142983	000454676	0.000201436	0.000189783	6.11255e-05	7.04235e-06

TABLE 3.3.17: Maximal error e_0 for the bet option at $t = T - k$ with $S_{\max} \simeq 4K$ and $K_\alpha = 0.5$ in the standard case with the backward Euler method

h \ k	.1	.01	.001	.0001	.00001	.000001
.5	0.00340489	0.000358709	3.59870e-05	3.59987e-06	3.59999e-07	3.60000e-08
.1	0.02724	0.00394572	0.000655884	6.59586e-05	6.59959e-06	6.59996e-07
.01	0.0192518	0.0205107	0262852	0.00381672	000602376	6.05635e-05

TABLE 3.3.18: Maximal error e_0 for the bet option at $t = T - 5k$ with $S_{\max} \simeq 4K$ and $K_\alpha = 0.5$ in the standard case with the backward Euler method

h \ k	.1	.01	.001	.0001	.00001	.000001
.5	0.0102349	0.00178064	0.000179806	1.79981e-05	1.79998e-06	1.80000e-07
.1	0.00944335	0.0160589	0.00315253	0.000329379	3.29938e-05	3.29994e-06
.01	0.0045153	0.00467452	0.00957738	0.0144031	0.00291284	0.000302454

3.4 Numerical results for the Crank Nicolson method

In this section we consider the Crank Nicolson method for the standard case $T = 1$, $K = 1$, $B = 0.3$, $r = 0.04$, $\gamma = 0$ and $\sigma = 0.2$ with the same computational setup as described in sections 3.2.1 and 3.3.1. Since the Crank Nicolson method is an implicit scheme like the backward Euler method, the computing times are similarly high.

3.4.1 Computational results for the standard case

First we compute the maximal error e_0 (see 3.4) at time $t = 0$ with $S_{\max} \simeq 4K, 2K, 1.5K$ and $1.25K$ for the put option in the standard case with the Crank Nicolson method. The results are shown in Tables 3.4.1–3.4.4 and in Figures 3.4.1–3.4.2.

TABLE 3.4.1: Maximal error e_0 for the put option at $t = 0$ for $S_{\max} \simeq 4K$ and $K_\alpha = 0.3$ in the standard case with the Crank Nicolson method.

h \ k	.3	.2	.1	.01	.001	.0001
.5	0.00672936	0.00671793	0.00671314	0.00671156	0.00671154	0.00671154
.4	0.00408546	0.00406345	0.00405426	0.00405125	0.00405122	0.00405122
.3	0.00322124	0.00325308	0.00326646	0.00327087	0.00327091	0.00327091
.2	0.00233565	0.00241369	0.00244614	0.00245679	0.0024569	0.0024569
.1	0.000501005	0.000536946	0.00055238	0.000557505	0.000557557	0.000557557
.08	0.000284197	0.000320717	0.000337337	0.000342817	0.000342872	0.000342872
.06	0.000651676	0.000174949	0.000204624	0.00021404	0.000214133	0.000214134
.05	0.00113038	0.000126523	0.00014705	0.0001561	0.00015619	0.00015619
.04	0.0018367	0.00024821	9.14746e-5	0.000101488	0.000101623	0.000101624
.03	0.00290236	0.000737749	4.7315e-5	5.60747e-5	5.61908e-5	5.6192e-5
.02	0.00400788	0.00150029	0.000119567	2.62052e-5	2.6316e-5	2.63171e-5
.01	0.00534424	0.00265056	0.000704856	6.56793e-6	6.68405e-6	6.68515e-6
.001	0.00666172	0.00391332	0.00181799	7.31236e-5	6.65842e-8	6.77993e-8

TABLE 3.4.2: Maximal error e_0 for the put option at $t = 0$ for $S_{\max} \simeq 2K$ and $K_\alpha = 0.3$ in the standard case with the Crank Nicolson method.

h \ k	.3	.2	.1	.01	.001	.0001
.5	0.00662353	0.00661279	0.00660828	0.00660679	0.00660677	0.00660677
.4	0.0040794	0.0040581	0.00404923	0.00404632	0.00404629	0.00404629
.3	0.00322131	0.00325312	0.00326649	0.00327089	0.00327094	0.00327094
.2	0.00233568	0.0024137	0.00244615	0.0024568	0.00245691	0.00245691
.1	0.000501005	0.000536946	0.00055238	0.000557505	0.000557557	0.000557557
.08	0.000284198	0.000320718	0.000337338	0.000342817	0.000342872	0.000342872
.06	0.000651674	0.00017495	0.000204624	0.00021404	0.000214133	0.000214134
.05	0.00113038	0.000126523	0.00014705	0.0001561	0.000156189	0.00015619
.04	0.00187367	0.00024821	9.14746e-5	0.000101488	0.000101623	0.000101624
.03	0.00290235	0.000737749	4.73149e-5	5.60746e-5	5.61908e-5	5.6192e-5
.02	0.00400788	0.00150029	0.000119568	2.62052e-5	2.6316e-5	2.63171e-5
.01	0.00534424	0.00265056	0.000704857	8.75748e-6	8.75748e-6	8.75748e-6
.001	0.00666172	0.00391332	0.00181799	7.31236e-5	8.29540e-6	8.21241e-6

TABLE 3.4.3: Maximal error e_0 for the put option at $t = 0$ for $S_{\max} \simeq 1.5K$ and $K_\alpha = 0.3$ in the standard case with the Crank Nicolson method.

h \ k	.3	.2	.1	.01	.001	.0001
.5	0.00661619	0.00661279	0.00660828	0.00660679	0.00660677	0.00660677
.4	0.00372853	0.00372142	0.00371196	0.00370885	0.00370882	0.00370882
.3	0.0032449	0.00325481	0.0032680	0.00327234	0.00327239	0.00327239
.2	0.00239739	0.00242142	00245322	0.00246365	0.00246375	0.00246375
.1	0.000657543	0.000657543	0.000657543	0.000657543	0.000657543	0.00065754
.08	0.00104401	0.00104401	0.00104401	0.00104401	0.00104401	0.00104401
.06	0.00105242	0.00105242	0.00105242	0.00105242	0.00105242	0.00105242
.05	0.000840836	0.000840836	0.000840836	0.000840836	0.00084084	0.00084084
.04	0.00106134	0.00106134	0.00106134	0.00106134	0.00106134	0.00106134
.03	0.00124797	0.000931848	0.000931848	0.000931848	0.00093185	0.00093185
.02	0.00214265	0.0014987	0.000976963	0.000976963	0.00097696	0.00097696
.01	0.0033607	0.00264872	0.00102750	0.0010275	0.00102750	0.0010275
.001	0.004640	0.00391119	00181926	0.00107541	0.00107541	0.00107541

TABLE 3.4.4: Maximal error e_0 for the put option at $t = 0$ for $S_{\max} \simeq 1.25K$ and $K_\alpha = 0.3$ in the standard case with the Crank Nicolson method.

h \ k	.3	.2	.1	.01	.001	.0001
.5	0.00612437	0.00612437	0.00612437	0.00612437	0.00612437	0.00612437
.4	0.00372853	0.00372142	0.00371196	0.00370885	0.00370882	0.00370882
.3	0.00332707	0.00333621	0.00334839	0.00335240	0.00335244	0.00335244
.2	0.00532862	0.00532862	0.00532862	0.00532862	0.00532862	0.00532862
.1	0.0087067	0.0087067	0.00870670	0.00870670	0.00870670	0.00870670
.08	0.00762432	0.00762432	0.00762432	0.00762432	0.00762432	0.00762432
.06	0.0080478	0.00804780	0.00804780	0.00804780	0.00804780	0.00804780
.05	0.0074617	0.00746170	0.00746170	0.0074617	0.00746170	0.00746170
.04	0.00851633	0.00851633	0.00851633	0.00851633	0.00851633	0.00851633
.03	0.00933452	0.00933452	0.00933452	0.00933452	0.00933452	0.00933452
.02	0.00942338	0.00942338	0.00942338	0.00942338	0.00942338	0.00942338
.01	0.00913899	0.00913899	0.00913899	0.00913899	0.00913899	0.00913899
.001	0.00956760	0.00956760	0.00956760	0.00956760	0.00956760	0.0095676

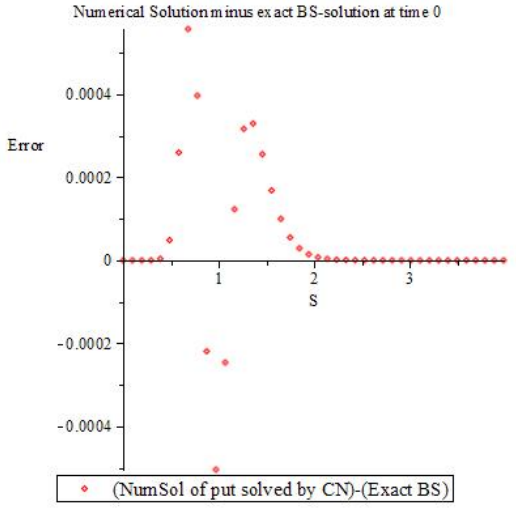

(a) CN error, coarse mesh, $S_{\max} \simeq 4K$.

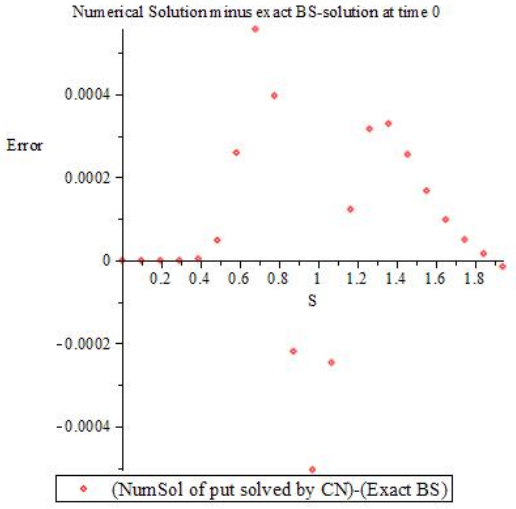

(b) CN error, coarse mesh, $S_{\max} \simeq 2K$.

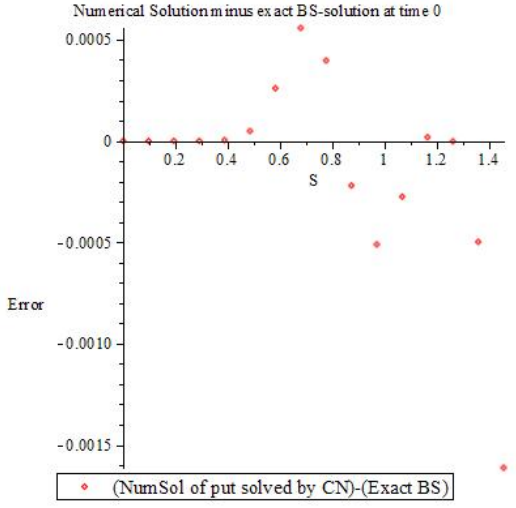

(c) CN error, coarse mesh, $S_{\max} \simeq 1,5K$.

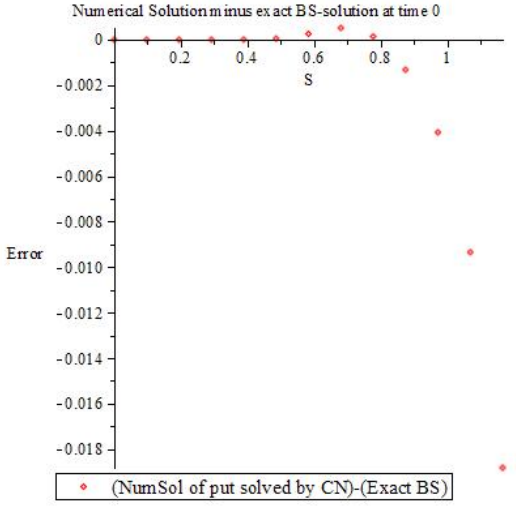

(d) CN error, coarse mesh, $S_{\max} \simeq 1.25K$.

FIGURE 3.4.1: Error $\{e_{0,n}\}_{n=1}^{N}$ at $t = 0$ for the put option and $S_{\max} \simeq$ (a) $4K$, (b) $2K$, (c) $1.5K$ and (d) $1.25K$ for stepsizes $h \simeq 0.1$ and $k \simeq 0.01$ and $K_\alpha = 0.3$ in the standard case with the Cranck Nicolson method.

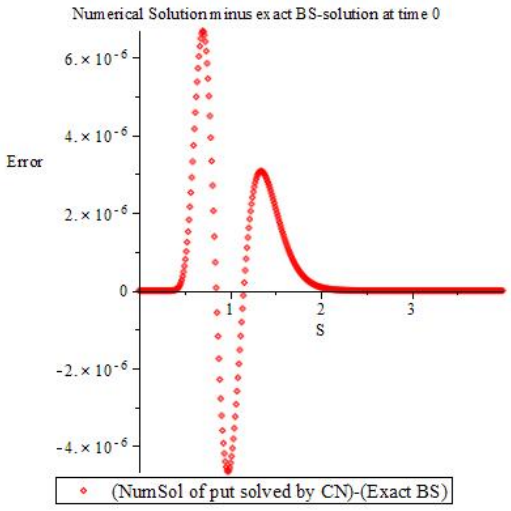

(a) CN error, fine mesh, $S_{\max} \simeq 4K$.

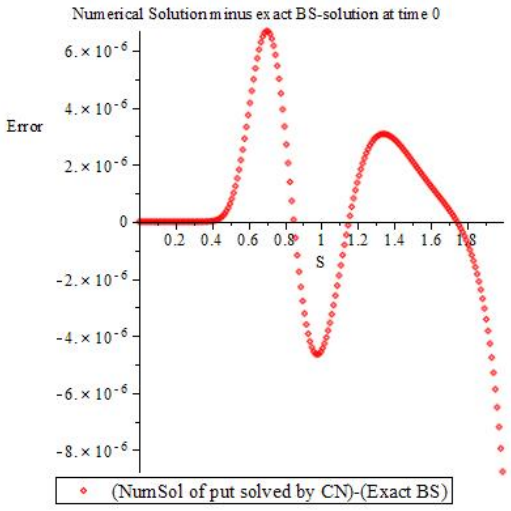

(b) CN error, fine mesh, $S_{\max} \simeq 2K$.

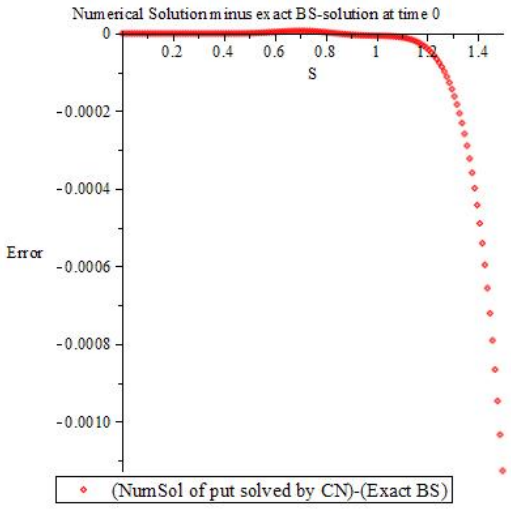

(c) CN error, fine mesh, $S_{\max} \simeq 1,5K$.

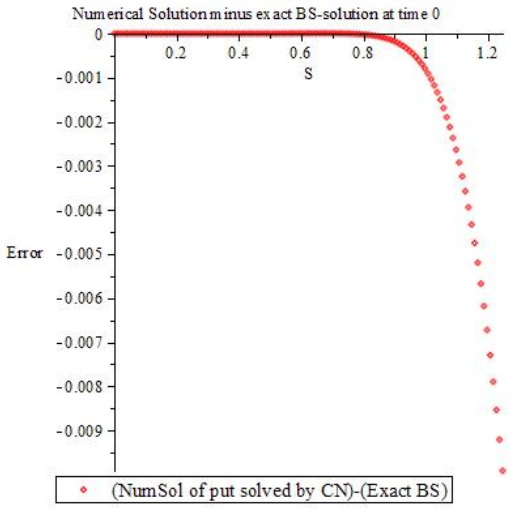

(d) CN error, fine mesh, $S_{\max} \simeq 1.25K$.

FIGURE 3.4.2: Error $\{e_{0,n}\}_{n=1}^{N}$ at $t = 0$ for the put option and $S_{\max} \simeq$ (a) $4K$, (b) $2K$, (c) $1.5K$ and (d) $1.25K$ for stepsizes $h \simeq 0.01$ and $k \simeq 0.001$ and $K_\alpha = 0.3$ in the standard case with the Cranck Nicolson method.

Now we consider the maximal error e_0 at time $t = 0$ with $S_{\max} \simeq 4K$ for the call option in the standard case with the Crank Nicolson method. The results are shown in Table 3.4.5.

TABLE 3.4.5: Maximal error e_0 for the call option at $t = 0$ for $S_{\max} \simeq 4K$ and $K_\alpha = 0.3$ in the standard case with the Crank Nicolson method.

h \ k	.3	.2	.1	.01	.001	.0001
.5	0.00672993	0.00671814	0.00671319	0.00671156	0.00671154	0.00671154
.4	0.00408603	0.00406365	0.00405431	0.00405125	0.00405122	0.00405122
.3	0.00322067	0.00325287	0.00326641	0.00327087	0.00327091	0.00327091
.2	0.00233508	0.00241348	0.00244609	0.00245679	0.0024569	0.0024569
.1	0.000501575	0.000537151	0.000552431	0.000557506	0.000557557	0.000557557
.08	0.000284767	0.000320923	0.000337389	0.000342817	0.000342872	0.000342872
.06	0.000652245	0.000175154	0.000204675	0.00021404	0.000214133	0.000214134
.05	0.00113095	0.000126728	0.000147102	0.0001561	0.00015619	0.00015619
.04	0.00187424	0.000248416	9.1526e-5	0.000101489	0.000101623	0.000101624
.03	0.00290292	0.000737954	4.73664e-5	5.60753e-5	5.61909e-5	5.6192e-5
.02	0.00400845	0.0015005	0.000119516	2.62058e-5	2.63161e-5	2.63172e-5
.01	0.0053448	0.00265076	0.000704805	6.56847e-6	6.68407e-6	6.68515e-6
.001	0.0066619	0.00391352	0.00181794	7.3123e-5	6.65894e-8	6.77994e-8

Finally we consider the maximal error e_0 at time $t = 0$ with $S_{\max} \simeq 4K$ for the bet option in the standard case with the Crank Nicolson method. The results are shown in Table 3.4.6.

TABLE 3.4.6: Maximal error e_0 for the bet option at $t = 0$ with $S_{\max} \simeq 4K$ and $K_\alpha = 0.5$ in the standard case with the Crank Nicolson method.

h \ k	.3	.2	.1	.01	.001	.0001
.5	0.0172728	0.0173101	0.0173257	0.0173308	0.0173309	0.0173309
.4	0.0172728	0.0173101	0.0173257	0.0173308	0.0173309	0.0173309
.3	0.0196424	0.0197403	0.0197813	0.0197948	0.0197949	0.0197949
.2	0.0105562	0.0110726	0.0112855	0.0113552	0.0113559	0.0113559
.1	0.0020692	0.0026026	0.0028317	0.0029045	0.0029052	0.00290525
.08	0.0020888	0.0016613	0.0017822	0.0018692	0.0018701	0.00187013
.06	0.0125431	0.0007964	0.0009074	0.0009828	0.0009836	0.000983583
.05	0.0211934	0.0019972	0.0006579	0.0007153	0.0007159	0.000715862
.04	0.0356145	0.0073694	0.0004022	0.0004553	0.0004559	0.000455861
.03	0.0554435	0.0202956	0.0004334	0.0002660	0.0002666	0.00026659
.02	0.0832861	0.0481960	0.0071909	0.0001160	0.0001166	0.000116588
.01	0.1156278	0.0931800	0.0479155	0.0000288	0.0000294	0.0000294
.001	0.1474289	0.1446246	0.1383441	0.0476325	2.90458e-7	4.83086e-7

3.4.2 Computational results for nonstandard cases

Here we consider robustness in the selection of $S_{\max}$ against variations in the other parameters in the problem when solving with the Crank Nicolson method like we have

done for the forward and backward Euler methods in sections 3.2.2 and 3.3.2. since Crank Nicolson method is an implicit method, we choose the same mesh sizes that we chose for the backward Euler method in section 3.3.2 therefore the coarse mesh with $h \simeq 0.1$ and $k \simeq 0.01$ and the fine mesh with $h \simeq 0.01$ and $k \simeq 0.001$. For each mesh, we shall find the smallest value of $S_{\max}$ where the error in $S = S_{\max}$ is negligible compared to the maximal error e_0.

As observed when solving with the forward Euler method, we expect no significant differences between the results for the put, call and bet options. Hence here we compute only for the put option as well. The results for the coarse mesh are shown in Tables 3.4.7 and 3.4.8 and the results for the fine mesh are shown in Tables 3.4.9 and 3.4.10.

TABLE 3.4.7: Smallest $S_{\max}$ not giving significant error at $S = S_{\max}$ with the coarse mesh $h \simeq 0.1$, $k \simeq 0.01$ and $K_\alpha = 0.3$ in various nonstandard cases for the put option with the Crank Nicolson method. "-" indicates a case where it has not been possible to establish a functional $S_{\max}$.

	$K = 10$				$K = 1$				$K = 0.1$			
	r \ σ	.01	.2	.9	r \ σ	.01	.2	.9	r \ σ	.01	.2	.9
$T = 10$	.001	$1.25K$	-	-	.001	$1.25K$	$8K$	-	.001	$2K$	$3K$	-
	.04	$1.25K$	-	-	.04	$1.5K$	$5K$	-	.04	$2K$	$2K$	-
	.1	$1.25K$	$5K$	-	.1	$1.5K$	$2K$	-	.1	$2K$	$2K$	-
$T = 1$	r \ σ	.01	.2	.9	r \ σ	.01	.2	.9	r \ σ	.01	.2	.9
	.001	$1.25K$	$3K$	-	.001	$1.5K$	$2K$	$24K$	.001	$2K$	$2K$	$7K$
	.04	$1.25K$	$3K$	-	.04	$1.5K$	$2K$	$23K$	.04	$2K$	$2K$	$6K$
	.1	$1.25K$	$2K$	-	.1	$1.5K$	$2K$	$22K$	.1	$2K$	$2K$	$6K$
$T = .1$	r \ σ	.01	.2	.9	r \ σ	.01	.2	.9	r \ σ	.01	.2	.9
	.001	$1.25K$	$1.25K$	$2K$	.001	$1.25K$	$1.25K$	$3K$	.001	$2K$	$2K$	$2K$
	.04	$1.25K$	$1.25K$	$2K$	.04	$1.25K$	$1.25K$	$3K$	.04	$2K$	$2K$	$2K$
	.1	$1.25K$	$1.25K$	$2K$	.1	$1.25K$	$1.25K$	$3K$	.1	$2K$	$2K$	$2K$

TABLE 3.4.8: Smallest $S_{\max}$ not giving significant error at $S = S_{\max}$ with the coarse mesh $h \simeq 0.1$, $k \simeq 0.01$ and $K_\alpha = 0.3$ in the standard case except for γ in the put option with the Crank Nicolson method.

γ	0	0.5	1.0
min $S_{\max}$	$2K$	$3K$	$4K$

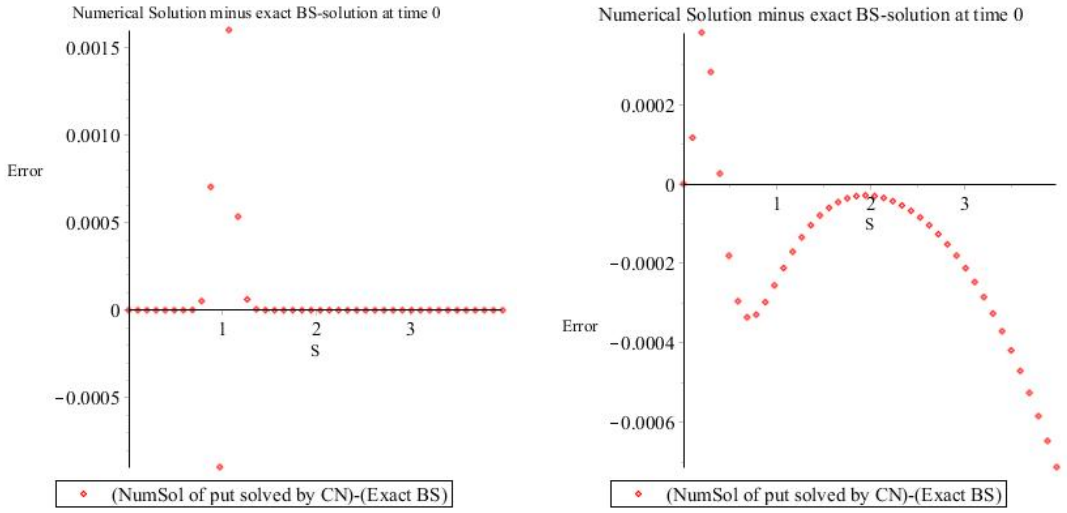

(a) CN error, coarse mesh, $T = 0.1$.

(b) CN error, coarse mesh, $T = 10$.

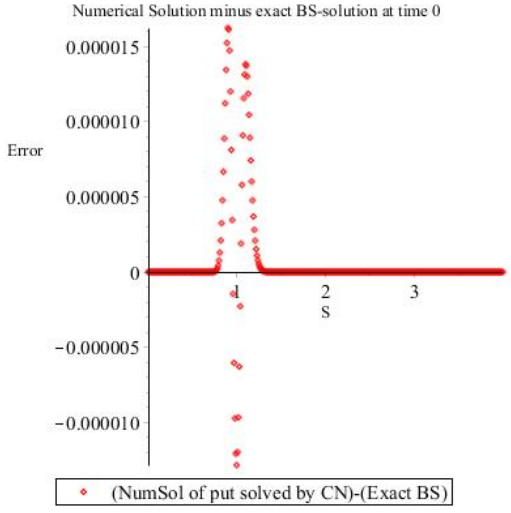

(c) CN error, fine mesh, $T = 0.1$.

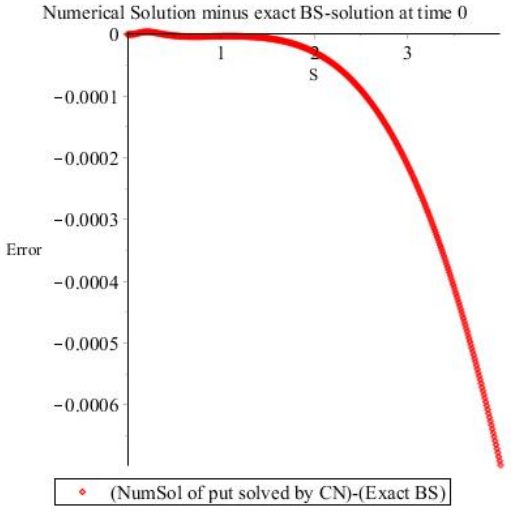

(d) CN error, fine mesh, $T = 10$.

FIGURE 3.4.3: Error $\{e_{0,n}\}_{n=1}^{N}$ at $t = 0$ for the put option with $S_{\max} \simeq 4K$ (a) $h \simeq 0.1$, $k \simeq 0.01$, $T = 0.1$, (b) $h \simeq 0.1$, $k \simeq 0.01$, $T = 10$, (c) $h \simeq 0.01$, $k \simeq 0.001$, $T = 0.1$ and (d) $h \simeq 0.01$, $k \simeq 0.001$, $T = 10$ and $K_\alpha = 0.3$, in the standard case apart from the value of T with the Crank Nicolson method.

TABLE 3.4.9: Smallest $S_{\max}$ not giving significant error at $S = S_{\max}$ with the fine mesh $h \simeq 0.01$, $k \simeq 0.001$ and $K_\alpha = 0.3$ in various nonstandard cases for the put option with the Crank Nicolson method. "-" indicates a case where it has not been possible to establish a functional $S_{\max}$.

	$K = 10$				$K = 1$				$K = 0.1$			
	r \ σ	.01	.2	.9	r \ σ	.01	.2	.9	r \ σ	.01	.2	.9
$T = 10$	.001	-	-	-	.001	$1.25K$	-	-	.001	$1.25K$	$8K$	-
	.04	-	-	-	.04	$1.25K$	-	-	.04	$1.25K$	$5K$	-
	.1	-	-	-	.1	$1.25K$	-	-	.1	$1.25K$	$2K$	-
$T = 1$	.001	$1.25K$	-	-	.001	$1.25K$	$3K$	-	.001	$1.25K$	$2K$	$25K$
	.04	$1.25K$	-	-	.04	$1.25K$	$3K$	-	.04	$1.25K$	$2K$	$25K$
	.1	$1.25K$	-	-	.1	$1.25K$	$2K$	-	.1	$1.25K$	$1.5K$	$25K$
$T = .1$	.001	$1.25K$	$1.5K$	$3K$	.001	$1.25K$	$1.25K$	$4K$	.001	$1.25K$	$1.25K$	$3K$
	.04	$1.25K$	$1.5K$	$3K$	.04	$1.25K$	$1.25K$	$4K$	.04	$1.25K$	$1.25K$	$3K$
	.1	$1.25K$	$1.5K$	$3K$	.1	$1.25K$	$1.25K$	$4K$	.1	$1.25K$	$1.25K$	$3K$

TABLE 3.4.10: Smallest $S_{\max}$ not giving significant error at $S = S_{\max}$ with the coarse mesh $h \simeq 0.01$, $k \simeq 0.001$ and $K_\alpha = 0.3$ in the standard case except for γ in the put option with the Crank Nicolson method.

γ	0	0.5	1.0
min $S_{\max}$	$3K$	$4K$	$5K$

3.4.3 Sensitivity to $S_{\max}$

Sensitivity to for the Crank-Nicolson method $S_{\max}$ shows there is no indication in the computations that have been performed that the results would differ from the forward or backward Euler methods. Thus $S_{\max} = 4K$ still seems to be a fairly good all round selection for most reasonable parameter values.

3.4.4 Convergence

First we consider the put option in the standard case with $S_{\max} = 4K$ solved with the Crank Nicolson method. Plotting the maximal errors e_0 (see 3.4) at time $t = 0$ from Table 3.4.1 with logarithmic axes, we get the result shown in Figure 3.4.4. Obviously there are 2 significantly different parts of the domain, that we shall refer to as "inside the bubble"($h \in]0, 0.08]$ and $k \in [0.3, 0.001]$) and "outside the bubble"($h \in [0.08, 0.5]$ and $k \in [0.001, 0.0001]$) respectively. Technically the "bubble" is where the error is increasing with decreasing $dS = h$. From the data in Table 3.4.1 we get the following

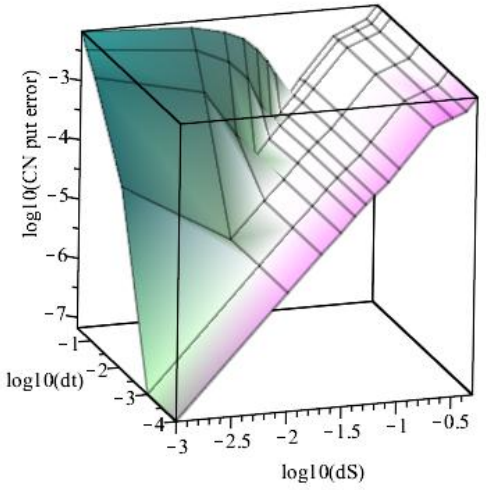

FIGURE 3.4.4: Plot of maximal error e_0 at time $t = 0$ (see 3.4) as a function of stepsizes $dS = h$ and $dt = k$ (logarithmic axes) for the put option in the standard case with $S_{\max} = 4K$ and $K_\alpha = 0.3$ with the Crank Nicolson method. In this case the maximal error is attained in the interior of the S-interval, close to $S = K$.

convergence result:

$$e_0 \simeq \begin{cases} 0.019k^{1.5} & \text{"in the bubble"} \\ 0.069h^2 & \text{"outside the bubble"} \end{cases} \tag{3.16}$$

Unlike what is observed for the forward Euler method, here we get the expected quadratic convergence in S and t, but only in the bubble.

In Figure 3.4.5 we show the error $e_{0,nm}$ (see 3.8) as a function of both S and t for 5 different meshes: Mesh 1: $h \simeq 0.1$, $k \simeq 0.1$, Mesh 2: $h \simeq 0.1$, $k \simeq 0.01$, Mesh 3: $h \simeq 0.1$, $k \simeq 0.001$, Mesh 4: $h \simeq 0.05$, $k \simeq 0.001$, Mesh 5: $h \simeq 0.03$, $k \simeq 0.001$.

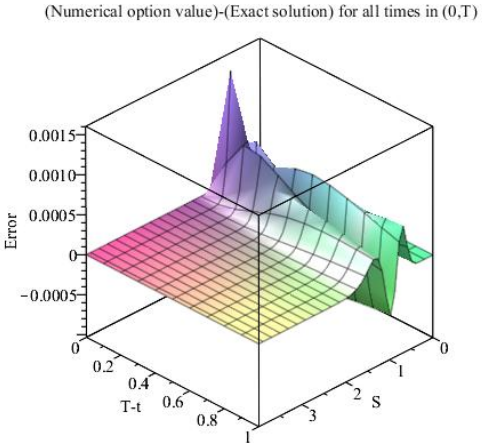

(a) Mesh 1 error.

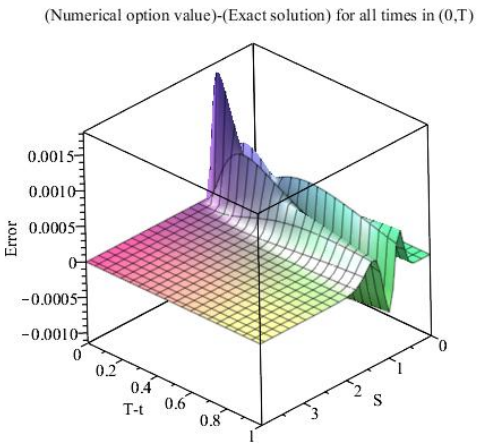

(b) Mesh 2 error.

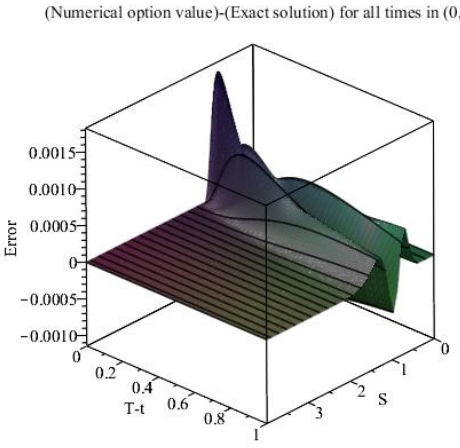

(c) Mesh 3 error.

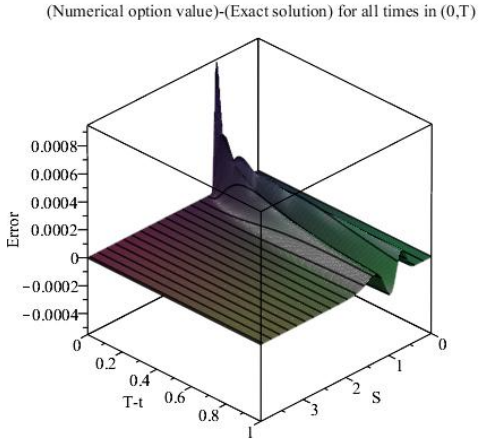

(d) Mesh 4 error.

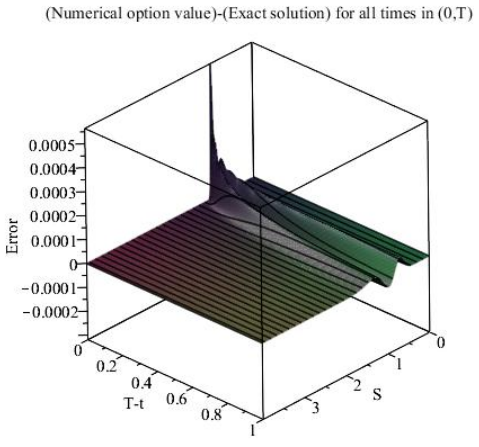

(e) Mesh 5 error.

FIGURE 3.4.5: Plot of the error as a function of S and t for the put option with $S_{\max} = 4K$ and $K_\alpha = 0.3$ with Cranck Nicolson method for mesh 1 (a), mesh 2 (b), mesh 3 (c), mesh 4 (d) and mesh 5 (e).

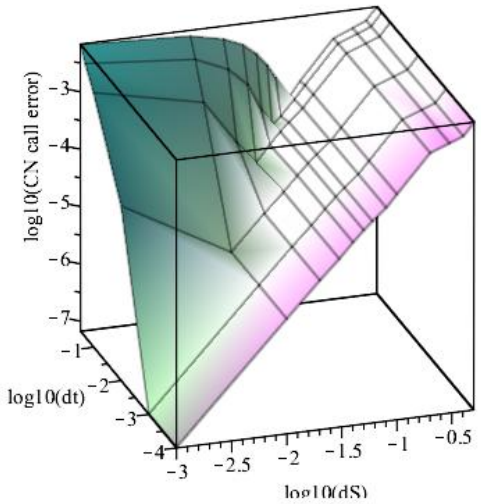

FIGURE 3.4.6: Plot of maximal error e_0 at time $t = 0$ (see 3.4) as a function of stepsizes $dS = h$ and $dt = k$ (logarithmic axes) for the call option in the standard case with $S_{\max} = 4K$ and $K_\alpha = 0.3$ with the Crank Nicolson method. In this case the maximal error is attained in the interior of the S-interval, close to $S = K$.

Next we turn to the call option in the standard case with $S_{\max} = 4K$ solved with the Crank Nicolson method. Plotting the maximal errors e_0 (see 3.4) at time $t = 0$ from Table 3.4.5 with logarithmic axes, we get the result shown in Figure 3.4.6. Obviously there are 2 significantly different parts of the domain, that we shall refer to as "inside the bubble" and "outside the bubble" respectively. From the data in Table 3.4.5 we get the following convergence result:

$$e_0 \simeq \begin{cases} 0.02k^{1.5} & \text{"in the bubble"} \\ 0.07h^2 & \text{"outside the bubble"} \end{cases} \tag{3.17}$$

Unlike what is observed for the forward Euler method, here we get the expected quadratic convergence in S and t, but only in the bubble.

Finally we consider the bet option in the standard case with $S_{\max} = 4K$ solved with the Crank Nicolson method. Plotting the maximal errors e_0 (see 3.4) at time $t = 0$ from Table 3.4.6 with logarithmic axes, we get the result shown in Figure 3.4.7. Obviously there are 2 significantly different parts of the domain, that we shall refer to as "inside the bubble" and "outside the bubble" respectively. From the data in Table 3.4.6 we get

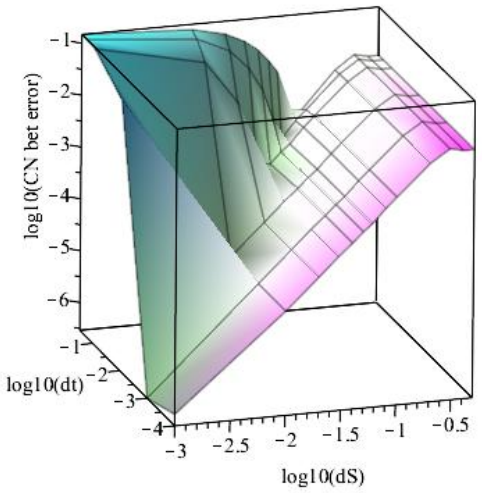

FIGURE 3.4.7: Plot of maximal error e_0 at time $t = 0$ (see 3.4) as a function of stepsizes $dS = h$ and $dt = k$ (logarithmic axes) for the bet option in the standard case with $S_{\max} = 4K$ and $K_\alpha = 0.5$ with the Crank Nicolson method. In this case the maximal error is attained in the interior of the S-interval, close to $S = K$.

the following convergence result:

$$e_0 \simeq \begin{cases} 0.118k^{0.6} & \text{"in the bubble"} \\ 0.017h^{1.4} & \text{"outside the bubble"} \end{cases} \tag{3.18}$$

Here we are far from getting the expected quadratic convergence in S and t.

For comparison, the convergence results with the Crank Nicolson method are repeated here:

$$\text{Put:} \quad e_0 \simeq \begin{cases} 0.019k^{1.5} & \text{"in the bubble"} \\ 0.069h^2 & \text{"outside the bubble"} \end{cases}$$

$$\text{Call:} \quad e_0 \simeq \begin{cases} 0.02k^{1.5} & \text{"in the bubble"} \\ 0.07h^2 & \text{"outside the bubble"} \end{cases}$$

$$\text{Bet:} \quad e_0 \simeq \begin{cases} 0.118k^{0.6} & \text{"in the bubble"} \\ 0.017h^{1.4} & \text{"outside the bubble"} \end{cases}$$

The conclusion is that the discontinuity in the derivative $\frac{\partial V}{\partial S}$ at $(S,t) = (K,T)$ for the put and call options means the loss of two orders of convergence in t (with respect to the expected quadratic convergence for the Crank Nicolson method) for bigger step sizes h in the computational domain. For smaller step sizes h in the computational

domain we observe the full quadratic convergence. Instead the expected quadratic order of convergence in S is observed in the computational domain. The discontinuity in V at $(S,t) = (K,T)$ for the bet option still means the loss of two orders of convergence in t (with respect to the expected quadratic convergence for the Crank Nicolson method) for bigger step sizes h in the computational domain. For smaller step sizes h in the computational domain we still lose more than one order in t because of the stronger singularity for the bet option than for the put and call options. The stronger singularity for the bet option (with respect to the put and call options) also means the loss of one order of convergence in S (with respect to the expected quadratic convergence for the Crank Nicolson method) in the entire computational domain. It would be expected that a quadratic convergence in S and t for the bet option would show up once h becomes small enough to "resolve the singularity". But because of the strong singularity this requires such small values of h that they are out of our computational domain. These speculations could merit further research but are not treated here.

3.4.5 Volatility limit

Now we consider the put option price computed with the Crank-Nicolson method when volatility tend to 0 and Table 3.4.11 shows the maximal error e_0 when σ tends to zero.

TABLE 3.4.11: Maximal error e_0 for the put option with the Crank-Nicolson method at time 0 with the standard case except σ at $S_{\max} \simeq 4K$ and $K_\alpha = 0.3$ with the coarse and fine meshes $h \simeq 0.1$, $k \simeq 0.01$ and $h \simeq 0.01$, $k \simeq 0.001$ respectively.

σ	0.4	0.2	0.01	0.001	0.0001	0.00001	0.
Coarse mesh	0.147924	0.0714919	0.00695045	0.00660321	0.00659973	0.00659969	0.00659969
Fine mesh	0.150188	0.0745654	0.00318953	0.00212712	0.00211662	0.00211651	0.00211651

In Figure 3.4.8 we show for the fine mesh $h \simeq 0.01$, $k \simeq 0.001$ the changes in option price when the volatility tends to zero to the left and the difference between the numerical solution with different values of σ and the exact solution with $\sigma = 0$ to the right.

We conclude, as for the forward and backward Euler methods, that the numerical solutions computed with the Crank-Nicolson method satisfy 1.12.

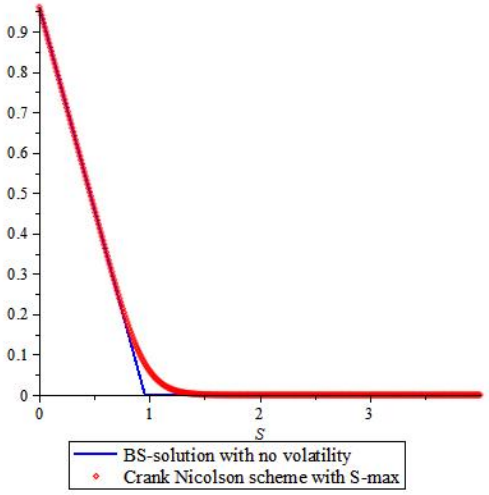

(a) Option Price, $\sigma = 0.2$, fine mesh.

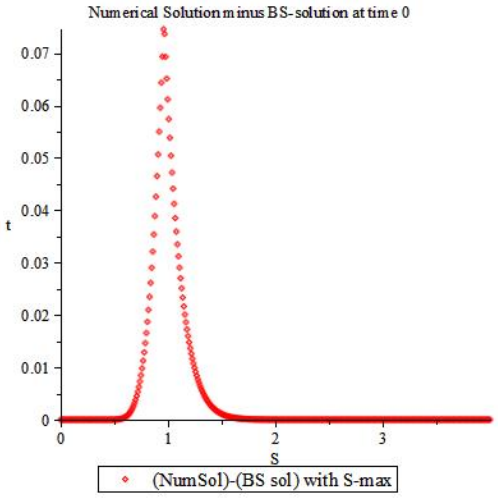

(b) Error curve, $\sigma = 0.2$, fine mesh.

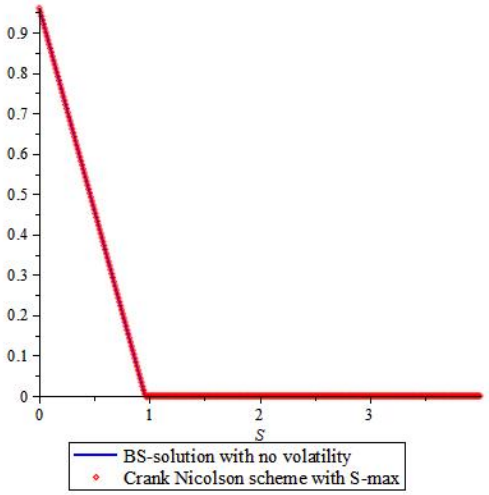

(c) Option Price, $\sigma = 0.001$, fine mesh.

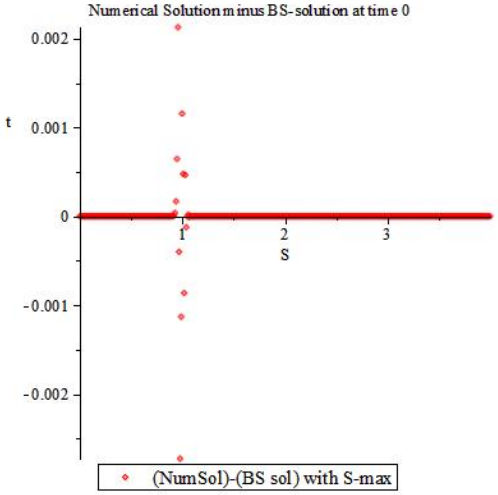

(d) Error curve, $\sigma = 0.001$, fine mesh.

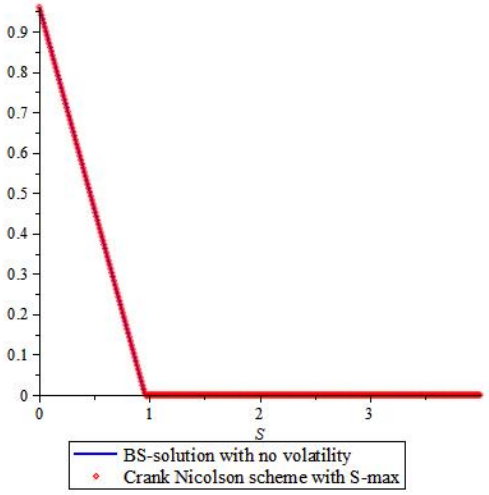

(e) Option Price, $\sigma = 0$, fine mesh.

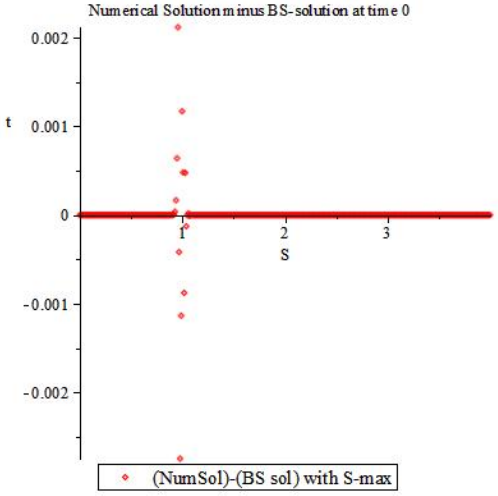

(f) Error curve, $\sigma = 0$, fine mesh.

FIGURE 3.4.8: The left curves show option price and the right curves error $\{e_{0,n}\}_{n=1}^{N}$ at $t = 0$ for the put option with $S_{\max} \simeq 4K$ and $K_\alpha = 0.3$ in the fine mesh $h \simeq 0.01$, $k \simeq 0.001$ (a)-(b) $\sigma = 0.2$, (c)-(d) $\sigma = 0.001$, and (e)-(f) $\sigma = 0$ in the standard case apart from the value of σ with the Crank-Nicolson method

3.4.6 Expiration limit

Here we compute the expiration limit for the options as we did in subsection 3.2.6 with the Crank Nicolson method.

TABLE 3.4.12: Maximal error e_0 for the put option at $t = T - k$ with $S_{\max} \simeq 4K$ and $K_\alpha = 0.3$ in the standard case with the Crank Nicolson method

h \ k	.1	.01	.001	.0001	.00001	.000001
.5	0.00331452	0.000365186	3.65214e-05	3.65217e-06	3.65217e-07	3.65217e-08
.1	0.0016035	0.000841773	0.000149326	1.49496e-05	1.49513e-06	1.49514e-07
.01	0.00491866	0.000711182	0.000176365	7.97703e-05	1.40759e-05	1.40955e-06

TABLE 3.4.13: Maximal error e_0 for the put option at $t = T - 5k$ with $S_{\max} \simeq 4K$ and $K_\alpha = 0.3$ in the standard case with the Crank Nicolson method

h \ k	.1	.01	.001	.0001	.00001	.000001
.5	0.00577972	0.00181334	0.000182601	1.82608e-05	1.82609e-06	1.82609e-07
.1	0.000698467	0.00180658	0.000646642	7.47104e-05	7.47526e-06	7.47568e-07
.01	0.00151497	3.37966e-05	7.15088e-05	0.000189811	6.12308e-05	7.04344e-06

TABLE 3.4.14: Maximal error e_0 for the call option at $t = T - k$ with $S_{\max} \simeq 4K$ and $K_\alpha = 0.3$ in the standard case with the Crank Nicolson method

h \ k	.1	.01	.001	.0001	.00001	.000001
.5	0.00331453	000365186	3.65214e-05	3.65217e-06	3.65217e-07	3.65217e-08
.1	0.00160351	0.000841773	0.000149326	1.49496e-05	1.49513e-06	1.49514e-07
.01	0.00491867	0.000711182	0.000176365	7.97703e-05	1.40759e-05	1.40955e-06

TABLE 3.4.15: Maximal error e_0 for the call option at $t = T - 5k$ with $S_{\max} \simeq 4K$ and $K_\alpha = 0.3$ in the standard case with the Crank Nicolson method

h \ k	.1	.01	.001	.0001	.00001	.000001
.5	0.00577974	0.00181334	0.000182601	1.82608e-05	1.82609e-06	1.82609e-07
.1	0.000698441	0.00180658	0.000646642	7.47104e-05	7.47526e-06	7.47568e-07
.01	0.00151499	3.37966e-05	7.15088e-05	0.000189811	6.12308e-05	7.04344e-06

TABLE 3.4.16: Maximal error e_0 for the bet option at $t = T - k$ with $S_{\max} \simeq 4K$ and $K_\alpha = 0.5$ in the standard case with the Crank Nicolson method

h \ k	.1	.01	.001	.0001	.00001	.000001
.5	0.00346605	0.000359353	3.59935e-05	3.59994e-06	3.59999e-07	3.60000e-08
.1	0.0180289	0.00413281	0.000657935	6.59793e-05	6.59979e-06	6.59998e-07
.01	0.113615	0.0458532	0.0179404	0.00398222	0.000604182	6.05818e-05

TABLE 3.4.17: Maximal error e_0 for the bet option at $t = T - 5k$ with $S_{\max} \simeq 4K$ and $K_\alpha = 0.5$ in the standard case with the Crank Nicolson method

h \ k	.1	.01	.001	.0001	.00001	.000001
.5	0.00985266	0.00178381	0.000179838	1.79984e-05	1.79998e-06	1.80000e-07
.1	0.00439463	0.0152823	0.0031625	0.000329483	3.29948e-05	3.29995e-06
.01	0.0723394	0.00358273	0.00440593	0.0137592	0.00292163	0.000302544

3.5 Conclusion

We considered some explicit and implicit finite difference schemes such as forward Euler, backward Euler and Crank-Nicolson methods for solving the standard linear Black-Scholes equation. We applied K_α method introduced in Chapter 2 for the given schemes here to reduce the schemes errors and reestablish the expected second oder of convergence in S-direction. We computed the order of convergence of the different schemes for different options and showed that we can not get the expected order of schemes convergences because of nonsmooth terminal condition of the equation.

We investigated the optimal value of S_{max} of the underlying asset as the right boundary condition of the Black-Scholes equation to have negligible errors around S_{max} in a standard case and some nonstandard case. we found that $S_{max} \simeq 4K$ is a good choice for different options such as put, call and bet option solved with the given three schemes. Also the computational results showed that S_{max} is fairly independent of the equation parameters like T, K, r, σ, γ and B except extreme value for dividends.

Furthermore volatility and expiration limits for these schemes have been considered. The volatility limit showed that when the volatility goes to zero the maximal errors tend to the maximal errors of the option price with no volatility. Also the expiration limit confirmed that when $t \to T$, the numerical solution tend to the exact terminal condition $V(S, T)$.

Chapter 4

Feedback Options in Nonlinear Numerical Finance

Jens Hugger and Sima Mashayekhi

Abstract. Feedback options are options where information about the trading of the underlying asset is fed back into the pricing model. This results in nonlinear pricing models. A survey of the literature about feedback options in finance is presented. The pricing model for the full feedback option on an infinite slab is presented and boundary values on a bounded domain are derived. This bounded, nonlinear, 2 dimensional initial-boundary value problem is solved numerically using a number of standard finite difference schemes and the methods incorporated in the symbolic software Maple^{TM}.

Keywords: Nonlinear PDE's, Feedback option, boundary value problem, numerical solution

Subjectclass: 35K61, 65M06

4.1 Introduction

In the classical Black-Scholes theory the price of financial derivatives is assumed to be independent on the trading strategy for the derivatives. The recent crisis on the European markets have proven otherwise as the price of the Greek, Italian and Spanish State bonds have fallen drastically. In this article we investigate feed back models where information about trading strategies are fed back into the model. This results in fully

nonlinear models that must be solved numerically. We investigate how liquidity(λ) can affect the option values. If we assume that a hedger holds the number of stocks dictated by the analytical Black- Scholes delta,then this leads to the linear PDE that is called First-order Feedback Model. But with assuming the trading strategy affect the price based on the actual delta of the modified price, it causes nonlinear PDE is called Full Feedback Model. At first in section 4.2 we present a survey of the literature about feedback options. After that in section 4.3 we present the partial differential equation model for the feedback option on the unbounded domain and derive boundary conditions to be used for numerical solution on a bounded domain. Then in section 4.4 we present the numerical methods to be used for solving the feedback option model. Finally in section 4.5 we present results obtained with the numerical methods presented in section 4.4 and conclude the work.

4.2 Literature survey on illiquid markets and feedback options

The classical Black-Scholes model is assumed on base of frictionless and perfectly liquid markets. Actually, it is assumed that buying arbitrarily large quantities of the underlying assets does not affect price of the underlying asset. Here we consider a realistic model for illiquid market that the effects of trading on the underlying asset price is considered [18], [12] and [14].

We suppose that the function $f(S,t)$ is the number of extra shares that should be held due to some deterministic hedging or trading strategy and therefore $df(S,t)$ will be the number of shares needed to be bought or sold at time t and price S. And also we assume that $\lambda(S,t)$ shows the form of price impact and liquidity factor. We can add these terms to the underlying process [18], so we will have

$$dS = \mu S dt + \sigma S dW + \lambda(S,t) df \tag{4.1}$$

where S is the price of the underlying, μ is the measure of the average rate of growth of the asset price, σ is the volatility of the underlying asset and W is a geometric Brownian motion.

We can expand $f(S+dS, t+dt)$ in a Taylor expansion at (S,t):

$$df = \frac{\partial f}{\partial t}dt + \frac{\partial f}{\partial S}dS + \frac{1}{2}\frac{\partial f}{\partial S^2}(dS)^2 + ...$$

and substituting in (4.1) to obtain

$$(1-\lambda\frac{\partial f}{\partial S})dS = (\mu S + \lambda\frac{\partial f}{\partial t})dt + \lambda\frac{\partial^2 f}{\partial S^2}(dS)^2 + \sigma S dW. \tag{4.2}$$

To find an expression for $(dS)^2$, we obtain squaring equation (4.2) and simply it when $dt \to 0$

$$(dS)^2 = \frac{\sigma^2 S^2 dt}{(1-\lambda\frac{\partial f}{\partial S})}^2 + o(dt)$$

where we have used this condition that $(dW)^2 \to dt$ as $dt \to 0$. Substituting above expression of $(dS)^2$ into (4.2), we obtain the following stochastic process:

$$dS = \hat{\mu}Sdt + \hat{\sigma}SdW \tag{4.3}$$

where

$$\mu(\hat{S},t) = \frac{1}{1-\lambda\frac{\partial f}{\partial S}}\Big[\mu S + \lambda(\frac{\partial f}{\partial S} + \frac{1}{2}\hat{\sigma^2}\frac{\partial^2 f}{\partial S^2})\Big]$$

We use Black-Scholes equation to option pricing under the modified stochastic process

$$\frac{\partial V}{\partial t} + \frac{\sigma^2 S^2}{2\Big(1-\lambda(S,t)\frac{\partial f}{\partial S}\Big)^2}\frac{\partial^2 V}{\partial S^2} + rS\frac{\partial V}{\partial S} - rV = 0 \tag{4.4}$$

Delta hedging is a trading strategy that could impact the price clearly. Therefore the trading strategy f can be an option delta under the option price V^*

$$f = \Delta^* = \frac{\partial V^*}{\partial S}.$$

Depends on which strategy the hedgers follow, we will have two pricing PDEs. If V^* were assumed the classical Black-Scholes value, from (4.4) we obtain

$$\frac{\partial V}{\partial t} + \frac{\sigma^2 S^2}{2\Big(1-\lambda(S,t)\frac{\partial^2 V^{BS}}{\partial S^2}\Big)^2}\frac{\partial^2 V}{\partial S^2} + rS\frac{\partial V}{\partial S} - rV = 0 \tag{4.5}$$

That is a linear PDE and is called *first-order feedback*. The second choice of V^* is when we assume that the hedger exactly know the feedback effect so accordingly changes the

hedging strategy therefore $V^* = V$ and the pricing PDE

$$\frac{\partial V}{\partial t} + \frac{\sigma^2 S^2}{2\Big(1 - \lambda(S,t)\frac{\partial^2 V}{\partial S^2}\Big)^2}\frac{\partial^2 V}{\partial S^2} + rS\frac{\partial V}{\partial S} - rV = 0 \tag{4.6}$$

that is a nonlinear PDE and is called *full feedback*.

Equation (4.6) have been considered with different forms of the function $\lambda(S,t)$. One case is a constant value of the liquidity factor which is discussed in [18] and [46] and will be discussed further in next sections. Furthermore, Bordag and Frey in [12] has introduced three different frameworks for modelling illiquid markets:

1) Transaction-cost models:

$$\frac{\partial V}{\partial t} + \frac{1}{2}\sigma^2 S^2\Big(1 + 2\rho S\frac{\partial^2 V}{\partial S^2}\Big)\frac{\partial^2 V}{\partial S^2}$$

2) Reduced-form SDE models:

$$\frac{\partial V}{\partial t} + \frac{1}{2}\frac{\sigma^2 S^2}{\Big(1 - \rho S\frac{\partial^2 V}{\partial S^2}\Big)^2}\frac{\partial^2 V}{\partial S^2}$$

3) Equilibrium or reaction-function models:

$$\frac{\partial V}{\partial t} + \frac{1}{2}\frac{\sigma^2 S^2}{\Big(1 - \rho\frac{g_\alpha(\rho V_S)}{g(\rho V_S)} S\frac{\partial^2 V}{\partial S^2}\Big)^2}\frac{\partial^2 V}{\partial S^2}$$

where ρ is a positive constant and the third model for $g(\alpha) = e^\alpha$ reduces to the second model, and for $g(\alpha) = \frac{1}{1-\alpha}$ [16] we will have:

$$\frac{\partial V}{\partial t} + \frac{1}{2}\frac{\sigma^2 S^2\big(1 - \rho\frac{\partial V}{\partial S}\big)^2}{\Big(1 - \rho\frac{\partial V}{\partial S} - \rho S\frac{\partial^2 V}{\partial S^2}\frac{\partial^2 V}{\partial S^2}\Big)^2}\frac{\partial^2 V}{\partial S^2}$$

4.3 PDE model for feedback options on an unbounded and on a bounded domain

The classical boundary value problem for a feedback European option posed over the financially relevant domain $\Omega_\infty = \{(S,t) \in]0,\infty[\times]0,T[\}$ is found in [18] (based on

[16, 14, 15] and for the special case of no dividend) to be

$$\begin{aligned}&\text{Find } V: \ (S,t) \in \bar{\Omega}_\infty \to R, \ V \in C^0(\bar{\Omega}_\infty) \cap C^{2,1}(\Omega_\infty) \text{ so that}\\ &\frac{\partial V}{\partial t} + \frac{\sigma^2(t)S^2}{2\Big(1-\lambda(S,t)\frac{\partial^2 V^*}{\partial S^2}\Big)^2}\frac{\partial^2 V}{\partial S^2} + \Big(r(t)S - \gamma(t)S\Big)\frac{\partial V}{\partial S} - r(t)V = 0 \text{ in } \Omega_\infty\\ &\text{and } V(S,T) = \kappa(S) \text{ in } \bar{\Omega}_\infty|_{t=T}.\end{aligned} \tag{4.7}$$

Here the dependent variable $V(S,t)$ is the value (price) of the option for a value S of the risky asset at time t. V^* is either V (giving the nonlinear *full feedback* case) or V^{BS} the "no feedback" Black-Scholes-price of the European vanilla option (giving the linear *first-order feedback* case). γ, $\sigma > 0$ and r — the *dividend yield*, *volatility* (on the underlying risky asset) and *market interest rate* (on the riskfree asset) — are all assumed to depend only on time t and be independent of the value S of the underlying risky asset. Instead $\lambda(S,t)$ and $\kappa(S)$ — the *market liquidity* and *payoff* — are functions of the value of the underlying risky asset — but not of any of the derivatives of S. While the liquidity is decided by the market and hence must be modeled, the payoff $\kappa(S)$ is negotiated at time 0 between the buyer and seller of the option. In (4.7) $\kappa(S)$ is given by:

$$\kappa^C(S) = \max\{S-K, 0\}, \tag{4.8}$$

$$\kappa^P(S) = \max\{K-S, 0\}, \tag{4.9}$$

$$\kappa^B(S) = B\mathcal{H}(S-K) = \begin{cases} B & \text{for } S-K \geq 0 \\ 0 & \text{for } S-K < 0 \end{cases}. \tag{4.10}$$

Whereas κ^C, κ^P and κ^B are the payoff functions for the call, put and simple bet options respectively.

For our 3 option cases the "no feedback" Black-Scholes-prices of the European vanilla options are known from basic finance text books as for example [46] §5.4–5.5. The focus in this work is on the challenges posed by the nonlinearity of the BVP(4.7) in the full feedback case when solving the problem numerically. As a warm up to this problem, we shall investigate also the linear first-order feedback case and address problems not connected to the nonlinearity here. To simplify we shall take r as a constant and $\gamma = 0$. Also we shall consider $\sigma \in (0,1)$ and $\lambda \in (0,\infty)$ constant. This results in the following *Backward* DEP [Differential Equation Problem] or IBVP [Initial, Boundary

Value Problem]:

$$
\begin{aligned}
&\text{Find } V: \ (S,t) \in \bar{\Omega} \to \mathbb{R} \text{ where } \Omega = (0, S_{\max}) \times (0,T) \text{ for some } S_{\max} >> K, \\
&\text{so that in a classical, weak or distributional sense} \\
&\frac{\partial V}{\partial t} + \frac{\sigma^2 S^2}{2\Big(1 - \lambda \frac{\partial^2 V^*}{\partial S^2}\Big)^2} \frac{\partial^2 V}{\partial S^2} + r\big(S\frac{\partial V}{\partial S} - V\big) = 0 \text{ in } \Omega \text{ and} \\
&V(0,t) = \kappa(0) e^{-r(T-t)}, \text{ in } \bar{\Omega}|_{S=0}, \\
&V(S_{\max},t) \simeq \begin{cases} S_{\max} - K e^{-r(T-t)} & \text{for } \kappa = \kappa^C \\ 0 & \text{for } \kappa = \kappa^P \\ B e^{-r(T-t)} & \text{for } \kappa = \kappa^B \end{cases}, \text{ in } \bar{\Omega}|_{S=S_{\max}}, \\
&V(S,T) = \kappa(S) \text{ in } \bar{\Omega}|_{t=T},
\end{aligned}
\tag{4.11}
$$

where we consider the 2 feedback cases

$$
\textit{Full Feedback case: } V^* = V \text{ and } \textit{First-order Feedback case: } V^* = V^{BS}, \tag{4.12}
$$

and the 3 payoff cases

$$
\textit{Call option: } \kappa = \kappa^C, \ \textit{Put option: } \kappa = \kappa^P \text{ and } \textit{Simple Bet option: } \kappa = \kappa^B. \tag{4.13}
$$

moreover for numerical computations it is convenient to have a bounded computational domain. This is obtained by restricting S to some bounded interval $S \in (0, S_{\max})$. As long as we require $S_{\max} >> K$.

4.4 Numerical methods for solving the feedback options

We consider the following consistent standard finite difference schemes for the numerical solution of (4.11-4.13).

a. *Forward Euler:* Forward in time t, central in S [FtCS]. Error and stability condition for the heat equation: $\mathcal{O}(k + h^2)$ and $k \leq \frac{h^2}{2}$ respectively.

b. *Backward Euler:* Backward in time t, central in S [BtCS]. Error and stability condition for the heat equation: $\mathcal{O}(k + h^2)$ and A- and L-stable respectively.

c. *Crank Nicolson:* Central in time t, central in S [CtCS]. Error and stability condition for the heat equation: $\mathcal{O}(k^2+h^2)$ and A- but not L-stable respectively.

The numerical schemes are constructed on a net of nodal points (S_n, t_m), $n = 1, \ldots, N$, $m = 1, \ldots, M$ with step sizes h and k respectively, so that $S_n = (n-1)h$ and $t_m = (M-m)k$ and in particular $S_1 = 0$, $S_N = S_{\max}$, $t_1 = T$ and $t_M = 0$. Then the schemes consist of simple replacements $[\rightsquigarrow]$ in (4.11): The Dirichlet terminal and boundary conditions are used as they are: $V(0,t_m) \rightsquigarrow \tilde{V}_{1,m}$, $V(S_{\max},t_m) \rightsquigarrow \tilde{V}_{N,m}$, $V(S_n,T) \rightsquigarrow \tilde{V}_{n,1}$ for $n = 1, \ldots, N$ and $m = 1, \ldots, M$. The derivatives $DV(S_n,t_m)$ in the relevant (mainly interior) nodal points in (4.11) are replaced by finite differences $\delta\tilde{V}_{n,m}$ varying from method to method:

$$
\begin{aligned}
&\text{Find } \tilde{V}_{n,m} \text{ for } n = 1, \ldots, N \text{ and } m = 1, \ldots, M: \\
&\delta_t \tilde{V}_{n,m} + \frac{\sigma^2 S_n^2}{2\left(1 - \lambda \delta_{SS} \tilde{V}^*_{n,m}\right)^2} \delta_{SS} \tilde{V}_{n,m} + r\left(S_n \delta_S \tilde{V}_{n,m} - \delta_0 \tilde{V}_{n,m}\right) = 0 \\
&\text{for } n = 2, \ldots, N-1 \text{ and} m = 1, \ldots, M-1, \\
&\tilde{V}_{1,m} = \kappa(0) e^{-r(T-t_m)}, \text{ for } m = 1, \ldots, M, \\
&\tilde{V}_{N,m} \simeq \begin{cases} S_{\max} - K e^{-r(T-t_m)} & \text{for } \kappa = \kappa^C \\ 0 & \text{for } \kappa = \kappa^P \\ B e^{-r(T-t_m)} & \text{for } \kappa = \kappa^B \end{cases}, \text{ for } m = 1, \ldots, M, \\
&\tilde{V}_{n,1} = \kappa(S) \text{ for } n = 1, \ldots, N,
\end{aligned}
\tag{4.14}
$$

where we consider the two feedback cases

$$
\begin{aligned}
&\textit{Full Feedback case: } \delta_{SS} \tilde{V}^*_{n,m} = \delta_{SS} \tilde{V}_{n,m} \text{ and} \\
&\textit{First-order Feedback case: } \delta_{SS} \tilde{V}^*_{n,m} = \delta_{SS} V^{BS}_{n,m}, \\
&\text{for } n = 1, \ldots, N \text{ and } m = 1, \ldots, M,
\end{aligned}
\tag{4.15}
$$

and the 3 payoff cases

$$
\textit{Call option: } \kappa = \kappa^C, \ \textit{Put option: } \kappa = \kappa^P \text{ and } \textit{Simple Bet option: } \kappa = \kappa^B. \tag{4.16}
$$

For the various finite difference schemes we have the following replacements:

a. *Forward Euler:*

$V(S_n, t_m) \rightsquigarrow \delta_0 \tilde{V}_{n,m} = \tilde{V}_{n,m}$,
$\frac{\partial V}{\partial t}(S_n, t_m) \rightsquigarrow \delta_t \tilde{V}_{n,m} = \frac{\tilde{V}_{n,m+1} - \tilde{V}_{n,m}}{k}$,
$\frac{\partial V}{\partial S}(S_n, t_m) \rightsquigarrow \delta_S \tilde{V}_{n,m} = \frac{\tilde{V}_{n+1,m} - \tilde{V}_{n-1,m}}{2h}$,
$\frac{\partial^2 V}{\partial S^2}(S_n, t_m) \rightsquigarrow \delta_{SS} \tilde{V}_{n,m} = \frac{\tilde{V}_{n+1,m} - 2\tilde{V}_{n,m} + \tilde{V}_{n-1,m}}{h^2}$,
$\frac{\partial^2 V^{BS}}{\partial S^2}(S_n, t_m) \rightsquigarrow \delta_{SS} \tilde{V}^{BS}_{n,m} = \frac{\partial^2 V^{BS}}{\partial S^2}(S_n, t_m)$,
for $n = 2, \ldots, N-1$, $m = 1, \ldots, M-1$.

b. *Backward Euler:*

$V(S_n, t_{m+1}) \rightsquigarrow \delta_0 \tilde{V}_{n,m} = \tilde{V}_{n,m+1}$,
$\frac{\partial V}{\partial t}(S_n, t_{m+1}) \rightsquigarrow \delta_t \tilde{V}_{n,m} = \frac{\tilde{V}_{n,m+1} - \tilde{V}_{n,m}}{k}$,
$\frac{\partial V}{\partial S}(S_n, t_{m+1}) \rightsquigarrow \delta_S \tilde{V}_{n,m} = \frac{\tilde{V}_{n+1,m+1} - \tilde{V}_{n-1,m+1}}{2h}$,
$\frac{\partial^2 V}{\partial S^2}(S_n, t_{m+1}) \rightsquigarrow \delta_{SS} \tilde{V}_{n,m} = \frac{\tilde{V}_{n+1,m+1} - 2\tilde{V}_{n,m+1} + \tilde{V}_{n-1,m+1}}{h^2}$,
$\frac{\partial^2 V^{BS}}{\partial S^2}(S_n, t_{m+1}) \rightsquigarrow \delta_{SS} \tilde{V}^{BS}_{n,m} = \frac{\partial^2 V^{BS}}{\partial S^2}(S_n, t_{m+1})$,
for $n = 2, \ldots, N-1$, $m = 1, \ldots, M-1$.

c. *Crank Nicolson:*

$V(S_n, t_{m+\frac{1}{2}}) \rightsquigarrow \delta_0 \tilde{V}_{n,m} = \frac{1}{2}\left(\tilde{V}_{n,m+1} + \tilde{V}_{n,m}\right)$,
$\frac{\partial V}{\partial t}(S_n, t_{m+\frac{1}{2}}) \rightsquigarrow \delta_t \tilde{V}_{n,m} = \frac{\tilde{V}_{n,m+1} - \tilde{V}_{n,m}}{k}$,
$\frac{\partial V}{\partial S}(S_n, t_{m+\frac{1}{2}}) \rightsquigarrow \delta_S \tilde{V}_{n,m} = \frac{1}{2}\left(\frac{\tilde{V}_{n+1,m+1} - \tilde{V}_{n-1,m+1}}{2h} + \frac{\tilde{V}_{n+1,m} - \tilde{V}_{n-1,m}}{2h}\right)$,
$\frac{\partial^2 V}{\partial S^2}(S_n, t_{m+\frac{1}{2}}) \rightsquigarrow \delta_{SS} \tilde{V}_{n,m} = \frac{1}{2}\left(\frac{\tilde{V}_{n+1,m+1} - 2\tilde{V}_{n,m+1} + \tilde{V}_{n-1,m+1}}{h^2} + \frac{\tilde{V}_{n+1,m} - 2\tilde{V}_{n,m} + \tilde{V}_{n-1,m}}{h^2}\right)$,
$\frac{\partial^2 V^{BS}}{\partial S^2}(S_n, t_{m+\frac{1}{2}}) \rightsquigarrow \delta_{SS} \tilde{V}^{BS}_{n,m} = \frac{\partial^2 V^{BS}}{\partial S^2}(S_n, t_{m+\frac{1}{2}})$,
for $n = 2, \ldots, N-1$, $m = 1, \ldots, M-1$.

4.5 Numerical results and conclusions

We define the error E for a test case with $S_{\max} = S^{\text{test}}_{\max}$ with respect to the reference case with $S_{\max} = S^{\text{ref}}_{\max} \simeq 4S^{\text{test}}_{\max}$ as

$$E(h, k, S^{\text{test}}_{\max}, \text{method}) = \max_{i,j} \left| \tilde{V}_{i,j}(h, k, S^{\text{test}}_{\max}, \text{method}) - \tilde{V}_{i,j}(h, k, S^{\text{ref}}_{\max}, \text{method}) \right|$$

where the maximum is taken over all nodal points for the test case ($S^{\text{ref}}_{\max}$ is selected so that all these point are also nodal points in the reference case) and $\tilde{V}_{i,j}(h, k, S^{\text{case}}_{\max}, \text{method})$ is the numerical solution in the nodal point indexed by i, j in the test case, with step

sizes h and k in the S and t directions respectively, with $S_{\max} = S^{\text{case}}_{\max}$ and using the finite difference scheme "method".

We consider for the first-order feedback and full feedback call option, two sets of step sizes: $h = k = 0.1$ and $h = 0.05$ and $k = 0.001$, five values of $S^{\text{test}}_{\max}$: $4K$, $3K$, $2K$, $1.5K$ and $1.1K$, and the 3 methods: Forward Euler [FE], Backward Euler [BE] and Crank-Nicolson [CN]. The goal is to find an appropriate scheme for the first-oder and full feedback options and select $S_{\max} = S^{\text{test}}_{\max}$ so that $E(h, k, S^{\text{test}}_{\max}, \text{method}) < 10^{-4}$. The relative errors for the first-order and full feedback call option solved with these three methods and with various values of $S^{\text{test}}_{\max}$ are given in Tables 4.1-4.4 for two step sizes $h = k = 0.1$ and $h = 0.05$ and $k = 0.001$ respectively.

TABLE 4.1: First-order feedback error $E(h = .1, k = .1, S^{\text{test}}_{\max}, \text{method})$

Method/$S^{\text{test}}_{\max}$	$1.1K$	$1.5K$	$2K$	$3K$	$4K$
FE	0.0136848	0.000930708	7.70656e-05	0.550371	329.79
BE	0.0130196	0.00120136	4.44045e-05	7.65906e-05	7.66613e-05
CN	0.0133154	0.00108415	1.40325e-05	5.63610e-08	5.12348e-08

TABLE 4.2: First-order feedback error $E(h = .05, k = .001, S^{\text{test}}_{\max}, \text{method})$

Method/$S^{\text{test}}_{\max}$	$1.1K$	$1.5K$	$2K$	$3K$	$4K$
FE	0.0207339	0.00108041	1.01585e-5	9.29013e+351	3.06264e+605
BE	0.0207211	0.00108332	8.94370e-6	7.67815e-07	7.68611e-07
CN	0.0207275	0.00108187	9.55081e-6	7.32806e-10	5.02608e-12

TABLE 4.3: Full feedback error $E(h = .1, k = .1, S^{\text{test}}_{\max}, \text{method})$

Method/$S^{\text{test}}_{\max}$	$1.1K$	$1.5K$	$2K$	$3K$	$4K$
FE	2.77760e-05	7.70689e-05	7.70689e-05	7.70656e-05	7.70656e-05
BE	0.00256037	0.000211262	8.01231e-05	7.66742e-05	7.66809e-05
CN	0.00828538	0.0217787	0.0422436	0.0829726	0.1237

TABLE 4.4: Full feedback error $E(h = .05, k = .001, S^{\text{test}}_{\max}, \text{method})$

Method/$S^{\text{test}}_{\max}$	$1.1K$	$1.5K$	$2K$	$3K$	$4K$
FE	1.90943e-05	7.68651e-07	7.68652e-07	7.68652e-07	7.68652e-07
BE	0.000843621	5.18059e-05	1.21166e-06	7.68647e-07	7.68612e-07
CN	0.00689234	0.0219523	0.0424089	0.0832193	0.124029

Based on these results for the first-order feedback the explicit scheme Forward Euler is not stable for bigger S_{max}. Therefore the implicit schemes backward Euler and Crank Nicolson solve the first-order feedback more accurately. Furthermore selecting $S_{\max} = 2K$ is sufficient for the given error (10^{-4}).

But for the full feedback option the explicit scheme is more accurate than implicit schemes since in implicit scheme we should solve a system of nonlinear equations by linearization of the nonlinear part of the equations and using an iterative method such as Newton method to solve the system of linearized equations. Moreover more complicated nonlinearity in Crank Nicolson scheme causes bigger errors than Backward Euler. Also for the given error (10^{-4}) in full feedback $S_{\max} = 2K$ is adequate.

Moreover all max errors are located in the last iteration and close to $S = S_{\max}$ however there is some oscillation around S=K. In Figure 4.1 we show two examples of numerical solutions of the first-order and full feedback call option with Crank Nicolson scheme in the above set up, namely $\tilde{V}_{i,j}(.05, .001, S_{\max}, \text{CN})$ and the 3-D plot of relative errors $(E(.05, .001, S^{\text{test}}_{\max}, \text{CN}))$ in all nodal points.

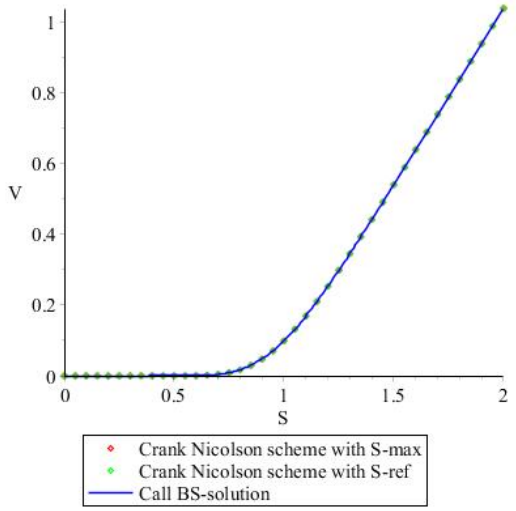

(a) First-order feedback call with $S_{\max}^{\text{test}} = 2K$.

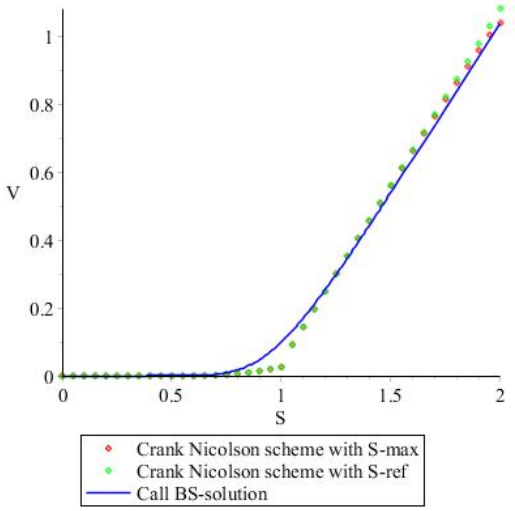

(b) Full feedback call with $S_{\max}^{\text{test}} = 2K$.

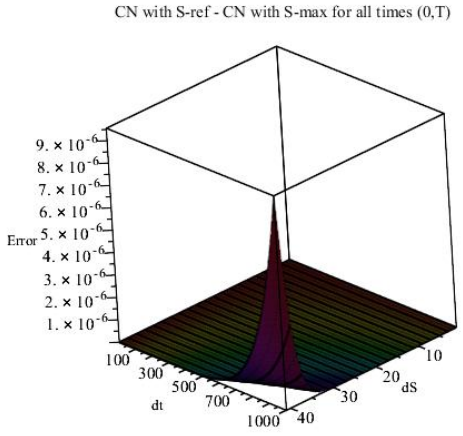

(c) First-order feedback errors with respect to $S_{\max}^{\text{ref}}$.

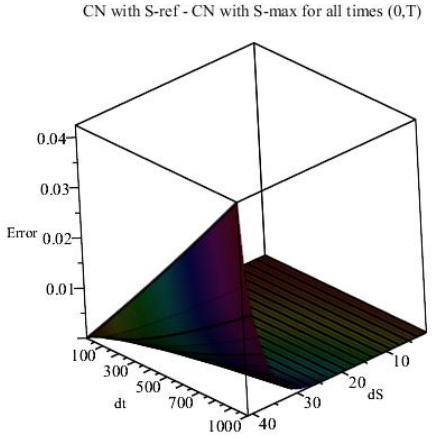

(d) Full feedback errors with respect to $S_{\max}^{\text{ref}}$.

FIGURE 4.1: Top curves are the first-order feedback (a) and full feedback (b) call option with $S_{\max}^{\text{test}} = 2K$, and two curves (c) and (d) are their errors in all nodal points with respect to $S_{\max}^{\text{ref}} = 4S_{\max}^{\text{test}}$ with step sizes $h = 0.05$ and $k = 0.001$.

Chapter 5

Finite Difference Schemes for a Nonlinear Black-Scholes Model with Transaction Cost and Volatility Risk

Sima Mashayekhi and Jens Hugger

Abstract. Several nonlinear Black-Scholes models have been proposed to take transaction cost, large investor performance and illiquid markets into account. One of the most comprehensive models was introduced by Barles and Soner in [4] and considers transaction cost in the hedging strategy and risk from an illiquid market. In this paper we compare several finite difference methods for the solution of this model with respect to precision and order of convergence within a computationally feasible domain allowing at most 200 space steps and 10000 time steps. We conclude that standard explicit Euler comes out as the preferred explicit method and standard Crank Nicolson with Rannacher time stepping as the preferred implicit method.

Keywords: Nonlinear Black-Scholes model, Transaction costs, Feedback and illiquidity, Finite difference schemes

Subjectclass: 35K20, 35K55, 35R99, 65M06, 65M12

5.1 Introduction

The classical linear Black-Scholes model for option pricing assumes a complete market without transaction cost, illiquidity or feedback issues like large investor performance. Several nonlinear Black-Scholes models have been proposed in recent years to deal with these inadequacies. Nonlinearity in the nonlinear Black-Scholes models always arises from a nonlinear volatility function depending not only on time t and underlying asset price S but also on the Greek Gamma i.e. the second derivative of the option price $V(S,t)$ with respect to S. Hence the nonlinear Black-Scholes model equation is

$$\frac{\partial V}{\partial t} + \frac{1}{2}\sigma^2(t, S, \frac{\partial^2 V}{\partial S^2})S^2\frac{\partial^2 V}{\partial S^2} + (r-\gamma)S\frac{\partial V}{\partial S} - rV = 0,\ (S,t) \in (0, S_{max}) \times (0,T) \quad (5.1)$$

with the following terminal and boundary Dirichlet conditions:

$$V(S,T) = \kappa(S,T),\ V(0,t) = \kappa(0,t),\ V(S_{\max},t) \simeq \kappa(S_{\max},t) \quad (5.2)$$

where we are using the utility function

$$\kappa(S,t) = \begin{cases} \max\{Se^{-\gamma(T-t)} - Ke^{-r(T-t)}, 0\} & \text{for the } \textit{call option} \\ \max\{Ke^{-r(T-t)} - Se^{-\gamma(T-t)}, 0\} & \text{for the } \textit{put option} \\ Be^{-r(T-t)}\mathcal{H}(S-K) & \text{for the } \textit{bet option} \end{cases} . \quad (5.3)$$

γ, σ and r are the *dividend yield*, *volatility* (on the underlying risky asset) and *market interest rate* (on the riskfree asset) respectively, K is the *Strike Price*, $\mathcal{H}$ the Heaviside function and $S_{\max} >> K$ is the upper bound on the computational domain in the S variable.

Two known "numerical issues" from the linear case are expected to carry over to the nonlinear case:

First of all many methods oscillate either around the strike price $S = K$ or around the upper bound for the computational domain $S = S_{\max}$. One way to eliminate such oscillations is to use a monotone method that cannot oscillate. Alternatively oscillations near $S = S_{\max}$ are easily observed and removed simply by increasing $S_{\max}$ of course at the cost of an increase in computational time. Initiating methods oscillating around $S = K$ by smaller timesteps (4 initial quartersteps has been suggested as optimal) with a

nonoscillating method tends to remove the oscillations without changing the convergence rate of the oscillating method. Most notable example is probably Crank-Nicolson with 4 initial quartersteps by implicit Euler explored in Chapter 2.

The second "numerical issue" is the degradation in observed convergence order caused by the singular terminal condition for options unless extremely small stepsizes are used. Stepsizes often lying outside what is computationally feasible.

In this article we will investigate these two problems for a number of finite difference schemes and one particular nonlinear model proposed by Barles and Soner in [4].

The nonlinearity of the nonlinear case may provide "numerical issues" of its own. Uniqueness of solution is typically an issue for nonlinear problems just as the "nice" smoothening feature of linear heat conduction may be lost. Such nonlinear features will not be dealt with here, but let us just note, that no practical problems in this direction have been observed.

In section 5.2 we review the Barles and Soner model for nonlinear volatility. In section 5.3 we present a number of different finite difference methods for the Barles and Soner model. In section 5.4 we present some numerical results with the different finite difference schemes for the Barles and Soner model. Finally in section 5.5 we discuss our results and present the conclusions.

5.2 The Barles and Soner nonlinear volatility model

Barles and Soner considers in [4] both transaction cost and risk from volatile portfolios. They take an approach based on utility maximization which results in the following adjustment of the volatility:

$$\sigma_{BS}^2(t,S,\frac{\partial^2 V}{\partial S^2}) = \sigma_0^2\left[1+\Psi\left(e^{r(T-t)}aS^2\frac{\partial^2 V}{\partial S^2}\right)\right]. \tag{5.4}$$

Here $a=\kappa^2 R$ where κ is the "Leland transaction cost" (denoted μ in [4]) and R is a *risk aversion factor* (denoted γ in [4]). Finally $\Psi(x)$ is the solution of the nonlinear ODE

$$\Psi'(x) = \frac{\Psi(x)+1}{2\sqrt{x\Psi(x)}-x},\ x\neq 0 \tag{5.5}$$

with the initial condition $\Psi(0) = 0$. In appendix A of [4] the existence of a unique continuous viscosity solution to this problem has been shown. It is also shown that $\Psi \geq 0$ i.e. that the adjustment factor to σ_0^2 is nonnegative for any argument of Ψ. For the numerical experiments an unspecified explicit time stepping finite difference scheme is used with small time steps near maturity ($t = T$) and larger time steps away from maturity. Lesmana and Wang present in [31] an implicit first order time stepping and upwind asset price stepping finite difference method that we here shall denote *ImpUp*. Zhou et al present in [48] a positivity-preserving scheme that we shall denote *PosPre*. Both schemes are used to solve the Barles and Soner model.

Note that σ_0 — the volatility of the underlying asset — is assumed constant and if we take $\sigma(t, S, V_{SS}) = \sigma_0$ we will have the classical linear Black-Scholes model.

5.3 Finite Difference Schemes

Arenas et al present in [2] a nonstandard explicit finite difference scheme for the numerical pricing of options in an illiquid market modeled by Frey et al in [16], [14] and [15]. González et al in [19] then applies the same scheme for the parameterized model by Bakstein and Howison from [3]. The method is shown to be nonnegative, nondecreasing, stable and consistent for both model problems. Here we shall consider this method for solving the option pricing problem with the Barles and Soner model (5.4–5.5) which has not previously been attempted (See Appendix 5.A-5.C for more details). For short the method will be denoted *NFDM* and we will compare NFDM to ImpUp and PosPre, both previously used to solve the Barles and Soner model. Finally we shall compare to two standard methods, namely explicit first order in time and central second order in S denoted *FtCS* and Crank-Nicolson denoted *CN*. CN is stabilized with "Rannacher time stepping" — starting up with 4 quarter steps using the fully implicit first order in time and second order in S "Implicit Euler" scheme — and hence the notation *CNR* is used. Also we shall apply $\boldsymbol{K_\alpha}$*-optimization* to all 5 methods minimizing the error by adjusting stepsizes so that the strike price K is situated in an optimal position in the element that it resides in (see Chapter 2).

The volatility function in (5.1) is then taken to be σ_{BS} from (5.4–5.5) and in order to follow the original presentation dividend is not considered ($\gamma = 0$) and time is reversed

by replacing the time variable t by $\tau = T - t$ and consequently $V(S,t)$ by $U(S,\tau)$. This transforms equation (5.1) into

$$\frac{\partial U}{\partial \tau} - \frac{1}{2}\sigma_{BS}^2(T-\tau, S, \frac{\partial^2 U}{\partial S^2})S^2\frac{\partial^2 U}{\partial S^2} - rS\frac{\partial U}{\partial S} + rU = 0 \tag{5.6}$$

with σ_{BS} given by (5.4–5.5) whereas the terminal and boundary conditions (5.2) for V are transformed into the obvious initial and boundary conditions for U

$$U(S,0) = \kappa(S,T),\ U(0,\tau) = \kappa(0,T-\tau),\ U(S_{\max},\tau) \simeq \kappa(S_{\max},T-\tau) \tag{5.7}$$

with κ still given by (5.3).

We describe our 5 FDM's using the following finite difference operators:

$$\begin{gathered}
\delta_\tau^+ u_j^n = \frac{u_j^{n+1} - u_j^n}{k}, \quad \tilde{\delta}_\tau^+ u_j^n = \frac{u_j^{n+1} - u_j^n}{\theta(k)}, \\
\delta_S^+ u_j^n = \frac{u_{j+1}^n - u_j^n}{h}, \quad \delta_S^0 u_j^n = \frac{u_{j+1}^n - u_{j-1}^n}{2h}, \\
\delta_{SS}^0 u_j^n = \frac{u_{j+1}^n - 2u_j^n + u_{j-1}^n}{h^2}, \quad \tilde{\delta}_{SS}^0 u_j^n = \frac{u_{j+1}^n - 2u_j^n + u_{j-1}^n}{\phi(h)}, \\
\bar{\delta}_{SS}^0 u_j^n = \frac{u_{j+1}^n - 2u_j^{n+1} + u_{j-1}^n}{h^2},
\end{gathered} \tag{5.8}$$

where $\phi(h) = (e^{\sqrt{r}h} - 2 + e^{-\sqrt{r}h})/r = h^2 + \mathcal{O}(h^4)$ and $\theta(k) = (1 - e^{-rk})/r = k + \mathcal{O}(k^2)$. Noting that the initial and boundary conditions are the same for all methods, our 5 FDM's are described by their main update equations:

$$\begin{aligned}
\text{NFDM} \quad & \tilde{\delta}_\tau^+ u_j^n - \frac{1}{2}\sigma_{BS}^2(T-\tau_n, S_j, \tilde{\delta}_{SS}^0 u_j^n)S_j^2\tilde{\delta}_{SS}^0 u_j^n - rS_j\delta_S^+ u_j^n + ru_j^n = 0 \\
\text{ImpUp} \quad & \delta_\tau^+ u_j^n - \frac{1}{2}\sigma_{BS}^2(T-\tau_{n+1}, S_j, \delta_{SS}^0 u_j^{n+1})S_j^2\delta_{SS}^0 u_j^{n+1} - rS_j\delta_S^+ u_j^{n+1} \\
& + ru_j^{n+1}n = 0 \\
\text{PosPre} \quad & \delta_\tau^+ \widehat{u}_j^n - \frac{1}{2}\sigma_{BS}^2(T-\tau_n, x_j^n, \bar{\delta}_{xx}^0 \widehat{u}_j^n)(x_j^n)^2\bar{\delta}_{xx}^0 \widehat{u}_j^n = 0 \\
\text{FtCS} \quad & \delta_\tau^+ u_j^n - \frac{1}{2}\sigma_{BS}^2(T-\tau_n, S_j, \delta_{SS}^0 u_j^n)S_j^2\delta_{SS}^0 u_j^n - rS_j\delta_S^0 u_j^n + ru_j^n = 0 \\
\text{CN} \quad & \delta_\tau^+ u_j^n - \frac{1}{2}\sigma_{BS}\left(T-\tau_{n+\frac{1}{2}}, S_j, \delta_{SS}^0\left(\frac{u_j^{n+1}+u_j^n}{2}\right)\right)S_j^2 \\
& \cdot \delta_{SS}^0\left(\frac{u_j^{n+1}+u_j^n}{2}\right) - rS_j\delta_S^0\left(\frac{u_j^{n+1}+u_j^n}{2}\right) + r\left(\frac{u_j^{n+1}+u_j^n}{2}\right) = 0
\end{aligned} \tag{5.9}$$

PosPre is solving $\widehat{u}_\tau - \frac{1}{2}\sigma_{BS}^2 x^2 \widehat{u}_{xx} = 0$ arising from equation (5.6) through the transformation $x(S,\tau) = e^{r\tau}S$ and $\widehat{u}(x,\tau) = e^{r\tau}U(S,\tau)$ used in [48]. PosPre for (5.6) is highly non standard.

NFDM is explicit, i.e. has short computational time, but is only conditionally stable. It is non negative and non oscillating and has order of convergence $\mathcal{O}(dt + dS)$.

ImpUp is implicit, i.e. has long computational time, but is unconditionally stable. It is non oscillating and has order of convergence $\mathcal{O}(dt + dS)$.

PosPre is explicit, i.e. has short computational time, and is unconditionally stable. It is non negative and non oscillating and has order of convergence $\mathcal{O}(dt + dS^2 + \frac{dt}{dS^2})$ and hence is only conditionally consistent with the condition $\frac{dt}{dS^2} \longrightarrow 0$ as dt and dS go to zero but the tough condition $dt = \mathcal{O}(dS^4)$ in order to not lose orders of convergence compared to the standard FtCS method.

FtCS is explicit, i.e. has short computational time, but is only conditionally stable. It may oscillate (but in practice only around $S = S_{\max}$) and has order of convergence $\mathcal{O}(dt + dS^2)$.

CN is implicit, i.e. has long computational time, but is unconditionally stable. It in not L-Stable and may oscillate (in practice both at $S = K$ and at $S = S_{\max}$) and has order of convergence $\mathcal{O}(dt^2 + dS^2)$.

The proof of the properties of NFDM, FtCS and CN for the Barles and Soner model will be presented elsewhere. The properties of ImpUp are shown in [31] and the properties of PosPre are shown in [48].

5.4 Numerical Results

We reuse the parameter values from [31] $\gamma = 0$, $r = 0.1$, $\sigma_0 = 0.2$, $K = 40$, $T = 1$, $S_{\max} = 80$ and $B = 1$. We compare results obtained with NFDM, ImpUp, PosPre, FtCS and CNR (see (5.8–5.9)) with these parameter values. For the transaction cost parameter a we shall consider the values 0 (linear Black-Scholes), 0.02 and 0.05 (considered in [31]) and also 0.1 and 0.4 (as extreme values). As it turns out, $S_{\max} = 2K = 80$ is sufficient to avoid oscillations in FtCS and CN at $S = S_{\max}$. Since in any case a

computational domain including $S \in [0, 2K]$ would seem reasonable, the non oscillatory methods provide no advantage when it comes to reducing the size of the computational domain.

The first step in solving the Barles and Soner model is the solution of the nonlinear ODE (5.5). This equation has been solved in [1] with the "ode45" solver in MATLAB based on the well known Ruge-Kutta-Fehlberg 45 scheme. Instead we shall follow the approach from [31] using an implicit exact solution derived in [8]. We then use Maple's `fsolve` command to find specific values of Ψ. The implicit exact solution takes the form

$$\sqrt{|x|} = \begin{cases} \frac{-\sinh^{-1}(\sqrt{\Psi(x)})}{\sqrt{\Psi(x)+1}} + \sqrt{\Psi(x)} & \text{for } x > 0 \\ \frac{-\sin^{-1}(\sqrt{-\Psi(x)})}{\sqrt{\Psi(x)+1}} - \sqrt{-\Psi(x)} & \text{for } x < 0 \end{cases} \tag{5.10}$$

We begin our numerical experiments by illustrating the effect of the transaction cost parameter a on the initial option price at $t = 0$ that we compute with NFDM for $h = dS = 2$, $k = dt = 0.00078125$ and $a = 0$, 0.02, 0.05, 0.1 and 0.4. The results for the bet (digital call) option are very similar to those for the put and call which are almost identical because of the put-call-parity. Hence we only show results for the put option. In the top left of Figure 5.1 we show the option price $V(S, 0) = U(S, T)$ for the put option and in the top right we show the difference between the nonlinear put option solved by NFDM and the exact solution to the linear put option ($a = 0$). Similarly, the bottom row shows the difference between two Greeks for the nonlinear put option and the exact Greeks for the linear put option. The Greeks (Delta ($\frac{\partial V}{\partial S}(S, 0) = \frac{\partial U}{\partial S}(S, T)$) and Gamma ($\frac{\partial^2 V}{\partial S^2}(S, 0) = \frac{\partial^2 U}{\partial S^2}(S, T)$)) are computed from the NFDM solution using second order finite differences. Note that only for the case $a = 0$ (the curves marked by circles in Figure 5.1) the differences actually constitute a numerical error. For other values of a the difference is only used for scaling. Figure 5.1 shows that bigger transaction cost parameters cause more extreme solution values without otherwise changing the overall picture. It should be noted however, that increasing the transaction cost parameter a heavily influences the stability condition for NFDM. For $dS = 2$ and $a \leq 0.1$, $dt = 0.0125$ is sufficient, whereas for $a = 0.4$ it has been necessary to take $dt = 0.00078125$ in order to get a stable numerical solution. In Figure 5.2 we show the stability regions for NFDM for $a = 0.02$ and $a = 0.4$ respectively with the boundary consisting of unstable points $(dS, dt = 0.1 \cdot 2^{-j})$ such that $(dS, dt = 0.1 \cdot 2^{-(j+1)})$ is stable. For

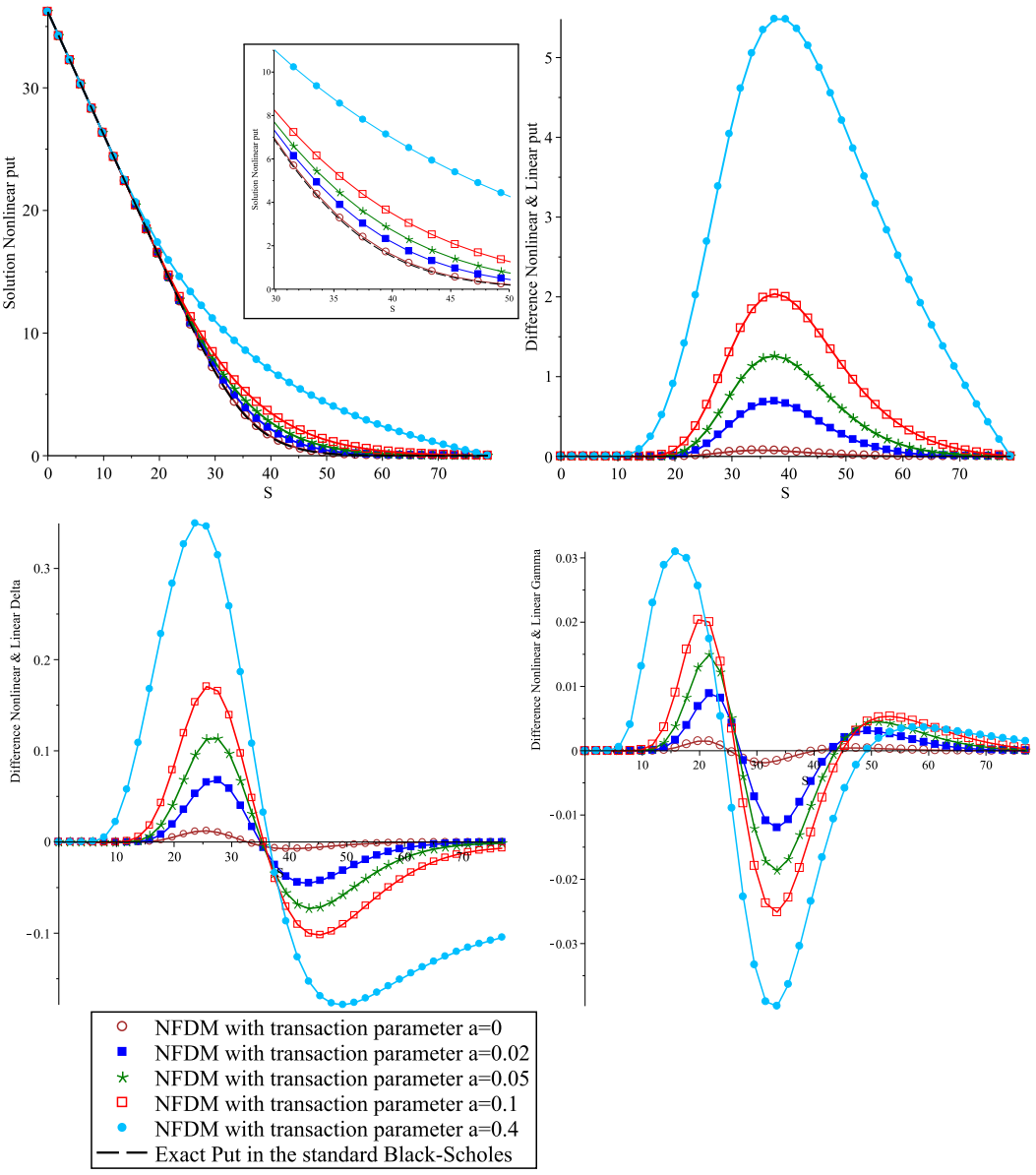

FIGURE 5.1: Nonlinear European Put option solved with NFDM for different transaction cost parameters at time 0 and differentiated with second order finite differences. Top left: Numerical option price. (Insert shows $(S, V) \in [30, 50] \times [0, 11]$). Top right: Numerical option price minus exact option price in the linear case $a = 0$. Bottom left: Numerical option Delta minus exact option delta in the linear case $a = 0$. Bottom right: Numerical option Gamma minus exact option gamma in the linear case $a = 0$

comparison we have included also the stability boundary for the classical FtCS. The results indicate that explicit FDM's become increasingly problematic with increasing transaction cost parameter a. In order to maintain a reasonably sized stability region within the computational domain, we shall compare the various methods for a low transaction cost parameter $a = 0.02$ below.

For a systematic comparison of the 5 finite difference methods we shall compute *base*

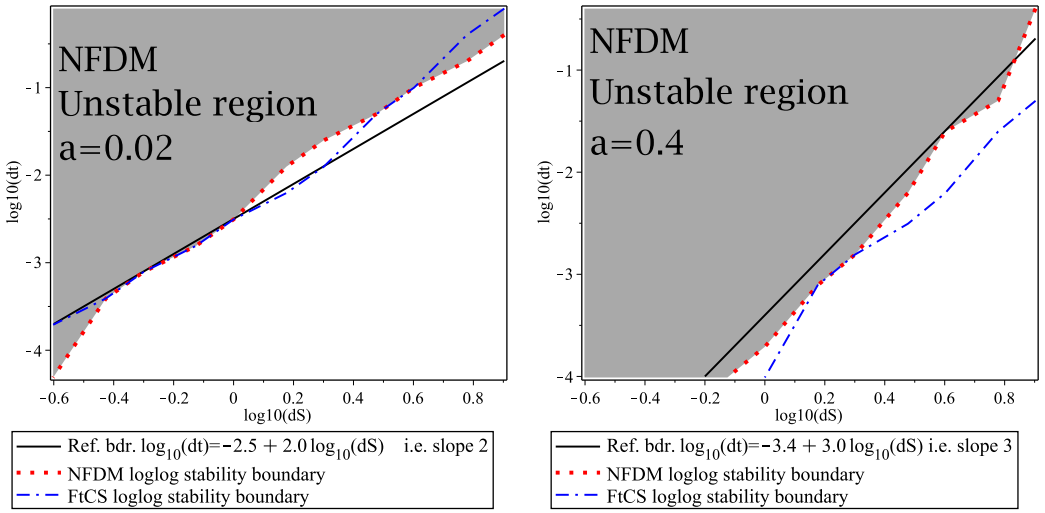

FIGURE 5.2: Log-Log-Stability region for NFDM and FtCS with transaction cost parameter $a = 0.02$ (Left figure) and $a = 0.4$ (Right figure)

solutions (BasSol) with a series of meshes with $dS \in [0.5, 8.0]$ and $dt \in [0.1, 0.0002]$. We need an estimate of the exact solution which is not known for the nonlinear models. The estimate will be based on a *Fine mesh reference solution (RefSol)* computed on a mesh with $dS = 0.375$ and $dt \simeq 0.0001$ which is finer than the base meshes. The fine mesh is defined as our limit for computational feasibility and takes several days to compute in our Maple setup. RefSol will either be computed with the method itself or with the CNR method which is found to be the better performing method for the linear problem ($a = 0$). (These results will be presented elsewhere).

We shall consider the *local error estimate* $E(S) = \text{RefSol} - \text{BasSol}$ at any $S \in [0, S_{\max}]$ and at time $t = 0$ which is a time discretization point for all methods. Instead the S grid of RefSol will be finer than that of BasSol and will generally not have overlapping nodes. When nodes are not overlapping a linear interpolation between the 2 closest neighbors is then performed resulting in a RefSol in the same nodal points as BasSol. We also consider the *global error estimate* $E_\infty = \max_S |E(S)|$, the maximum taken over all S-nodal points for BasSol.

The local error estimate $E(S)$ with transaction cost parameter $a = 0.02$ at time $t = 0$ and with CNR as reference method is shown in Figure 5.3 for step sizes $h = dS = 2$ and $k = dt = 0.0125$. For this particular snapshot clearly FtCS is providing the smallest global error estimate, closely followed by CNR while NFDM, ImpUp and PosPre are falling significantly behind. Note that the 10 times smaller $E(S)$ for the bet option than for the call option is countered by the 40 times smaller maximal solution value for the bet ($V_{\max}^{\text{bet}} = 1$) than for the call ($V_{\max}^{\text{call}} = 40$).

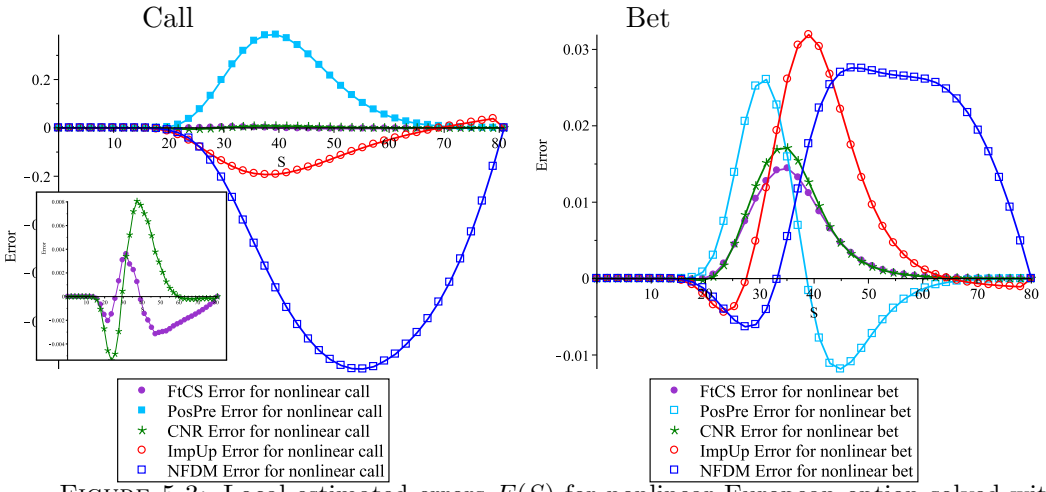

FIGURE 5.3: Local estimated errors $E(S)$ for nonlinear European option solved with NFDM, ImpUp, PosPre, FtCS and CNR with $dS = 2$ and $dt = 0.01245$ for transaction cost parameter $a = 0.02$. The reference solution is computed with CNR for a fine mesh with $dS = 0.375$ and $dt = 0.00009765625$. Left: Call option. (Insert shows FtCS and CNR with $(S, E(S)) \in [0, 80] \times [-0.0055, 0.008]$). Right: Bet option

TABLE 5.1: Convergence results for the nonlinear call option solved with NFDM and FtCS

Nodes		**NFDM**			**FtCS**		
S	***t***	**Error**	**Difference**	**Ratio**	**Error**	**Difference**	**Ratio**
10	320	0.969558			0.126505		
20	640	0.362126	0.607432		0.032240	0.094265	
40	1280	0.161670	0.200456	3.03	0.009176	0.023064	4.09
80	2560	0.090007	0.071663	2.80	0.002706	0.006470	3.56
160	5120	0.026759	0.063248	1.13	0.000986	0.001720	3.76

For a more thorough investigation the global error estimate is computed for call and bet options for all 5 FDM's, and for all BasSol using the FDM itself for RefSol. A selection of convergence plots with logarithmic axes showing the global error estimate E_∞ for the call option solved with NFDM, PosPre, FtCS and CNR and for all BasSol are shown in Figure 5.4. The bet options are omitted since they show very similar results. ImpUp is omitted since it in the linear case ($a = 0$) shows a behavior very similar to CNR only with significantly bigger errors (smaller order of convergence).

Since the exact solution is not known for the nonlinear options, we estimate convergence orders based on the numerical solutions in two different ways: Tables 5.1–5.2 illustrate the convergence of the error $e_R \simeq CR^q$ (not knowing whether R is dS or dt) for NFDM, PosPre, FtCS and CNR when halving both step sizes in each iteration so that Ratio $= 2^q = \frac{|e_h - e_{h/2}|}{|e_{h/2} - e_{h/4}|}$. We obtain quadratic convergence for FtCS and CNR, linear but decreasing order of convergence for NFDM and sublinear but increasing order

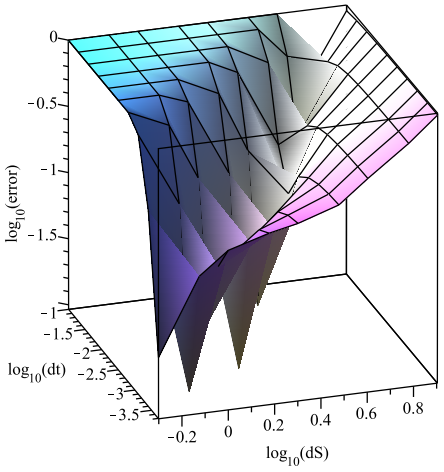

(a) $\log_{10}$(estimated NFDM error)

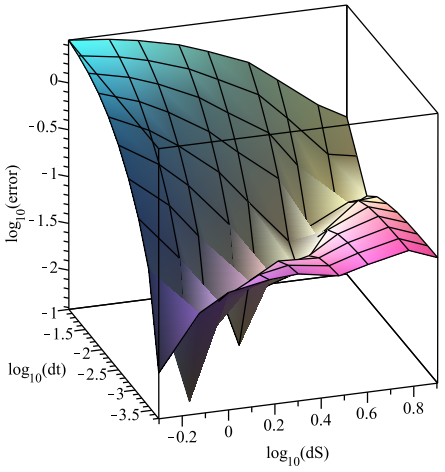

(b) $\log_{10}$(estimated PosPre error)

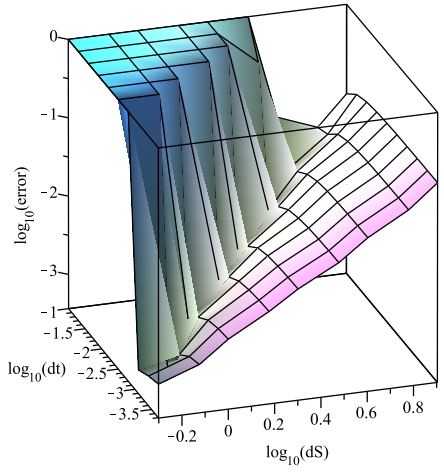

(c) $\log_{10}$(estimated FtCS error)

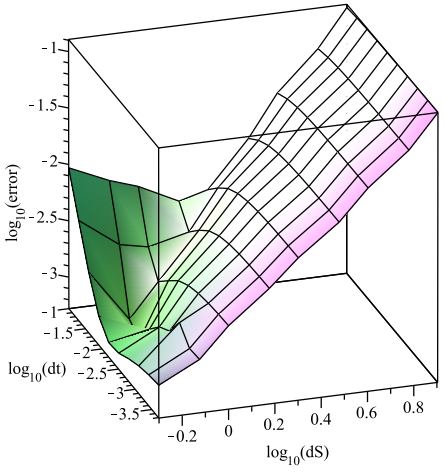

(d) $\log_{10}$(estimated CNR error)

FIGURE 5.4: Global estimated errors E_∞ for nonlinear European Call options when solved with NFDM (a), PosPre (b), FtCS (c) and CNR (d) for transaction cost parameter $a = 0.02$ at time $t = 0$. The reference solution is computed with NFDM, PosPre, FtCS and CNR respectively for a fine mesh with $dS = 0.375$ and $dt = 0.00009765625$

TABLE 5.2: Convergence results for the nonlinear call option solved with CNR and PosPre

Nodes		**CNR**			**PosPre**		
S	***t***	**Error**	**Difference**	**Ratio**	**Error**	**Difference**	**Ratio**
10	320	0.127837			0.077035		
20	640	0.032952	0.094885		0.075434	0.001601	
40	1280	0.009476	0.023476	4.04	0.065135	0.010299	0.16
80	2560	0.002836	0.006640	3.53	0.040396	0.024739	0.42
160	5120	0.001026	0.001810	3.66	0.011714	0.028682	0.86

of convergence for PosPre. Clearly, neither NFDM nor PosPre stabilize with respect to order of convergence within the computationally feasible domain. We also propose a more thorough approach focusing on convergence order in both variables S and t simultaneously and utilizing data from all BasSol in a weighted least squares approximation over all stable data points $(dS_i, dt_j, (E_\infty)_{i,j})$ of the form

$$\min_{a,b,\alpha,\beta} \sum_{i,j} w_{i,j} \cdot ((E_\infty)_{i,j} - (a \cdot dS_i^\alpha + b \cdot dt_j^\beta))^2. \tag{5.11}$$

The stepsizes are recorded so that they decrease with increasing index, i.e. $dS_{i+1} \leq dS_i$ and $dt_{j+1} \leq dt_j$, and the simple weight function $w_{i,j} = i \cdot j$ putting higher weight on smaller step sizes is applied. Obviously selecting a different weight function may change the results somewhat. Points where the error is increasing with decreasing dS are omitted. In the least squares minimizations the side conditions $0 \leq a$, $0 \leq b$, $0 \leq \alpha \leq 2.5$ and $0 \leq \beta \leq 2.5$ are imposed. The following convergence orders are computed. For the implicit PosPre and CNR the results in the square braces $[\cdot]$ are for the "bubbles" for large dt and small dS where the error start increasing with decreasing dS(see Figure 5.4):

$$\begin{array}{lll}
\text{NFDM} & E_\infty^{\text{Call}} = 0.067 dS^{1.3} & E_\infty^{\text{Bet}} = 0.012 dS^{1.1} \\
\text{FtCS} & E_\infty^{\text{Call}} = 0.002 dS^{2.0} & E_\infty^{\text{Bet}} = 0.008 dS^{1.1} \\
\text{CNR} & E_\infty^{\text{Call}} = 0.002 dS^{2.0}\ [0.089 dt^{1.1}] & E_\infty^{\text{Bet}} = 0.007 dS^{1.2} \\
\text{PosPre} & E_\infty^{\text{Call}} = 0.058\ [7.170 dt^{0.5}] & E_\infty^{\text{Bet}} = \text{"Oscillating error"}
\end{array} \tag{5.12}$$

The oscillating error for the PosPre bet is consistent with the conditional consistency condition $\frac{dt}{dS^2} \longrightarrow 0$, indicating that smaller dt's are required.

We venture the following conclusions based on the graphs and the least squares calculations: The implicit methods PosPre and CNR show convergence with decreasing dt of order 0.5 and 1.1 respectively in the bubble. For the explicit methods NFDM and FtCS the bubbles are covered by the instability region. In order to get errors below 0.001 smaller values of dS are required which is computationally infeasible. A better alternative to investigate obviously is mesh grading the S-mesh, or some transformation method as suggested in [41] (ch. 11, for a nonlinear jumping volatility model) but this is beyond the scope of the current article. For the call option FtCS and CNR show

the expected quadratic convergence with dS outside the bubble whereas NFDM only shows an order slightly above linear and PosPre shows no convergence at all. For the bet option both FtCS, CNR and NFDM show orders of convergence in dS slightly above linear. The stability area for FtCS is comparable to the one for NFDM (see Figure 5.2). Comparing the methods clearly FtCS and CNR stand out above the rest, the choice being whether to go for the fast computational times for the explicit FtCS, dealing with the instability area increasing in size with the transaction cost parameter a and reducing the usable area for the explicit methods to approximately $0 \leq a \leq 0.1$, or whether to accept the longer computational times of the implicit CNR, avoiding the concerns about feasible dt–dS combinations for the implicit, absolutely stable CNR.

5.5 Conclusions

The "classical Explicit Euler" is the better explicit method and the "classical with a twist Crank-Nicolson with Rannacher time stepping" is the better implicit method among the FDM's tested on the Barles and Soner nonlinear Black-Scholes model. The non oscillating methods do not offer any enhancement of the performance in the cases considered. The explicit methods suffer from an instability region growing with the transaction cost parameter a rendering them somewhat useless for $a \geq 0.1$. None of the methods considered show significant convergence with dt — the error from the S-direction dominating except for the coarsest time step sizes. Because of computer time limitations the brute force solution (smaller dS) seems out of reach pointing instead towards graded S-meshes as the obvious solution to get in the ideal zone where the errors from t and S are balanced.

Appendix

5.A NFDM Scheme

The nonstandard finite difference scheme [NFDM] is based on an "exact finite difference scheme" for the linear first order reaction and convection terms removing the diffusion term by taking $\sigma_0 = 0$. Then this scheme is applied to the complete problem only adding nonstandard finite difference approximations of the diffusion term. So first we consider the problem

$$\frac{\partial U}{\partial \tau} - rS\frac{\partial U}{\partial S} + rU = 0 \text{ for } (S,\tau) \in (0, S_{\max}) \times (0,T)$$

$$U(S,0) = \kappa(S,T) \text{ for } S \in (0, S_{\max})$$

where $\kappa(S,t)$ is the utility function defined in (5.3). The solution to this problem is $U(S,\tau) = \kappa(Se^{r\tau}, T)e^{-r\tau}$ and it is easily seen that this function satisfies

$$\frac{U(S,\tau+\Delta\tau) - U(\widehat{S},\tau)}{\theta(\Delta\tau)} = -rU(\widehat{S},\tau)$$

where

$$\theta(\Delta\tau) = \frac{1-e^{-r\Delta\tau}}{r} = \Delta\tau + \mathcal{O}(\Delta\tau^2)$$

and

$$\widehat{S} = Se^{r\Delta\tau} = \frac{S}{1-r\theta(\Delta\tau)} \Rightarrow \widehat{S} - S = S\frac{r\theta(\Delta\tau)}{1-r\theta(\Delta\tau)}.$$

This is in the form of an "exact finite difference scheme" for the above linear equation. By Taylor expansion using $\frac{\Delta\tau}{\theta(\Delta\tau)} = 1 + \mathcal{O}(\Delta\tau)$ it is easily seen that (for any smooth U)

$$\frac{\partial U}{\partial \tau}(S,\tau) - rS\frac{\partial U}{\partial S}(S,\tau) + rU(S,\tau) = \frac{U(S,\tau+\Delta\tau) - U(\widehat{S},\tau)}{\theta(\Delta\tau)} + rU(\widehat{S},\tau) + \mathcal{O}(\Delta\tau). \tag{5.13}$$

Note that the approximation retains the order if $\theta(\Delta\tau)$ is replaced by $\Delta\tau$.
In order to reach a useful finite difference scheme the solution in the ghost point $\widehat{S}$ is "split" between the two adjacent mesh points S and $S + \Delta S$ by Taylor expansion. Arenas et el [2] use the following 1st order Taylor expansion:

$$\begin{aligned} &U(\widehat{S},\tau) = \tilde{U}^0_{\Delta S,\Delta\tau}(S,\tau) + \mathcal{O}(\Delta S\Delta\tau + \Delta\tau^2) \text{ where} \\ &\tilde{U}^0_{\Delta S,\Delta\tau}(S,\tau) = U(S,\tau) + (\widehat{S} - S)\frac{U(S+\Delta S,\tau) - U(S,\tau)}{\Delta S}. \end{aligned} \tag{5.14}$$

Requiring $S \le \widehat{S} \le S + \Delta S \ \forall S \in [0, S_{\max}]$ which is equivalent to the condition

$$S_{\max}(e^{r\Delta\tau} - 1) \le \Delta S \Leftrightarrow \Delta\tau \le \frac{1}{r\ln(1 + \frac{\Delta S}{S_{\max}})} \le \frac{\Delta S}{rS_{\max}} + \mathcal{O}(\Delta S^2) \tag{5.15}$$

we end up with the truncation error $\mathcal{O}(\Delta S^2)$. Inserting $\tilde{U}^0_{\Delta S,\Delta\tau}(S,\tau)$ instead of $U(\widehat{S},\tau)$ in (5.13) we get

$$\begin{aligned} &\frac{\partial U}{\partial \tau}(S,\tau) - rS\frac{\partial U}{\partial S}(S,\tau) + rU(S,\tau) \\ &= \frac{U(S,\tau+\Delta\tau) - \tilde{U}^0_{\Delta S,\Delta\tau}(S,\tau)}{\theta(\Delta\tau)} + r\tilde{U}^0_{\Delta S,\Delta\tau}(S,\tau) + \mathcal{O}(\Delta\tau) + \mathcal{O}(\Delta S) \\ &= \frac{U(S,\tau+\Delta\tau) - U(S,\tau)}{\theta(\Delta\tau)} - rS\frac{U(S+\Delta S,\tau) - U(S,\tau)}{\Delta S} + rU(S,\tau) \\ &+\mathcal{O}(\Delta\tau) + \mathcal{O}(\Delta S). \end{aligned} \tag{5.16}$$

Clearly, this does not lead to 2nd order consistency in S as claimed in [2]. The method is only first order consistent in S as well as t. Following [34] Arenas et al then suggest the approximation arising from

$$\begin{aligned} &\frac{\partial^2 U}{\partial S^2}(S,\tau) = \frac{U(S-\Delta S,\tau) - 2U(S,\tau) + U(S+\Delta S,\tau)}{\phi(\Delta S)} + \mathcal{O}(\Delta S^2) \text{ where} \\ &\phi(\Delta S) = \frac{1}{r}(e^{\sqrt{r}\Delta S} - 2 + e^{-\sqrt{r}\Delta S}) = \Delta S^2 + \mathcal{O}(\Delta S^4) \end{aligned} \tag{5.17}$$

for the second derivatives (noting that $\frac{\Delta S^2}{\phi(\Delta S)} = 1 + \mathcal{O}(\Delta S^2)$) whereas the remaining S and τ in the diffusion term are left unaltered. Note that the approximation retains the order if $\phi(\Delta S)$ is replaced by ΔS^2. This results in the following approximation:

$$\begin{aligned}
&\frac{\partial U}{\partial \tau}(S,\tau) - rS\frac{\partial U}{\partial S}(S,\tau) + rU(S,\tau) - \frac{1}{2}\sigma_{BS}^2(T-\tau,S,U_{SS})S^2\frac{\partial^2 U}{\partial S^2}(S,\tau)\\
&= \frac{U(S,\tau+\Delta\tau)-U(S,\tau)}{\theta(\Delta\tau)} - rS\frac{U(S+\Delta S,\tau)-U(S,\tau)}{\Delta S} + rU(S,\tau)\\
&-\frac{1}{2}\sigma_{BS}^2(T-\tau,S,U_{SS})S^2\frac{U(S-\Delta S,\tau)-2U(S,\tau)+U(S+\Delta S,\tau)}{\phi(\Delta S)}\\
&+\mathcal{O}(\Delta\tau)+\mathcal{O}(\Delta S). \qquad (5.18)
\end{aligned}$$

Now consider a uniform mesh $S_j = jh$ for $j = 0,\ldots,M$ and $\tau^n = nk$ for $n = 0,\ldots,N$ where the condition (5.15) takes the form $\frac{T}{N} = k \le \frac{1}{r}\ln(1+\frac{h}{S_{\max}}) = \frac{1}{r}\ln(1+\frac{1}{M})$ or $N \gtrsim rT\cdot M$ which is a very mild condition satisfied for sufficiently small time stepsizes k. We use u_j^n as our approximation to $U(S_j,\tau_n)$, U being the solution to (5.6–5.7). Also introduce the following difference operators:

$$\delta_\tau^+ u_j^n = \frac{u_j^{n+1}-u_j^n}{k}, \quad \tilde\delta_\tau^+ u_j^n = \frac{u_j^{n+1}-u_j^n}{\theta(k)},$$

$$\delta_S^+ u_j^n = \frac{u_{j+1}^n - u_j^n}{h}, \quad \delta_S^0 u_j^n = \frac{u_{j+1}^n - u_{j-1}^n}{2h},$$

$$\delta_{SS}^0 u_j^n = \frac{u_{j+1}^n - 2u_j^n + u_{j-1}^n}{h^2}, \quad \tilde\delta_{SS}^0 u_j^n = \frac{u_{j+1}^n - 2u_j^n + u_{j-1}^n}{\phi(h)}, \quad \bar\delta_{SS}^0 u_j^n = \frac{u_{j+1}^n - 2u_j^{n+1} + u_{j-1}^n}{h^2}.$$

Discarding the truncation error terms in (5.18) we arrive at the explicit nonstandard finite difference scheme for (5.6–5.7) [NFDM]

$$\begin{aligned}
&\tilde\delta_\tau^+ u_j^n - \frac{1}{2}\sigma_{BS}^2(T-\tau_n,S_j,\tilde\delta_{SS}^0 u_j^n)S^2\tilde\delta_{SS}^0 u_j^n - rS_j\delta_S^+ u_j^n + ru_j^n = 0\\
&\quad \text{for } j = 1,\ldots,M-1,\ n = 0,\ldots,N-1\ (h = \frac{S_{\max}}{M},\ k = \frac{T}{N},\ N \gtrsim rT\cdot M),\\
&u_j^0 = \kappa(jh,T),\ u_0^n = \kappa(0,T-nk),\ u_M^n = \kappa(S_{\max},T-nk)\\
&\quad \text{for } j = 1,\ldots,M-1,\ n = 0,\ldots,N. \qquad (5.19)
\end{aligned}$$

This is easily recognized as an explicit upwinding method except for the nonstandard first order approximations to h and k in most of the derivatives. By construction and by the boundedness and smoothness of U and its derivatives this scheme is first order

consistent in τ and S in any L^p-norm (also L^∞) under the assumption that

$$\Psi(e^{rnk}\kappa^2 R(jh)^2 \delta^0_{SS} U^n_j) - \Psi(e^{rnk}\kappa^2 R(jh)^2 U_{SS}(jh, nk)) = \mathcal{O}(h^{1+q}) = \mathcal{O}(\Delta S^{1+q})$$
$$\text{for } q = 0, 1 \text{ and any smooth } U. \tag{5.20}$$

$q = 0$ is required for NFDM using (5.14) whereas $q = 1$ is required for FtCS using (5.21) below, where (5.20) results in second order consistency in S in any L^p norm. Note that these orders of consistency are valid also if replacing $\theta(k)$ by k and $\phi(h)$ by h^2.

Note that FtCS may actually be created from NFDM simply by splitting $\hat{S}$ between the mesh points $S - \Delta S$ and $S + \Delta S$ instead of between S and $S + \Delta S$ and hence replacing (5.14) by

$$\begin{aligned} &U(\widehat{S}, \tau) = \tilde{U}^1_{\Delta S, \Delta\tau}(S, \tau) + \mathcal{O}(\Delta S^2 \Delta\tau + \Delta\tau^2) \text{ where} \\ &\tilde{U}^1_{\Delta S, \Delta\tau}(S, \tau) = U(S, \tau) + (\widehat{S} - S)\frac{U(S + \Delta S, \tau) - U(S - \Delta S, \tau)}{2\Delta S} \end{aligned} \tag{5.21}$$

still assuming (5.15). Combining (5.13) and (5.21) we get

$$\begin{aligned} &\frac{\partial U}{\partial \tau}(S, \tau) - rS\frac{\partial U}{\partial S}(S, \tau) + rU(S, \tau) \\ &= \frac{U(S, \tau + \Delta\tau) - \tilde{U}^1_{\Delta S, \Delta\tau}(S, \tau)}{\theta(\Delta\tau)} + r\tilde{U}^1_{\Delta S, \Delta\tau}(S, \tau) + \mathcal{O}(\Delta\tau) + \mathcal{O}(\Delta S^2) \\ &= \frac{U(S, \tau + \Delta\tau) - U(S, \tau)}{\theta(\Delta\tau)} - rS\frac{U(S + \Delta S, \tau) - U(S - \Delta S, \tau)}{2\Delta S} + rU(S, \tau) \\ &+ \mathcal{O}(\Delta\tau) + \mathcal{O}(\Delta S^2). \end{aligned} \tag{5.22}$$

Note that also this approximation retains the order if $\theta(\Delta\tau)$ is replaced by $\Delta\tau$. Using (5.17) and replacing $\theta(\Delta\tau)$ by $\Delta\tau$ and $\phi(\Delta S)$ by ΔS^2 without the loss of consistency order we arrive at FtCS. Since $\Delta\tau \leq \mathcal{O}(\Delta S)$ by (5.15) the practical difference between the different orders of NFDM and FtCS needs to be investigated further.

Now we focus on NFDM and FtCS who may be rewritten in a unified fashion as follows ($q = 0$ for NFDM and $q = 1$ for FtCS):

$$
\begin{aligned}
&u_j^{n+1} = (1 - r\theta(k))\left\{u_j^n + \frac{r\theta(k)}{(1+q)(1-r\theta(k))} j(u_{j+1}^n - u_{j-q}^n)\right\} \\
&+\frac{\theta(k)}{2}\sigma_0^2\left(1 + \Psi(e^{rnk}\kappa^2 R(jh)^2 \tilde{\delta}_{SS}^0 u_j^n)\right) j^2 h^2 \tilde{\delta}_{SS}^0 u_j^n \\
&\quad \text{for } q = 0, 1,\ j = 1, \ldots, M-1,\ n = 0, \ldots, N-1\ (h = \frac{S_{\max}}{M},\ k = \frac{T}{N},\ N \gtrsim rT \cdot M), \\
&u_j^0 = \kappa(jh, T),\ u_0^n = \kappa(0, T - nk),\ u_M^n = \kappa(S_{\max}, T - nk) \\
&\quad \text{for } j = 1, \ldots, M-1,\ n = 0, \ldots, N. \qquad (5.23)
\end{aligned}
$$

Note that Arenas et al [2] apply the boundary conditions $\frac{\partial^2 U}{\partial S^2} = 0$ in $(0, \tau)$ and $(S_{\max}, \tau)$ in hard form by $\delta_{SS}^0 u_0^n = \delta_{SS}^0 u_M^n = 0$ thus introducing the ghost points $S_{-1} = -h$ and $S_{M+1} = S_{\max} + h$ and at the same time extending the finite difference scheme (5.23) to include also $j = 0$ and $j = M$. We shall do the same for our theoretical investigations even though we for the practical computations are using the Dirichlet conditions from (5.7) only approximately satisfying these conditions. By rearranging the terms (5.23) can be written as

$$
\begin{aligned}
&u_j^{n+1} = a_j^n u_{j+1}^n + b_j^n u_j^n + c_j^n u_{j-1}^n \\
&\quad \text{for } j = 1, \ldots, M-1,\ n = 0, \ldots, N-1 \text{ and} \\
&u_j^0 = \kappa(jh, T),\ u_0^n = \kappa(0, T - nk),\ u_M^n = \kappa(S_{\max}, T - nk) \\
&\quad \text{for } j = 1, \ldots, M-1,\ n = 0, \ldots, N\ (h = \frac{S_{\max}}{M},\ k = \frac{T}{N},\ N \gtrsim rT \cdot M) \qquad (5.24)
\end{aligned}
$$

or with derivative boundary conditions

$$
\begin{aligned}
&u_j^{n+1} = a_j^n u_{j+1}^n + b_j^n u_j^n + c_j^n u_{j-1}^n \\
&\quad \text{for } j = 0, \ldots, M,\ n = 0, \ldots, N-1\ (h = \frac{S_{\max}}{M},\ k = \frac{T}{N},\ N \gtrsim rT \cdot M) \text{ and} \\
&u_j^0 = \kappa(jh, T),\ \delta_{SS}^0 u_0^n = \delta_{SS}^0 u_M^n = 0 \\
&\quad \text{for } j = 0, \ldots, M,\ n = 0, \ldots, N\ (h = \frac{S_{\max}}{M},\ k = \frac{T}{N},\ N \gtrsim rT \cdot M) \qquad (5.25)
\end{aligned}
$$

where

$$
\begin{aligned}
a_j^n &= \frac{r\theta(k)j}{1+q} + \frac{\theta(k)\omega_j^n}{2\phi(h)},\\
b_j^n &= 1 - r\theta(k)\left(\frac{1-q}{1+q}j + 1\right) - \frac{\theta(k)\omega_j^n}{\phi(h)},\\
c_j^n &= -\frac{qr\theta(k)j}{1+q} + \frac{\theta(k)\omega_j^n}{2\phi(h)},\\
\omega_j^n &= \sigma_0^2(jh)^2\left[1 + \Psi\left(e^{rnk}\kappa^2 R(jh)^2\delta_{SS}^0 u_j^n\right)\right] = S_j^2\sigma_{BS}^2(T-\tau^n, S_j, \delta_{SS}^0 u_j^n) \geq 0\\
&\text{for } q = 0,1,\ j = 0,\ldots,M,\ n = 0,\ldots,N\ \left(h = \frac{S_{\max}}{M},\ k = \frac{T}{N},\ N \gtrsim rT\cdot M\right). \qquad (5.26)
\end{aligned}
$$

Here $q = 0$ corresponds to NFDM while $q = 1$ corresponds to FtCS. The theoretical properties of NFDM (and FtCS) are covered by Appendix 5.B

5.B NFDM Perperties Theorem

Theorem 5.1. *If*

$$
\theta(k)\left(rM + \frac{r^2\theta(k)M^2}{1-r\theta(k)} + \frac{1}{\phi(h)}\max_{\substack{j=0,\ldots,M\\ n=0,\ldots,N-1}}\omega_j^n\right) \leq 1 \qquad (5.27)
$$

(which will be satisfied for sufficiently small time stepsizes k) then

1. *the nonstandard finite difference schemes (5.24) and (5.25) for $q = 0$ are nonnegative, i.e. $u_j^n \geq 0$ for all $j = 0,\ldots,M$ and $n = 0,\ldots,N$.*

2. *the nonstandard finite difference scheme (5.25) for $q = 0$ is monotonicity preserving in S, i.e. $u_{j+1}^n \geq (\leq)\ u_j^n$ for all $j = 0,\ldots,M-1$ and any $n = 0,\ldots,N-1 \Rightarrow u_{j+1}^{n+1} \geq (\leq)\ u_j^{n+1}$ for all $j = 0,\ldots,M-1$.*

3. *the nonstandard finite difference scheme (5.25) for $q = 0$ for the put option is monotone nonincreasing with S, i.e. $u_0^n \geq \ldots \geq u_M^n$ for all $n = 0,\ldots,N$. For the call and bet options the scheme is monotone nondecreasing with S, i.e. $u_0^n \leq \ldots \leq u_M^n$ for all $n = 0,\ldots,N$.*

4. *the nonstandard finite difference schemes (5.24) and (5.25) are consistent in any L^p norm ($p \in [1,\infty]$) of order 1 in τ and order $1+q$ in S (for $q = 0,1$) assuming (5.20).*

5. *the nonstandard finite difference schemes (5.24) and (5.25) are stable in the* L^∞ *norm (for* $q = 0, 1$*), i.e.* $\|\mathbf{u}^n\|_\infty \leq Ce^{\beta\tau^n}\|\mathbf{u}^0\|_\infty$ *for all* $n = 0, 1, \ldots$ *for some* $C, \beta \geq 0$ *where* $\mathbf{u}^n = [u_0^n, \ldots, u_M^n]^T$.

6. *the nonstandard finite difference schemes (5.24) and (5.25) are convergent in the* L^∞ *norm of order 1 in* τ *and order* $1 + q$ *in* S *(for* $q = 0, 1$*) to the solution to (5.6–5.7) assuming (5.20).*

Proof.

1.

Here we provide the proof for the nonnegativity of (5.24), the details for (5.25) following from the exposition in [19].

For all $j = 1, \ldots, M-1$, $n = 0, \ldots, N$ with initial data given by (5.24) and by definition of the put, call and bet options, $u_j^0 \geq 0$, $u_0^n \geq 0$ and $u_M^n \geq 0$. By (5.26) also $a_j^n \geq 0$ for $q = 0, 1$ and $c_j^n \geq 0$ for $q = 0$. In order to have $c_j^n \geq 0$ also for $q = 1$ we would need

$$\phi(h) \leq \frac{1}{rM} \min_{\substack{j=0,\ldots,M \\ n=0,\ldots,N-1}} \omega_j^n \text{ for } q = 1 \tag{5.28}$$

but since $\omega_j^n \simeq 0$ close to the S-boundaries, this condition is not satisfied. Hence FtCS cannot be shown to be nonnegative by this method, which is consistent with the practical observations that FtCS may oscillate near $S = S_{\max}$ but does not oscillate near $S = K$. If only $b_j^n \geq 0$ for $j = 1, \ldots, M-1$, $n = 0, \ldots, N-1$, (5.24) implies that $u_j^n \geq 0$ for $j = 0, \ldots, M$, $n = 0, \ldots, N$, i.e. the scheme is nonnegative.

The nonnegativity of b_j^n hinges on the properties of δ_j^n and the function Ψ and is here only stated in general terms as the assumption (5.27).

Obviously (5.27) $\Rightarrow \min_{\substack{j=1,\ldots,M-1 \\ n=0,\ldots,N-1}} \left(1 - r\theta(k)\left(\frac{1-q}{1+q}j + 1\right) - \frac{qr^2\theta(k)^2j^2}{1-r\theta(k)} - \frac{\theta(k)}{\phi(h)}\omega_j^n\right) \geq 0 \Leftrightarrow \min_{\substack{j=1,\ldots,M-1 \\ n=0,\ldots,N-1}} b_j^n \geq 0$.

2.

Let us consider only the nondecreasing case, since the nonincreasing case is identical apart from the orientation of the inequality signs. Hence assume that

$$u_{j+1}^n \geq u_j^n \text{ for all } j = 0, \ldots, M-1 \text{ and any } n = 0, \ldots, N-1. \tag{5.29}$$

Note that $\delta_0^n = 0 \Leftrightarrow u_{-1}^n = 2u_0^n - u_1^n = u_0^n + (u_0^n - u_1^n) \overset{(5.29)}{\leq} u_0^n$. Hence (5.29) can be extended to $j = -1$.

Also $\delta_M^n = 0 \Leftrightarrow u_{M+1}^n = 2u_M^n - u_{M-1}^n = u_M^n + (u_M^n - u_{M-1}^n) \overset{(5.29)}{\geq} u_M^n$. Hence (5.29) can be extended to $j = M$.

Thus we have

$$u_{j+1}^n \geq u_j^n \text{ for all } j = -1, \ldots, M \text{ and some } n = 0, \ldots, N-1. \tag{5.30}$$

Also note that by simple computation from (5.26)

$$a_j^n + (b_j^n + r\theta(k)) + c_j^n = 1 \text{ for all } j = 0, \ldots, M. \tag{5.31}$$

For $j = 0, \ldots, M-1$:

$u_j^{n+1} - u_j^n \overset{(5.24)}{=} a_j^n u_{j+1}^n + b_j^n u_j^n + c_j^n u_{j-1}^n - u_j^n \overset{(5.30)}{\leq} a_j^n u_{j+1}^n + b_j^n u_j^n + c_j^n u_j^n - u_j^n$

$= a_j^n(u_{j+1}^n - u_j^n) + (a_j^n + b_j^n + c_j^n - 1)u_j^n \overset{(5.31)}{=} a_j^n(u_{j+1}^n - u_j^n) - r\theta(k)u_j^n$

and

$u_{j+1}^{n+1} - u_{j+1}^n \overset{(5.24)}{=} a_{j+1}^n u_{j+2}^n + b_{j+1}^n u_{j+1}^n + c_{j+1}^n u_j^n - u_{j+1}^n \overset{(5.30)}{\geq} a_{j+1}^n u_{j+1}^n + b_{j+1}^n u_{j+1}^n +$

$c_{j+1}^n u_j^n - u_{j+1}^n$

$= -c_{j+1}^n(u_{j+1}^n - u_j^n) + (c_{j+1}^n + a_{j+1}^n + b_{j+1}^n - 1)u_{j+1}^n \overset{(5.31)}{=} -c_{j+1}^n(u_{j+1}^n - u_j^n) - r\theta(k)u_{j+1}^n.$

and hence

$u_{j+1}^{n+1} - u_j^{n+1} = (u_{j+1}^{n+1} - u_{j+1}^n) + (u_{j+1}^n - u_j^n) - (u_j^{n+1} - u_j^n) \geq \left(-c_{j+1}^n + 1 - a_j^n - r\theta(k)\right)\left(u_{j+1}^n - u_j^n\right)$

≥ 0 where the last term is nonnegative by (5.30) and the first term is nonnegative by (5.27) and the following argument:

$-c_{j+1}^n + 1 - a_j^n - r\theta(k) \overset{(5.26)}{=} -\frac{\theta(k)}{2\phi(h)}\omega_{j+1}^n + 1 - rj\theta(k) - \frac{\theta(k)}{2\phi(h)}\omega_j^n + 1 - r\theta(k)$

$= 1 - r(j+1)\theta(k) - \frac{\theta(k)}{2\phi(h)}(\omega_j^n + \omega_{j+1}^n) \geq 1 - rM\theta(k) - \frac{\theta(k)}{2\phi(h)}(\max_{j=0,\ldots,M-1}\omega_j^n + \max_{j+1=1,\ldots,M}\omega_{j+1}^n)$

$\geq 1 - rM\theta(k) - \frac{\theta(k)}{\phi(h)} \max_{\substack{j=0,\ldots,M \\ n=0,\ldots,N-1}} \omega_j^n \overset{(5.27)}{\geq} 0.$

3.

For the put option, $u_{j+1}^0 \leq u_j^0$ for all $j = 0, \ldots, M-1$.

For the call and bet options $u_{j+1}^0 \geq u_j^0$ for all $j = 0, \ldots, M-1$.

The results then follow from monotonicity preservation.

4.

For (5.24) see below (5.19). The consistency in the L^∞ norm for (5.25) follows from the exposition in [19] and the general L^p-norm is a simple generalization.

5.

Here we provide the proof for the stability of (5.24), the details for (5.25) following from the exposition in [19].

First $u_0^n = [0 \vee Ke^{-r\tau} \vee 0] \leq [0 \vee K \vee 0] = u_0^0 \leq \|\mathbf{u}^0\|_\infty$ satisfying the stability requirement with $C = 1$ and $\beta = 0$.

Also $u_M^n = [S_{\max} - Ke^{-r\tau} \vee 0 \vee Be^{-r\tau}] \leq [\frac{S_{\max} - Ke^{-r\tau}}{S_{\max} - K}(S_{\max} - K) \vee 0 \vee B] \leq [\alpha(S_{\max} - K) \vee 0 \vee B] \leq \max\{\alpha, 1\} u_0^0 \leq \max\{\alpha, 1\}\|\mathbf{u}^0\|_\infty$ where $\alpha = \frac{S_{\max} - Ke^{-rT}}{S_{\max} - K} \geq \frac{S_{\max} - Ke^{-r\tau}}{S_{\max} - K}$.

Hence the stability requirement is satisfied with $C = \max\{\alpha, 1\}$ and $\beta = 0$.

Finally for $j = 1, \ldots, M-1$:

$u_j^{n+1} \overset{(5.24)}{=} a_j^n u_{j+1}^n + b_j^n u_j^n + c_j^n u_{j-1}^n \leq (a_j^n + b_j^n + c_j^n)\|\mathbf{u}^n\|_\infty$

where $0 \leq a_j^n + b_j^n + c_j^n \overset{(5.31)}{=} 1 - r\theta(k) \leq 1$ so that $u_j^{n+1} \leq \|\mathbf{u}^n\|_\infty \Rightarrow u_j^n \leq \|\mathbf{u}^0\|_\infty$ which satisfies the stability requirement with $C = 1$ and $\beta = 0$.

In conclusion $\|\mathbf{u}^n\|_\infty \leq C\|\mathbf{u}^0\|_\infty$ where $C = \max\{\alpha, 1\}$.

6.

This follows from Lax's convergence theorem and bullets 4 and 5. □

5.C $\Psi(x)$ Plot

A plot of Ψ is shown in Figure 5.C.1.

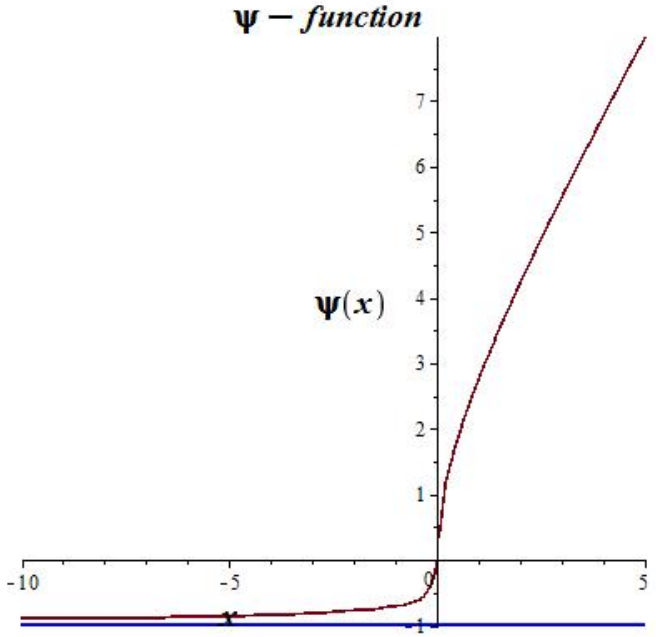

FIGURE 5.C.1: The Barles and Soner Ψ function satisfying (5.5).

Bibliography

[1] J. Ankudinova and M. Ehrhardt, *On the numerical solution of nonlinear black–scholes equations*, Computers & Mathematics with Applications, 56 (2008), pp. 799–812.

[2] A. J. Arenas, G. González-Parra, and B. M. Caraballo, *A nonstandard finite difference scheme for a nonlinear black–scholes equation*, Mathematical and Computer Modelling, 57 (2013), pp. 1663–1670.

[3] D. Bakstein and S. Howison, *A non-arbitrage liquidity model with observable parameters for derivatives*, Mathematical Finance, (2003).

[4] G. Barles and H. M. Soner, *Option pricing with transaction costs and a nonlinear black-scholes equation*, Finance and Stochastics, 2 (1998), pp. 369–397.

[5] F. Black and M. Scholes, *The pricing of options and corporate liabilities*, The journal of political economy, (1973), pp. 637–654.

[6] P. P. Boyle and T. Vorst, *Option replication in discrete time with transaction costs*, The Journal of Finance, 47 (1992), pp. 271–293.

[7] M. J. Brennan and E. S. Schwartz, *Finite difference methods and jump processes arising in the pricing of contingent claims: A synthesis*, Journal of Financial and Quantitative Analysis, 13 (1978), pp. 461–474.

[8] R. Company, L. Jodar, and J. R. Pintos, *A numerical method for european option pricing with transaction costs nonlinear equation*, Mathematical and Computer Modelling, 50 (2009), pp. 910–920.

[9] R. Cont and E. Voltchkova, *A finite difference scheme for option pricing in jump diffusion and exponential lévy models*, SIAM Journal on Numerical Analysis, 43 (2005), pp. 1596–1626.

[10] D. J. Duffy, *A critique of the crank nicolson scheme strengths and weaknesses for financial instrument pricing*, 70+ DVDs FOR SALE & EXCHANGE, (2004), p. 333.

[11] ——, *Finite Difference methods in financial engineering: a Partial Differential Equation approach*, John Wiley & Sons, 2006.

[12] M. Ehrhardt, *Nonlinear models in mathematical finance: new research trends in option pricing*, Nova Science Publishers, 2008.

[13] P. A. Forsyth and G. Labahn, *Numerical methods for controlled hamilton-jacobi-bellman pdes in finance*, Journal of Computational Finance, 11 (2007), p. 1.

[14] R. Frey, *Market illiquidity as a source of model risk in dynamic hedging*, in Model Risk, Risk Publications, London, 2000, pp. 125–136.

[15] R. Frey and P. Patie, *Risk management for derivatives in illiquid markets: A simulation study*, in Advances in finance and stochastics, Springer, 2002, pp. 137–159.

[16] R. Frey and A. Stremme, *Market volatility and feedback effects from dynamic hedging*, Mathematical finance, 7 (1997), pp. 351–374.

[17] M. B. Giles and R. Carter, *Convergence analysis of crank-nicolson and rannacher time-marching*, (2005).

[18] K. J. Glover, *The analysis of PDEs arising in nonlinear and non-standard option pricing*, PhD thesis, University of Manchester, 2008.

[19] G. González-Parra, A. J. Arenas, and B. M. Chen-Charpentier, *Positive numerical solution for a nonarbitrage liquidity model using nonstandard finite difference schemes*, Numerical Methods for Partial Differential Equations, 30 (2014), pp. 210–221.

[20] E. G. Haug, *The complete guide to option pricing formulas*, vol. 2, McGraw-Hill New York, 1998.

[21] T. Hoggard, A. E. Whalley, and P. Wilmott, *Hedging option portfolios in the presence of transaction costs*, Advances in Futures and Options Research, 7 (1994), pp. 21–35.

[22] M. H. Holmes, *Introduction to numerical methods in differential equations*, vol. 52, Springer, 2007.

[23] J. Hugger, *The boundary value formulation of the asian call option*, in Numerical Mathematics and Advanced Applications, Springer, 2003, pp. 409–418.

[24] ——, *Wellposedness of the boundary value formulation of a fixed strike asian option*, Journal of computational and applied mathematics, 185 (2006), pp. 460–481.

[25] M. Jandačka and D. Ševčovič, *On the risk-adjusted pricing-methodology-based valuation of vanilla options and explanation of the volatility smile*, Journal of Applied Mathematics, 2005 (2005), pp. 235–258.

[26] R. Korn and E. Korn, *Option pricing and portfolio optimization*, American Math. Soc., Providence, (2001).

[27] M. Kratka, *No mystery behind the smile*, Risk, 9 (1998), pp. 67–71.

[28] P. Kútik and K. Mikula, *Finite volume schemes for solving nonlinear partial differential equations in financial mathematics*, in Finite Volumes for Complex Applications VI Problems & Perspectives, Springer, 2011, pp. 643–651.

[29] Y.-K. Kwok, *Mathematical models of financial derivatives*, Springer, 2008.

[30] H. E. Leland, *Option pricing and replication with transactions costs*, The journal of finance, 40 (1985), pp. 1283–1301.

[31] D. C. Lesmana and S. Wang, *An upwind finite difference method for a nonlinear black–scholes equation governing european option valuation under transaction costs*, Applied Mathematics and Computation, (2013).

[32] H. Liu and J. Yong, *Option pricing with an illiquid underlying asset market*, Journal of Economic Dynamics and Control, 29 (2005), pp. 2125–2156.

[33] R. C. Merton et al., *Theory of rational option pricing*, (1971).

[34] R. E. Mickens, *Nonstandard finite difference models of differential equations*, World Scientific, 1994.

[35] E. Navarro, J. R. Pintos, E. Ponsoda, et al., *Numerical solution of linear and nonlinear black–scholes option pricing equations*, Computers & Mathematics with Applications, 56 (2008), pp. 813–821.

[36] C. W. Oosterlee, C. C. W. Leentvaar, and X. Huang, *Accurate american option pricing by grid stretching and high order finite differences*, tech. report, Working papers, DIAM, Delft University of Technology, the Netherlands, 2005.

[37] O. Østerby, *Five ways of reducing the crank–nicolson oscillations*, BIT Numerical Mathematics, 43 (2003), pp. 811–822.

[38] D. M. Pooley, K. R. Vetzal, and P. A. Forsyth, *Convergence remedies for non-smooth payoffs in option pricing*, Journal of Computational Finance, 6 (2003), pp. 25–40.

[39] R. Rannacher, *Finite element solution of diffusion problems with irregular data*, Numerische Mathematik, 43 (1984), pp. 309–327.

[40] C. Reisinger and A. Whitley, *The impact of a natural time change on the convergence of the crank–nicolson scheme*, IMA Journal of Numerical Analysis, (2013), p. drt029.

[41] D. Ševcovic, B. Stehliková, and K. Mikula, *Analytical and numerical methods for pricing financial derivatives*, Nova Science Publ. ISBN, (2011), pp. 978–1.

[42] R. Seydel, *Tools for computational finance*, Springer, 2012.

[43] D. Y. Tangman, A. Gopaul, and M. Bhuruth, *Numerical pricing of options using high-order compact finite difference schemes*, Journal of Computational and Applied Mathematics, 218 (2008), pp. 270–280.

[44] D. Tavella and C. Randall, *Pricing financial instruments: The finite difference method*, John Wiley & Sons New York, 2000.

[45] J. Wang and P. A. Forsyth, *Maximal use of central differencing for hamilton-jacobi-bellman pdes in finance*, SIAM Journal on Numerical Analysis, 46 (2008), pp. 1580–1601.

[46] P. Wilmott, *The mathematics of financial derivatives: a student introduction*, Cambridge University Press, 1995.

[47] Y. Zhao and W. T. Ziemba, *On leland's option hedging strategy with transaction costs*, tech. report, Humboldt University, Berlin, Germany, 2003.

[48] S. Zhou, W. Li, Y. Wei, and C. Wen, *A positivity-preserving numerical scheme for nonlinear option pricing models*, Journal of Applied Mathematics, 2012 (2012).